

Universiteit
Leiden
The Netherlands

Genetic and environmental factors determining heterogeneity in preservation stress resistance of Aspergillus niger conidia

Seekles, S.J.

Citation
Seekles, S. J. (2022, January 18). *Genetic and environmental factors determining heterogeneity in preservation stress resistance of Aspergillus niger conidia*. Retrieved from https://hdl.handle.net/1887/3250007

Version:	Publisher's Version
License:	Licence agreement concerning inclusion of doctoral thesis in the Institutional Repository of the University of Leiden
Downloaded from:	https://hdl.handle.net/1887/3250007

Note: To cite this publication please use the final published version (if applicable).

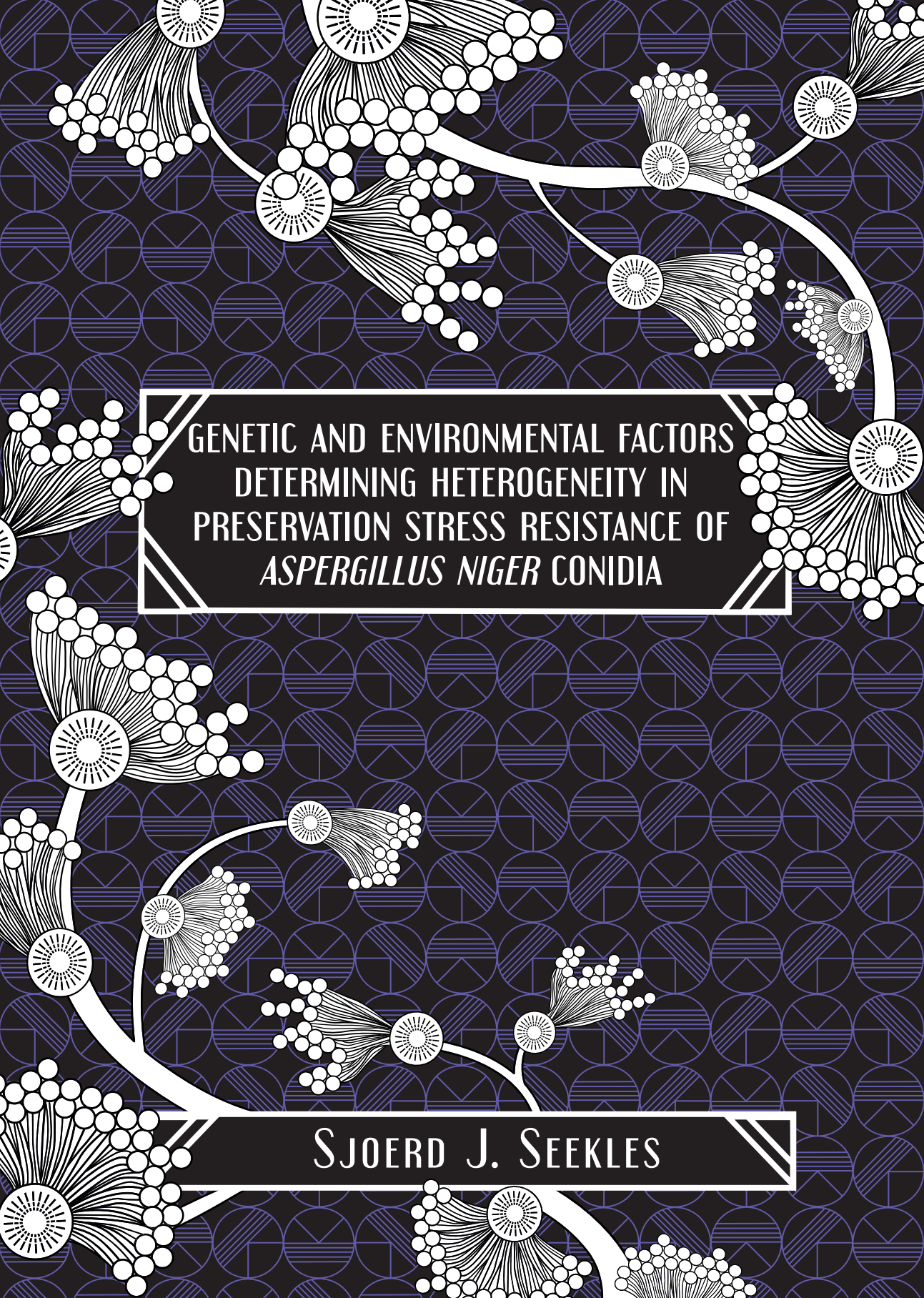
GENETIC AND ENVIRONMENTAL FACTORS DETERMINING HETEROGENEITY IN PRESERVATION STRESS RESISTANCE OF *ASPERGILLUS NIGER* CONIDIA
SJOERD J. SEEKLES

Genetic and environmental factors determining heterogeneity in preservation stress resistance of *Aspergillus niger* conidia

Sjoerd J. Seekles

ISBN: 978-94-6458-018-1

Author: Sjoerd Johan Seekles

Cover & Layout design: Raden Lerika Ratri Noorshanti, Hadiastri Kusumawardhani

Printing: Ridderprint B.V., Netherlands | www.ridderprint.nl

This work is financed by Topsector Agri & Food project “Heterogeneity in spores of food spoilage fungi” (project number AF-15507). The studies presented in this thesis were performed within the framework of TiFN.

Copyright © S. J. Seekles, 2021. All rights reserved.

Genetic and environmental factors determining heterogeneity in preservation stress resistance of *Aspergillus niger* conidia

Proefschrift

ter verkrijging van

de graad van doctor aan de Universiteit Leiden,

op gezag van rector magnificus prof.dr.ir. H. Bijl,

volgens besluit van het college voor promoties

te verdedigen op dinsdag 18 Januari 2022

klokke 11.15 uur

door

Sjoerd Johan Seekles

geboren te Alkmaar

in 1993

Promotors: Dr. A. F. J. Ram

Prof. dr. P. J. Punt

Promotiecommissie: Prof. dr. J. H. de Winde

Prof. dr. G. P. van Wezel

Prof. dr. D. Claessen

Prof. dr. S. Brul

Prof. dr. V. Meyer

Dr. D. E. Rozen

Table of Contents

CHAPTER 1 Introduction **9**

Introduction 11

Scope and outline of this thesis 19

References 22

CHAPTER 2 **29**

Natural variation and the role of Zn_2Cys_6 transcription factors SdrA, WarA and WarB in sorbic acid resistance of *Aspergillus niger*

Abstract 30

Introduction 31

Results 35

Discussion 42

Material and Methods 45

References 49

Additional files 52

CHAPTER 3 **65**

Interkingdom microbial variability in heat resistance

Abstract 66

Introduction 67

Results 68

Discussion 74

Experimental Procedures 78

References 82

Additional files 87

CHAPTER 4 **91**

Genome sequencing of the neotype strain CBS 554.65 reveals the MAT1-2 locus of *Aspergillus niger*

Abstract 92

Background 93

Materials and methods 94

Results and discussion 98

Conclusions 115

References 116

List of additional files 122

CHAPTER 5 **125**

Genome sequences of 24 *Aspergillus niger sensu stricto* strains to study heterokaryon compatibility and sexual reproduction

Abstract 126

Introduction 127

Materials and Methods 131

Results 140

Discussion 150

References 153

Additional files 160

CHAPTER 6 **167**

Preservation stress resistance of melanin deficient conidia from *Paecilomyces variotii* and *Penicillium roqueforti* mutants generated via CRISPR/Cas9 genome editing

Abstract 168

Introduction 169

Results 172

Conclusions 186

Materials and Methods 188

References 192

Additional files 196

CHAPTER 7 **205**

Dissecting the pivotal role of mannitol and trehalose as compatible solutes in heat resistance of conidia, germination, and population heterogeneity in the filamentous fungus *Aspergillus niger*

Abstract 206

Introduction 207

Results 211

Discussion 226

Materials and Methods 230

References 239

Additional files 243

CHAPTER 8 **257**

The impact of cultivation temperature on the transcriptome, proteome and heat resistance of *Aspergillus niger* conidia

Introduction 259

Results 261

Discussion 269

Materials and Methods 272

References 281

Additional Files 287

CHAPTER 9 Discussion **299**

Discussion 300

Conclusion 309

References 310

Summary **315**

Samenvatting **321**

Curriculum vitae **327**

Publication list **329**

CHAPTER 1

Introduction

Introduction

Food and the preservation of food are a crucial part of human existence and a central part of many human societies. Humans have been preserving food since pre-historic times. The oldest evidence of food preservation dates back to the Middle Pleistocene; archeological data suggests that prehistoric humans saved the bones of animals inside a cave (Israel) for delayed consumption of the bone marrow and grease safely stored inside [1]. Food preservation is necessary to protect food from microbial food spoilage, thereby securing food products for human consumption. Although food preservation has become more sophisticated since pre-historic times, still around 25% of the global food supply is lost, post-harvest, due to microbial spoilage [2]. A significant portion of this post-harvest food spoilage is due to filamentous fungi, commonly referred to as “moulds” [3,4]. Most isolated food spoilage moulds are part of the phylum Ascomycota and include several species belong to the genus *Penicillium*, *Paecilomyces* and *Aspergillus* [5]. In general preservation strategies are aimed at preventing the outgrowth of fungal spores. Both sexual (ascospores) and asexual (conidiospores) spores from these fungi are relevant for spoilage (see a recent review on food spoilage by heat-resistant molds [6]). In this thesis we focus on the asexual spores (conidia) of these food spoiling fungi.

Filamentous fungi produce asexually spores (conidia) that are everywhere

Filamentous fungi produce conidia as a means of reproduction. Conidia have general characteristics that are shared among all species, six of these characteristics are listed here. First, conidia are dormant structures, meaning they are thought to be metabolically inactive, although this has been topic of debate [7]. Second, the conidia are the offspring of the fungus, meant to germinate and thrive after arriving at a place where the proper conditions are met [8]. Third, conidia are per definition the asexual (clonal) offspring of the fungus, meaning that they are genetically identical to the parent. Fourth, to increase the chance of successful reproduction, large quantities of these asexual spores are spread into the environment. Conidia tend to be easily dispersed in these large quanti-

ties through water or wind [8]. Fifth, conidia, meant for reproduction and long-distance travel through water and air, are heavily protected cells. They are meant to survive harsh conditions (drought, heat) and long periods of time before the proper conditions are met that support germination [9]. Sixth, the large airborne population of conidia is reported to be heterogenous with regards to their resistance against environmental stressors. Especially these last two characteristics make conidia well suited as reproductive structures for survival in nature, an therefore challenging structures to inactivate by commonly used preservation techniques.

Modern techniques of food preservation

In modern food preservation, various techniques are used to protect foods against spoilage by fungal spores. The most commonly used food preservation methods belong to one of three groups [10]. First, inactivation methods (for example inactivation by heating or applying radiation) are meant to kill the fungal spore and thereby protecting the food from spoilage. Second, growth inhibition methods (for example inhibition by adding preservatives or storing foods in cold environments) are meant to delay or prevent outgrowth of the fungus. Third, prevention methods (for example prevention by packaging) are meant to prevent recontamination after inactivation methods have been applied. In practice, these three methods are often combined where food is treated, packaged and subsequently stored in a way that inhibits fungal growth [11]. Studies have shown that 10 – 1000 conidia from genus *Aspergillus* are present in every cubic meter of air [12] and that these amounts vary with the season [13–15]. This makes preventing contamination nearly impossible. Even the air inside food factories contains many conidia that can potentially contaminate the food product throughout the production line. There are, however, ways to mitigate this challenge. Air filters are often installed inside clean rooms being part of these production lines [16]. Also, inactivation of contaminants present on the food product is commonly followed by instant packaging, thereby preventing contact with new potential contaminators from the air [17]. In this thesis, I will focus on the conidia of the

food spoiler *Aspergillus niger* and I will specifically explore the mechanisms that make these conidia resilient against commonly used preservation techniques such as UV-C inactivation, heat inactivation and inhibition by weak acid preservatives.

The life cycle of *Aspergillus niger*

Most filamentous fungi belonging the Ascomycota are heterothallic, meaning that a haploid strain has a single mating type, commonly addressed as mating type MAT1-1 or MAT1-2 [18]. It requires fusion of two haploid strains of opposite mating type to form a diploid, which in turn, after going through meiosis, is able to form ascospores to complete the sexual cycle [19,20]. However, a sexual cycle of *A. niger* has not been observed yet and this organism is thought to be a truly asexual species, thereby only reproducing through conidia. Besides asexual and sexual reproduction, a third means of 'reproduction' has been explored under laboratory conditions in this fungus: the para-sexual cycle [21]. In this life cycle, the offspring is not a perfect genetical clone, as in the asexual cycle, but is also not the result of meiosis as seen in the sexual cycle. In the parasexual cycle the diploid phase undergoes chromosomal reshuffling resulting in haploid offspring with chromosomes of either parent. An overview of the three life cycles is given in Figure 1.1.

Molecular genetics in *Aspergillus niger*

The filamentous fungus *A. niger* is most commonly known as a biotechnologically relevant producer of citric acid [24]. The production of almost all commercially available citric acid is produced by fermentation of *A. niger*, and its usefulness as a cell factory has since then been expanded to the production of other organic acids and proteins [25]. However, *A. niger* is also a common food contaminant, found for example in yoghurt, on grapes, coffee beans or the onion in your kitchen drawer [26–28]. The filamentous fungus *A. niger* has been used as a cell factory for decades, therefore our knowledge on the

organism is relatively large compared to other food spoiling moulds [25]. This includes our understanding of the genetics of *A. niger* and the genetic toolbox available for this organism, including CRISPR-Cas9 mediated genome editing [29–31], making it a prime candidate to use molecular genetic tools to study biological interesting aspects such as the resistance of food spoilage fungi towards food preservation techniques. In this thesis, we expand the genetic toolbox of *A. niger* to *Penicillium roqueforti* and *Paecilomyces variotii*, two other filamentous fungi that are common food spoilers. The research described in this thesis is part of a TIFN funded project entitled "Heterogeneity in spores of food spoilage fungi" in which the molecular mechanisms and heterogeneity of spores against food preservation strategies in *A. niger*, *P.roqueforti* and *P. variotii* are studied (https://topsectoragrifood.nl/project/heterogeneity-in-spores-of-food-spoilage-fungi/).

Compatible solutes are part of the fungal response to deal with harsh conditions

Finding the optimal preservation strategies against fungi can be challenging due to the large array of molecular stress resistance mechanisms present in these organisms. As mentioned above, conidia are relatively stress resistant cells and are able to survive common preservation techniques such as inactivation by heat. One of the major contributors to the high (preservation) stress resistance of fungal spores is considered to be the high concentrations of internal compatible solutes [32]. These molecules are defined as 'compatible' with the cytoplasm, as they accumulate to high concentrations without becoming toxic for the cell. These compatible solutes are thought to be quickly accumulated in vegetative cells upon encountering a stressful environment such as drought or heat. Different kind of molecules have been reported to act as compatible solutes, including trehalose, polyols, betaines and specific amino acids such as proline [33]. There are many synonyms to 'compatible solute' that are commonly used throughout the literature, such as osmoprotectant, osmolyte, chemical chaperone, co-solvent or kosmotropic solute. The most important characteristic of these compounds is that they protect the cell against stressors by stabilizing macromolecules (mainly proteins, but also structures

such as the plasma membrane). There are three main theories proposed on how these molecules protect macro-molecules.

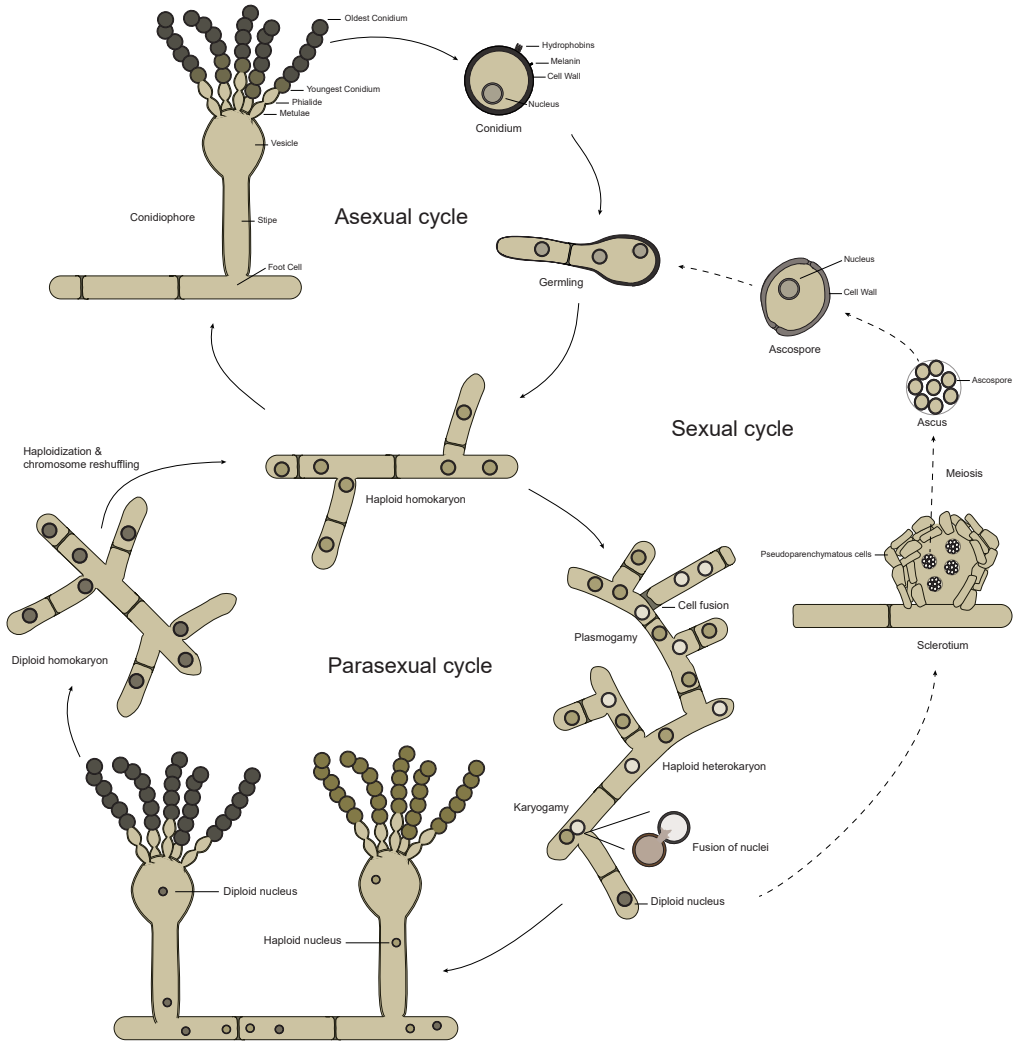

Figure 1.1. Life cycle of *Aspergillus niger*. The sexual cycle depicted here has not yet been proven to exist in *A. niger,* therefore this depiction was based on the sexual cycle found in closely related species *Aspergillus tubingensis* [22,23]. Offspring of the fungus is either a genetic copy of the parent (asexual cycle), has undergone meiosis (sexual cycle), or has undergone haploidization and chromosome reshuffling (parasexual cycle).

One theory is the so-called ‘water replacement theory’ [34,35]. This theory states that the compatible solutes effectively replace water on a molecular level, creating water

bridges and thereby stabilizing proteins and membranes [36–38]. Another theory is the vitrification theory, also known as the 'glassy state theory' [39–41]. This theory proposes that compatible solutes in high concentrations establish a so-called glassy state inside the cell. This glassy state is a chemically steady state that looks like a glass, in which the non-covalent intramolecular bonds (such as water bridges) are preserved, thereby preventing denaturation of proteins. Intramolecular bonds in this state become extremely rigid, and therefore stable, even when the cell is treated with stressors such as extreme heat or cold. This is one of the main arguments raised as to why the compatible solute glycerol is so essential in keeping bacterial and fungal stocks alive in freezers kept at -80 °C [42]. A less often discussed theory is the preferential exclusion theory [43]. This theory stems from thermodynamics and has to do with the so-called 'folding equilibrium' of proteins in liquid. Depending on the amount of compatible solute present, the folding equilibrium will shift, making it thermodynamically more favorable for the protein to stay in the folded form. This has to do with the interaction between protein, water and compatible solute, where the water molecules are favored to interact with the compatible solute, thereby 'drying' or depriving the proteins from water molecules. This 'dried' and strongly folded protein would in turn be better protected against most forms molecular damage. Some adjusted versions of each theory exist, but these three form the basis for most theories currently proposed on the mode of action of compatible solutes [44]. It is also good to note that the three theories are not thought to be mutually exclusive [45].

Stress signaling pathways, transcription factors and their target genes

How does a fungus recognize it needs to protect itself against a stressor? Several kinase dependent signal transduction pathways are known in fungi that respond to stressors, often adapted to specific stressors the cell might face from the environment. These stress signaling pathways are best-described in *Saccharomyces cerevisiae* and *Candida albicans*, but overall are preserved among fungi, and some have been described in *Aspergillus* species as well [46]. Most stressors are first recognized by a receptor, many

of which reside in the cell membrane [47]. Receptors directly activate a kinase-dependent signaling cascade machinery, belonging to either a two-component signaling (TCS) system or the mitogen-activated protein kinase (MAPK) dependent system. At the end of these, sometimes very complex, cascading pathways often resides a transcription factor (TF) which is activated. This protein activates or represses the expression of multiple genes, thereby creating a molecular response by the fungus to the observed environmental stressor. For example, upon sensing oxidative stress via the HOG pathway, the fungal cell will activate transcription factors that induce the production of catalases and superoxide dismutases [48,49], enzymes that can detoxify reactive oxygen species (ROS). In terms of conidial preservation stress resistance, transcription factor AtfA is important for the oxidative and heat stress resistance of conidia from *Aspergillus fumigatus*, *Aspergillus nidulans* and *Aspergillus oryzae* [50–53]. AtfA is known to regulate gene *tpsA*, important for trehalose accumulation in conidia. AtfA also regulates other genes encoding conidia specific proteins such as catalase *catA*, dehydrin *dprA* and "conidiation specific" gene *conJ* which are all thought to be involved in conidial stress resistance [54–56].

However, not all stress signaling pathways in fungi are fully understood, and some do not require a cell signaling cascade by kinases. The activation of the main heat shock response in *S. cerevisiae* is regulated by transcription factor "Heat shock factor 1" (Hsf1) and its homologues are conserved and active in filamentous fungi [57–59]. Upon heat shock, the Hsf1 proteins undergoes a confirmational change and forms a trimer, which is the activate form of the transcription factor, subsequently adjusting expression ~3% of all genes on the genome of *S. cerevisiae* [60], however it is not clear if additional molecules and steps are involved in this conformational change [61]. This transcription factor Hsf1 induces expression of heat shock proteins including Hsp26 and Hsp104, required for heat stress resistance [62]. Similarly, the main weak acid stress response in *S. cerevisiae* is regulated by "Weak acid resistance 1" (War1p) [63]. This transcription factor, important in the weak acid stress response, has direct interactions with the weak acid anions inside the fungal cell, leading to its activation [64,65]. Upon activation,

War1p induces the expression of Pdr12, an ABC-type efflux pump meant to extrude weak acid anions out of the cell [66].

The heterogeneity of *Aspergillus niger* conidia.

Food preservation becomes even more challenging when considering that conidia are heterogeneous in their stress resistance and germination capacity. Therefore, inactivation or inhibition of the germination of one conidium might not inactivate or inhibit another fungal conidium. The most well-described source of spore heterogeneity is caused by species and strain diversity. For example, the heat resistance of fungal conidia varies greatly depending on which species or strain is analysed [67,68]. However, a scarcely studied phenomenon is the heterogeneity in stress resistance and germination capacity of fungal spores within a single spore population, thus obtained from a single strain. Researchers have shown that conidia from a single *A. niger* strain are heterogeneous in their stress resistance towards sorbic acid [69] and heat [70]. It is remarkable that differences between individual conidia are observed when considering that these spores are clonal offspring and therefore genetically identical to each other (see Figure 1.1). Additionally, previous research has shown that cultivation temperature [71] and spore maturation [72] impact physical properties and potentially preservation stress resistance of *Aspergillus* conidia. Taken together with the fact that conidia are dispersed in large quantities, it illustrates the possibility of individual differences between conidia in terms of preservation or environmental stress resistance and germination capacity within a given spore population. These individual differences between conidia can be beneficial for survival of the fungus as a bet-hedging strategy, where individual conidia vary from one another, therein protected against specific stressors or able to germinate under specific conditions, ensuring propagation of the fungus. In this thesis, I will contribute to our understanding of the molecular mechanisms behind conidial stress resistance and heterogeneity between conidia of *A. niger*.

Scope and outline of this thesis

The conidia produced by filamentous fungi pose a constant threat to food preservation. Two major treatments to prevent food spoilage fungi from colonizing food are (1) the heat treatment of food, in order to heat inactivate the conidia, and (2) to include weak acid preservatives (especially sorbic acid) in the food, in order to inactivate the conidia or inhibit fungal growth. Fungi have evolved several mechanisms to survive heat stress and sorbic acid stress in order to survive and proliferate. In addition, earlier research has already indicated that different strains of the same species and spore populations from a single strain are highly heterogenic in their resistance to these stressors. The aim of the thesis is to study the heterogeneity in stress resistance of conidia between strains and between the spore populations of the same strain, and subsequently to identify important factors determining stress resistance.

In **Chapter 2** we investigate the strain diversity in stress resistance of *A. niger* against sorbic acid, a common chemical preservative used by food industries. The sorbic acid stress resistance of 100 *A. niger* strains isolated from various sources, including contaminated foods, was investigated. Additionally, a total of 240 transcription factor knock-out strains were screened for their weak acid stress resistance, revealing transcription factors that are involved in the weak acid stress response of *A. niger*. A novel transcription factor involved in weak acid stress resistance, named *warB*, was identified and further investigated.

In **Chapter 3** we investigate the role of strain diversity in the stress resistance of *P. variotii*, *P. roqueforti* and *A. niger* against heat. The heat stress resistance of ~20 strains of each species was investigated. The degree of variation in conidial heat resistance due to factor “strain” was quantified, and results were compared to previous reports in other organisms. The strain variability observed between conidia of the three food spoiling fungi were in the same order of magnitude as spores from bacterial species.

Genomes of 24 *Aspergillus niger* strains displaying various sensitivities towards heat and weak acids were sequenced with the aim to perform genome wide association studies (GWAS) and bulk-segregant analyses in order to find genetic elements involved in conidial heat resistance and weak acid stress resistance. However, GWAS studies were inconclusive, providing too many target genes putatively involved in both heat resistance and weak acid stress resistance. Additionally, the parasexual crossing of *A. niger* strains, which is required for bulk segregant analysis, turned out to be highly challenging due to widespread heterokaryon incompatibility (described in **Chapter 5**). However, the 24 genomes of *A. niger* revealed an equal distribution of mating types in this presumably asexual species. As a first step to further explore the possible sexual state of *A. niger*, which would be interesting for many future genetic studies, including studies on conidial stress resistance, a high-quality genome of the *A. niger* neotype strain CBS 554.65 containing the MAT1-2 mating type locus was analysed and presented in **Chapter 4**.

In **Chapter 5** the analysis and comparison of the 24 genomes of *A. niger sensu stricto* strains is described in more detail. Together with publicly available genomes, we show that the 32 *A. niger* genome sequenced strains cluster in three distinct phylogenetic groups. A successful parasexual cross between two *A. niger sensu stricto* strains with two different mating types is described, creating the first diploid *A. niger* strain containing both mating types.

In **Chapter 6** the CRISPR/Cas9 genome editing tool for *A. niger* was adopted for genetically less well characterised food spoiling fungi *P. roqueforti* and *P. variotii*. CRISPR/Cas9 was successfully implemented to create targeted mutations in a *pks* gene required for DHN-melanin synthesis. The role of melanin in mediating conidial heat stress and UV stress was studied in more detail using the generated melanin mutants in all three species.

In **Chapter 7** the impact of both the age of conidia and the internal compatible solute compositions of conidia on heat resistance and germination kinetics in *A. niger*

is described. Young conidia contained limited compatible solutes and were found heat stress sensitive. Knock-out strains deleted in trehalose and/or mannitol biosynthesis genes were made using CRISPR/Cas9 genome editing to investigate the role of compatible solutes in heat resistance and germination. The results indicate that trehalose and mannitol levels are important parameters in relation to mediating heat resistance and that the higher sensitivity to heat stress observed in relatively young conidia is due to low levels of compatible solutes.

In **Chapter 8** the impact of cultivation temperature on the resulting heat resistance of conidia was studied at transcriptome, proteome and physiology level. The analyses suggest that apart from increased trehalose levels also the induced expression of heat shock proteins could be responsible for the observation that conidia were more heat resistant when the mycelium was cultivated at 37 °C compared to 28 °C.

In **Chapter 9** the results are discussed and reflected upon. The genetic factors (species and strain) as well as the environmental factors (age, cultivation temperature) all contribute to the observed heterogeneity in preservation stress resistance of *A. niger* conidia. Internal compatible solutes, as well as protein levels from protective proteins such as heat shock proteins, potentially contribute to the individual differences observed between conidia.

The work described in this thesis may contribute in a further understanding of the genetic and environmental factors determining the heterogeneity observed in preservation stress resistance of *A. niger* conidia.

1

References

1. Blasco R, Rosell J, Arilla M, Margalida A, Villalba D, Gopher A, et al. Bone marrow storage and delayed consumption at Middle Pleistocene Qesem Cave, Israel (420 to 200 ka). Sci Adv. 2019;5:eaav9822.

2. Gram L, Ravn L, Rasch M, Bruhn JB, Christensen AB, Givskov M. Food spoilage - Interactions between food spoilage bacteria. Int J Food Microbiol. 2002;78:79–97.

3. Sperber WH. Introduction to the microbiological spoilage of foods and beverages. In: Sperber WH, Doyle MP, editors. Compend Microbiol spoilage foods beverages. New York: Springer; 2009. p. 1–40.

4. Snyder AB, Worobo RW. Fungal spoilage in food processing. J Food Prot. International Association for Food Protection; 2018;81:1035–40.

5. Snyder AB, Churey JJ, Worobo RW. Association of fungal genera from spoiled processed foods with physicochemical food properties and processing conditions. Food Microbiol. 2019;83:211–8.

6. Rico-Munoz E. Heat resistant molds in foods and beverages: recent advances on assessment and prevention. Curr Opin Food Sci. 2017;17:75–83.

7. Novodvorska M, Stratford M, Blythe MJ, Wilson R, Beniston RG, Archer DB. Metabolic activity in dormant conidia of *Aspergillus niger* and developmental changes during conidial outgrowth. Fungal Genet Biol. 2016;94:23–31.

8. Wyatt TT, Wösten HAB, Dijksterhuis J. Fungal spores for dispersion in space and time. Adv Appl Microbiol. 2013;85:43–91.

9. Dijksterhuis J. Fungal spores : Highly variable and stress-resistant vehicles for distribution and spoilage. J Food Microbiol. 2019;81:2–11.

10. Garnier L, Valence F, Mounier J. Diversity and control of spoilage fungi in dairy products: an update. Microorganisms. 2017;5:42.

11. Davies CR, Wohlgemuth F, Young T, Violet J, Dickinson M, Sanders JW, et al. Evolving challenges and strategies for fungal control in the food supply chain. Fungal Biol Rev. 2021;36:15–26.

12. Jara D, Portnoy J, Dhar M, Barnes C. Relation of indoor and outdoor airborne fungal spore levels in the Kansas City metropolitan area. Allergy asthma Proc. 2017;38:130–5.

13. Guinea J, Peláez T, Alcalá L, Bouza E. Outdoor environmental levels of Aspergillus spp. conidia over a wide geographical area. Med Mycol. 2006;44:349–56.

14. Abu-Dieyeh MH, Barham R, Abu-Elteen K, Al-Rashidi R, Shaheen I. Seasonal variation of fungal spore populations in the atmosphere of Zarqa area, Jordan. Aerobiologia (Bologna). 2010;26:263–76.

15. De Antoni Zoppas BC, Valencia-Barrera RM, Vergamini Duso SM, Fernández-González D. Fungal spores prevalent in the aerosol of the city of Caxias do Sul, Rio Grande do Sul, Brazil, over a 2-year period (2001-2002). Aerobiologia (Bologna). 2006;22:119–26.

16. Price DL, Simmons RB, Crow Jr SA, Ahearn DG. Mold colonization during use of preservative-treated and untreated air filters, including HEPA filters from hospitals and commercial locations over an 8-year period (1996–2003). J Ind Microbiol Biotechnol. 2005;32:319–21.

17. Scaramuzza N, Cigarini M, Mutti P, Berni E. Sanitization of packaging and machineries in the food industry: Effect of hydrogen peroxide on ascospores and conidia of filamentous fungi. Int J Food Microbiol. 2020;316:108421.

18. Coppin E, Debuchy R, Arnaise S, Picard M. Mating types and sexual development in filamentous ascomycetes. Microbiol Mol Biol Rev. 1997;61:411–28.

19. Ojeda-López M, Chen W, Eagle CE, Gutiérrez G, Jia WL, Swilaiman SS, et al. Evolution of asexual and sexual reproduction in the aspergilli. Stud Mycol. 2018;91:37–59.

20. Glass NL, Nelson MA. Mating-type genes in mycelial ascomycetes. In: Wessels JGH, Meinhardt F, editors. Growth, Differ Sex. Heidelberg: Springer, Berlin; 1994. p. 295–306.

21. Pontecorvo G. The parasexual cycle in fungi. Annu Rev Microbiol. 1956;10:393–400.

22. Horn BW, Olarte RA, Peterson SW, Carbone I. Sexual reproduction in *Aspergillus tubingensis* from section *Nigri*. Mycologia. 2013;105:1153–63.

23. Olarte RA, Horn BW, Singh R, Carbone I. Sexual recombination in *Aspergillus tubingensis*. Mycologia. 2015;107:307–12.

24. Currie JN. The citric acid fermentation of *Aspergillus niger*. J Biol Chem. 1917;31:15–37.

25. Cairns TC, Nai C, Meyer V. How a fungus shapes biotechnology: 100 years of *Aspergillus niger* research. Fungal Biol Biotechnol. 2018;5:1–14.

26. Noonim P, Mahakarnchanakul W, Nielsen KF, Frisvad JC, Samson RA. Fumonisin B2 production by *Aspergillus niger* in Thai coffee beans. Food Addit Contam Part A. 2009;26:94–100.

27. Gougouli M, Koutsoumanis KP. Risk assessment of fungal spoilage: A case study of *Aspergillus niger* on yogurt. Food Microbiol. 2017;65:264–73.

28. Perrone G, Susca A, Cozzi G, Ehrlich K, Varga J, Frisvad JC, et al. Biodiversity of Aspergillus species in some important agricultural products. Stud Mycol. 2007;59:53–66.

29. Nødvig CS, Nielsen JB, Kogle ME, Mortensen UH. A CRISPR-Cas9 system for genetic engineering of filamentous fungi. PLoS One. 2015;10:1–18.

30. van Leeuwe TM, Arentshorst M, Ernst T, Alazi E, Punt PJ, Ram AFJ. Efficient marker free CRISPR/Cas9 genome editing for functional analysis of gene families in filamentous fungi. Fungal Biol Biotechnol. 2019;6:1–13.

31. Zheng X, Zheng P, Zhang K, Cairns TC, Meyer V, Sun J, et al. 5S rRNA Promoter for guide RNA expression enabled highly efficient CRISPR/Cas9 genome editing in *Aspergillus niger*. ACS Synth Biol. 2018;8:1568–74.

32. Dijksterhuis J, de Vries RP. Compatible solutes and fungal development. Biochem J. 2006;399:e3-5.

33. Welsh DT. Ecological significance of compatible solute accumulation by micro-organisms: from single cells to global climate. FEMS Microbiol Rev. 2000;24:263–90.

34. Mensink MA, Frijlink HW, van der Voort Maarschalk K, Hinrichs WLJ. How sugars protect proteins in the solid state and during drying (review): Mechanisms of stabilization in relation to stress conditions. Eur J Pharm Biopharm. 2017;114:288–95.

35. Crowe JH, Clegg JS, Crowe LM. Anhydrobiosis: the water replacement hypothesis. In: Reid D, editor. Prop Water Foods ISOPOW 6. Boston: Springer; 1998. p. 440–55.

36. Carpenter JF, Crowe JH. An infrared spectroscopic study of the interactions of carbohydrates with dried proteins. Biochemistry. 2002;28:3916–22.

37. Allison SD, Chang B, Randolph TW, Carpenter JF. Hydrogen bonding between sugar and protein is responsible for inhibition of dehydration-induced protein unfolding. Arch Biochem Biophys. 1999;365:289–98.

38. Mensink MA, Van Bockstal PJ, Pieters S, De Meyer L, Frijlink HW, Van Der Voort Maarschalk K, et al. In-line near infrared spectroscopy during freeze-drying as a tool to measure efficiency of hydrogen bond formation between protein and sugar, predictive of protein storage stability. Int J Pharm. 2015;496:792–800.

39. Slade L, Levine H. Beyond water activity: recent advances based on an alternative approach to the assessment of food quality and safety. Crit Rev Food Sci Nutr. 1991;30:115–360.

40. Ubbink J. Structural and thermodynamic aspects of plasticization and antiplasticization in glassy encapsulation and biostabilization matrices. Adv Drug Deliv Rev. 2016;100:10–26.

41. Chang L, Shepherd D, Sun J, Ouellette D, Grant KL, Tang X, et al. Mechanism of protein stabilization by sugars during freeze-drying and storage: Native structure preservation, specific interaction, and/or immobilization in a glassy matrix? J Pharm Sci. 2005;94:1427–44.

42. Bhattacharya S. Cryoprotectants and their usage in cryopreservation process. In: Bozkurt Y, editor. Cryopreserv Biotechnol Biomed Biol Sci. London: IntechOpen; 2018. p. 7–20.

43. Canchi DR, Jayasimha P, Rau DC, Makhatadze GI, Garcia AE. Molecular mechanism for the preferential exclusion of TMAO from protein surfaces. J Phys Chem B. 2012;116:12095.

44. Jain NK, Roy I. Effect of trehalose on protein structure. Protein Sci. 2009;18:24–36.

45. Christensen D, Kirby D, Foged C, Agger EM, Andersen P, Perrie Y, et al. α,α′-trehalose 6,6′-dibehenate in non-phospholipid-based liposomes enables direct interaction with trehalose, offering stability during freeze-drying. Biochim Biophys Acta - Biomembr. 2008;1778:1365–73.

46. Hagiwara D, Sakamoto K, Abe K, Gomi K. Signaling pathways for stress responses and adaptation in Aspergillus species: stress biology in the post-genomic era. Biosci Biotechnol Biochem. 2016;80:1667–80.

47. Grice C, Bertuzzi M, Bignell E. Receptor-mediated signaling in *Aspergillus fumigatus*. Front Microbiol.

2013;4:26.

48. Angelova MB, Pashova SB, Spasova BK, Vassilev S V., Slokoska LS. Oxidative stress response of filamentous fungi induced by hydrogen peroxide and paraquat. Mycol Res. 2005;109:150–8.

49. Paris S, Wysong D, Debeaupuis J-P, Shibuya K, Philippe B, Diamond RD, et al. Catalases of *Aspergillus fumigatus*. Infect Immun. 2003;71:3551–62.

50. Hagiwara D, Suzuki S, Kamei K, Gonoi T, Kawamoto S. The role of AtfA and HOG MAPK pathway in stress tolerance in conidia of *Aspergillus fumigatus*. Fungal Genet Biol. 2014;73:138–49.

51. Lara-Rojas F, Sánchez O, Kawasaki L, Aguirre J. *Aspergillus nidulans* transcription factor AtfA interacts with the MAPK SakA to regulate general stress responses, development and spore functions. Mol Microbiol. 2011;80:436–54.

52. Sakamoto K, Iwashita K, Yamada O, Kobayashi K, Mizuno A, Akita O, et al. *Aspergillus oryzae* AtfA controls conidial germination and stress tolerance. Fungal Genet Biol. 2009;46:887–97.

53. Emri T, Szarvas V, Orosz E, Antal K, Park HS, Han KH, et al. Core oxidative stress response in *Aspergillus nidulans*. BMC Genomics. BMC Genomics; 2015;16:478.

54. Hoi JWS, Lamarre C, Beau R, Meneau I, Berepiki A, Barre A, et al. A novel family of dehydrin-like proteins is involved in stress response in the human fungal pathogen *Aspergillus fumigatus*. Mol Biol Cell. 2011;22:1896.

55. Suzuki S, Sarikaya Bayram Ö, Bayram Ö, Braus GH. *conF* and *conJ* contribute to conidia germination and stress response in the filamentous fungus *Aspergillus nidulans*. Fungal Genet Biol. Academic Press; 2013;56:42–53.

56. Navarro RE, Stringer MA, Hansberg W, Timberlake WE, Aguirre J. *catA*, a new *Aspergillus nidulans* gene encoding a developmentally regulated catalase. Curr Genet. 1996;29:352–9.

57. Sorger PK, Pelham HRB. Yeast heat shock factor is an essential DNA-binding protein that exhibits temperature-dependent phosphorylation. Cell. 1988;54:855–64.

58. Nicholls S, Leach MD, Priest CL, Brown AJP. Role of the heat shock transcription factor, Hsf1, in a major fungal pathogen that is obligately associated with warm-blooded animals. Mol Microbiol. 2009;74:844.

59. Fabri JHTM, Rocha MC, Fernandes CM, Persinoti GF, Ries LNA, Cunha AF da, et al. The heat shock transcription factor HsfA is essential for thermotolerance and regulates cell wall integrity in *Aspergillus fumigatus*. Front Microbiol. 2021;12:656548.

60. Hahn J-S, Hu Z, Thiele DJ, Iyer VR. Genome-wide analysis of the biology of stress responses through heat shock transcription factor. Mol Cell Biol. 2004;24:5249–56.

61. Calderwood SK, Xie Y, Wang X, Khaleque MA, Chou SD, Murshid A, et al. Signal transduction pathways leading to heat shock transcription. Sign Transduct Insights. 2010;2:13–24.

62. Chowdhary S, Kainth AS, Pincus D, Gross DS. Heat Shock Factor 1 drives intergenic association of its

target gene loci upon heat shock. Cell Rep. 2019;26:18.

63. Kren A, Mamnun YM, Bauer BE, Schüller C, Wolfger H, Hatzixanthis K, et al. War1p, a novel transcription factor controlling weak acid stress response in yeast. Mol Cell Biol. 2003;23:1775–85.

64. Kim MS, Cho KH, Park KH, Jang J, Hahn J-S. Activation of Haa1 and War1 transcription factors by differential binding of weak acid anions in *Saccharomyces cerevisiae*. Nucleic Acids Res. 2019;47:1211–24.

65. Gregori C, Schüller C, Frohner IE, Ammerer G, Kuchler K. Weak organic acids trigger conformational changes of the yeast transcription factor War1 in vivo to elicit stress adaptation. J Biol Chem. 2008;283:25752–64.

66. Piper P, Mahé Y, Thompson S, Pandjaitan R, Holyoak C, Egner R, et al. The Pdr12 ABC transporter is required for the development of weak organic acid resistance in yeast. EMBO J. 1998;17:4257–65.

67. van den Brule T, Punt M, Teertstra W, Houbraken J, Wösten H, Dijksterhuis J. The most heat-resistant conidia observed to date are formed by distinct strains of *Paecilomyces variotii*. Environ Microbiol. 2019;22:986–99.

68. Dijksterhuis J. The fungal spore and food spoilage. Curr Opin Food Sci. 2017;17:68–74.

69. Geoghegan IA, Stratford M, Bromley M, Archer DB, Avery S V. Weak acid resistance A (WarA), a novel transcription factor required for regulation of weak-acid resistance and spore-spore heterogeneity in *Aspergillus niger*. mSphere. 2020;5:e00685-19.

70. Fujikawa H, Itoh T. Tailing of thermal inactivation curve of *Aspergillus niger* spores. Appl Environ Microbiol. 1996;62:3745–9.

71. Hagiwara D, Sakai K, Suzuki S, Umemura M, Nogawa T, Kato N, et al. Temperature during conidiation affects stress tolerance, pigmentation, and trypacidin accumulation in the conidia of the airborne pathogen *Aspergillus fumigatus*. PLoS One. 2017;12:e0177050.

72. Teertstra WR, Tegelaar M, Dijksterhuis J, Golovina EA, Ohm RA, Wösten HAB. Maturation of conidia on conidiophores of *Aspergillus niger*. Fungal Genet Biol. 2017;98:61–70.

CHAPTER 2

Natural variation and the role of Zn_2Cys_6 transcription factors SdrA, WarA and WarB in sorbic acid resistance of *Aspergillus niger*

Sjoerd J. Seekles, Jisca van Dam, Mark Arentshorst and Arthur F.J. Ram

Manuscript in preparation

Abstract

Weak acids, such as sorbic acid, are used as chemical food preservatives by industry. Fungi overcome this weak acid stress by inducing cellular responses mediated by transcription factors. In our research, a large-scale sorbic acid resistance screening was performed on 100 *A. niger* wild-type *sensu stricto* strains isolated from various sources to study strain variability in sorbic acid resistance. The minimal inhibitory concentration of undissociated (MIC_u) sorbic acid at pH = 4 in MEB of the *A. niger* strains varies between 4.0 mM and 7.0 mM, with the average out of 100 strains being 4.8 ± 0.8 mM, when scored after 28 days. MIC_u values were roughly 1 mM lower when tested in commercial ice tea instead of MEB. Genome sequencing of the most sorbic acid sensitive strain among the isolates, CBS 147320, was found to have a premature stop codon inside the sorbic acid response regulator encoding gene *sdrA*. Repairing this missense mutation to using CRISPR-Cas9 mediated genome editing increased the sorbic acid resistance, showing that the sorbic acid sensitive phenotype of this strain is caused by the loss of SdrA function. To identify additional transcription factors involved in weak acid resistance, a transcription factor knock-out library consisting of 240 *A. niger* deletion strains each lacking a single transcription factor was screened. The screen identified a novel transcription factor WarB, contributing to the resistance against a broad range of weak acids, including sorbic acid. The SdrA and WarA Zn_2Cys_6 transcription factors were previously shown to mediate sorbic acid resistance. The role of SdrA, WarA and WarB in weak acid resistance, including sorbic acid, was investigated by creating single, double and the triple knock-out strains. All three transcription factors were found to have an additive effect to the sorbic acid stress response, and the *ΔwarB* strain was found significantly more sensitive to benzoic acid compared to the *ΔsdrA* and *ΔwarA* strains.

Introduction

A significant portion of microbial food spoilage is caused by filamentous fungi, commonly referred to as moulds [1]. Several fungal species have the capacity to infect foods and beverages, and are able to proliferate in conditions with limited water availability, a lack of nitrogen or after heat treatment [2]. Fungal spoilage can affect the visual appearance, taste and other properties of food products [3]. Additionally, the production of mycotoxins by food spoiling fungi forms a direct risk for human health [4].

There are several ways in which the food industry preserves food and reduces microbial spoilage. Firstly, by the use of packaging thereby preventing microbes with access to food. Secondly, by inactivation of microorganisms in food by ionizing radiation and heat treatments such as pasteurization and sterilization [5]. Another tactic involves growth inhibition of microorganisms present on the foods; this includes storage at lowered temperatures, reducing the water activity of foods by drying products or reducing oxygen availability by vacuum packaging. One other growth inhibition technique relies on the addition of chemical substances which reduce microbial growth, such as the addition of weak acid preservatives. [2,5]

Weak acids are food preservatives that cause growth inhibition on a broad spectrum of microorganisms. Weak acids are both fungistatic and bacteriostatic [6]. Commonly used weak acids in the food industry include sorbic acid, benzoic acid [7,8], propionic acid [9], lactic acid, acetic acid [10] and citric acid [11]. Sorbic acid can be added in its acid form, recognized by the European food additive number E200, but is more commonly added as the salt components sodium sorbate (E201), potassium sorbate (E202) or calcium sorbate (E203). Sorbic acid is added to food products such as condiments, bread, fruit jams, juices and soft drinks [12]. The concentration of weak acids allowed in foods and beverages is tightly controlled by governmental organizations such as the Food and Drug Administration (FDA) and the European Food and Safety Authority (EFSA). The maximum concentration of sorbates strongly depends on the food product, for example, the EFSA states that a maximum of 300 mg/L (2.67 mM) sorbate is

allowed in flavored drinks (excluding dairy products), whereas a maximum of 500 mg/L (4.46 mM) sorbate is allowed in fruit and vegetable juices, and 2000 mg/L (17.84 mM) is allowed in processed cheeses [13]. The mode of action of these weak acids as preservatives is most commonly described in the “classical weak acid theory” [14].

The classic weak acid theory explains that weak acids, when present in low pH, can cause the acidification of cells. In a liquid solution, a weak acid can be present in its undissociated form, in which the weak acid is present in its full molecule formation, or in its dissociated form in which the molecule has dissociated into the charged anion (WA^-) and proton (H^+). In solutions where the pH is equal to the pKa of the weak acid, the amount of undissociated acid (WAH) is equal to the amount dissociated acid (WA^- and H^+). When the pH decreases, the proportion of undissociated acid (WAH) increases. Only weak acids in their undissociated form (WAH) are able to diffuse through the plasma membrane into the cytoplasm [15,16]. Therefore, when the pH < pKa, the weak acid molecules diffuse through the plasma membrane, and because of the near neutral pH of the cytoplasm, the undissociated acids (WAH) are forced to dissociate into charged ions (WA^- and H^+) [17,18]. The charged ions (WA^- and H^+) are not able to diffuse back through the plasma membrane and accumulate in the cytoplasm, resulting in acidification of the cytoplasm [19]. In this classic theory, weak acids are thought to be most effective in solutions with a low pH.

However, recent studies show that not all weak acids inhibit growth equally, and some weak acids do not even cause a lowered internal pH [20]. Therefore, alternative mode of actions have been proposed in literature, describing the function of specific weak acids in food preservation. For example, a study in *Saccharomyces cerevisiae* suggested that sorbic acid accumulates in mitochondrial membranes [20]. This study proposed that sorbic acid inhibits the O_2 uptake by inducing ROS and thereby negatively influencing the respiration of yeast. Similarly, in *Aspergillus niger* sorbic acid acts as a membrane active compound which inhibits glucose and O_2 uptake, thereby inhibiting conidial germination [21]. These examples show that weak acid preservatives can have inhibiting effects on cells besides acidification of the cytoplasm as described in the clas-

sical weak acid theory.

Several food spoiling fungi have been reported with resistance to these weak acid preservatives, the most well-known species being spoilage yeasts. The spoilage yeast *Zygosaccharomyces bailii* has been reported to survive up to 9.45 mM of sorbic acid and 11 mM of benzoic acid [3]. However, besides yeast species, mostly Ascomycetes are found as food contaminants [1]. Commonly found food spoiling Ascomycetes include for example *A. niger*, *Paecilomyces variotii* and *Penicillium roqueforti* [2]. Therefore, preservative resistance of Ascomycetes have been investigated before, especially in relation to specific food products such as bread [22–25]. Investigation on the stress responses and molecular mechanisms behind weak acid resistance in filamentous fungi has been limited, however the role of two transcription factors has been revealed in *A. niger*.

Transcription factors play an important role in acquiring weak acid resistance by food spoiling fungi. *A. niger* has the ability to decarboxylate the weak acids sorbic acid and cinnamic acid, mediated by the enzymes phenyl transferase PadA, and cinnamic acid decarboxylase CdcA [26,27]. These enzymes provide resistance towards sorbic acid and cinnamic acid, and is most effective during conidial germination and outgrowth [6]. CdcA and PadA are regulated by the Zn_2Cys_6-finger transcription factor sorbic acid decarboxylase regulator SdrA [27]. These genes are also present in other *Aspergilli* which are able to grow on sorbic acid and cinnamic acid [27]. The deletion of *cdcA*, *padA*, or *sdrA* results in increased sensitivity towards sorbic acid and cinnamic acid, but did not completely eliminate it [27]. This suggests the presence of a separate yet uncharacterized set of genes that also add to the sorbic acid resistance in *A. niger*.

The transcription factor ‘weak acid resistance A’ (WarA) has been recently described in *A. niger*, and is required for resistance against a range of weak acid preservatives [28]. The knock-out strain (*ΔwarA*) showed sensitivity to propionic, butanoic, pentanoic, hexanoic, sorbic and benzoic acids. WarA is described as having a CdcA-independent role in the sorbic acid resistance of *A. niger*, since the double knock-out strain

lacking WarA and CdcA shows increased sensitivity to sorbic acid when compared to either of the single knock-out strains. Geoghegan and colleagues propose that WarA is possibly required for weak acid resistance by regulating the expression of PdrA, an ATP binding cassette (ABC) type transporter, which the authors show is a homologue to Pdr12p, an ABC-type transporter known to pump out weak-acid anions in *S. cerevisiae* [29]. In *S. cerevisiae* Pdr12p is regulated by War1p, a Zn_2Cys_6-finger transcription factor, which binds to weak acid response element, WARE, in the Pdr12p promotor [30]. It should be noted that the *S. cerevisiae* War1p and *A. niger* WarA protein are both Zn_2Cys_6 transcription factors, but they do not shown significant sequence similarity apart from the DNA binding domain [28].

In our research, a large-scale sorbic acid resistance screening was performed on 100 *A. niger* wild-type strains to study strain variability in sorbic acid resistance. Additionally, the screening of 240 transcription factor knock-out strains revealed the importance of multiple transcription factors in the weak acid stress response, including WarB. We show that WarB is important for sorbic, benzoic, cinnamic, propionic and acetic acid stress resistance, and that the *warB* deletion has an additive effect on the sorbic acid resistance when combined with the *sdrA* and *warA* deletions.

Results

Natural variation of sorbic acid resistance among 100 *A. niger* sensu stricto strains

All 100 wild-type *A. niger sensu stricto* strains were obtained from the CBS collection, Westerdijk Fungal Biodiversity Institute, Utrecht, the Netherlands. These strains originate from all over the word and were isolated from diverse sources (Table 2.S1). In order to investigate food spoiling capacity of these strains, a 96-wells plate assay was performed testing sorbic acid resistance of *A. niger* strains in two types of liquid media; malt extract broth (MEB) (Figure 2.1) and commercial ice tea (Lipton Peach Ice Tea) (Figure 2.2). The 100 *A. niger* strains were subjected to 0 – 9 mM of undissociated sorbic acid and scored for growth after seven and 28 days.

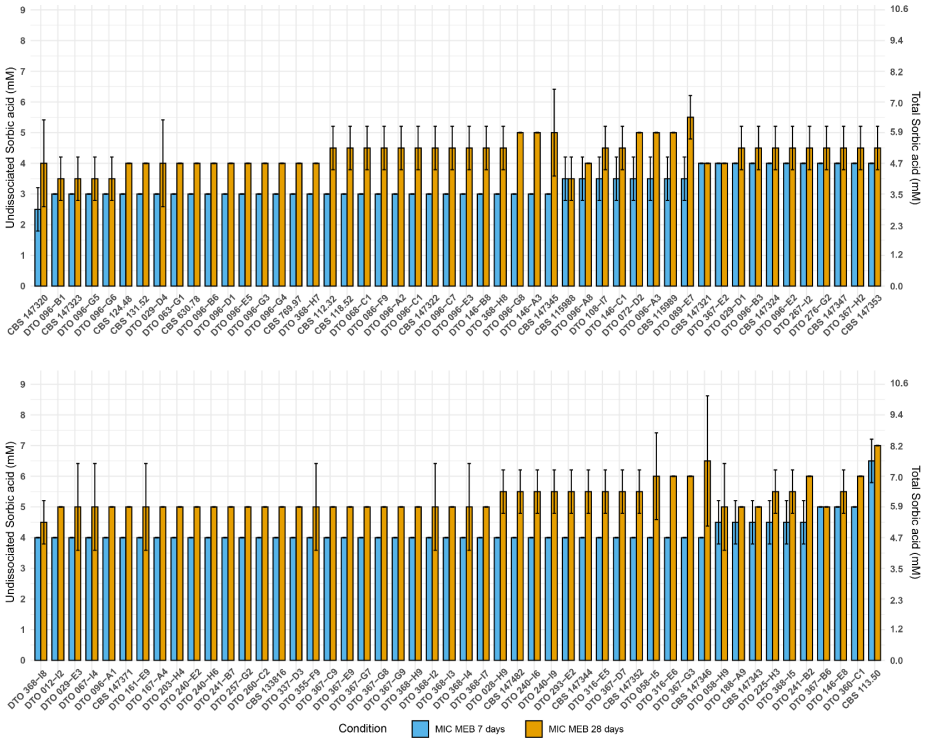

Figure 2.1. MIC assay showing strain diversity of 100 *A. niger* strains grown in MEB. Mean MIC values for each strain was determined after 7 days (blue), and 28 days (orange) of growth at 25 °C, from biological duplicates. The error bar indicates the standard deviation between the duplicates. The primary Y-axis indicates the undissociated sorbic acid concentration, whereas the secondary Y-axis indicates the total sorbic acid concentration.

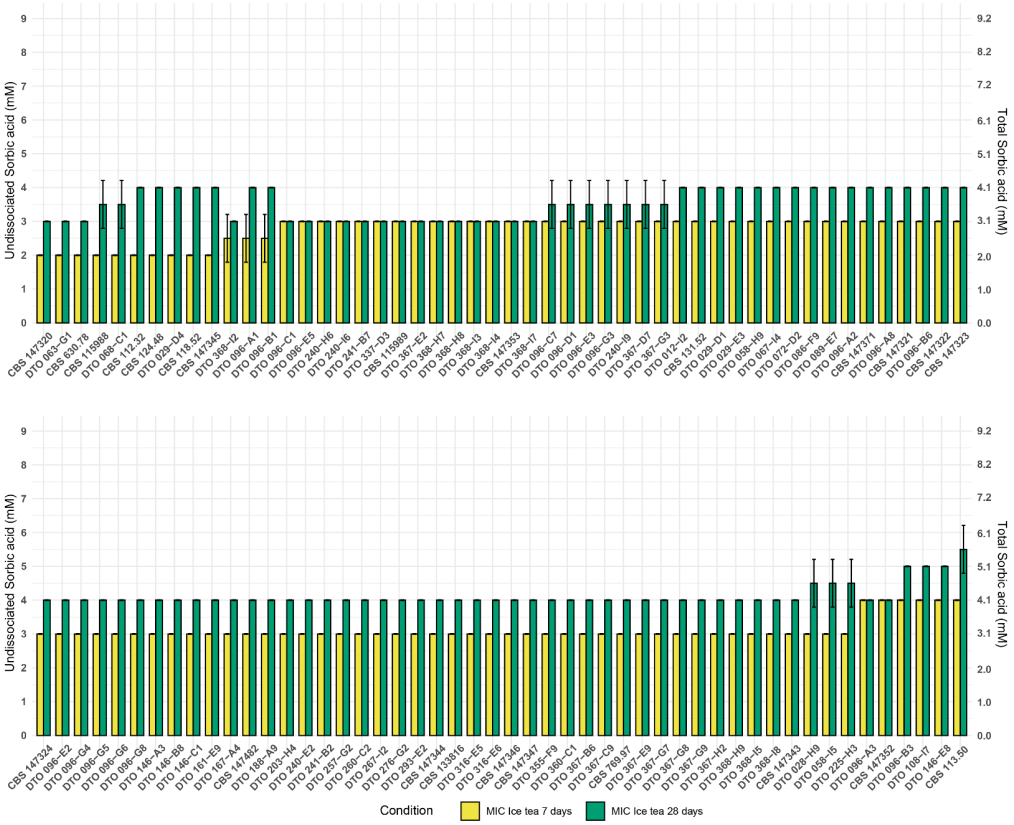

Figure 2.2. MIC assay showing strain diversity of 100 *A. niger* strains grown in ice tea. Mean MIC values for each strain was determined after 7 days (yellow), and 28 days (green) of growth at 25 °C, from biological duplicates. The error bar indicates the standard deviation between the duplicates. The primary Y-axis indicates the undissociated sorbic acid concentration, whereas the secondary Y-axis indicates the total sorbic acid concentration.

The average MIC_u of the 100 *A. niger* strains was determined in both MEB and a commercial ice tea, and shown together with the MIC_u of the most resistant and sensitive strain in Table 2.1. The fungal static effect of sorbic acid became apparent by determining the MIC after prolonged incubation (28 days) compared to 7 days. After 28 days the MIC increased 1.1 mM and 0.9 mM in MEB and Ice tea respectively. The average MIC_u of sorbic acid when tested in commercial ice tea was roughly 1 mM lower than the values obtained in MEB (Table 2.1).

Table 2.1. The average and most extreme sorbic MIC_u values (average ± SD) out of 100 *A. niger* strains grown in MEB and commercial ice tea.

Sample	MIC_u in MEB (mM)		MIC_u in ice tea (mM)	
	7 days	28 days	7 days	28 days
Average of 100 strains	3.7 ± 0.6	4.8 ± 0.8	2.9 ± 0.4	3.8 ± 0.5
CBS 147320 (sorbic acid sensitive strain)	2.5 ± 0.7	4.0 ± 1.4	2.0 ± 0.0	3.0 ± 0.0
CBS 113.50 (sorbic acid resistant strain)	6.5 ± 0.7	7.0 ± 0.0	4.0 ± 0.0	5.5 ± 0.7

Genome sequencing and SNP analysis of the most sorbic acid sensitive strain CBS147320

The genome of CBS 147320 was previously sequenced (Chapter 3). When analysing the genome of this strain, we discovered a SNP inside the *sdrA* gene (G1296A, located in the Fungal specific transcription factor domain PF04082), resulting in a premature stop codon. Therefore, the SdrA protein (originally 657 amino acids long) is truncated in the sorbic acid sensitive wild-type strain CBS 147320 and only 384 amino acids long. In order to test whether the missense mutation in *sdrA* is responsible for the high sensitivity towards sorbic acid, a complementation study was designed to restore the mutation resulting in a stop codon (TGA) back to the codon (TGG) found in the wild type *sdrA* gene found in other isolates and the N402 strain (for complementation methodology see Figure 2.S1). In short, fungal transformations were performed in which a double strand break (DSB) was introduced in the *sdrA* locus in CBS 147320 using CRISPR/Cas9. Donor DNA containing a truncated copy of *sdrA* amplified from lab strain N402 (containing the wild-type gene of *sdrA*) was provided during the transformation. Transformants with a putatively restored *sdrA* locus were created in this way, and subsequently screened for sorbic acid resistance. Thirteen transformants were obtained and analysed for their sorbic acid resistance by performing a spot-assay on MM plates containing 1, 2, 3 and 4 mM sorbic acid at pH = 4 (Figure 2.3). Parental strain CBS 147320, a *sdrA* deletion strain and sorbic acid resistant strain CBS 113.50 were taken along as controls. Trans-

formants could be grouped in three different groups based on the phenotypes seen in the sorbic acid spot-assay. Seven transformants (group 1) have similar sorbic acid sensitivity as parental strain CBS 147320, indicating that the SNP in the *sdrA* gene has not been restored in these transformants. The double-stranded break in these transformants had been most likely repaired by non-homologous end-joining and not by homologous recombination of the donor DNA. Four transformants (group 2) show increased sorbic acid resistance compared to parental strain CBS 147320, having visible growth after 4 days on MM plates containing 3 mM sorbic acid. For now, we assume that in these transformants the mutated *srdA* gene is repaired by homologous recombination of the donor DNA. Two transformants (group 3) have a higher sorbic acid resistance, comparable to the sorbic acid resistant strain CBS 113.50. We assume that in these transformants, the missense mutation in sdrA is repaired by the donor DNA and that additional copies of the donor DNA have been integrated. These results indicate that the weak acid sensitivity of wild-type strain CBS 147320 could be restored by introducing the wild-type *sdrA* gene back into the genome. An additional diagnostic PCR or Southern blot analysis is needed to further confirm the genomic alterations in all groups of transformants.

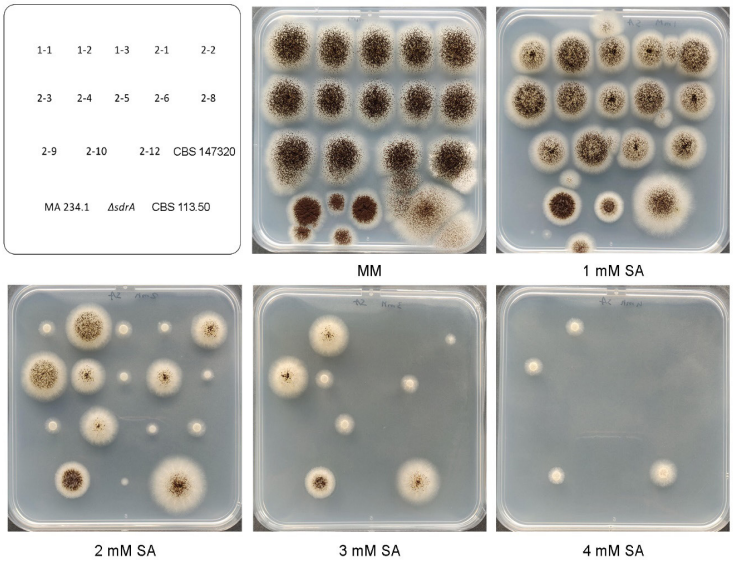

Figure 2.3. Phenotypic screen of CBS 147320 transformants with a putatively restored *sdrA* locus on sorbic acid. The transformants, JvD1-1 until JvD2-12, with a potentially restored *sdrA* locus were tested on sorbic acid resistance. The spot assay was done on MM + glucose with the

addition of sorbic acid (SA), concentrations given of undissociated sorbic acid. Conidia were spotted and plates were subsequently grown for 4 days at 30 °C. Several controls were taken along; sorbic acid sensitive wild-type strain CBS 147320, parental strain MA 234.1, knock-out strain (*ΔsdrA*) and sorbic acid resistant strain CBS 113.50. Transformants showed three phenotypes, (1) like parental strain CBS 147320, (2) semi-resistant showing growth in the presence of 3 mM SA or (3) very resistant to SA, comparable to the most resistant wild-type strain CBS 113.50.

Screening for transcription factors that are related to weak acid stress resistance

In order to identify additional transcription factors involved in weak acid stress resistance of *A. niger*, a library of 240 *A. niger* transcription factor knock-out strains was screened for sorbic acid, cinnamic acid, benzoic acid and propionic acid resistance (knock-out library made by Arentshorst, van Peij, Pel and Ram, unpublished data). A selection of transcription factor knock-out strains with interesting phenotypes were re-evaluated using smaller concentration steps (Figure 2.4).

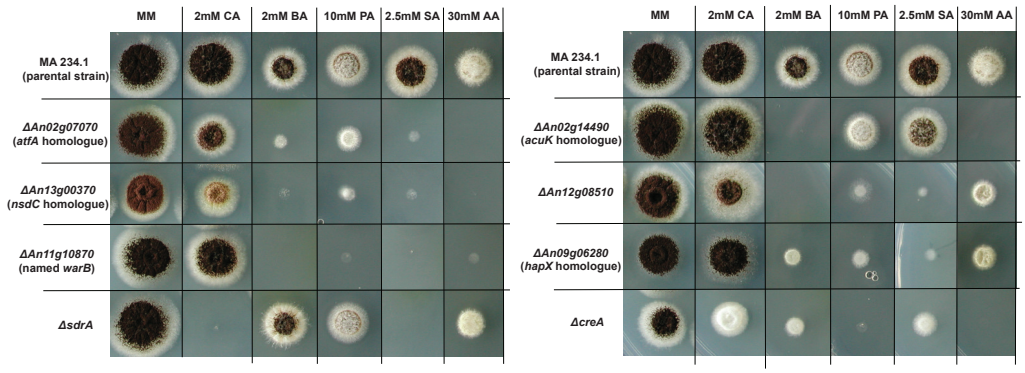

Figure 2.4. Transcription factor knock-out strains sensitive to weak acid stress. The spot assay was conducted on MM containing glucose (pH = 4). The weak acids tested were 2 mM cinnamic acid (CA), 2 mM benzoic acid (BA), 10 mM propionic acid (PA), 2.5 mM sorbic acid (SA) and 30 mM acetic acid (AA). Weak acid concentrations listed are total weak acid concentrations added, the undissociated acid concentrations (pH = 4) are 1.5 mM CA, 1.2 mM BA, 8.8 mM PA, 2.1 mM SA and 25.6 mM AA. Growth was scored and pictures were taken after 5 days of incubation at 30°C. The top row contains parental strain MA 234.1 (ΔkusA), two times the same spots, as a control for growth comparison.

The screening of 240 transcription factor knock-out strains revealed multiple candidate transcription factors involved in weak acid stress resistance in *A. niger*, including the *atfA* homologue putatively involved in the general stress response [31] the

nsdC homologue, the *hapX* homologue, the *acuK* homologue and *creA* which is the main regulator of carbon catabolite repression [32]. Additionally, knock-out strains lacking transcription factors An12g08510 and An11g10870, with no clear homologues, showed reduced growth on plates containing weak acids. The knock-out strain lacking gene An11g10870 was specifically interesting, showing a severe growth reduction on four out of the five weak acids tested: benzoic acid, propionic acid, benzoic acid and acetic acid. This gene was studied further and named WarB for 'weak acid resistance B'. WarB is a Zn_2Cys_6 transcription factor consisting of only 307 amino acids and is significantly shorter than other sorbic acid response regulators SdrA (628 amino acids) and WarA (777 amino acids). No clear homology exists between WarB and previously described transcription factors WarA, SdrA or the sorbic acid response regulator in yeast; War1p [28,30]. In order to further investigate the effects of the *warB* deletion, single and combination knock-out strains lacking *sdrA*, *warA* and *warB* were made using CRISPR/Cas9 genome editing. The proper deletion of the strain was verified by diagnostic PCR (Figure 2.S2) and these strains were tested for their resistance against weak acid preservatives, using a spot assay (Figure 2.5).

The single knock-out strain *ΔwarB* was more sensitive towards sorbic acid, benzoic acid and cinnamic acid compared to its parental strain. The *ΔwarB* single knock-out strain was more sensitive towards benzoic acid when compared to the *ΔsdrA* or *ΔwarA* single knock-out strains. The double knock-out strain *ΔsdrA, ΔwarB* showed severely reduced growth in the presence of cinnamic acid when compared to either *ΔsdrA* or *ΔwarB* single knock-out strains. All three transcription factors, *sdrA* and *warA* and *warB*, were involved in sorbic acid resistance, as shown by the higher sensitivity of the triple knock-out strain than any double knock-out strain, indicating that these three transcription factors work side-by-side to generate the regular sorbic acid stress response. Additionally, sorbic acid sensitivity of the knock-out strains was investigated in a liquid assay (MEB) in 96-wells plates, similar to the experiment performed on wild types in Figure 2.1, confirming the same impact of *sdrA*, *warA* and *warB* on sorbic acid resistance in liquid (Figure 2.S3).

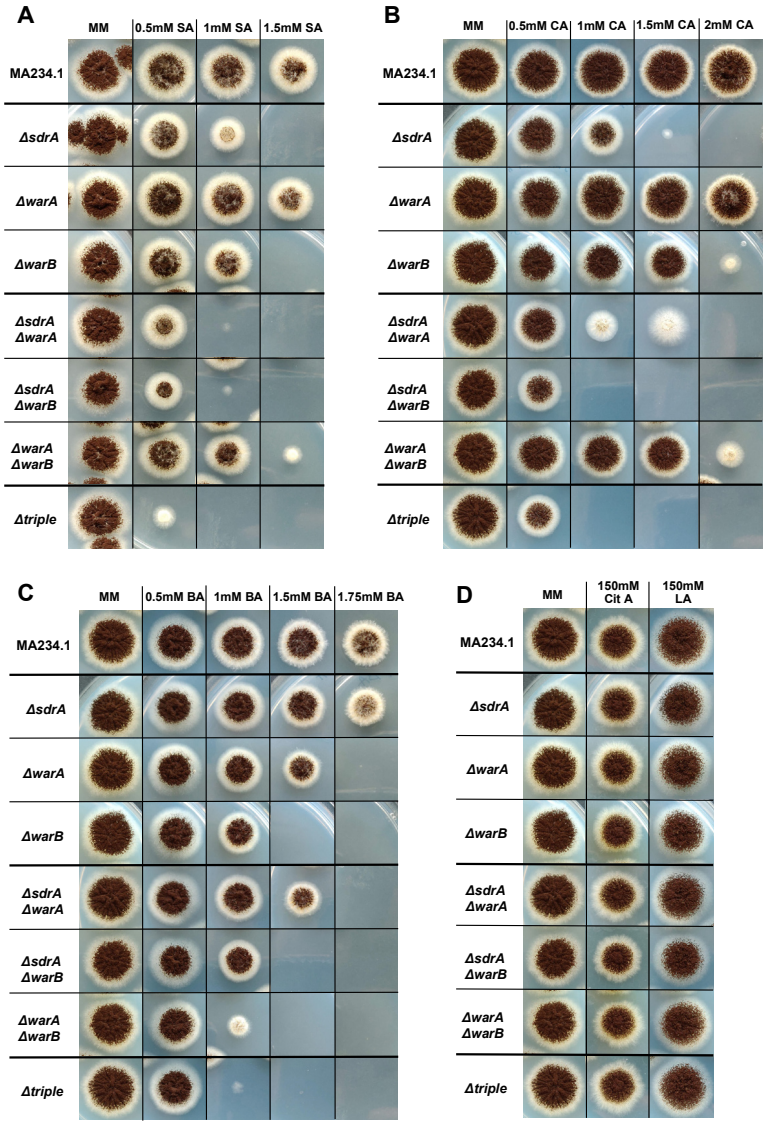

Figure 2.5. Weak acid stress resistance of knock-out strains lacking *sdrA*, *warA* and/or *warB*. Conidia are spotted on MM containing glucose and weak acid, pH 4, grown for 4 days at 30 °C. Growth was compared to the growth phenotype of the parental strain MA234.1 (*ΔkusA*). All concentrations of weak acids added listed are total weak acid concentrations. A. Sorbic acid (SA) stress resistance. The triple knock-out strain is the most sensitive for sorbic acid stress. A double knock-out strain *ΔwarA*, *ΔwarB* is less sensitive than the single knock-out strain *ΔwarB*. B. Cinnamic acid (CA) stress resistance. The Δ*sdrA, ΔwarB* strain is the most sensitive to cinnamic acid, the *warA* deletion does not seem to affect cinnamic acid stress resistance. C. Benzoic acid (BA) stress resistance. The *warB* deletion has the largest effect on the benzoic acid resistance. D. Citric acid (Cit A) and lactic acid (LA) stress resistance seemed not affected.

Discussion

Heterogeneity among different (natural) isolates of the same species in relation to weak acid stress resistance of fungi has been reported before. For example in the case of spoilage yeast *Z. bailii* [3], variation in MIC values among strains were reported to vary between 4.5 mM and 9.5 mM (mean 7.1 mM). In our study, the sorbic acid MIC_u of *A. niger* was determined for 100 strains, and showed and average of 4.8 ± 0.8 mM in MEB and 3.8 ± 0.5 mM in commercial ice tea when scored after 28 days (Table 2.1). These findings for *A. niger* are consistent with earlier reports. A recent study tested three *A. niger* strains and one *Aspergillus tubingensis* strain and reported sorbic acid MIC_u values of these strains between 2.88 mM – 4.80 mM [22]. Therefore, most *A. niger* strains will survive the maximum allowed sorbates in flavored drinks (2.67 mM), some will survive the limits allowed in fruit juices (4.46 mM) and no strains will survive limits allowed in processed cheeses (17.84 mM) [13]. However, it is important to note the outliers, specifically the most sorbic acid resistant *A. niger* strain out of the 100 reported in our study (Table 2.1), CBS 113.50, with a sorbic acid MIC_u of 7 mM. This means that, depending on the strains found in any specific food processing facility, one might need 7 mM of undissociated sorbic acid to reliably prevent growth of *A. niger*. Additionally, MIC_u values are depending on the medium used, as strains consistently showed lower MIC_u values in commercial ice tea when compared to relatively rich medium MEB. We noticed that sporulation was limited in the ice tea medium, and the 96-wells plates showing growth were not as densely packed with mycelium when compared to the same assay performed in MEB. Perhaps ice tea is a relatively poor growth medium for *A. niger*, thereby lowering the minimal concentration of sorbic acid needed to prevent outgrowth. No clear relationship between isolated source and sorbic acid resistance was found. *A. niger* strains isolated as food contaminants were not the most sorbic acid resistant strains in our study. Only two strains, CBS 113.50 and DTO 146-E8, belong consistently to the top 5 most sorbic acid resistant strains in both MEB and commercial ice tea, and these strains were isolated from leather and indoor environment, respectively (Table 2.S1). The most sorbic acid sensitive strain in both MEB and commercial ice tea, CBS 147320,

was isolated from grape.

The most sorbic acid sensitive strain, CBS 147320, had a SNP inside the *sdrA* gene resulting in a premature stop codon. The sorbic acid resistance could be increased again by replacing the SNP with the 'normal' base present in all other *A. niger* strains (Figure 2.3). Therefore, the most sorbic acid sensitive wild-type strain found, originally isolated from a grape in Australia, was in fact a strain lacking SdrA activity. This indicates that the transcription factors involved in the sorbic acid response are important, not solely for our understanding of the molecular mechanisms behind fungal sorbic acid resistance, but are also an important factor within the observed strain variability of *A. niger*.

A spot-assay testing weak acid resistance of 240 *A. niger* knock-out strains, each lacking a single transcription factor, revealed transcription factors that are potentially involved in the weak acid stress response. One transcription factor is a homologue of general stress response regulator AtfA [31]. Three transcription factors which upon deletion reduced the resistance towards sorbic acid are homologues of genes regulating siderophores and iron uptake, HapX, NsdC and AcuK [33–35]. AcuK is known to be essential for growth on gluconeogenic carbon sources and its reduced resistance could possibly be caused by a metabolic imbalance an reduced catabolism of sorbic acid. However, AcuK is also required for iron uptake in *Aspergillus fumigatus* and regulates a set of genes involved in iron homeostasis, including gene *hapX* [33]. Recently, researchers have shown that NsdC regulates many genes in *A. fumigatus* and impacts stress resistance against cell wall damaging agents, however NsdC also regulates expression of siderophores and genes involved in iron-uptake, again including *hapX* [35]. Transcription factor HapX is best known for its role in iron homeostasis, however researchers have shown that the HapX protein also has a putative role in mitochondrial metabolism in *A. fumigatus*, more than 30% of the target genes of HapX have a function in the mitochondria [36]. As discussed in the introduction, a recent publication has disputed the classical weak acid theory of cytosolic acidification, and instead proposes that weak acids disrupt mitochondrial respiration by localizing in the mitochondrial membrane [20]. It is interesting to note that the effectivity of weak acids in the mitochondrial membrane

could perhaps explain why *acuK*, *nsdC* and *hapX* knock-out strains were linked to weak acid stress sensitivity. The *ΔcreA* strain also seems impacted by weak acids. Since the *ΔcreA* strain is impacted in the carbon catabolite repression, the strain does not limit itself to glucose uptake and metabolism. Perhaps the active uptake of the weak acids as a potential carbon source in the *ΔcreA* strain is causing its weak acid sensitive phenotype.

Another interesting gene was putative transcription factor An11g10870, dubbed WarB. We analysed available expression data of *A. niger* growing in the presence of sorbic acid to investigate the expression of the *warB* gene [28]. The *warB* gene shows induction (logFC = 5.5) in the presence of sorbic acid compared to the control, indicating the possible involvement of WarB in the sorbic acid stress response. The deletion of *warB* resulted in increased sensitivity towards benzoic, sorbic, cinnamic, propionic and acetic acid (Figure 2.3 and Figure 2.4). Double and triple knock-out strains were made in *A. niger* lacking *sdrA*, *warA* and/or *warB* to investigate the relative importance of each transcription factor in the weak acid stress response. All three transcription factors seem to contribute to the sorbic acid resistance of *A. niger*, as indicated by the high sorbic acid sensitivity of the triple knock-out strain. Interestingly, the *ΔwarA*, *ΔwarB* double knock-out strain seems to be slightly more resistant to both sorbic acid and cinnamic acid than the *ΔwarB* single knock-out strain. Perhaps this finding indicates a compensatory effect, where *sdrA* is upregulated in the absence of *warA* and *warB*, but further research is needed to confirm this hypothesis. Future research could focus on the target genes regulated by WarB, thereby expanding our knowledge on the weak acid stress response of *A. niger*.

Material and Methods

Strains and growth conditions

All strains used in this study are listed in Table 2.S1. The 100 *A. niger* wild-type strains were obtained from the CBS strain collection of the Westerdijk Institute of Fungal Biodiversity, Utrecht, the Netherlands. The *A. niger* strains were cultivated on malt extract agar (MEA, CM0059, Oxoid) plates for 7 days at 30 °C to harvest conidia for weak acid stress resistance assays. Conidia were harvested by adding saline solution, consisting of 0.9% NaCl + 0.02% Tween 80 in demi water, to the plates and gently scraping the spores with a sterile cotton swab, after which the spore solution is filtered through a sterile filter (Amplitude EcoCloth, Contec).

Sorbic acid sensitivity screening by liquid assay

The sorbic acid (SA) minimal inhibitory concentration (MIC) of 100 *A. niger* strains was determined using a liquid assay using 96-wells plates based on previous research (van den Brule *et al.* unpublished results). In short, 96-wells plates contained malt extract broth (MEB, CM0057, Oxoid) and a concentration range of undissociated sorbic acid (0 – 9 mM in steps of 1 mM). MEB was adjusted to pH 4 by the addition of NaOH/HCl after autoclaving. The sorbic acid stock of 10 mM undissociated sorbic acid was made by dissolving 11.78 mM sorbic acid in warm MEB after autoclaving and subsequently adjusted to pH 4 with NaOH/HCl and filter sterilized. The undissociated sorbic acid concentrations were calculated with the Henderson-Hasselbalch equation as defined by pH = pKa + log ($[A^-]/[HA]$) [37]. Each well contained a total volume of 200 µL with a total of 10^4 spores, by adding 10 µL of 10^6 spores/mL spore stock, counted and diluted by using TC20 automated cell counter (Bio-Rad). Growth was scored after 7 days and 28 days of growth at 25 °C using biological duplicates. The wells at the borders of the 96-well plates are used as water reservoirs and filled with 200 µL Milli-Q in order to prevent dehydration. To further limit dehydration and cross-contamination, the lids of the 96-wells plates are kept closed during the experiment. Additionally, the 96-well plates are kept inside a closed box con-

taining a falcon tube of water that functions as an additional water reservoir preventing dehydration of the wells.

The same assay was also performed to determine the MIC of 100 *A. niger* strains in ice tea peach. Filter sterilized and uncarbonated ice tea peach (Lipton) was used. The pH of the ice tea was measured at 3.1 and not adjusted. A total of 10.2 mM sorbic acid was added to ice tea and was subsequently filter sterilized, resulting in a sorbic acid stock with a concentration of 10 mM undissociated sorbic acid.

Weak acid sensitivity screening by spot assays

Spot assays were performed on minimal medium plates (MM) containing 27,75 mM glucose and varying concentrations of weak acids. For the initial spot assay testing 240 transcription factor knock-out strains, the following concentrations of (total) weak acids (pH = 4) were used: 4.5 mM sorbic acid, 2 mM and 3 mM benzoic acid, 2 mM and 3 mM cinnamic acid and 10 mM and 20 mM propionic acid. Minimal medium is prepared as described before [38], and set to pH 4 by the addition of NaOH/HCl after autoclaving. The weak acids tested were sorbic acid (Fluka chemika), cinnamic acid (Fluka chemika), benzoic acid (p-hydroxy-benzoic acid, Sigma), propionic acid (Propionic acid sodium salt, Sigma), lactic acid (Sigma Aldrich), citric acid (tri-sodium citrate dihydrate, VWR chemicals) and acetic acid (acetic acid glacial, Biosolve chemicals). Sorbic acid and cinnamic acid stock solutions were made in 70 % ethanol. Acetic acid was used directly from the liquid stock solution. All other weak acids stocks were made in Milli-Q and filter sterilized before use.

Spot assays on MM containing weak acids were performed by spotting 5 µL of a 10^6 conidia/mL spore stock solution, concentration determined by using TC20 automated cell counter (Bio-Rad), thereby inoculating a total of 5000 conidia per spot. Spot assay plates were cultivated for 4 days at 30 °C after which pictures were taken and growth was determined unless noted otherwise.

CRISPR/Cas9 genome editing in *A. niger*

Knock-out strains were constructed using a marker-free CRISPR/Cas9 genome editing approach as described previously [39]. All primers and plasmids used in this study are listed in Table 2.S2 and Table 2.S3, respectively. Single knock-out strains lacking the genes *sdrA* (An03g06580), *warA* (An08g08340) and *warB (*An11g10870) were made in MA234.1. Additionally, all possible combination knock-out strains were made; (*ΔsdrA*, *ΔwarA*), (*ΔwarA, Δwar*B), (*ΔsdrA, ΔwarB*) and (*ΔsdrA, ΔwarA, ΔwarB*) (Table 2.S1).

A schematic overview of the technique used for complementation to replace *sdrA* in wild-type strain CBS 147320 by the *sdrA* locus obtained from laboratory strain N402 is shown in Figure 2.S1. CRISPR/Cas9 plasmid SdrA gRNA2 in pFC332 (Figure 2.S1B) was used to obtain a double strand break in *sdrA*. The repair DNA was constructed by amplifying the gene as present in N402 by PCR. The donor DNA contained two newly introduced silent point mutations in order to eliminate further Cas9 endonuclease activity after a homology directed repair event has taken place. In short, the reverse primer of 5' part of the gene (p2r sjs28) and the forward primer of the 3' part of the gene (p3f sjs28) were designed to contain an overlapping sequence. This overlapping sequence contained the two newly introduced silent point mutations. The repair DNA was subsequently constructed by fusion PCR (Figure 2.S1C). PCR reactions to obtain repair DNA for the complementation were performed using Phusion™ High-Fidelity DNA Polymerase (Thermo scientific) with its appropriate buffer and protocol as prescribed by the manufacturer. Transformation was performed using a PEG-mediated protocol described previously [38], with few exceptions. Protoplast formation of wild-type *A. niger* strain CBS 147320 was seen after 2.5 hours of incubating. After 5 days of growth, transformants were single streaked on MM+ hygromycin (100 µg/mL) for purification and afterwards on MM, and MM +hygromycin for subsequent removal of selection pressure to select for transformants that lost the CRISPR/Cas9 containing plasmid.

Data availability

All data is included in the manuscript. Knock-out strains and plasmids used are available

upon request. Wild-type strains are available as part of the CBS collection, Westerdijk Fungal Biodiversity Institute, Utrecht, the Netherlands. Figure 2.S1 contains a detailed overview the SNP complementation methodology in wild-type *A. niger* strain CBS 147320. Figure 2.S2 contains the diagnostic PCRs performed to confirm *warA, sdrA* and *warB* deletions. Figure 2.S3 contains the MICu values of transcription factor knock-out strains lacking any combination of *sdrA*, *warA* and/or *warB* determined in MEB.

References

1. Snyder AB, Churey JJ, Worobo RW. Association of fungal genera from spoiled processed foods with physicochemical food properties and processing conditions. Food Microbiol. 2019;83:211–8.

2. Rico-Munoz E, Samson RA, Houbraken J. Mould spoilage of foods and beverages: Using the right methodology. Food Microbiol. 2019;81:51–62.

3. Stratford M, Steels H, Nebe-von-Caron G, Novodvorska M, Hayer K, Archer DB. Extreme resistance to weak-acid preservatives in the spoilage yeast Zygosaccharomyces bailii. Int J Food Microbiol. Elsevier B.V.; 2013;166:126–34.

4. Agriopoulou S, Stamatelopoulou E, Varzakas T. Advances in occurrence, importance, and mycotoxin control strategies: Prevention and detoxification in foods. Foods. 2020;9:137.

5. Gould GW. New methods of food preservation. 1st ed. New York: Springer US; 1995.

6. Plumridge A, Hesse SJA, Watson AJ, Lowe KC, Stratford M, Archer DB. The weak acid preservative sorbic acid inhibits conidial germination and mycelial growth of Aspergillus niger through intracellular acidification. Appl Environ Microbiol. American Society for Microbiology; 2004;70:3506–11.

7. Chichester DF, Tanner Jr FW. Handbook of Food Additives. CRC Press, Cleveland; 1972. p. 142–7.

8. Piper JD, Piper PW. Benzoate and sorbate salts: a systematic review of the potential hazards of these invaluable preservatives and the expanding spectrum of clinical uses for sodium benzoate. Compr Rev Food Sci Food Saf. 2017;16:868–80.

9. Dijksterhuis J, Meijer M, van Doorn T, Houbraken J, Bruinenberg P. The preservative propionic acid differentially affects survival of conidia and germ tubes of feed spoilage fungi. Int J Food Microbiol. 2019;306:108258.

10. Dagnas S, Gauvry E, Onno B, Membré JM. Quantifying effect of lactic, acetic, and propionic acids on growth of molds isolated from spoiled bakery products. J Food Prot. International Association for Food Protection; 2015;78:1689–98.

11. Nielsen MK, Arneborg N. The effect of citric acid and pH on growth and metabolism of anaerobic Saccharomyces cerevisiae and Zygosaccharomyces bailii cultures. Food Microbiol. Academic Press; 2007;24:101–5.

12. Jorge K. SOFT DRINKS | Chemical Composition. In: Caballero B, editor. Encycl Food Sci Nutr. 2nd ed. Cambridge, Massachusetts: Academic Press; 2003. p. 5346–52.

13. EFSA AP. Scientific opinion on the re-evaluation of sorbic acid (E 200), potassium sorbate (E 202) and calcium sorbate (E 203) as food additives. EFSA J. 2015;13:4144.

14. Neal AL, Weinstock JO, Lampen JO. Mechanisms of fatty acid toxicity for yeast. J Bacteriol. 1965;90:126–31.

15. Stratford M, Rose AH. Transport of sulphur dioxide by Saccharomyces cerevisiae. Microbiology. 1986;132:1–6.

16. Macris BJ. Mechanism of benzoic acid uptake by Saccharomyces cerevisiae. Appl Microbiol. 1975;30:503–6.

17. Pearce AK, Booth IR, Brown AJP. Genetic manipulation of 6-phosphofructo-1-kinase and fruc-

tose 2,6-bisphosphate levels affects the extent to which benzoic acid inhibits the growth of Saccharomyces cerevisiae. Microbiology. 2001;147:403–10.

18. Krebs HA, Wiggins D, Stubbs M, Sols A, Bedoya F. Studies on the mechanism of the antifungal action of benzoate. Biochem J. 1983;214:657–63.

19. Lambert RJ, Stratford M. Weak-acid preservatives: Modelling microbial inhibition and response. J Appl Microbiol. 1999;86:157–64.

20. Stratford M, Vallières C, Geoghegan I, Archer D, Avery S. The preservative sorbic acid targets respiration, explaining the resistance of fermentative spoilage yeast species. mSphere. 2020;5:e00273-20.

21. Novodvorska M, Stratford M, Blythe MJ, Wilson R, Beniston RG, Archer DB. Metabolic activity in dormant conidia of Aspergillus niger and developmental changes during conidial outgrowth. Fungal Genet Biol. 2016;94:23–31.

22. Alcano M de J, Jahn RC, Scherer CD, Wigmann ÉF, Moraes VM, Garcia M V., et al. Susceptibility of Aspergillus spp. to acetic and sorbic acids based on pH and effect of sub-inhibitory doses of sorbic acid on ochratoxin A production. Food Res Int. 2016;81:25–30.

23. Marín S, Guynot ME, Sanchis V, Arbonés J, Ramos AJ. Aspergillus flavus, Aspergillus niger, and Penicillium corylophilum spoilage prevention of bakery products by means of weak-acid preservatives. J Food Sci. 2002;67:2271–7.

24. Levinskaite L. Susceptibility of food-contaminating Penicillium genus fungi to some preservatives and disinfectants. Ann Agric Environ Med. 2012;19:85–9.

25. Garcia MV, Garcia-Cela E, Magan N, Copetti MV, Medina A. Comparative growth inhibition of bread spoilage fungi by different preservative concentrations using a rapid turbidimetric assay system. Front Microbiol. 2021;12:1364.

26. Plumridge A, Melin P, Stratford M, Novodvorska M, Shunburne L, Dyer PS, et al. The decarboxylation of the weak-acid preservative, sorbic acid, is encoded by linked genes in Aspergillus spp. Fungal Genet Biol. 2010;47:683–92.

27. Lubbers RJM, Dilokpimol A, Navarro J, Peng M, Wang M, Lipzen A, et al. Cinnamic acid and sorbic acid conversion are mediated by the same transcriptional regulator in Aspergillus niger. Front Bioeng Biotechnol. 2019;7:249.

28. Geoghegan IA, Stratford M, Bromley M, Archer DB, Avery S V. Weak acid resistance A (WarA), a novel transcription factor required for regulation of weak-acid resistance and spore-spore heterogeneity in Aspergillus niger. mSphere. 2020;5:e00685-19.

29. Piper P, Mahé Y, Thompson S, Pandjaitan R, Holyoak C, Egner R, et al. The Pdr12 ABC transporter is required for the development of weak organic acid resistance in yeast. EMBO J. 1998;17:4257–65.

30. Kren A, Mamnun YM, Bauer BE, Schüller C, Wolfger H, Hatzixanthis K, et al. War1p, a novel transcription factor controlling weak acid stress response in yeast. Mol Cell Biol. 2003;23:1775–85.

31. Hagiwara D, Suzuki S, Kamei K, Gonoi T, Kawamoto S. The role of AtfA and HOG MAPK pathway in stress tolerance in conidia of Aspergillus fumigatus. Fungal Genet Biol. 2014;73:138–49.

32. Ruijter GJG, Visser J. Carbon repression in Aspergilli. FEMS Microbiol Lett. 1997;151:103–14.

33. Monsicha P, Hong L, Wenjie X, D. SB, C. SD, P. MA, et al. Divergent targets of Aspergillus fu-

migatus AcuK and AcuM transcription factors during growth in vitro versus invasive disease. Infect Immun [Internet]. 2015;83:923–33. Available from: https://doi.org/10.1128/IAI.02685-14

34. Hortschansky P, Eisendle M, Al-Abdallah Q, Schmidt AD, Bergmann S, Thön M, et al. Interaction of HapX with the CCAAT-binding complex--a novel mechanism of gene regulation by iron. EMBO J [Internet]. 2007/06/14. Nature Publishing Group; 2007;26:3157–68. Available from: https://pubmed.ncbi.nlm.nih.gov/17568774

35. Patrícia A de C, Clara V, Jéssica C, Cristina CA, Lakhansing P, Lilian PS, et al. Novel biological functions of the NsdC transcription factor in Aspergillus fumigatus. MBio. 2021;12:e03102-20.

36. Schrettl M, Beckmann N, Varga J, Heinekamp T, Jacobsen ID, Jöchl C, et al. HapX-mediated adaption to iron starvation is crucial for virulence of Aspergillus fumigatus. PLOS Pathog. 2010;6:e1001124.

37. Po HN, Senozan NM. The Henderson-Hasselbalch equation: Its history and limitations. J Chem Educ. 2001;78:1499–503.

38. Arentshorst M, Ram AFJ, Meyer V. Using non-homologous end-joining-deficient strains for functional gene analyses in filamentous fungi. Methods Mol Biol. 2012;835:133–50.

39. van Leeuwe TM, Arentshorst M, Ernst T, Alazi E, Punt PJ, Ram AFJ. Efficient marker free CRISPR/Cas9 genome editing for functional analysis of gene families in filamentous fungi. Fungal Biol Biotechnol. 2019;6:1–13.

40. Park J, Hulsman M, Arentshorst M, Breeman M, Alazi E, Lagendijk EL, et al. Transcriptomic and molecular genetic analysis of the cell wall salvage response of Aspergillus niger to the absence of galactofuranose synthesis. Cell Microbiol. 2016;18:1268–84.

41. Nødvig CS, Nielsen JB, Kogle ME, Mortensen UH. A CRISPR-Cas9 system for genetic engineering of filamentous fungi. PLoS One. 2015;10:e0133085.

Additional files

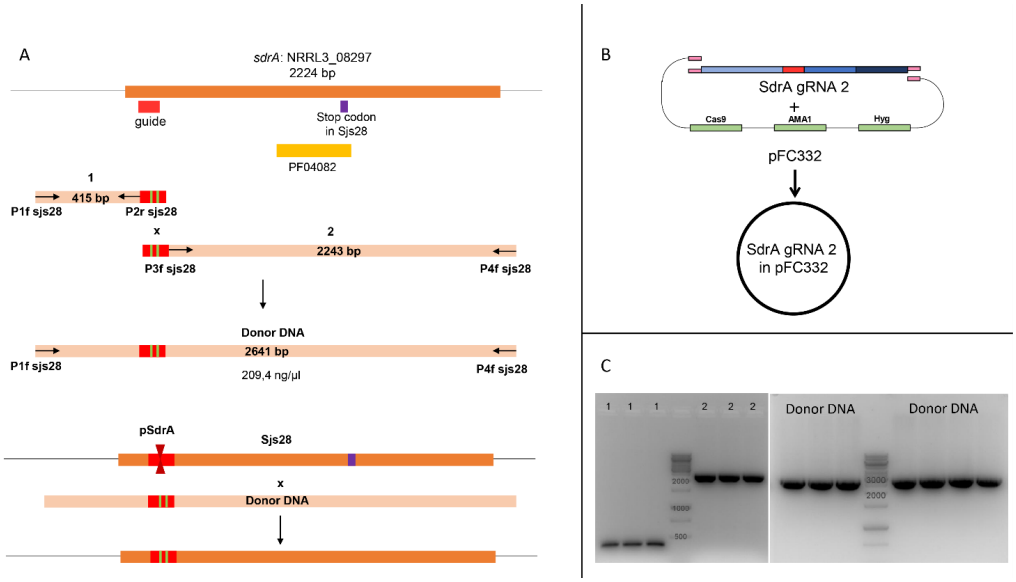

Figure 2.S1. Complementation of the premature stop codon of *sdrA* in CBS 147320 using CRISPR/Cas9. A. Schematic overview of the complementation methodology with *sdrA* (orange), the location of the guide of sdrA gRNA2 (red), the location of the stop codon in CBS 147320 (purple), and the location of the PFAM domain PF04082, fungal transcription factor domain (yellow). Also includes a schematic overview of the amplification method of the repair DNA (pink), with SNPs in the guide indicated (green). B. A schematic overview of the construction of the CRISPR/Cas9 containing plasmid pSdrA containing a guideRNA specifically targeting the *sdrA* locus. C. A PCR showing the fragments 1 (415 bp) and 2 (2243 bp), with fusion PCR obtaining the complete Donor DNA (2641 bp). Gels are run on 1% agarose gel with GeneRuler 1 kb DNA ladder.

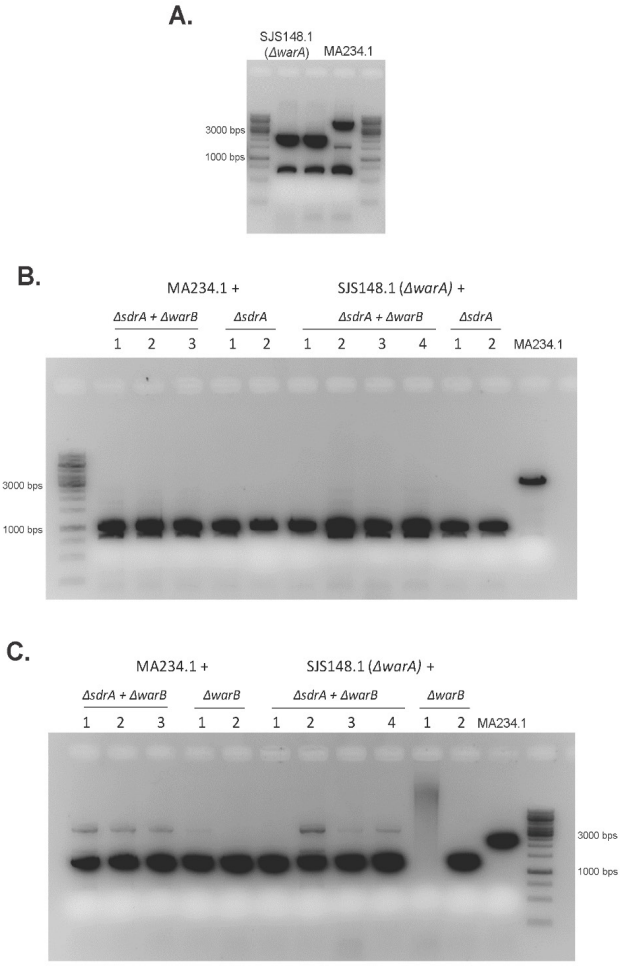

Figure 2.S2. Diagnostic PCR confirming the *warA*, *sdrA* and *warB* deletions. A. First, the *ΔwarA* deletion strain SJS148.1 was created. Diagnostic PCR was performed using forward primer DIAG_warA_fw and reverse primer DIAG_warA_rv to amplify the gene and flanking regions. A bandsize of 4800 bps is expected when *warA* is present, and a bandsize of 2166 bps is expected when *warA* is deleted. B. Diagnostic PCR was performed using forward primer DIAG_sdrA_fw and reverse primer DIAG_sdrA_rv to amplify the gene and flanking regions. A bandsize of 3181 bps is expected when *sdrA* is present, and a bandsize of 964 bps is expected when *sdrA* is deleted. C. Diagnostic PCR was performed using forward primer DIAG_warB_fw and reverse primer DIAG_warB_rv to amplify the gene and flanking regions. A bandsize of 2345 bps is expected when *warB* is present, and a bandsize of 1299 bps is expected when *warB* is deleted.

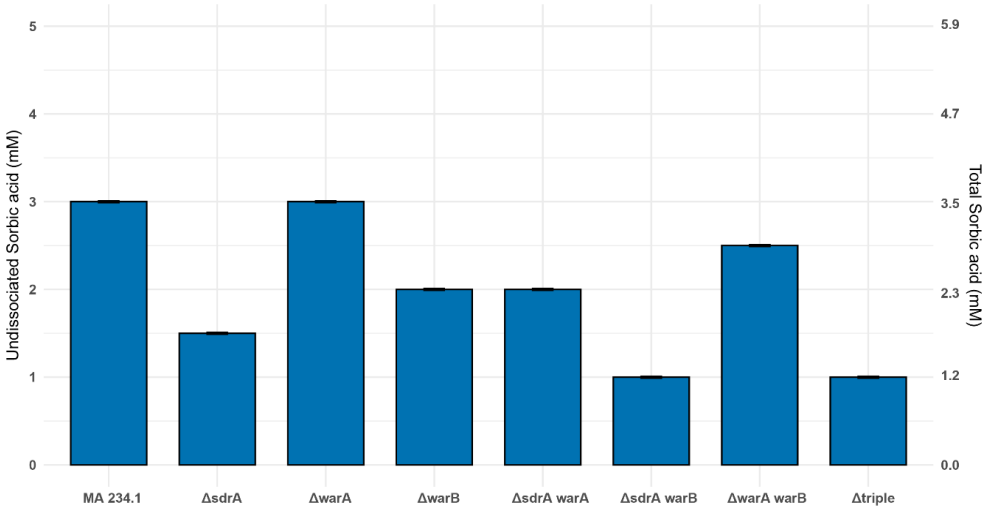

Figure 2.S3. The sorbic acid MIC values in liquid MEB assay of the knock-out strains lacking *sdrA*, *warA* and/or *warB*. Average MIC values of transcription factor knock-out strains in liquid MEB (pH = 4). MIC of each strain was identified in biological duplicates, the mean MIC is visualized in blue, with the error bar indicating the standard deviation (all duplicates gave the same MIC so the standard deviations are 0 in all cases). The growth was scored after 4 days of growth at 30 °C. The primary Y-axis indicates the undissociated sorbic acid concentration, while the secondary Y-axis indicates the total sorbic acid concentration added.

Table 2.S1. Strains used in this study

CBS number strain	DTO number strain	Genotype	Parental strain	Isolated from	Species	Obtained from
CBS 113.50	DTO 008-C3	wild type	-	Leather	*Aspergillus niger*	Westerdijk Fungal Biodiversity Institute
CBS 554.65	DTO 012-I2	wild type	-	Tannic-gallic acid fermentation, Connecticut, USA	*Aspergillus niger*	Westerdijk Fungal Biodiversity Institute
CBS 110.30	DTO 028-H9	wild type	-	Göttingen, Germany	*Aspergillus niger*	Westerdijk Fungal Biodiversity Institute
CBS 112.32	DTO 028-I3	wild type	-	Japan	*Aspergillus niger*	Westerdijk Fungal Biodiversity Institute
CBS 124.48	DTO 029-B1	wild type	-	Unknown	*Aspergillus niger*	Westerdijk Fungal Biodiversity Institute
CBS 131.52	DTO 029-C3	wild type	-	Leather	*Aspergillus niger*	Westerdijk Fungal Biodiversity Institute
CBS 263.65	DTO 029-D1	wild type	-	Copenhagen, Denmark	*Aspergillus niger*	Westerdijk Fungal Biodiversity Institute
CBS 103.66	DTO 029-D4	wild type	-	Unknown	*Aspergillus niger*	Westerdijk Fungal Biodiversity Institute
CBS 623.78	DTO 029-E3	wild type	-	France	*Aspergillus niger*	Westerdijk Fungal Biodiversity Institute
CBS 117.52	DTO 058-H9	wild type	-	Unknown	*Aspergillus niger*	Westerdijk Fungal Biodiversity Institute
CBS 118.52	DTO 058-I1	wild type	-	Unknown	*Aspergillus niger*	Westerdijk Fungal Biodiversity Institute
CBS 139.52	DTO 058-I5	wild type	-	Kuro-koji, Japan	*Aspergillus niger*	Westerdijk Fungal Biodiversity Institute
CBS 115988	DTO 059-C7	wild type	-	Unknown	*Aspergillus niger*	Westerdijk Fungal Biodiversity Institute
CBS 123906	DTO 063-G1	wild type	-	Ryuku, Japan	*Aspergillus niger*	Westerdijk Fungal Biodiversity Institute
CBS 630.78	DTO 067-H7	wild type	-	Army equipment, South Pacific Islands	*Aspergillus niger*	Westerdijk Fungal Biodiversity Institute
CBS 118.36	DTO 067-I4	wild type	-	Chemical, USA	*Aspergillus niger*	Westerdijk Fungal Biodiversity Institute
CBS 126.49	DTO 068-C1	wild type	-	Unknown	*Aspergillus niger*	Westerdijk Fungal Biodiversity Institute
-	DTO 072-D2	wild type	-	Indoor air of archive, the Netherlands	*Aspergillus niger*	Westerdijk Fungal Biodiversity Institute
-	DTO 086-F9	wild type	-	Filter flow cabinet, Westerdijk institute, Utrecht, the Netherlands	*Aspergillus niger*	Westerdijk Fungal Biodiversity Institute
-	DTO 089-E7	wild type	-	Air in crawling space, Eindhoven, the Netherlands	*Aspergillus niger*	Westerdijk Fungal Biodiversity Institute
-	DTO 096-A1	wild type	-	Wall down in the Lechuguilla Cave, Carlsbad, New Mexico, USA	*Aspergillus niger*	Westerdijk Fungal Biodiversity Institute

CBS number strain	DTO number strain	Genotype	Parental strain	Isolated from	Species	Obtained from
-	DTO 096-A2	wild type	-	Soil from dirt road, Isla Santa Cruz, Galapagos islands, Ecuador	*Aspergillus niger*	Westerdijk Fungal Biodiversity Institute
-	DTO 096-A3	wild type	-	Spent coffee (mouldy growth), Denmark	*Aspergillus niger*	Westerdijk Fungal Biodiversity Institute
CBS 147371	DTO 096-A5	wild type	-	Green coffee bean, Coffee Research Station, Netrakonda, India	*Aspergillus niger*	Westerdijk Fungal Biodiversity Institute
CBS 147320	DTO 096-A7	wild type	-	Grape, Australia	*Aspergillus niger*	Westerdijk Fungal Biodiversity Institute
-	DTO 096-A8	wild type	-	Artic soil, Svalbard, Norway	*Aspergillus niger*	Westerdijk Fungal Biodiversity Institute
CBS 147321	DTO 096-A9	wild type	-	Artic soil, Svalbard, Norway	*Aspergillus niger*	Westerdijk Fungal Biodiversity Institute
-	DTO 096-B1	wild type	-	Rice starch, imported to Denmark	*Aspergillus niger*	Westerdijk Fungal Biodiversity Institute
-	DTO 096-B3	wild type	-	Pepper, imported to Denmark	*Aspergillus niger*	Westerdijk Fungal Biodiversity Institute
-	DTO 096-B6	wild type	-	Saffron powder, from Kenya imported to Denmark	*Aspergillus niger*	Westerdijk Fungal Biodiversity Institute
-	DTO 096-C1	wild type	-	Unknown	*Aspergillus niger*	Westerdijk Fungal Biodiversity Institute
CBS 147322	DTO 096-C6	wild type	-	Coffee, Brazil	*Aspergillus niger*	Westerdijk Fungal Biodiversity Institute
-	DTO 096-C7	wild type	-	Unknown	*Aspergillus niger*	Westerdijk Fungal Biodiversity Institute
-	DTO 096-D1	wild type	-	Unknown	*Aspergillus niger*	Westerdijk Fungal Biodiversity Institute
CBS 147323	DTO 096-D7	wild type	-	Raisin, Fabula, Turkey	*Aspergillus niger*	Westerdijk Fungal Biodiversity Institute
CBS 147324	DTO 096-E1	wild type	-	Unknown	*Aspergillus niger*	Westerdijk Fungal Biodiversity Institute
-	DTO 096-E2	wild type	-	Unknown	*Aspergillus niger*	Westerdijk Fungal Biodiversity Institute
-	DTO 096-E3	wild type	-	Unknown	*Aspergillus niger*	Westerdijk Fungal Biodiversity Institute
-	DTO 096-E5	wild type	-	Unknown	*Aspergillus niger*	Westerdijk Fungal Biodiversity Institute
CBS 101700	DTO 096-G3	wild type	-	Japan	*Aspergillus niger*	Westerdijk Fungal Biodiversity Institute
CBS 101706	DTO 096-G4	wild type	-	Soy bean	*Aspergillus niger*	Westerdijk Fungal Biodiversity Institute
CBS 101707	DTO 096-G5	wild type	-	Broiler mixed feed	*Aspergillus niger*	Westerdijk Fungal Biodiversity Institute
CBS 101708	DTO 096-G6	wild type	-	Uknown	*Aspergillus niger*	Westerdijk Fungal Biodiversity Institute

CBS number strain	DTO number strain	Genotype	Parental strain	Isolated from	Species	Obtained from
CBS 121047	DTO 096-G8	wild type	-	Coffee bean, Thailand	*Aspergillus niger*	Westerdijk Fungal Biodiversity Institute
-	DTO 108-I7	wild type	-	Indoor environment, Thailand	*Aspergillus niger*	Westerdijk Fungal Biodiversity Institute
CBS 120.49	DTO 146-A3	wild type	-	USA	*Aspergillus niger*	Westerdijk Fungal Biodiversity Institute
CBS 101698	DTO 146-B8	wild type	-	Mesocarp finga – coffee bean, Kenya	*Aspergillus niger*	Westerdijk Fungal Biodiversity Institute
CBS 101705	DTO 146-C1	wild type	-	Carpet dust from school, Canada	*Aspergillus niger*	Westerdijk Fungal Biodiversity Institute
-	DTO 146-E8	wild type	-	Indoor environment, Hungary	*Aspergillus niger*	Westerdijk Fungal Biodiversity Institute
-	DTO 161-E9	wild type	-	Bamboo sample, Ho Chi Minh city, Vietnam	*Aspergillus niger*	Westerdijk Fungal Biodiversity Institute
-	DTO 167-A4	wild type	-	Margarine, Belgium	*Aspergillus niger*	Westerdijk Fungal Biodiversity Institute
CBS 147482	DTO 175-I5	wild type	-	Surface water, Portugal	*Aspergillus niger*	Westerdijk Fungal Biodiversity Institute
-	DTO 188-A9	wild type	-	Cinnamon, imported to the Netherlands	*Aspergillus niger*	Westerdijk Fungal Biodiversity Institute
-	DTO 203-H4	wild type	-	Soil, Kabodan island, Iran	*Aspergillus niger*	Westerdijk Fungal Biodiversity Institute
-	DTO 225-H3	wild type	-	Raisins, imported to Denmark	*Aspergillus niger*	Westerdijk Fungal Biodiversity Institute
-	DTO 240-E2	wild type	-	Breakfast cereal, Turkey	*Aspergillus niger*	Westerdijk Fungal Biodiversity Institute
-	DTO 240-H6	wild type	-	Muesli, Turkey	*Aspergillus niger*	Westerdijk Fungal Biodiversity Institute
-	DTO 240-I6	wild type	-	Dried fig, Turkey	*Aspergillus niger*	Westerdijk Fungal Biodiversity Institute
-	DTO 240-I9	wild type	-	Dried fruit, Turkey	*Aspergillus niger*	Westerdijk Fungal Biodiversity Institute
-	DTO 241-B2	wild type	-	Breakfast cereal, Turkey	*Aspergillus niger*	Westerdijk Fungal Biodiversity Institute
-	DTO 241-B7	wild type	-	Muesli, Turkey	*Aspergillus niger*	Westerdijk Fungal Biodiversity Institute
-	DTO 257-G2	wild type	-	Filling, the Netherlands	*Aspergillus niger*	Westerdijk Fungal Biodiversity Institute
-	DTO 260-C2	wild type	-	Indoor, school, Turkey	*Aspergillus niger*	Westerdijk Fungal Biodiversity Institute
-	DTO 267-I2	wild type	-	House dust, Thailand	*Aspergillus niger*	Westerdijk Fungal Biodiversity Institute
-	DTO 276-G2	wild type	-	BAL, Iran	*Aspergillus niger*	Westerdijk Fungal Biodiversity Institute
CBS 147343	DTO 291-B7	wild type	-	Coffee bean, Thailand	*Aspergillus niger*	Westerdijk Fungal Biodiversity Institute
-	DTO 293-E2	wild type	-	Coffee beans (Arabica), Thailand	*Aspergillus niger*	Westerdijk Fungal Biodiversity Institute

CBS number strain	DTO number strain	Genotype	Parental strain	Isolated from	Species	Obtained from
CBS 147344	DTO 293-G7	wild type	-	Coffee beans (Robusta), Thailand	*Aspergillus niger*	Westerdijk Fungal Biodiversity Institute
CBS 133816	DTO 316-E3	wild type	-	Black pepper, Denmark	*Aspergillus niger*	Westerdijk Fungal Biodiversity Institute
CBS 147345	DTO 316-E4	wild type	-	USA	*Aspergillus niger*	Westerdijk Fungal Biodiversity Institute
-	DTO 316-E5	wild type	-	Raisins, California, USA	*Aspergillus niger*	Westerdijk Fungal Biodiversity Institute
-	DTO 316-E6	wild type	-	Raisins, California, USA	*Aspergillus niger*	Westerdijk Fungal Biodiversity Institute
CBS 147346	DTO 321-E6	wild type	-	CF patient material, the Netherlands	*Aspergillus niger*	Westerdijk Fungal Biodiversity Institute
CBS 147347	DTO 326-A7	wild type	-	Petridish in soft drink factory, the Netherlands	*Aspergillus niger*	Westerdijk Fungal Biodiversity Institute
-	DTO 337-D3	wild type	-	Fruit, Belgium	*Aspergillus niger*	Westerdijk Fungal Biodiversity Institute
-	DTO 355-F9	wild type	-	Patient material, the Netherlands	*Aspergillus niger*	Westerdijk Fungal Biodiversity Institute
-	DTO 360-C1	wild type	-	Liquorice solution, the Netherlands	*Aspergillus niger*	Westerdijk Fungal Biodiversity Institute
CBS 115.50	DTO 367-B6	wild type	-	Unknown	*Aspergillus niger*	Westerdijk Fungal Biodiversity Institute
CBS 281.95	DTO 367-C9	wild type	-	Unknown	*Aspergillus niger*	Westerdijk Fungal Biodiversity Institute
CBS 769.97	DTO 367-D1	wild type	-	Leather	*Aspergillus niger*	Westerdijk Fungal Biodiversity Institute
CBS 115989	DTO 367-D6	wild type	-	Unknown	*Aspergillus niger*	Westerdijk Fungal Biodiversity Institute
CBS 116681	DTO 367-D7	wild type	-	Imported kernels of apricots, the Netherlands	*Aspergillus niger*	Westerdijk Fungal Biodiversity Institute
CBS 119394	DTO 367-E2	wild type	-	USA	*Aspergillus niger*	Westerdijk Fungal Biodiversity Institute
CBS 121997	DTO 367-E9	wild type	-	Coffee bean, Chiangmai, Thailand	*Aspergillus niger*	Westerdijk Fungal Biodiversity Institute
CBS 129379	DTO 367-G3	wild type	-	Soil, Cedrus deodar forest, Mussoorie, India	*Aspergillus niger*	Westerdijk Fungal Biodiversity Institute
CBS 132413	DTO 367-G7	wild type	-	Soil, 200m from W. mirabilis, Swakop, Namibia	*Aspergillus niger*	Westerdijk Fungal Biodiversity Institute
CBS 133817	DTO 367-G8	wild type	-	Black pepper, Denmark	*Aspergillus niger*	Westerdijk Fungal Biodiversity Institute
CBS 133818	DTO 367-G9	wild type	-	Raisins, Denmark	*Aspergillus niger*	Westerdijk Fungal Biodiversity Institute
CBS 140837	DTO 367-H2	wild type	-	Soil, Rudňany, Slovakia	*Aspergillus niger*	Westerdijk Fungal Biodiversity Institute

CBS number strain	DTO number strain	Genotype	Parental strain	Isolated from	Species	Obtained from
-	DTO 368-H7	wild type	-	K-sorbate free margarine, the Netherlands	*Aspergillus niger*	Westerdijk Fungal Biodiversity Institute
-	DTO 368-H8	wild type	-	Beverages factory, India	*Aspergillus niger*	Westerdijk Fungal Biodiversity Institute
-	DTO 368-H9	wild type	-	Ice Tea Red, Philippines	*Aspergillus niger*	Westerdijk Fungal Biodiversity Institute
CBS 147352	DTO 368-I1	wild type	-	Air next to bottle blower, Mexico	*Aspergillus niger*	Westerdijk Fungal Biodiversity Institute
-	DTO 368-I2	wild type	-	Decaffinated tea bags, Belgium	*Aspergillus niger*	Westerdijk Fungal Biodiversity Institute
-	DTO 368-I3	wild type	-	Environment in factory, Uzbekistan	*Aspergillus niger*	Westerdijk Fungal Biodiversity Institute
-	DTO 368-I4	wild type	-	Potassium sorbate containing margarine, Ghana	*Aspergillus niger*	Westerdijk Fungal Biodiversity Institute
-	DTO 368-I5	wild type	-	Foods factory of Sanquinetto, Italy	*Aspergillus niger*	Westerdijk Fungal Biodiversity Institute
CBS 147353	DTO 368-I6	wild type	-	Foods factory of Sanquinetto, Italy	*Aspergillus niger*	Westerdijk Fungal Biodiversity Institute
-	DTO 368-I7	wild type	-	Used in soy sauce fermentation process, China	*Aspergillus niger*	Westerdijk Fungal Biodiversity Institute
CBS 554.65	DTO 368-I8	wild type	-	Connecticut, USA	*Aspergillus niger*	Westerdijk Fungal Biodiversity Institute
JvD 1-1		putative *sdrA* G1296A	CBS 147320	-	*Aspergillus niger*	This study
JvD 1-2		putative *sdrA* G1296A	CBS 147320	-	*Aspergillus niger*	This study
JvD 1-3		putative *sdrA* G1296A	CBS 147320	-	*Aspergillus niger*	This study
JvD 2-1		putative *sdrA* G1296A	CBS 147320	-	*Aspergillus niger*	This study
JvD 2-2		putative *sdrA* G1296A	CBS 147320	-	*Aspergillus niger*	This study
JvD 2-3		putative *sdrA* G1296A	CBS 147320	-	*Aspergillus niger*	This study
JvD 2-4		putative *sdrA* G1296A	CBS 147320	-	*Aspergillus niger*	This study
JvD 2-5		putative *sdrA* G1296A	CBS 147320	-	*Aspergillus niger*	This study
JvD 2-6		putative *sdrA* G1296A	CBS 147320	-	*Aspergillus niger*	This study

CBS number strain	DTO number strain	Genotype	Parental strain	Isolated from	Species	Obtained from
JvD 2-8		putative *sdrA* G1296A	CBS 147320	-	*Aspergillus niger*	This study
JvD 2-9		putative *sdrA* G1296A	CBS 147320	-	*Aspergillus niger*	This study
JvD 2-10		putative *sdrA* G1296A	CBS 147320	-	*Aspergillus niger*	This study
JvD 2-12		putative *sdrA* G1296A	CBS 147320	-	*Aspergillus niger*	This study
MA234.1		Δ*kusA*	N402	-	*Aspergillus niger*	[40]
SJS148.1		*ΔwarA*	MA234.1	-	*Aspergillus niger*	This study
SJS157.1		*ΔsdrA*	MA234.1	-	*Aspergillus niger*	This study
SJS158.1		*ΔwarB*	MA234.2	-	*Aspergillus niger*	This study
SJS159.1		*ΔsdrA*, *ΔwarA*	SJS148.1	-	*Aspergillus niger*	This study
SJS160.2		*ΔwarA*, *ΔwarB*	SJS148.2	-	*Aspergillus niger*	This study
SJS161.1		*ΔsdrA*, *ΔwarB*	MA234.1	-	*Aspergillus niger*	This study
SJS162.1		*ΔsdrA*, *ΔwarA*, *ΔwarB*	SJS148.1	-	*Aspergillus niger*	This study

Table 2.S2. Primers used in this study

Primer name	Sequence	Function
p1f sjs28	TCCCGCATCGGCTAAGTCTCCA	*sdrA repair DNA 1 for CBS 147320*
p2r sjs28	CTGATTCCGCTTCATTCGCAGCACGCGGT-CAATCTCT	*sdrA repair DNA 1 for CBS 147320*
p3f sjs28	GAATGAAGCGGAATCAGCGCGAGGCTCGAGCGT-GTTA	*sdrA repair DNA 2 for CBS 147320*
p4r sjs28	AGTCCGAGGCCTCCGAACCA	*sdrA repair DNA 2 for CBS 147320*
TS1_sdrA_fw	TCCCGCATCGGCTAAGTCTCCA	*Creation of 5' sdrA flank, 367 bp*
TS1_sdrA_rv	GGAGTGGTACCAATATAAGCCGGCGGTGTGTCG-GAACCTCAAAAGC	*Creation of 5' sdrA flank, 367 bp*
TS2_sdrA_fw	CCGGCTTATATTGGTACCACTCCCCATGACGTTATG-CGGCCCCTC	*Creation of 3' sdrA flank, 502 bp*
TS2_sdrA_rv	AGTGGCACCCGTCATGGCTACT	*Creation of 3' sdrA flank, 502 bp*
sdrA_sgRNA2_fw	AATGAAACGCAATCAGCGCGGTTTTAGAGCTAGAAAT	*Create the sdrA target for the CRISPR/Cas9 plasmid*
sdrA_sgRNA2_rv	CGCGCTGATTGCGTTTCATTGACGAGCTTACTCGTTT	*Create the sdrA target for the CRISPR/Cas9 plasmid*
diag_sdrA_fw	ACTTAGGGGGTGGGACCAGTGG	*diagnostic PCR sdrA deletion*
diag_sdrA_rv	GGACTTTGATGCCGAGCATGGC	*diagnostic PCR sdrA deletion*
5_warA_fw	GGCGTCCTCCAGGGTCTCATCT	*Creation of 5' warA flank, 368 bp*
5_warA_rv	GGAGTGGTACCAATATAAGCCGGTGGCTTGCTGT-TATTCTAGAGAGGG	*Creation of 5' warA flank, 368 bp*
3_warA_fw	CCGGCTTATATTGGTACCACTCCTGTGTATTTGTCTG-GAGTGGATGT	*Creation of 3' warA flank, 1002 bp*
3_warA_rv	AGCTCCCGCTCAATCCTCGAGA	*Creation of 3' warA flank, 1002 bp*
warA_sgRNA_fw	CGATAGACGATGCTTACCTGGTTTTAGAGCTAGAAAT	*Create the warA target for the CRISPR/Cas9 plasmid*
warA_sgRNA_rv	CAGGTAAGCATCGTCTATCGGACGAGCTTACTCGTTT	*Create the warA target for the CRISPR/Cas9 plasmid*
diag_warA_fw	CACAATGCCATGTAGCGCGCAA	*diagnostic PCR warA deletion*
diag_warA_rv	ACACGATCTGACCGCGATGACG	*diagnostic PCR warA deletion*
TS1_warB_fw	TCGACCCTCCCGGTTTGGTCAA	*Creation of 5' warB flank, 599 bp*

Primer name	Sequence	Function
TS1_warB_rv	GGAGTGGTACCAATATAAGCCGGTGAAGGAG-GTTTGGTTGCGGGT	*Creation of 5' warB flank, 599 bp*
TS2_warB_fw	CCGGCTTATATTGGTACCACTCCACGATACGAC-GAAGTTCAGCAT	*Creation of 3' warB flank, 544 bp*
TS2_warB_rv	AGTTCGGCCACTTCTCGGACCA	*Creation of 3' warB flank, 544 bp*
warB_sgRNA2_rv	CGGTGTTCTCTTCGAAGCGCGACGAGCTTACTC-GTTT	*Create the warB target for the CRISPR/Cas9 plasmid*
warB_sgRNA2_fw	GCGCTTCGAAGAGAACACCGGTTTTA-GAGCTAGAAAT	*Create the warB target for the CRISPR/Cas9 plasmid*
diag_warB_fw	TCGCCCTCGTCTTACTCCTCCC	*diagnostic PCR warB deletion*
diag_warB_rv	CCATGACGTCCTCCATCACCGC	*diagnostic PCR warB deletion*

Table 2.S3. Plasmids used in this study

Plasmid name	Target sequence	Function	Origin
pTLL108.1	-	Template for the amplification of guide RNA	[39]
pTLL109.2	-	Template for the amplification of guide RNA	[39]
pFC332	-	Vector containing CRISPR/ Cas9	[41]
sdrA gRNA2 in pFC332	AATGAAACGCAATCAGCGCG	Targeted double stranded break in *sdrA* gene	This study
warA gRNA in pFC332	CGATAGACGATGCTTACCTG	Targeted double stranded break in *sdrA* gene	This study
warB gRNA2 in pFC332	GCGCTTCGAAGAGAACAC-CG	Targeted double stranded break in *sdrA* gene	This study

CHAPTER 3

Interkingdom microbial variability in heat resistance

Tom van den Brule, Maarten Punt, Sjoerd J. Seekles, Frank J. J. Segers, Jos Houbraken, Wilma C. Hazeleger, Arthur F. J. Ram, Han A. B. Wösten, Marcel H. Zwietering, Jan Dijksterhuis, Heidy M. W. den Besten

Submitted for publication

Abstract

Microbial species are inherently variable, which is reflected in intraspecies genotypic and phenotypic differences. Strain-to-strain variation gives rise to variability in stress resistance and plays a crucial role in microbial ecology. Here, strain variability in heat resistance of asexual spores (conidia) of the fungal species *Aspergillus niger*, *Penicillium roqueforti* and *Paecilomyces variotii* was quantified and compared to variability found in the literature. After heat treatment, a 5.4- to 8.6-fold difference in inactivation rate was found between individual strains within each species, while the strain variability of the three fungal species was not statistically different. We hypothesised that the degree of intraspecies variability is uniform, not only within the fungal kingdom, but also between different microbial kingdoms. Comparison with three spore-forming bacteria and two non-spore-forming bacteria revealed that the variability of the different species was indeed in the same order of magnitude, which hints to a microbial signature of variation that exceeds kingdom boundaries.

Introduction

Diversity of microbial species is key to adapt to environmental changes and to thrive in different niches. Intraspecies variability includes all variation within a species, including genotypic and phenotypic differences. Unravelling drivers for intraspecies variability has been a broadly studied subject the past decade including elucidating mechanistic differences between strains [1–3] and sources of phenotypic heterogeneity of genetic identical cell populations [4,5]. Strain diversity can have huge consequences on diagnostics, virulence and antimicrobial treatments in clinical microbiology, or on the efficacy of food preservation methods [6–10].

As microbial species are inherently variable, strains of the same species may differ in their response to environmental stresses. Indeed, large differences in stress robustness have been reported in bacterial species [11]. This suggests that microbial stress robustness is a relevant trait to quantify strain variability. Recently, strain variability in heat resistance has been quantified for bacterial vegetative cells of the pathogen *Listeria monocytogenes* [12] and the food-borne organism *Lactiplantibacillus plantarum* [13] (previously known as *Lactobacillus plantarum* [14]) and for bacterial spores of the pathogen *Bacillus cereus* [11], and the food spoilers *Bacillus subtilis* [8] and *Geobacillus stearothermophilus* [15]. Notably, the quantified strain variability was high for the tested organisms and inactivation rates of the most heat sensitive and most heat resistance strains of the same species could differ a factor ten. This means that when a similar temperature/time regime is applied, the most heat resistant strain will be reduced with a factor 10, while the most heat sensitive strains will be reduced with a factor 10^{10}. This results in huge differences in heat treatment efficacies, depending on the heat stress robustness of the microbial contaminant [11].

Spores of bacteria and fungi are considered more stress resistant than vegetative cells [16]. The stress resistance of fungal spores varies strongly, ranging from spores that display stress resistance similar to that of vegetative cells to very high stress resistance that can be comparable to bacterial spores [16–18]. Filamentous Ascomyce-

te fungi that belong to the order Eurotiales can produce asexual spores called conidia. Airborne conidia are resistant to various environmental stresses including ultra violet (UV) radiation, desiccation, cold and heat stress [16]. Conidia are an integral part of the fungal life cycle, and can be distributed in space by air, wind or other vectors and are abundantly present in the environment. For example, *Penicillium chrysogenum* conidia are so widespread that they are considered being cosmopolitan [19] and these airborne conidia are found in the air and soil in many different habitats [20]. Studies have shown that conidia can travel large distances. For instance, conidia of *Aspergillus sydowii* have been suggested to be transported over thousands of kilometres from the Sahara desert to the Caribbean reefs [21]. Being airborne and widely present, fungal airborne conidia are often related to food spoilage, leading to considerable losses of food and feed [22].

Recently, conidial heat resistance of various strains of the food spoilage fungus *Paecilomyces variotii* was reported to be highly variable. Decimal reduction times of thermal treatments at 60°C (D_{60}-values) ranged from 3.5 to 27.6 minutes when different strains were used of the same species [23]. This prompted us to study a larger selection of isolates and to quantify variability in conidial heat resistance among strains of *Pae. variotii* in detail. Furthermore, we also assessed strain variability in conidial heat resistance of the fermentative fungus *Penicillium roqueforti*, and for *Aspergillus niger*, which is commonly used as model fungus. Both species are also known as food spoilers. The quantified strain variabilities were compared between the fungal species, and also compared to strain variability in heat resistance of bacterial vegetative cells and spores, to assess strain variability across kingdom borders.

Results

Verification of strain identity

In total, 21 *A. niger*, 20 *P. roqueforti* and 20 *Pae. variotii* strains were selected (Table 3.S1) and their identity was verified by sequencing genetic marker genes according to the phylogenetic standards [24]. Based on the partial sequences of *caM*, all *A. niger*

strains grouped together with type strain *A. niger* NRRL 326, with *Aspergillus welwitschiae*, the most closely related species, being the sister clade (Fig. 3.1a). Similarly, the partial *benA* sequences of the *P. roqueforti* strains grouped with type strain CBS 221.30 and segregated from the closely related *Penicillium mediterraneum* (Fig. 3.1b). In agreement with previous studies [25,26], we found more intraspecies variation in the partial *benA* sequences of *Pae. variotii* compared to *A. niger* and *P. roqueforti*. However, all *Pae. variotii* strains clustered with type strain CBS 102.74, while *Paecilomyces brunneolus* was sister to this cluster (Fig. 3.1c).

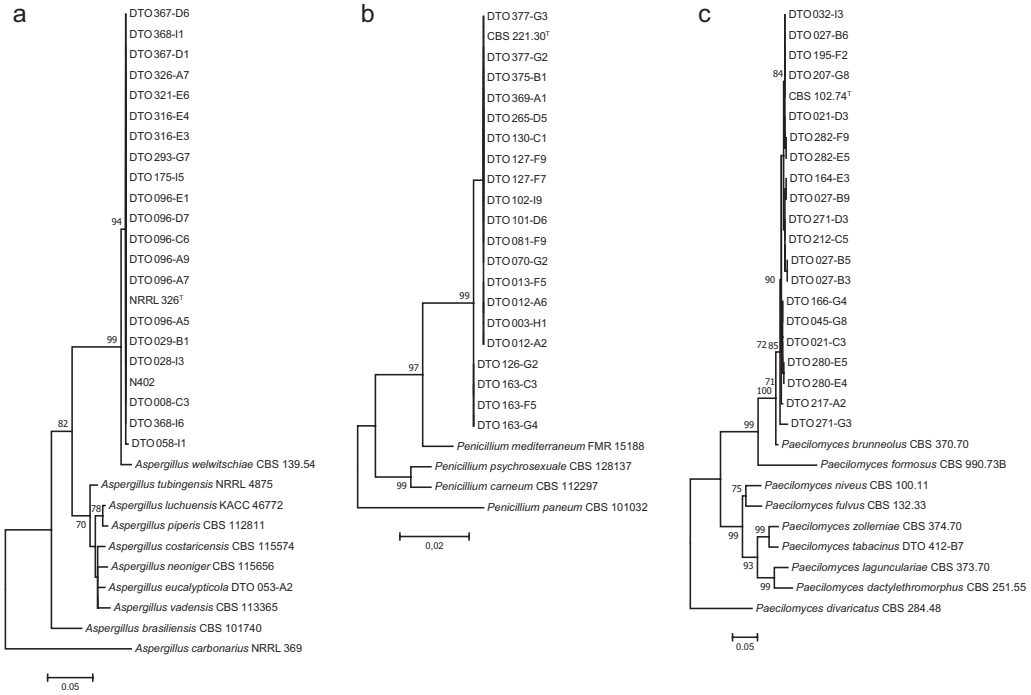

Figure 3.1. Maximum likelihood trees for strain identification. (a) Phylogram based on partial *caM* sequence of studied *A. niger* strains, including type strain NRRL 326 and other closely related *Aspergillus* species with *Aspergillus carbonarius* used as outgroup. (b) Phylogram based on partial *benA* sequences of *P. roqueforti* strains, including type strain CBS 221.30 and other closely related *Penicillium* species with *Penicillium paneum* as outgroup. (c) Phylogram based on partial *benA* gene sequences of *Pae. variotii* strains, including type strain CBS 102.74 and other closely related *Paecilomyces* species with *Paecilomyces divaricatus* as outgroup.

Quantification of heat resistance

Strains of *A. niger*, *P. roqueforti*, and *Pae. variotii* were heat-treated using biologically independent batches of conidia and technical duplicates. The differences between the technical replicates were rather small for all strains of the three species (Figure 3.2a, d, g). The differences between the biological replicates were clearly higher than those of the experimental duplicates (Figure 3.2b, e, h), but much higher differences were found between the individual strains per species (Figure 3.2c, f, i). Most inactivation kinetics, *i.e.* 237 out of 366, did not show a significant tailing or a shoulder curvature, and a linear model was used to calculate the *D*-value. For the other data sets the reparameterized Weibull model (Eq. 1) was used to calculate the average *D*-value (Table 3.S2).

The most heat-resistant *P. roqueforti* strain was DTO 013-F5, while the most heat-sensitive strain was DTO 130-C1 with D_{56}-values of 13.6 ± 3.0 and 1.6 ± 0.38 minutes, respectively. Similar to *P. roqueforti*, about an eight-fold difference was found between the most heat-resistant *Pae. variotii* strain DTO 195-F2 and the most heat-sensitive strain DTO 212-C5, with corresponding D_{60}-values of 26.6 ± 3.4 and 3.5 ± 0.30 minutes, respectively. This indicates that for this specific heat treatment, one out of ten cells will survive for the most resistant strain, while only one out of 10^8 cells will survive for the most sensitive strain. Three out of 21 *A. niger* strains, DTO 028-I3, DTO 029-B1 and DTO 058-I1, did not sporulate well after 7 days growth on MEA at 25°C. A better sporulation was achieved when cultivating at 30°C instead of 25°C, and therefore this temperature was used to culture conidia. Interestingly, these three strains belonged to the most heat sensitive strains, with D_{54}-values of 12.6 ± 1.7, 3.7 ± 0.60 and 9.9 ± 2.2 minutes, respectively. Impeded sporulation can be a sign of degeneration of a strain [27]. Indeed, these three strains were deposited more than six decades ago into the CBS culture collection and it cannot be excluded that the strains degenerated over the years or arrived in a degenerated state when deposited. Because growing cultures at higher temperatures can significantly enhance heat resistance in the case of *Aspergillus fumigatus* [28] and *P. roqueforti* conidia [29], it was decided to exclude DTO 028-I3, DTO 029-B1 and DTO 058-I1 for further analysis. This made DTO 367-D1 the most sensitive

and DTO 326-A2 the most resistant *A. niger* strain with D_{54}-values of 9.4 ± 0.85 and 50.4 ± 11.9 minutes, respectively.

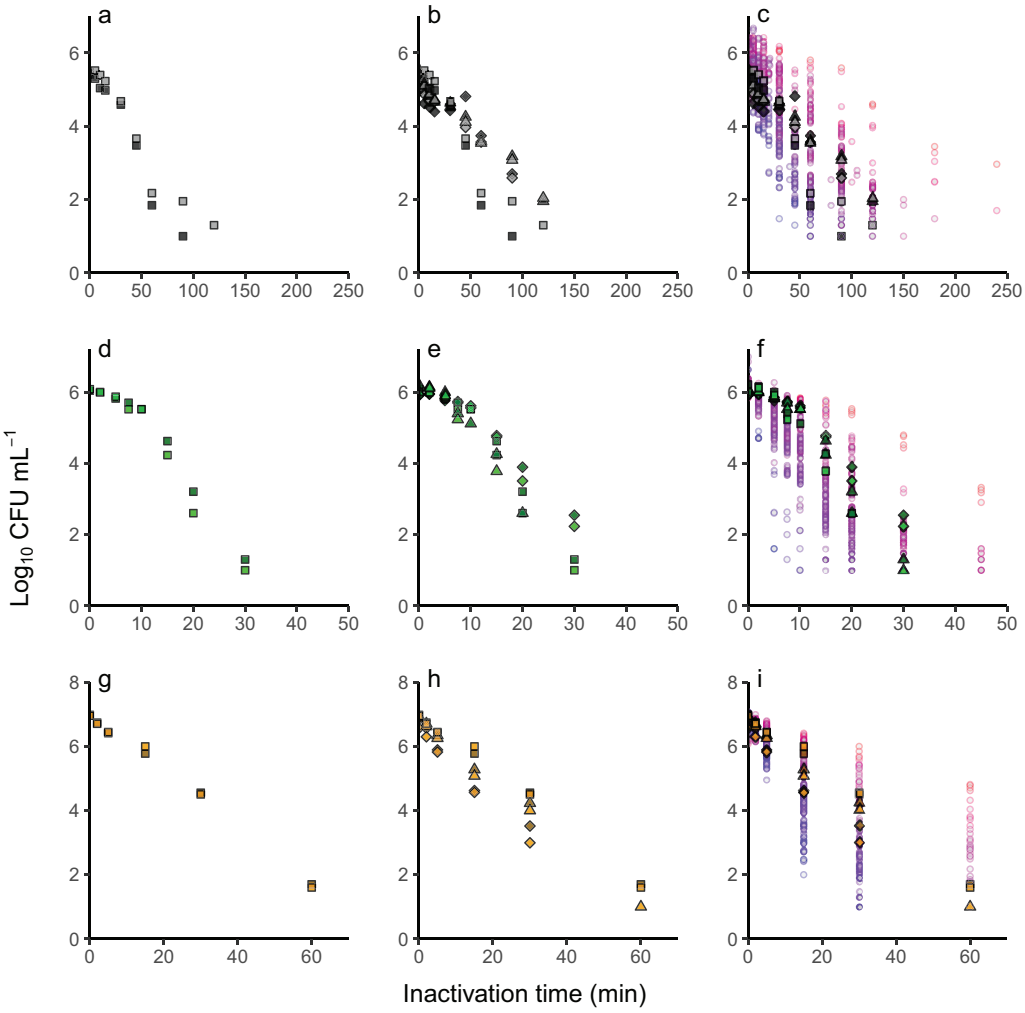

Figure 3.2. Variability in thermal inactivation of species. Thermal inactivation was performed at 54°C for *A. niger* (a-c), 56°C for *P. roqueforti* (d-f) and 60°C for *Pae. variotii* (g-i). Experimental variability (a, d, g), biological variability (b, e, h) and strain variability (c, f, i) is depicted by the $\log_{10}$ CFU mL^{-1} data of each experiment. The strains *A. niger* DTO 316-E3 (black; a-c), *P. roqueforti* DTO 163-C3 (green; d-f) and *Pae. variotii* DTO 166-G4 (orange; g-i) are highlighted, showing two experimental replicates (dark fill, light fill) of three biological replicates (□, ◇ and Δ). All other strains (○; c, f, i) are coloured using a gradient from blue (heat-sensitive) to red (heat-resistant) based on the mean *D*-values presented in Table 3.S2.

Quantification of variability

The experimental, biological and strain variability of the three species was quantitatively expressed in $\sqrt{MSE}$ (*i.e.* the standard deviation, σ) of the $\log_{10}$ *D*-values, which is a measure of variability (Fig. 3.3). Indeed, as observed in Fig. 3.2, experimental variability was the lowest variability factor with σ_e values of 0.045, 0.044 and 0.033 for *A. niger*, *P. roqueforti* and *Pae. variotii*, respectively. Biological variability values were larger with a σ_b of 0.092, 0.096 and 0.084 for *A. niger*, *P. roqueforti* and *Pae. variotii*, respectively. Strain variability was clearly higher, with σ_s of 0.197, 0.179 and 0.230 for the three fungi, respectively. Interestingly, the 95% confidence intervals of the three species were overlapping for each of the variability factors. This indicates that there are no differences in the magnitude of the variability between the species. However, the variability factors were clearly different, with strain variability being higher than biological variability, and both being higher than experimental variability.

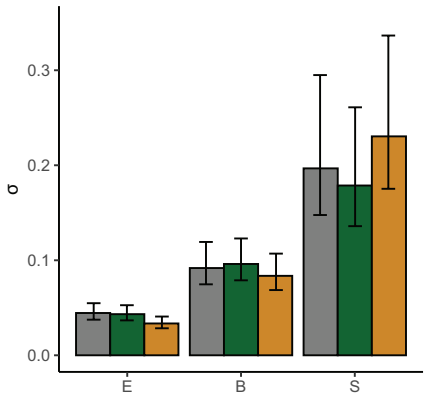

Figure 3.3. Quantification of variability. Experimental variability (E), biological variability (B) and strain variability (S) of *A. niger* (grey), *P. roqueforti* (green) and *Pae. variotii* (orange). For strain variability 18 *A. niger*, 20 *P. roqueforti* and 20 *Pae. variotii* strains were used to determine σ_s values. Error bars represent the 95% confidence interval of the σ values.

Meta-analysis

The conidial heat resistance of *A. niger* and *P. roqueforti* strains presented in this study was compared with available data from the literature. Only recently, two studies described the heat resistance for *Pae. variotii* conidia [23,30] and therefore this fungus was

excluded for the meta-analysis. The *D*-values from literature for *A. niger* and *P. roqueforti* and the *D*-values collected in the current study are shown in Figure 3.4a and 3.4b, respectively. The linear correlation between the $\log_{10}$ *D*-values and temperature allowed to calculate the *z*-value, indicating the temperature increase needed to decrease *D*-values 10-fold. The *z*-values were 8.9°C for *A. niger* and 7.8°C for *P. roqueforti*, which is comparable to *z*-values found for multiple bacterial species [31]. The deviation of each data point to the linear regression between $\log_{10}$ *D*-value and temperature was used to quantify the overall variability σ_T, which was 0.432 for *A. niger* and 0.413 for *P. roqueforti*. With σ_s values 46% and 43% of the σ_T values for *A. niger* and *P. roqueforti*, respectively, these results indicate that strain variability is a substantial source of variability in the overall variability found.

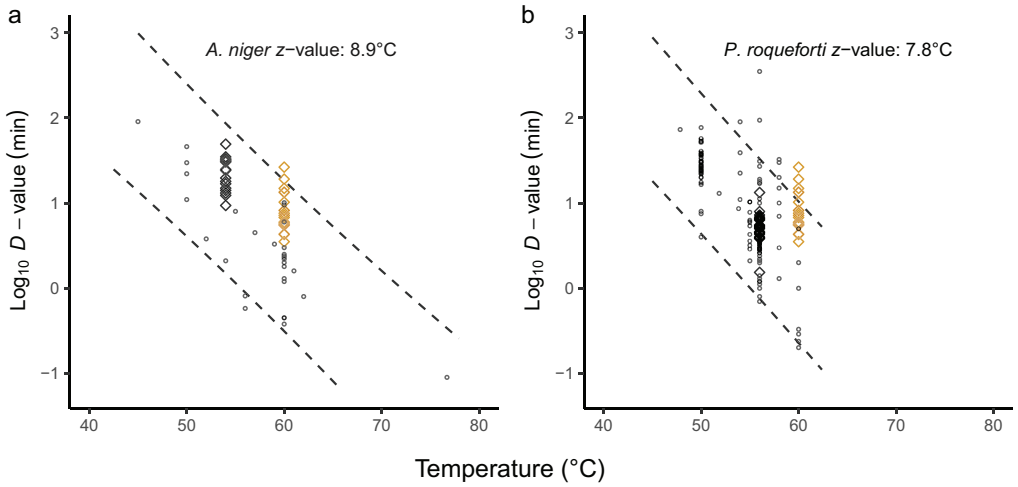

Figure 3.4. Meta-analysis of *A. niger* and *P. roqueforti* *D*-values. $\log_{10}$ *D*-values from literature (○) and mean $\log_{10}$ *D*-values per strain presented in this study (◇) were combined to determine *z*-values and overall variability for *A. niger* (a) and *P. roqueforti* (b). Mean $\log_{10}$ *D*-values of *Pae. variotii* strains presented in this study are depicted as orange ◇ in both panels. The 95% prediction intervals of the linear regression analysis are depicted as dashed lines in both panels.

Interkingdom comparison

It is well known that heat resistance of bacterial spores and vegetative cells differs enormously among species, and consequently the *D*-values are very different when determined at the same temperature. Interestingly, contrary to the magnitude, the intraspecies

variability of bacterial species inactivation rates were in the same order of magnitude when five different bacterial species were compared [11], including 3 spore-forming bacteria, *B. subtilis*, *B. cereus*, *G. stearothermophilus*, and 2 non-spore-forming bacteria, *L. monocytogenes* and *Lpb. plantarum*. Because the current study used a similar experimental set up to determine heat resistance between fungal strains, taking into account the variability between biologically independent replicates and variability between technical duplicates, we could compare the σ_e, σ_b and σ_s values of the three fungal species to those of the five bacterial species (Fig. 3.5). Note that the *B. subtilis* strains were grouped in a high-level heat resistant group and a low-level heat resistant group for quantification of strain variability. The *B. subtilis* strains that produced high-level heat resistant spores proved to harbour a mobile genetic element, *spoVA*^{2mob}, that confers high-level heat resistance to spores [32], giving genetic evidence for clustering the corresponding strains into two groups. Interestingly, for all microbial species, strain variability was larger than biological and experimental variabilities. Altogether, these data suggest that the different levels of variability in heat resistance of fungal conidia are very similar to those of bacterial spores and cells.

Discussion

Intraspecies variability is inherent in microbial species. We scrutinized conidial heat resistance of three fungal species and quantified variability at experimental, biological and strain level. In total, 18 *A. niger*, 20 *P. roqueforti* and 20 *Pae. variotii* strains were used to quantify strain variability. Although some reference strains were included in the strain selection it is of importance to select the strains randomly in order to represent variability found in nature. In mycological research, it can be challenging to identify fungal isolates to species level as some are cryptic species. For instance, *A. niger* is difficult to distinguish from *Aspergillus luchuensis* and *Aspergillus welwitschiae* based on morphology [33]. Even identification by sequencing of genetic marker genes can be puzzling since databases can contain sequences of previously misidentified isolates [34,35]. Identifica-

tion of the strains used in this study by phylogenetic analysis of marker genes sequences of reference strains provided a robust identification of the current species. Therefore, the selection of fungal strains and the genetic locus used for comparison indicate that the observed variation in conidial heat resistance is truly intraspecies.

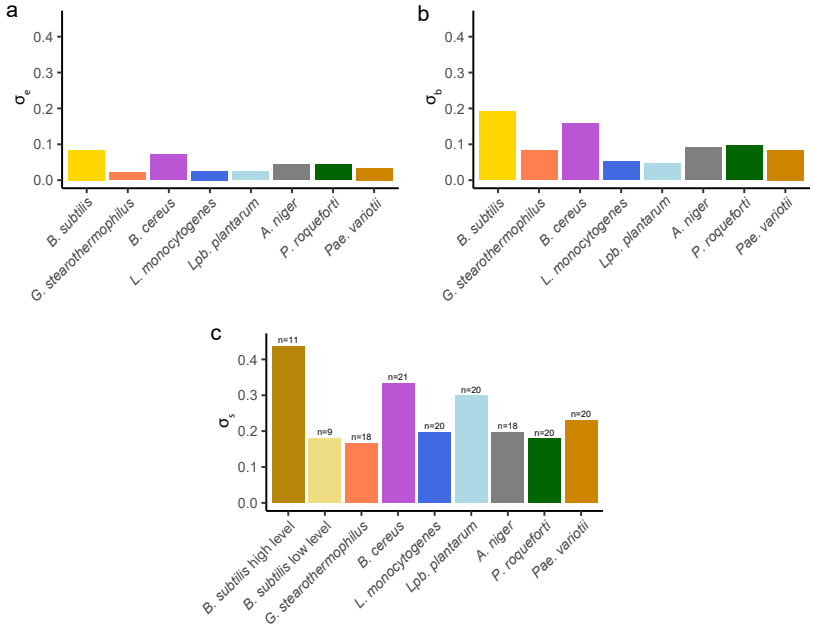

Figure 3.5. Comparison of variability in heat resistance between bacterial spores, vegetative cells and fungal conidia. The y-axes represent experimental σ_e (a), biological σ_b (b) and strain σ_s variability (c) in heat resistance of bacterial spores of *B. subtilis*, *B. cereus* and *G. stearothermophilus*, bacterial vegetative cells of *L. monocytogenes* and *Lpb. plantarum* and fungal conidia of *A. niger*, *P. roqueforti* and *Pae. variotii*. For strain variability, *n* represents the number of strains used to determine σ_s values. Data of bacterial species was adapted from den Besten *et al.*, 2018.

Differences in heat resistance are not only caused by variation in genetic background. Heterogeneity in genetically uniform cells can contribute to survival against environmental stress in yeast species [36]. Some strains of *Pae. variotii* can produce conidia populations that are heterogeneous in size [23]. The same study stated that strains producing conidia with a larger mean size tend to be more heat resistant; hinting that the larger conidia within spore populations could be more heat resistant compared to small size conidia. In addition to these examples of phenotypic heterogeneity, environmental growth conditions can have a significant effect on heat resistance. Besides cultivation

temperature [28,29], the maturation of conidia also plays a role in the development of heat resistance as conidia from older colonies of *A. niger* and *P. roqueforti* showed higher robustness to heat treatments [29,37]. On the other hand, environmental conditions during conidiation can also reduce heat resistance of fungal conidia. Growth at pH 4.6 resulted in sensitive conidia compared to the more optimal conditions at pH 8.0 of the insect-pathogenic fungus *Metarhizium robertsii* [38]. Intracellular compatible solutes and protective proteins are known to provide heat robustness to fungal species [16,39]. Conidia of *A. niger* contain large amounts of Hsp70 transcripts [40] and mannitol [37], while arabitol, the hydrophilins con-6 and con-10 and 17 predicted proteins with unknown function were implied to play a role in heat resistance of *P. roqueforti* conidia [29]. On the other hand, *Pae. variotii* conidia contain predominantly trehalose as compatible solute [25] and in higher amount than *A. niger* [37] and *P. roqueforti* [29], which might explain, at least in part, the higher heat resistance of this species.

Our experimental set up was aimed to reduce environmental variation as much as possible by spreading many conidia over one plate for inoculation. This way, we anticipated to differences due to colony age, which could be interpreted as environmental variation. In the meta-analysis, we compared our data with data available in literature, where different growth conditions and heating menstrua were applied, to visualize this overall variability. This demonstrated that strain variability is a large, if not the largest source of the overall variability. This is consistent with bacterial species, where σ_s values are typically 40% to 75% of the overall variability found in literature [11]. For two other bacterial species, *Escherichia coli* O157:H7 and *Staphylococcus aureus*, *D*-values have been for a large number of strains at one or two temperatures, allowing us also to quantify the strain variability for these two species using our approach (Eq. 4). This showed that the strain variability of *Escherichia coli* O157:H7 was 0.206 (n=17) as calculated by the $\log_{10}$ *D*-value at 55°C and 60°C, whereas for *S. aureus* the strain variability was 0.360 (n=15) as calculated by the $\log_{10}$ *D*-value at 58°C. Interestingly, these values are in the same order of magnitude as presented in Fig. 3.4c. To the best of our knowledge, for one species, namely *Salmonella* spp., reported differences in heat resistance among

strains isolated from various sources tend to be much smaller with σ_s values of 0.07 and 0.09 [6,11,41], and this supports the relevance to quantify the strain variability of this species in more detail. Quantified microbial variability is crucial information to be included in risk assessments to realistically predict microbial behaviour.

In conclusion, strain variability in conidial heat resistance of the three fungal species was in the same order of magnitude as for bacterial species, which hints to a natural diversity that stretches beyond kingdoms. In other fields of research, intraspecies variability also occurs in virulence, growth and biofilm formation [9], and an intriguing question is whether the impact of strain variability is also comparable for other microbial traits.

Experimental Procedures

Strain selection and identification

All strains were selected and obtained from the CBS culture collection and the working collection of the Food and Indoor Mycology (DTO) group, both housed at the Westerdijk Fungal Biodiversity Institute (Table 3.S1). Strains included the previously studied *A. niger* N402 [42], *P. roqueforti* DTO 377-G3 [29] and *Pae. variotii* DTO 032-I3, DTO 212-C5, DTO 217-A2 and DTO 280-E5 (CBS 101075) [25,43]. The other strains were selected from both food and non-food sources. Identity of strains was confirmed by sequencing the partial calmodulin (*caM*) gene for *A. niger* and the partial beta-tubulin (*benA*) gene for *P. roqueforti* and *Pae. variotii* that can be used as identification marker [44–46]. After alignment using MUSCLE, a maximum likelihood tree of each species was computed with 1,000 bootstrap replications using MEGA7 [47]. Reference sequences of closely related species and the type strain were included in the phylograms [24]. For each tree, the model with the lowest Bayesian Information Criterion (BIC) score was used. The Kimura 2-parameter model including gamma distribution (K2+G) was used for *A. niger*, and the Jukes-Cantor (JC) model and the Kimura 2-parameter model including invariant sites (K2+I) model were used for *P. roqueforti* and *Pae. variotii*, respectively.

Growth conditions and harvesting conidia

Culturing and harvesting of conidia were performed as described [25]. In short, fungal strains stored in 30% (w/v) glycerol at -20°C were spot-inoculated on malt extract agar (MEA, Oxoid, Hampshire, UK) and incubated for 7 days at 25°C. *A. niger* strains DTO 028-I3 and DTO 058-I1 were cultured at 30°C because sporulation was not sufficient at 25°C. Freshly harvested conidia were used to spread-inoculate a new MEA plate to anticipate on differences in age within the conidia population. Conidia were harvested after 7 days of incubation in ACES buffer (10 mM N(2-acetamido)-2-aminoethanesulfonic acid, 0.02% Tween 80, pH 6.8) and filtered using either sterile glass wool in a syringe or sterilized Amplitude EcoCloth wipes (Contec Europe, Vannes, France). Subsequently,

conidia were washed two times in ACES buffer. The concentration of conidia in suspension was determined using a Coulter Counter Multisizer 3 (Beckman Coulter, Life Sciences, Indianapolis, USA) [23], a Bio-Rad TC20 Automated Cell Counter (Bio-Rad Laboratories, Lunteren, The Netherlands), or a Bürker-Türk heamocytometer (VWR, Amsterdam, The Netherlands) and the conidia suspension was set at 2 * 10^8 conidia ml^{-1}.

Thermal treatments

A volume of 0.2 to 1 mL of conidia suspension was added to pre-heated ACES buffer to a total volume of 20 mL in Erlenmeyer flasks in a water bath. Conidia of *A. niger*, *P. roqueforti* and *Pae. variotii* were treated at 54°C, 56°C and 60°C, respectively. At various time points, 1 mL samples were taken, immediately chilled on ice, and decimally diluted. One hundred µL was surface-inoculated on MEA and plates were incubated at 25°C. The non-heated conidia suspension was also decimally diluted and subsequently plated to determine the initial viable concentration of conidia at *t*=0 minutes. Colonies of *Pae. variotii* were counted after three days of incubation, while *A. niger* and *P. roqueforti* colonies were counted after 7 days. The $\log_{10}$ colony forming units (CFU) mL^{-1} was calculated for each sampling time point.

Quantification of heat resistance

The reparameterised Weibull model (Eq. 1) [48] was fitted to the $\log_{10}$ CFU mL^{-1} data of each inactivation experiment with the R package Growthrates using the Levenberg-Marquardt algorithm [49]. The Weibull model allows fitting linear, concave, and convex inactivation curves and was able to fit the different thermal inactivation curves of the strains.

$$Log_{10}(N_t) = Log_{10}(N_0) - \Delta \cdot \left(\frac{t}{t_{\Delta D}}\right)^{\beta} \qquad (1)$$

where N_0 is the initial concentration of conidia (CFU mL^{-1}), N_t is the number of surviving conidia (CFU mL^{-1}) at time point t, Δ is the reference number of decimal reductions, $t_{\Delta D}$ represents the time needed to reduce the initial number of conidia with Δ decimals, and

the shape parameter where β > 1 gives a concave and β < 1 a convex behaviour. When β was significantly different from 1, the average *D*-value was estimated as $\frac{t_{\Delta D}}{\Delta}$. If not, the negative reciprocal of the linear regression slope, $\frac{-1}{slope}$, was used to estimate the *D*-value as described [25].

Quantification of variability

Experimental, biological and strain variabilities were quantified per species using the Aryani method [12]. For each strain, three biologically independent batches of conidial spores were prepared, and conidial heat resistance was tested in duplicate for each batch of conidial spores. Experimental variability (σ_e) was defined as the variability between parallel experimental replicates, and expressed by the root mean square error ($\sqrt{MSE_e}$) of Eq. 2

$$MSE_e = \frac{RSS_e}{DF_e} = \frac{\sum_{S=1}^{i}\sum_{B=1}^{3}\sum_{E=1}^{2}(X_{EBS}-X_{BS})^2}{n-p} \quad (2)$$

where MSE_e is mean square error, RSS_e is Residual Sum of Squares, DF_e is Degrees of Freedom, X_{EBS} is the $\log_{10}$ *D*-value of each experiment 'E' of biological replicate 'B' and strain 'S',X_{BS} is the average of the $\log_{10}$ *D*-value of the experimental duplicates of each biological replicate 'B' of strain 'S', *i* is the number of strains used per species and is the number of data points (*n = 2 * 3 * i*) minus the number of parameters (p = 3 * i).

Biological variability (σ_b) was expressed by $\sqrt{MSE_b}$ of Eq. 3

$$MSE_b = \frac{RSS_b}{DF_b} = \frac{\sum_{S=1}^{i}\sum_{B=1}^{3}(X_{BS}-X_S)^2}{n-p} \quad (3)$$

where X_s is the average of X_{BS} from the biological triplicates of strain 'S' and is the number of data points (*n = 3 * i*) minus the number of parameters (*p = 1 * i*).

Strain variability (σ_s) was expressed by $\sqrt{MSE_s}$ of Eq. 4

$$MSE_s = \frac{RSS_s}{DF_s} = \frac{\sum_{S=1}^{i}(X_S-X)^2}{n-p} \quad (4)$$

where *X* is the average of X_s of all *i* strains and DF_s is the number of data points (*n = i*) minus the number of parameters (*p = i*).

The 95% confidence intervals of σ_e, σ_b and σ_s were calculated according to Eq. 5

$$\sqrt{\frac{RSS}{\chi^2_{DF;\,\alpha/2}}} \leq \sigma \leq \sqrt{\frac{RSS}{\chi^2_{DF;\,1-\alpha/2}}} \quad (5)$$

where X^2 is the critical Chi-square value at α/2 and 1 - α/2 with α = 0.05, using the same *RSS* and *DF* definitions as in Eq. 2-4.

Meta-analysis

Data describing the inactivation kinetics of conidia of *A. niger* [50–57] and *P. roqueforti* [29,54,58–61] were collected from literature. The obtained *D*-values were $\log_{10}$ transformed and the mean $\log_{10}$ *D*-value of each strain tested in this study were added to the data set, resulting in 48 and 148 data points for *A. niger* and *P. roqueforti*, respectively. The $\log_{10}D$-values versus the temperature were used to calculated the *z*-value for each species, being negative reciprocal of the linear regression slope, $\frac{-1}{slope}$. Subsequently, the 95% prediction interval of the linear regression was calculated using Eq. 6

$$Log_{10}D_{ref} \pm t_{DF;\,1-0.5\alpha}\sqrt{\frac{RSS}{DF}} \quad (6)$$

Where D_{ref} is the reference $\log_{10}$ *D*-value at the reference temperature, *t* is the Student *t*-value with degrees of freedom (*DF*) *n - 2* and α = 0.05, *RSS* is the residual sum of squares calculated from the deviation of the data to the linear regression line. The overall variability (σ_t) was defined as the deviation of the data to the linear regression line, $\sqrt{\frac{RSS}{DF}}$ with *RSS* the residual sum of squares calculated from the deviation of the data to the linear regression line, and *n - 2*.

References

1. Papke RT, Ward DM. The importance of physical isolation to microbial diversification. FEMS Microbiol Ecol. 2004;48:293–303.

2. Andersson JO. Gene transfer and diversification of microbial eukaryotes. Annu Rev Microbiol. 2009;63:177–93.

3. Choudoir MJ, Panke-Buisse K, Andam CP, Buckley DH. Genome surfing as driver of microbial genomic diversity. Trends Microbiol. 2017;25:624–36.

4. Avery S V. Microbial cell individuality and the underlying sources of heterogeneity. Nat Rev Microbiol. 2006;4:577–87.

5. Ackermann M. A functional perspective on phenotypic heterogeneity in microorganisms. Nat Rev Microbiol. 2015;13:497–508.

6. Lianou A, Koutsoumanis KP. Evaluation of the strain variability of *Salmonella enterica* acid and heat resistance. Food Microbiol. 2013;34:259–67.

7. Stratford M, Steels H, Nebe-von-Caron G, Novodvorska M, Hayer K, Archer DB. Extreme resistance to weak-acid preservatives in the spoilage yeast *Zygosaccharomyces bailii*. Int J Food Microbiol. 2013;166:126–34.

8. den Besten HMW, Berendsen EM, Wells-Bennik MHJ, Straatsma H, Zwietering MH. Two complementary approaches to quantify variability in heat resistance of spores of *Bacillus subtilis*. Int J Food Microbiol. 2017;253:48–53.

9. Lianou A, Nychas GJE, Koutsoumanis KP. Strain variability in biofilm formation: A food safety and quality perspective. Food Res Int. 2020;137:109424.

10. Davies CR, Wohlgemuth F, Young T, Violet J, Dickinson M, Sanders JW, et al. Evolving challenges and strategies for fungal control in the food supply chain. Fungal Biol Rev. 2021;36:15–26.

11. Den Besten HMW, Wells-Bennik MHJ, Zwietering MH. Natural diversity in heat resistance of bacteria and bacterial spores: impact on food safety and quality. Annu Rev Food Sci Technol. 2018;9:383–410.

12. Aryani DC, den Besten HMW, Hazeleger WC, Zwietering MH. Quantifying variability on thermal resistance of *Listeria monocytogenes*. Int J Food Microbiol. 2015;193:130–8.

13. Aryani DC, den Besten HMW, Zwietering MH. Quantifying variability in growth and thermal inactivation kinetics of *Lactobacillus plantarum*. Appl Environ Microbiol. 2016;82:4896–908.

14. Zheng J, Wittouck S, Salvetti E, Franz CMAP, Harris HMB, Mattarelli P, et al. A taxonomic note

on the genus *Lactobacillus*: Description of 23 novel genera, emended description of the genus *Lactobacillus* Beijerinck 1901, and union of *Lactobacillaceae* and *Leuconostocaceae*. Int J Syst Evol Microbiol. 2020;70:2782–858.

15. Wells-Bennik MHJ, Janssen PWM, Klaus V, Yang C, Zwietering MH, Den Besten HMW. Heat resistance of spores of 18 strains of *Geobacillus stearothermophilus* and impact of culturing conditions. Int J Food Microbiol. 2019;291:161–72.

16. Wyatt TT, Wösten HAB, Dijksterhuis J. Fungal spores for dispersion in space and time. Adv Appl Microbiol. 2013;85:43–91.

17. Beuchat LR. Extraordinary heat resistance of *Talaromyces flavus* and *Neosartorya fischeri* ascospores in fruit products. J Food Sci. 1986;51:1506–10.

18. Van Leeuwen MR, Van Doorn TM, Golovina EA, Stark J, Dijksterhuis J. Water- and air-distributed conidia differ in sterol content and cytoplasmic microviscosity. Appl Environ Microbiol. 2010;76:366–9.

19. Henk DA, Eagle CE, Brown K, Van Den Berg MA, Dyer PS, Peterson SW, et al. Speciation despite globally overlapping distributions in *Penicillium chrysogenum*: The population genetics of Alexander Fleming's lucky fungus. Mol Ecol. 2011;20:4288–301.

20. Amend AS, Seifert KA, Samson R, Bruns TD. Indoor fungal composition is geographically patterned and more diverse in temperate zones than in the tropics. Proc Natl Acad Sci U S A. 2010;107:13748–53.

21. Shinn EA, Smith GW, Prospero JM, Betzer P, Hayes ML, Garrison V, et al. African dust and the demise of Caribbean coral reefs. Geophys Res Lett. 2000;27:3029–32.

22. Dijksterhuis J. The fungal spore and food spoilage. Curr Opin Food Sci. 2017;17:68–74.

23. van den Brule T, Lee CLS, Houbraken J, Haas PJ, Wösten H, Dijksterhuis J. Conidial heat resistance of various strains of the food spoilage fungus *Paecilomyces variotii* correlates with mean spore size, spore shape and size distribution. Food Res Int. 2020;137:109514.

24. Houbraken J, Kocsubé S, Visagie CM, Yilmaz N, Wang XC, Meijer M, et al. Classification of *Aspergillus*, *Penicillium*, *Talaromyces* and related genera (*Eurotiales*): An overview of families, genera, subgenera, sections, series and species. Stud Mycol. 2020;95:5–169.

25. van den Brule T, Punt M, Teertstra W, Houbraken J, Wösten H, Dijksterhuis J. The most heat-resistant conidia observed to date are formed by distinct strains of *Paecilomyces variotii*. Environ Microbiol. 2019;22:986–99.

26. Houbraken J, Varga J, Rico-Munoz E, Johnson S, Samson RA. Sexual reproduction as the cause of heat resistance in the food spoilage fungus *Byssochlamys spectabilis* (anamorph *Paeci-*

lomyces variotii). Appl Environ Microbiol. 2008;

27. Li L, Hu X, Xia Y, Xiao G, Zheng P, Wang C. Linkage of oxidative stress and mitochondrial dysfunctions to spontaneous culture degeneration in *Aspergillus nidulans*. Mol Cell Proteomics. 2014;13:449–61.

28. Hagiwara D, Sakai K, Suzuki S, Umemura M, Nogawa T, Kato N, et al. Temperature during conidiation affects stress tolerance, pigmentation, and trypacidin accumulation in the conidia of the airborne pathogen *Aspergillus fumigatus*. PLoS One. 2017;12:e0177050.

29. Punt M, van den Brule T, Teertstra WR, Dijksterhuis J, den Besten HMW, Ohm RA, et al. Impact of maturation and growth temperature on cell-size distribution, heat-resistance, compatible solute composition and transcription profiles of *Penicillium* roqueforti conidia. Food Res Int. 2020;136:109287.

30. van den Brule T, Punt M, Teertstra W, Houbraken J, Wösten H, Dijksterhuis J. The most heat-resistant conidia observed to date are formed by distinct strains of *Paecilomyces variotii*. Environ Microbiol. 2019;22:986–99.

31. Van Asselt ED, Zwietering MH. A systematic approach to determine global thermal inactivation parameters for various food pathogens. Int J Food Microbiol. 2006;107:73–82.

32. Berendsen EM, Boekhorst J, Kuipers OP, Wells-Bennik MHJ. A mobile genetic element profoundly increases heat resistance of bacterial spores. ISME J. Nature Publishing Group; 2016;10:2633–42.

33. Samson RA, Houbraken J, Thrane U, Frisvad JC, Andersen B. Food and Indoor Fungi. 2nd ed. Samson RA, Houbraken J, Thrane U, Frisvad JC, Andersen B, editors. Utrecht: Centraalbureau voor Schimmelcultures; 2019.

34. Hofstetter V, Buyck B, Eyssartier G, Schnee S, Gindro K. The unbearable lightness of sequenced-based identification. Fungal Divers. 2019.

35. Lücking R, Aime MC, Robbertse B, Miller AN, Ariyawansa HA, Aoki T, et al. Unambiguous identification of fungi: Where do we stand and how accurate and precise is fungal DNA barcoding? IMA Fungus. 2020;11:14.

36. Holland SL, Reader T, Dyer PS, Avery S V. Phenotypic heterogeneity is a selected trait in natural yeast populations subject to environmental stress. Environ Microbiol. 2014;16:1729–40.

37. Teertstra WR, Tegelaar M, Dijksterhuis J, Golovina EA, Ohm RA, Wösten HAB. Maturation of conidia on conidiophores of *Aspergillus niger*. Fungal Genet Biol. 2017;98:61–70.

38. Rangel DEN, Braga GUL, Fernandes ÉKK, Keyser CA, Hallsworth JE, Roberts DW. Stress tolerance and virulence of insect-pathogenic fungi are determined by environmental conditions

during conidial formation. Curr Genet. 2015;61:383–404.

39. van Leeuwen MR, Wyatt TT, van Doorn TM, Lugones LG, Wösten HAB, Dijksterhuis J. Hydrophilins in the filamentous fungus *Neosartorya fischeri* (*Aspergillus fischeri*) have protective activity against several types of microbial water stress. Environ Microbiol Rep. 2016;8:45–52.

40. van Leeuwen MR, Krijgsheld P, Bleichrodt R, Menke H, Stam H, Stark J, et al. Germination of conidia of *Aspergillus niger* is accompanied by major changes in RNA profiles. Stud Mycol. 2013;74:59–70.

41. Gurtler JB, Hinton A, Bailey RB, Cray WC, Meinersmann RJ, Ball TA, et al. *Salmonella* isolated from ready-to-eat pasteurized liquid egg products: Thermal resistance, biochemical profile, and fatty acid analysis. Int J Food Microbiol. 2015;206:109–17.

42. Bos CJ, Debets AJM, Swart K, Huybers A, Kobus G, Slakhorst SM. Genetic analysis and the construction of master strains for assignment of genes to six linkage groups in *Aspergillus niger*. Curr Genet. 1988;14:437–43.

43. Urquhart AS, Mondo SJ, Mäkelä MR, Hane JK, Wiebenga A, He G, et al. Genomic and genetic insights into a cosmopolitan fungus, *Paecilomyces variotii* (*Eurotiales*). Front Microbiol. 2018;9:3058.

44. Samson RA, Houbraken J, Varga J, Frisvad JC. Polyphasic taxonomy of the heat resistant ascomycete genus *Byssochlamys* and its *Paecilomyces* anamorphs. Persoonia Mol Phylogeny Evol Fungi. 2009;22:14–27.

45. Varga J, Frisvad JC, Kocsubé S, Brankovics B, Tóth B, Szigeti G, et al. New and revisited species in *Aspergillus* section *Nigri*. Stud Mycol. 2011;69:1–17.

46. Visagie CM, Houbraken J, Frisvad JC, Hong SB, Klaassen CHW, Perrone G, et al. Identification and nomenclature of the genus *Penicillium*. Stud Mycol. 2014;78:343–71.

47. Kumar S, Stecher G, Tamura K. MEGA7: Molecular Evolutionary Genetics Analysis version 7.0 for bigger datasets. Mol Biol Evol. 2016;33:1870–4.

48. Metselaar KI, Den Besten HMW, Abee T, Moezelaar R, Zwietering MH. Isolation and quantification of highly acid resistant variants of *Listeria monocytogenes*. Int J Food Microbiol. 2013;166:508–14.

49. Hall BG, Acar H, Nandipati A, Barlow M. Growth rates made easy. Mol Biol Evol. 2014;31:232–8.

50. Baggerman WI. Heat resistance of yeast cells and fungal spores. In: Samson RA, Hoekstra ES, van Oorschot CAN, editors. Introd to food-borne fungi. Utrecht: Centraalbureau voor Schimmelcultures (CBS); 1981. p. 227–31.

51. Ballestra P, Cuq J-L. Influence of pressurized carbon dioxide on the thermal inactivation of bacterial and fungal spores. LWT-Food Sci Technol. 1998;31:84–8.

52. Rege AR, Pai JS. Development of thermal process for clarified pomegranate (*Punica granatum*) juice. J Food Sci Technol. 1999;36:261–3.

53. Fujikawa H, Morozumi S, Smerage GH, Teixeira AA. Comparison of capillary and test tube procedures for analysis of thermal inactivation kinetics of mold spores. J Food Prot. 2000;63:1404–9.

54. Shearer AEH, Mazzotta AS, Chuyate R, Gombas DE. Heat resistance of juice spoilage microorganisms. J Food Prot. 2002;65:1271–5.

55. Reveron IM, Barreiro JA, Sandoval AJ. Thermal death characteristics of *Lactobacillus paracasei* and *Aspergillus niger* in Pilsen beer. J Food Eng. 2005;66:239–43.

56. Esbelin J, Mallea S, Ram AFJ, Carlin F. Role of pigmentation in protecting *Aspergillus niger* conidiospores against pulsed light radiation. Photochem Photobiol. 2013;89:758–61.

57. Belbahi A, Bohuon P, Leguérinel I, Meot JM, Loiseau G, Madani K. Heat resistances of *Candida apicola* and *Aspergillus niger* spores isolated from date fruit surface. J Food Process Eng. 2017;40:e12272.

58. Kunz B. Untersuchungen über den einfluß der temperatur auf konidiensuspensionen ausgewählter Penicillienspecies. Food/Nahrung. 1981;25:185–91.

59. Broker U, Spicher G, Ahrens E. Zur frage der hitzeresistenz der erreger der schimmelbildung bei backwaren. 3. Mitteilung: Einfluß exogener faktoren auf die hitzeresistenz von schimmelsporen. Getreide, Mehl und Brot. 1987;41:344–50.

60. Broker U, Spicher G, Ahrens E. Zur frage der hitzeresistenz der erreger der schimmelbildung bei backwaren. 2. Mitteilung: Einfluß endogener faktoren auf die hitzeresistenz von schimmelsporen. Getreide, Mehl und Brot. 1987;41:278–84.

61. Blank G, Yang R, Scanlon MG. Influence of sporulation a_w on heat resistance and germination of *Penicillium roqueforti* spores. Food Microbiol. 1998;15:151–6.

Additional files

Table 3.S1. Overview of the strains used in this study

	Strain No.	Other collections	Substrate	Location	Genbank accession number[A]	Reference
Aspergillus niger	DTO 008-C3	CBS 113.50	Leather	Germany	MW148182	1
	DTO 028-I3	CBS 112.32	Unknown	Japan	MW148184	1
	DTO 029-B1	CBS 124.48	Unknown	Ghana	MW148185	
	DTO 058-I1	CBS 118.52	Unknown	Unknown	MW148186	
	DTO 096-A5	CBS 147371; IBT 20381	Green coffee bean	India	GU195635	2
	DTO 096-A7	CBS 147320; IBT 22937	Grape	Australia	MW148187	
	DTO 096-A9	CBS 147321; IBT 23366	Artic soil	Svalbard, Norway	MW148188	
	DTO 096-C6	CBS 147322; IBT 27294	Coffee	Brazil	MW148189	
	DTO 096-D7	CBS 147323; IBT 29331	Raisin	Turkey	MW148190	
	DTO 096-E1	CBS 147324; IBT 29884; NRRL 615			MW148191	3
	DTO 175-I5	CBS 147482	Surface Water	Portugal	MW148192	
	DTO 293-G7	CBS 147344	Coffee beans (Robusta)	Thailand	MW148193	
	DTO 316-E3	CBS 133816; IBT 24631	Black pepper	Denmark	GU195636	2
	DTO 316-E4	CBS 147345; IBT 26389; NRRL 599			MW148194	4
	DTO 321-E6	CBS 147346	CF patient material	the Netherlands	MW148195	
	DTO 326-A7	CBS 147347	Petridish from soft drink factory	the Netherlands	MW148196	
	DTO 367-D1	CBS 769.97	Leather	Germany	MW148197	
	DTO 367-D6	CBS 115989; NRRL 3122			MW148198	5
	DTO 368-I1	CBS 147352	Air next to bottle blower	Mexico	MW148199	
	DTO 368-I6	CBS 147353	Food factory	Italy	MW148200	
	N402	ATCC 64974			MW148183	6
Penicillium roqueforti	DTO 003-H1	CBS 147308	Environment dairy factory	the Netherlands	MW148162	
	DTO 012-A2	CBS 147309	Tortilla (flour)	California, USA	MW148163	
	DTO 012-A6	CBS 147310	Tortilla (corn)	California, USA	MW148164	
	DTO 013-F5	CBS 147311	Margarine	the Netherlands	MW148165	
	DTO 070-G2	CBS 147317	Wood	Unknown	MW148166	
	DTO 081-F9	CBS 147318	Air in cheese warehouse	the Netherlands	MW148167	
	DTO 101-D6	CBS 147325	Cheese surface	the Netherlands	MW148168	
	DTO 102-I9	CBS 147326	Drink	The Netherlands	MW148169	
	DTO 126-G2	CBS 147330	Air in bakery	USA	MW148170	
	DTO 127-F7	CBS 147331	Chicory root extract	the Netherlands	MW148171	
	DTO 127-F9	CBS 147332	Chicory root extract	the Netherlands	MW148172	
	DTO 130-C1	CBS 147333	Air of cheese factory	the Netherlands	MW148173	
	DTO 163-C3	CBS 147337	Single ascospore isolate of DTO 006-G1 and DTO 027-I6	the Netherlands	MW148174	
	DTO 163-F5	CBS 147338	Cheese, Garstang Blue	UK	MW148175	
	DTO 163-G4	CBS 147339	Barley	Denmark	MW148176	
	DTO 265-D5	CBS 147372	Edge of brine bath	the Netherlands	MW148177	
	DTO 369-A1	CBS 147354	From mayonnaise, containing K-sorbate	The Netherlands	MW148178	
	DTO 375-B1	CBS 147355	Cheese	Mexico	MW148179	
	DTO 377-G2	LCP 96.3914	Stewed fruit	France	MW148180	7
	DTO 377-G3	LCP 97.4111	Wood	France	MW148181	7
Paecilomyces variotii	DTO 021-C3	CBS 145656	Spoiled sports drink	USA	MN153215	8
	DTO 021-D3	CBS 145657	Heat shocked sucrose	USA	MN153219	8
	DTO 027-B3	CBS 121577	Spoiled sports drink	USA	EU037084	9
	DTO 027-B5	CBS 121579	Sucrose	USA	EU037082	9
	DTO 027-B6	CBS 121580	Spoiled apple juice	The Netherlands	EU037081	9
	DTO 027-B9	CBS 121583	Spoiled sports drink	USA	EU037078	9
	DTO 032-I3	CBS 121585	High Fructose Corn Syrup after heat shock	USA	EU037077	9
	DTO 045-G8	CBS 145658	Drink	USA	MN153224	8
	DTO 164-E3	CBS 145659	Blue berry ingredients	The Netherlands	MN153240	8
	DTO 166-G4	CBS 145660	Pectin, heat treated	The Netherlands	MN153245	8
	DTO 195-F2	CBS 145663	Margarine	Belgium	MN153269	8
	DTO 207-G8	CBS 145664	Fruit, ingredient	The Netherlands	MN153270	8
	DTO 212-C5	CBS 145665	Vanilla	The Netherlands	MN153271	8
	DTO 217-A2	CBS 145666	Ice pop, heat treated	The Netherlands	MN153275	8
	DTO 271-D3	CBS 145667	Industry environment	Guatamala	MN153286	8
	DTO 271-G3	CBS 145668	Ice tea	South Africa	MN153287	8
	DTO 280-E4	CBS 109073	Pectin	The Netherlands	EU037070	9
	DTO 280-E5	CBS 101075	Heat processed fruit beverage	Japan	EU037069	9
	DTO 282-E5	CBS 145669	Margarine	Italy	MN153294	8
	DTO 282-F9	CBS 145670	Wall covering, industry environment	UK	MN153297	8

[A]Genbank accession numbers of partial *caM* gene sequences for the studied *A. niger* strains and partial *benA* gene sequences for the *P. roqueforti* and *P. variotii* strains.

References

1 Meijer M, Houbraken J, Dalhuijsen S, Samson R, De Vries R. 2011. Growth and hydrolase profiles can be used as characteristics to distinguish *Aspergillus niger* and other black aspergilli. Stud Mycol 69:19-30.

2 Mogensen JM, Nielsen KF, Samson RA, Frisvad JC, Thrane U. 2009. Effect of temperature and water activity on the production of fumonisins by *Aspergillus niger* and different Fusarium species. BMC Microbiol 9:281.

3 Moyer AJ. 1953. Effect of alcohols on the mycological production of citric acid in surface and submerged culture. II. Fermentation of crude carbohydrates. Appl Microbiol 1:7-13.

4 Ramachandran K, Walker TK. 1951. A biosynthesis of dimethylpyruvic acid. Arch Biochem Biophys 31:224-233.

5 Van Lanen JM, Smith MB. 1968. Process of producing glucamylase and an alcohol product. Hiram Walker & Sons Inc. US patent 3418211.

6 Bos CJ, Debets AJM, Swart K, Huybers A, Kobus G, Slakhorst SM. 1988. Genetic analysis and the construction of master strains for assignment of genes to six linkage groups in *Aspergillus niger*. Curr Genet 14:437-443.

7 Ropars J, Cruaud C, Lacoste S, Dupont J. 2012. A taxonomic and ecological overview of cheese fungi. Int J Food Microbiol 155:199-210.

8 van den Brule T, Punt M, Teertstra W, Houbraken J, Wösten H, Dijksterhuis J. 2020. The most heat-resistant conidia observed to date are formed by distinct strains of *Paecilomyces variotii*. Environ Microbiol 22:986-999.

9 Houbraken J, Varga J, Rico-Munoz E, Johnson S, Samson RA. 2008. Sexual reproduction as the cause of heat resistance in the food spoilage fungus *Byssochlamys spectabilis* (anamorph *Paecilomyces variotii*). Appl Environ Microbiol 74:1613-9.

Table 3.S2. D-values of experimental replicates (E) and biological replicates (B) of all strains used in this study. Shaping parameter β including 95% confidence interval (CI) of the Weibull model was used to check significance of the model.

A. niger Strain	B	E	D_{90}-value	β [95% CI]	*P. roquefortii* Strain	B	E	D_{90}-value	β [95% CI]	*Pae. variotii* Strain	B	E	D_{90}-value	β [95% CI]
DTO 008-C3	1	1	12.6	1.3 [0.82 - 1.78]	DTO 003-H1	1	1	4.3	1.11 [0.65 - 1.58]	DTO 021-C3	1	1	12.9	1.18 [1.04 - 1.31]
		2	11.6	1.16 [0.8 - 1.52]			2	4.4	1.06 [0.64 - 1.47]			2	13.5	1.05 [0.8 - 1.3]
	2	1	16.3	1.61 [0.55 - 2.67]		2	1	5.5	0.91 [0.53 - 1.3]		2	1	15.4	1.27 [0.68 - 1.85]
		2	15.5	1.51 [0.44 - 2.59]			2	5.7	0.82 [0.5 - 1.14]			2	15.5	1.37 [1.09 - 1.66]
	3	1	11.8	1.33 [0.63 - 2.02]		3	1	5.3	1.02 [0.28 - 1.77]		3	1	11.8	1.34 [0.86 - 1.83]
		2	11.7	1.48 [1.21 - 1.75]			2	7.7	0.7 [0.13 - 1.28]			2	12.1	1.17 [1.11 - 1.22]
DTO 028-I3	1	1	13.3	0.51 [0.32 - 0.7]	DTO 012-A2	1	1	5.2	1.15 [0.81 - 1.5]	DTO 021-D3	1	1	3.3	1.12 [0.47 - 1.77]
		2	13.1	0.47 [0.27 - 0.66]			2	5.0	1.26 [0.94 - 1.58]			2	3.5	1.27 [-0.98 - 3.51]
	2	1	14.3	0.43 [0.23 - 0.63]		2	1	4.0	1.11 [0.82 - 1.39]		2	1	4.6	1.2 [0.12 - 2.28]
		2	13.9	0.42 [0.22 - 0.63]			2	3.9	1.11 [0.53 - 1.69]			2	4.4	1.07 [-0.92 - 3.07]
	3	1	10.1	0.29 [0.15 - 0.44]		3	1	4.5	1.19 [0.53 - 1.86]		3	1	5.4	0.83 [0.28 - 1.39]
		2	11.0	0.3 [0.13 - 0.48]			2	4.6	1.28 [0.78 - 1.79]			2	5.2	0.83 [0.3 - 1.37]
DTO 029-B1	1	1	3.7	0.58 [0.17 - 0.99]	DTO 012-A6	1	1	7.9	0.94 [0.2 - 1.67]	DTO 027-B3	1	1	4.0	0.89 [0.76 - 1.02]
		2	4.7	0.83 [-0.54 - 2.2]			2	8.0	0.88 [0.11 - 1.65]			2	4.0	1 [0.66 - 1.34]
	2	1	3.4	1.01 [0.27 - 1.75]		2	1	7.6	2.43 [1.96 - 2.9]		2	1	7.3	0.88 [0.48 - 1.28]
		2	3.0	1.08 [0.41 - 1.75]			2	9.2	1.27 [0.45 - 2.09]			2	7.4	0.94 [0.43 - 1.45]
	3	1	3.7	1.08 [0.32 - 1.84]		3	1	7.4	2.61 [2.06 - 3.16]		3	1	6.4	0.79 [0.39 - 1.19]
		2	3.9	1.23 [-0.18 - 2.65]			2	7.7	2.51 [1.95 - 3.07]			2	6.0	0.8 [0.63 - 0.97]
DTO 058-I1	1	1	7.3	0.61 [0.32 - 0.9]	DTO 013-F5	1	1	14.8	1.94 [1.6 - 2.28]	DTO 027-B5	1	1	7.1	0.96 [0.36 - 1.56]
		2	6.8	0.6 [0.31 - 0.89]			2	15.6	1.6 [1.29 - 1.91]			2	6.7	1.45 [0.94 - 1.96]
	2	1	11.4	0.7 [0.5 - 0.9]		2	1	16.0	2 [1.88 - 2.13]		2	1	10.3	1.16 [0.54 - 1.77]
		2	11.5	0.7 [0.48 - 0.92]			2	15.8	2.26 [1.9 - 2.61]			2	11.1	0.99 [0.76 - 1.22]
	3	1	11.3	0.87 [0.53 - 1.21]		3	1	9.1	1.56 [1.1 - 2.02]		3	1	7.7	0.85 [0.47 - 1.22]
		2	11.2	1.11 [0.69 - 1.53]			2	10.5	1.86 [1.39 - 2.34]			2	7.1	0.98 [0.36 - 1.61]
DTO 096-A5	1	1	13.3	1.05 [0.62 - 1.47]	DTO 070-G2	1	1	8.1	1.01 [0.4 - 1.62]	DTO 027-B6	1	1	4.1	1.51 [0.57 - 2.44]
		2	12.7	1.09 [0.43 - 1.75]			2	7.5	1.7 [1.28 - 2.12]			2	4.0	1.19 [0.04 - 2.34]
	2	1	13.6	0.94 [0.12 - 1.76]		2	1	6.6	0.53 [0.18 - 0.89]		2	1	6.1	0.95 [0.46 - 1.43]
		2	14.9	0.87 [0.05 - 1.69]			2	4.5	1.02 [0.8 - 1.24]			2	6.1	1.05 [0.68 - 1.43]
	3	1	15.0	1.05 [0.63 - 1.48]		3	1	7.8	1.18 [0.38 - 1.97]		3	1	7.0	0.95 [0.44 - 1.45]
		2	15.3	1.31 [0.67 - 1.96]			2	7.2	1.97 [1.05 - 2.89]			2	6.8	0.99 [0.39 - 1.59]
DTO 096-A7	1	1	18.5	1.35 [1.14 - 1.57]	DTO 081-F9	1	1	7.3	2.14 [1.74 - 2.54]	DTO 027-B9	1	1	11.6	0.88 [0.62 - 1.14]
		2	17.4	1.2 [0.8 - 1.6]			2	7.5	2.04 [1.79 - 2.29]			2	9.4	1.05 [0.96 - 1.14]
	2	1	21.3	1.14 [0.77 - 1.5]		2	1	6.0	1.75 [0.72 - 2.77]		2	1	6.6	0.83 [0.57 - 1.08]
		2	22.0	1.03 [0.48 - 1.58]			2	7.8	5 [-0.71 - 10.71]			2	6.2	0.82 [0.64 - 1]
	3	1	19.5	1.18 [0.97 - 1.39]		3	1	2.5	1.8 [1.38 - 2.23]		3	1	8.1	0.73 [0.39 - 1.06]
		2	19.8	1.24 [0.9 - 1.57]			2	2.5	1.63 [1.22 - 2.04]			2	8.4	0.74 [0.09 - 1.38]
DTO 096-A9	1	1	15.3	0.62 [-0.06 - 1.3]	DTO 101-D6	1	1	6.8	0.9 [0.54 - 1.25]	DTO 032-I3	1	1	5.4	1.03 [0.64 - 1.42]
		2	14.1	0.68 [-0.03 - 1.39]			2	8.1	0.77 [0.47 - 1.06]			2	4.8	0.8 [-0.02 - 1.63]
	2	1	13.7	0.6 [0.16 - 1.04]		2	1	5.9	1.11 [0.89 - 1.33]		2	1	6.8	0.94 [0.51 - 1.36]
		2	10.6	0.58 [0.17 - 0.99]			2	6.1	1.26 [1.14 - 1.39]			2	6.6	0.98 [0.5 - 1.45]
	3	1	10.6	0.7 [0.2 - 1.2]		3	1	6.5	0.95 [0.77 - 1.14]		3	1	5.9	1.03 [0.71 - 1.34]
		2	10.6	0.7 [0.16 - 1.23]			2	6.3	0.95 [0.88 - 1.02]			2	5.8	1.06 [0.91 - 1.2]
DTO 096-C6	1	1	43.4	0.66 [0.02 - 1.3]	DTO 102-I9	1	1	7.5	1.09 [0.62 - 1.55]	DTO 045-G8	1	1	7.3	1.21 [1.04 - 1.37]
		2	46.4	1.78 [1.14 - 2.42]			2	9.8	0.79 [0.51 - 1.07]			2	6.3	1.42 [1.2 - 1.65]
	2	1	29.6	1.32 [0.74 - 1.89]		2	1	7.8	0.64 [0.38 - 0.9]		2	1	6.4	0.92 [0.6 - 1.24]
		2	30.3	1.32 [0.69 - 1.95]			2	7.4	0.82 [0.37 - 1.27]			2	6.2	1.01 [0.82 - 1.2]
	3	1	31.9	1.31 [0.66 - 1.96]		3	1	5.7	0.58 [0.17 - 0.98]		3	1	10.0	0.75 [0.41 - 1.09]
		2	31.1	1.54 [1.18 - 1.89]			2	6.1	0.62 [0.26 - 0.98]			2	7.5	0.96 [0.67 - 1.25]
DTO 096-D7	1	1	28.0	1.27 [0.73 - 1.81]	DTO 126-G2	1	1	3.9	1.38 [0.85 - 1.92]	DTO 164-E3	1	1	5.1	0.81 [0.6 - 1.02]
		2	31.2	1.43 [0.17 - 2.69]			2	4.1	1.37 [1 - 1.74]			2	6.0	0.83 [0.4 - 1.26]
	2	1	28.1	1.39 [1.32 - 1.46]		2	1	3.7	1.43 [0.91 - 1.95]		2	1	4.5	0.89 [-0.07 - 1.84]
		2	25.5	1.99 [1.28 - 2.7]			2	3.8	1.39 [0.91 - 1.87]			2	5.1	0.88 [0.82 - 0.94]
	3	1	44.6	2.8 [-0.08 - 5.68]		3	1	4.2	1.61 [1.3 - 1.93]		3	1	6.3	0.79 [0.28 - 1.3]
		2	39.0	2 [1.29 - 2.71]			2	4.5	1.64 [-0.01 - 3.28]			2	6.7	0.8 [0.69 - 0.92]
DTO 096-E1	1	1	26.2	1.19 [0.83 - 1.55]	DTO 127-F7	1	1	3.9	1.44 [1.14 - 1.75]	DTO 166-G4	1	1	9.0	0.69 [0.23 - 1.16]
		2	19.6	1.07 [0.7 - 1.44]			2	3.9	1.82 [1.53 - 2.11]			2	8.4	0.86 [0.7 - 1.02]
	2	1	32.5	0.66 [0.42 - 0.89]		2	1	4.3	1.51 [0.66 - 2.37]		2	1	11.2	0.82 [0.41 - 1.23]
		2	30.9	0.71 [0.55 - 0.88]			2	5.2	0.83 [0.24 - 1.42]			2	10.4	0.92 [0.69 - 1.15]
	3	1	21.8	0.6 [0.34 - 0.86]		3	1	3.1	1.39 [1.08 - 1.71]		3	1	11.6	1.11 [0.9 - 1.32]
		2	20.8	0.67 [0.4 - 0.93]			2	3.0	1.67 [1.28 - 2.06]			2	11.4	1.2 [0.91 - 1.48]
DTO 175-I5	1	1	14.2	1.57 [0.1 - 3.03]	DTO 127-F9	1	1	5.3	1.66 [1.2 - 2.12]	DTO 195-F2	1	1	24.2	0.72 [0.32 - 1.12]
		2	15.3	1.4 [0.33 - 2.48]			2	4.9	1.86 [1.14 - 2.57]			2	21.3	0.71 [0.48 - 0.94]
	2	1	21.9	0.74 [0.32 - 1.15]		2	1	5.5	1.55 [0.76 - 2.35]		2	1	28.2	0.84 [0.67 - 1.02]
		2	20.2	0.86 [0.45 - 1.26]			2	5.6	1.16 [0.77 - 1.54]			2	26.4	1 [0.67 - 1.32]
	3	1	19.5	0.67 [0.41 - 0.92]		3	1	6.0	1.67 [1.28 - 2.06]		3	1	30.4	1.22 [0.42 - 2.02]
		2	18.0	0.92 [0.56 - 1.28]			2	6.0	1.65 [1.22 - 2.08]			2	29.2	0.79 [0.44 - 1.14]
DTO 293-G7	1	1	30.5	0.62 [0.33 - 0.92]	DTO 130-C1	1	1	1.9	0.99 [0.1 - 1.87]	DTO 207-G8	1	1	5.6	0.97 [0.27 - 1.67]
		2	33.9	0.57 [0.29 - 0.85]			2	1.7	1.02 [0.59 - 1.46]			2	5.8	1.07 [0.93 - 1.2]
	2	1	16.1	0.96 [0.19 - 1.73]		2	1	2.0	0.72 [0.14 - 1.31]		2	1	6.9	0.9 [0.26 - 1.53]
		2	16.3	0.96 [0.23 - 1.68]			2	1.6	0.93 [-0.36 - 2.23]			2	6.9	0.96 [0.54 - 1.38]
	3	1	28.6	0.79 [0.31 - 1.27]		3	1	1.1	NA		3	1	8.2	0.83 [0.61 - 1.06]
		2	26.1	0.81 [0.29 - 1.32]			2	1.1	NA			2	7.8	0.89 [0.51 - 1.12]
DTO 316-E3	1	1	47.5	2.43 [0.19 - 4.67]	DTO 163-C3	1	1	9.0	1.54 [1.12 - 1.97]	DTO 212-C5	1	1	3.6	0.97 [-1.73 - 3.68]
		2	39.9	1.38 [1.01 - 1.74]			2	7.6	1.54 [0.89 - 2.19]			2	4.0	1.22 [-2.85 - 5.28]
	2	1	37.7	0.97 [0.57 - 1.37]		2	1	6.1	1.62 [1.17 - 2.07]		2	1	3.4	1.08 [-0.44 - 2.59]
		2	37.6	0.9 [0.6 - 1.21]			2	5.5	1.41 [0.83 - 2]			2	3.2	1.03 [-1.29 - 3.35]
	3	1	18.9	1.15 [0.53 - 1.77]		3	1	5.4	1.79 [1.25 - 2.32]		3	1	3.8	1.24 [0.27 - 2.01]
		2	25.1	0.82 [0.33 - 1.32]			2	6.2	1.7 [-0.07 - 3.46]			2	3.2	1.24 [-2 - 4.49]
DTO 316-E4	1	1	15.8	1.2 [0.77 - 1.63]	DTO 163-F5	1	1	5.2	1.24 [1.03 - 1.44]	DTO 217-A2	1	1	24.5	0.79 [0.56 - 1.03]
		2	26.3	1.05 [0.63 - 1.46]			2	5.6	1 [0.74 - 1.26]			2	22.5	0.91 [0.54 - 1.29]
	2	1	18.0	0.96 [0.43 - 1.5]		2	1	6.3	2.17 [1.15 - 3.2]		2	1	19.2	1.02 [0.86 - 1.19]
		2	17.5	0.98 [0.5 - 1.47]			2	7.3	2.32 [0.91 - 3.72]			2	18.7	1.07 [0.98 - 1.16]
	3	1	14.5	0.54 [0.29 - 0.78]		3	1	3.9	1.21 [0.87 - 1.55]		3	1	16.3	1.28 [1.03 - 1.53]
		2	12.2	0.78 [0.58 - 0.97]			2	4.6	1.04 [0.67 - 1.41]			2	15.2	1.24 [0.95 - 1.53]
DTO 321-E6	1	1	47.1	0.41 [0.17 - 0.65]	DTO 163-G4	1	1	4.1	1.16 [0.92 - 1.39]	DTO 271-D3	1	1	7.2	0.83 [0.56 - 1.09]
		2	37.8	0.68 [0.35 - 1]			2	4.4	0.91 [0.5 - 1.32]			2	8.6	0.91 [0.61 - 1.21]
	2	1	28.3	0.74 [0.18 - 1.3]		2	1	5.1	0.67 [0.29 - 1.05]		2	1	8.4	1.03 [0.83 - 1.24]
		2	26.5	0.77 [0.25 - 1.29]			2	4.5	0.86 [0.63 - 1.09]			2	7.4	1.06 [0.94 - 1.18]
	3	1	23.8	0.71 [0.35 - 1.06]		3	1	4.3	0.87 [0.68 - 1.06]		3	1	7.8	1.26 [0.66 - 1.86]
		2	24.9	0.63 [0.22 - 1.04]			2	3.7	0.83 [0.34 - 1.32]			2	6.4	1.09 [0.88 - 1.3]
DTO 326-A7	1	1	59.8	1.03 [0.31 - 1.74]	DTO 265-D5	1	1	5.8	1.13 [0.63 - 1.64]	DTO 271-G3	1	1	5.9	0.85 [0.57 - 1.14]
		2	45.9	1.3 [1.04 - 1.56]			2	5.3	0.81 [0.43 - 1.19]			2	6.3	0.86 [0.29 - 1.43]
	2	1	50.9	1.32 [0.95 - 1.69]		2	1	4.2	1.1 [0.86 - 1.35]		2	1	3.7	1.41 [0.42 - 2.39]
		2	66.5	1.18 [0.79 - 1.56]			2	4.2	1.17 [0.85 - 1.49]			2	2.9	1.25 [0.7 - 1.8]
	3	1	47.5	0.9 [0.53 - 1.27]		3	1	4.5	1.08 [0.5 - 1.66]		3	1	3.2	1.37 [0.78 - 1.96]
		2	32.2	1.75 [0.8 - 2.7]			2	3.9	1.06 [0.03 - 2.1]			2	4.7	0.83 [-0.5 - 2.16]
DTO 367-D1	1	1	10.8	1.06 [-0.3 - 2.43]	DTO 369-A1	1	1	3.8	0.77 [0.25 - 1.3]	DTO 280-E4	1	1	6.3	0.7 [0.58 - 0.82]
		2	8.9	1.05 [0.4 - 1.7]			2	5.5	0.57 [0.06 - 1.08]			2	6.5	0.85 [0.6 - 1.1]
	2	1	9.2	0.69 [0.52 - 0.86]		2	1	3.6	1 [0.53 - 1.47]		2	1	4.5	0.78 [-0.43 - 1.98]
		2	9.8	0.77 [0.57 - 0.97]			2	4.0	0.99 [0.7 - 1.28]			2	3.8	0.86 [-0.6 - 2.32]
	3	1	9.5	0.91 [0.48 - 1.34]		3	1	3.2	1.09 [0.46 - 1.73]		3	1	6.2	0.85 [0.63 - 1.07]
		2	8.3	0.72 [0.34 - 1.09]			2	3.7	0.82 [0.42 - 1.23]			2	6.4	0.84 [0.67 - 1.02]
DTO 367-D6	1	1	15.9	1.01 [0.41 - 1.61]	DTO 375-B1	1	1	5.2	1.32 [0.76 - 1.89]	DTO 280-E5	1	1	5.1	0.81 [0.6 - 1.02]
		2	15.1	0.9 [0.46 - 1.35]			2	4.3	1.69 [0.45 - 2.94]			2	6.0	0.83 [0.4 - 1.26]
	2	1	15.3	1.06 [0.57 - 1.55]		2	1	4.7	1.37 [0.63 - 2.11]		2	1	6.8	0.74 [0.34 - 1.15]
		2	15.0	0.95 [0.58 - 1.31]			2	3.9	1.36 [0.68 - 2.04]			2	6.5	0.75 [0.39 - 1.11]
	3	1	14.0	0.8 [0.48 - 1.12]		3	1	4.7	1.28 [0.91 - 1.66]		3	1	6.0	0.9 [0.66 - 1.13]
		2	14.6	0.71 [0.39 - 1.03]			2	4.4	1.17 [0.7 - 1.63]			2	5.8	0.94 [0.67 - 1.21]
DTO 368-I1	1	1	39.5	1.91 [1.36 - 2.45]	DTO 377-G2	1	1	5.2	0.99 [0.77 - 1.22]	DTO 282-E5	1	1	16.1	0.73 [0.36 - 1.1]
		2	40.1	1.92 [1.23 - 2.61]			2	6.2	0.88 [0.7 - 1.07]			2	13.7	0.72 [0.48 - 0.96]
	2	1	22.7	1.01 [0.57 - 1.46]		2	1	6.2	0.67 [0.3 - 1.03]		2	1	11.7	0.87 [0.76 - 0.97]
		2	20.5	1.29 [0.79 - 1.79]			2	5.9	0.63 [0.32 - 0.94]			2	11.5	0.8 [0.51 - 1.09]
	3	1	33.3	0.69 [0.37 - 1.02]		3	1	7.2	1.11 [0.86 - 1.36]		3	1	14.2	0.72 [0.49 - 0.96]
		2	34.8	0.65 [0.26 - 1.04]			2	7.5	0.99 [0.83 - 1.16]			2	13.5	0.67 [0.44 - 0.89]
DTO 368-I6	1	1	34.4	0.9 [0.6 - 1.2]	DTO 377-G3	1	1	7.0	0.97 [0.35 - 1.59]	DTO 282-F9	1	1	17.0	1.12 [0.84 - 1.39]
		2	31.4	1.32 [0.89 - 1.76]			2	7.5	0.99 [0.64 - 1.35]			2	15.4	1.2 [1.07 - 1.33]
	2	1	31.3	1.3 [0.35 - 2.26]		2	1	5.1	0.83 [0.63 - 1.02]		2	1	13.8	1.17 [0.9 - 1.44]
		2	37.0	1.87 [1.28 - 2.47]			2	3.9	1.19 [0.67 - 1.71]			2	14.2	1.26 [1.1 - 1.43]
	3	1	32.1	1.59 [1 - 2.18]		3	1	4.6	1.5 [1.09 - 1.92]		3	1	14.5	1.01 [0.89 - 1.13]
		2	31.2	1.27 [1.01 - 1.54]			2	4.1	1.69 [1.17 - 2.2]			2	14.5	1 [0.9 - 1.09]
N402	1	1	28.5	1.32 [0.54 - 2.09]										
		2	26.7	1.24 [0.75 - 1.73]										
	2	1	33.3	1.54 [0.92 - 2.16]										
		2	32.2	1.6 [1.08 - 2.12]										
	3	1	34.8	1.24 [0.88 - 1.59]										
		2	33.4	1.15 [0.83 - 1.48]										

CHAPTER 4

Genome sequencing of the neotype strain CBS 554.65 reveals the MAT1-2 locus of *Aspergillus niger*

Valeria Ellena, Sjoerd J. Seekles, Gabriel A. Vignolle, Arthur F.J. Ram,

Matthias G. Steiger

Published in: BMC Genomics (2021), 22, 679.
DOI: https://doi.org/10.1186/s12864-021-07990-8

Abstract

Background

Aspergillus niger is a ubiquitous filamentous fungus widely employed as a cell factory thanks to its abilities to produce a wide range of organic acids and enzymes. Its genome was one of the first *Aspergillus* genomes to be sequenced in 2007, due to its economic importance and its role as model organism to study fungal fermentation. Nowadays, the genome sequences of more than 20 *A. niger* strains are available. These, however, do not include the neotype strain CBS 554.65.

Results

The genome of CBS 554.65 was sequenced with PacBio. A high-quality nuclear genome sequence consisting of 17 contigs with a N50 value of 4.07 Mbp was obtained. The assembly covered all the 8 centromeric regions of the chromosomes. In addition, a complete circular mitochondrial DNA assembly was obtained. Bioinformatic analyses revealed the presence of a MAT1-2-1 gene in this genome, contrary to the most commonly used *A. niger* strains, such as ATCC 1015 and CBS 513.88, which contain a MAT1-1-1 gene. A nucleotide alignment showed a different orientation of the MAT1-1 locus of ATCC 1015 compared to the MAT1-2 locus of CBS 554.65, relative to conserved genes flanking the MAT locus. Within 24 newly sequenced isolates of *A. niger* half of them had a MAT1-1 locus and the other half a MAT1-2 locus. The genomic organization of the MAT1-2 locus in CBS 554.65 is similar to other *Aspergillus* species. In contrast, the region comprising the MAT1-1 locus is flipped in all sequenced strains of *A. niger*.

Conclusions

This study, besides providing a high-quality genome sequence of an important *A. niger* strain, suggests the occurrence of genetic flipping or switching events at the MAT1-1 locus of *A. niger.* These results provide new insights in the mating system of *A. niger* and could contribute to the investigation and potential discovery of sexuality in this species long thought to be asexual.

Background

Aspergillus niger is a filamentous fungus classified in the section *Nigri* of the genus *Aspergillus.* Its versatile metabolism allows it to grow in a wide variety of environments [1]. Since the early 20th century it has become a major industrial producer of organic acids, such as citric and gluconic acid, and enzymes, including amylases and phytases [2,3]. The United States Food and Drug Administration has given it GRAS (Generally Regarded As Safe) status because of its long history of industrial use [3].

First genome sequencing projects were focused on industrial relevant strains. In 2007, the genome sequence of the enzyme-producing strain CBS 513.88 was published [4], followed by the sequencing of the citric acid-producing strain ATCC 1015 in 2011 [5]. At the moment, the genome sequences of 23 *A. niger* strains are available in GenBank. Surprisingly, the *A. niger* strain CBS 554.65 has not yet been sequenced although it is the official neotype strain of this species [6]. This strain was isolated from a tannic-gallic acid fermentation in Connecticut (USA) and it is listed as the (neo-)type strain by international strain collections, such as the Westerdijk Institute (CBS 554.65), the American Type Culture Collection (ATCC 16888) and the ARS Culture Collection (NRRL 326). According to the International Code of Nomenclature for algae, fungi and plants (Shenzhen Code) a neotype is “a specimen or illustration selected to serve as nomenclatural type if no original material exists, or as long as it is missing” [7]. The importance of strain CBS 554.65 lies in its use as biological model and reference strain for morphological observations and taxonomical studies. *A. niger* was previously shown to be able to form sclerotia [8–11], which are an important prerequisite for the sexual development in closely related species. In 2016 the presence of a MAT1-2 locus in the genome of CBS 554.65 was mentioned in a study [12], making this strain an interesting candidate for investigating sexuality in *A. niger*.

The MAT loci are regions of the genome which contain one or more open reading frames of which at least one encodes a transcription factor [13,14]. Conventionally, the MAT locus containing a transcription factor with an α1 domain similar to the MATα1 of *S. cerevisiae* is called MAT1-1, while the MAT locus containing a transcription factor with

a high mobility group (HMG) domain is called MAT1-2 [13]. The corresponding genes are usually called MAT1-1-1 and MAT1-2-1 [13]. The first number indicates that the two sequences are found in the same locus. Due to their sequence dissimilarities they are not termed alleles but idiomorphs [15]. MAT1-1-1 and MAT1-2-1 are major players in the sexual cycle of fungi. They contain DNA binding motifs and were shown to control the expression of pheromone and pheromone-receptor genes during the mating process [16–18]. In heterothallic species, which are self-incompatible, only one of the two MAT genes is found and mating can occur only between strains of opposite mating-type [13]. In homothallic species, which are self-fertile, both MAT genes are present, either linked or unlinked, in the same genome [19]. In the ascomycetes, the sequences flanking the MAT loci are highly conserved [13,20,21]. In the aspergilli, as well as in other fungi, including yeasts, the MAT idiomorphs are usually flanked by the genes *slaB*, encoding for a cytoskeleton assembly control factor, and the DNA lyase *apnB*. An anaphase promoting complex gene (*apcE*) is also sometimes present [21].

Although present in previously sequenced genomes, the second mating-type locus of *A. niger* has not been described in detail. In this study, we present the full genome sequence of a MAT1-2 *A. niger* strain and compare its MAT locus to the one of strain ATCC 1015 and those of 24 *de novo* sequenced *A. niger* isolates containing both MAT1-1 and MAT1-2 loci.

Materials and methods

Strains

The genetic organization of the MAT locus present in *A. niger* CBS 554.65 (ATCC 16888, NRRL 326) was analyzed and compared to the MAT locus of *A. niger* ATCC 1015 and 24 *A. niger* isolates obtained from the Westerdijk Fungal Biodiversity Institute, Uppsalalaan 8, Utrecht, the Netherlands. The isolates analyzed are listed in Table S1 (Additional file 1).

Media

The morphology of strain CBS 554.65 was inspected on minimal medium [22] and malt

extract agar (30 g/L malt extract (AppliChem, Darmstadt, Germany) and 5 g/L peptone from casein (Merck KGaA, Darmstadt, Germany)). The strain was 4-point inoculated and incubated at 30°C for one week.

Genome sequencing and annotation

The genome of the *A. niger* neotype strain CBS 554.65 was sequenced with the PacBio® technology using the PacBio SEQUEL system (Sequencing Chemistry S/P2-C2/5.0) by the Vienna Biocenter Core Facilities (VBCF). The genome was assembled with the default HGAP4 pipeline in PacBio SMRTlink version 5.1.0.26412. The mitochondrial DNA was assembled using CLC Genomic Workbench 12.0 (QIAGEN). The genome annotation of CBS 554.65 was performed with Augustus [23], by training the tool on the genome annotation of the strain ATCC 1015 as reference.

PCRs were performed on the genomic DNA of CBS 554.65 to confirm sequencing and assembly results. Primer pairs chr5_left_fwd/chr5_left_rev and chr5_right_fwd_1/chr5_right_rev_1 were used to amplify 1756 bp and 1638 bp respectively in the left and in the right region of chr5_00008F. Primers B150 and B151 were used to amplify 1644 bp in the MAT1-1 locus of ATCC 1015. Primers B151 and B152 were used to amplify 2009 bp in the MAT1-2 locus of CBS 554.65. PCR products were sequenced by Microsynth AG.

The MAT locus sequences of 24 *A. niger* isolates were extracted from the complete genome sequences obtained with the Illumina technology and assembled using SPADes [24] (data not published). Homologues of the MAT genes in these isolates were determined based on local Blastn searches using genes obtained from CBS 554.65 and ATCC 1015 as query. In 18 out of the 24 *A. niger* isolates the MAT locus was distributed over multiple scaffolds. In order to verify the location of the MAT genes and their orientation in these strains, diagnostic PCRs and subsequent sequencing were performed to fill *in silico* gaps within the MAT locus. Primers used in this study are listed in Table S2 (Additional file 2).

Bioinformatic analyses

The genome and the gene set of CBS 554.65 were evaluated using Quast v5.0.2 [25,26],

which includes a benchmarking with Benchmarking Universal Single-Copy Orthologs (BUSCO) v3.0.2. This was performed with the fungal dataset of 290 BUSCOs from 85 fungal species [27]. The genome was masked using RepeatMasker v4.0.9 to identify repetitive elements [28]. Transfer RNA genes were detected using tRNAscan-SE v1.3.1 [29].

The unprocessed reads were mapped to the assembly with the Burrows-Wheeler Alignment Tool (bwa) [30,31] and the mapping was sorted with SAMtools [32]. The average coverage based on the sorted mapping was calculated in the R environment [33]. The mappings for each individual scaffold were plotted in R and coverage graphs for each scaffold obtained.

The proteomes of the strains CBS 554.65 and NRRL3 were aligned using DIAMOND blastp [34,35] with an E-value of e^{-10}. The output, consisting of the unique proteins of CBS 554.65 compared to NRRL3, was filtered with a blastx analysis to remove unannotated proteins and analyzed with pannzer2 [36]. The same analysis was performed on the complete proteome of strain CBS 554.65. A singular enrichment analysis (SEA) was performed on the GO term set of unique proteins of CBS 554.65 referenced to the entire GO term set of CBS 554.65 with agriGO [37,38].

The genome sequences of strains ATCC 1015, NRRL3 and CBS 513.88 were retrieved from JGI [39]. Analyses of the position of the MAT genes within the MAT locus for *A. niger* strains were performed either on BLAST, by searching in the whole-genome shotgun contig database (wgs) of *A. niger*, or on CLC Main Workbench 20.0.2 (QIAGEN). The same analysis was performed for *A. welwitschiae* strains on BLAST against the whole-genome shotgun contig database (wgs) limited by organism (*Aspergillus*) and with FungiDB for the other *Aspergillus* species [40]. Sequence analyses and alignments were performed with CLC Main Workbench 20.0.2 (QIAGEN).

Availability of data and material

This Whole Genome Shotgun project has been deposited at DDBJ/ENA/GenBank under the bioproject PRJNA715116 (accession JAGRPH000000000) [https://www.ebi.ac.uk/ena/browser/view/PRJNA715116]. The version described in this paper is version

JAGRPH010000000. The genome reads of strain CBS 554.65 are available in the European Nucleotide Archive (ENA) at EMBL-EBI under accession numbers PRJEB42544 [https://www.ebi.ac.uk/ena/browser/view/PRJEB42544]. The mitochondrial genome of strains CBS 554.65 has been deposited at GenBank under the accession MW816869 [https://www.ncbi.nlm.nih.gov/nuccore/MW816869.1]. The MAT loci sequences of the *A. niger* isolates have been deposited at GenBank under the accessions: MW809487-MW809508.

[https://www.ncbi.nlm.nih.gov/nuccore/MW809487,
https://www.ncbi.nlm.nih.gov/nuccore/MW809488,
https://www.ncbi.nlm.nih.gov/nuccore/MW809489,
https://www.ncbi.nlm.nih.gov/nuccore/MW809490,
https://www.ncbi.nlm.nih.gov/nuccore/MW809491,
https://www.ncbi.nlm.nih.gov/nuccore/MW809492,
https://www.ncbi.nlm.nih.gov/nuccore/MW809493,
https://www.ncbi.nlm.nih.gov/nuccore/MW809494,
https://www.ncbi.nlm.nih.gov/nuccore/MW809495,
https://www.ncbi.nlm.nih.gov/nuccore/MW809496,
https://www.ncbi.nlm.nih.gov/nuccore/MW809497,
https://www.ncbi.nlm.nih.gov/nuccore/MW809498,
https://www.ncbi.nlm.nih.gov/nuccore/MW809499,
https://www.ncbi.nlm.nih.gov/nuccore/MW809500,
https://www.ncbi.nlm.nih.gov/nuccore/MW809501,
https://www.ncbi.nlm.nih.gov/nuccore/MW809502,
https://www.ncbi.nlm.nih.gov/nuccore/MW8094503,
https://www.ncbi.nlm.nih.gov/nuccore/MW8094504,
https://www.ncbi.nlm.nih.gov/nuccore/MW809505,
https://www.ncbi.nlm.nih.gov/nuccore/MW809506,
https://www.ncbi.nlm.nih.gov/nuccore/MW809507,
https://www.ncbi.nlm.nih.gov/nuccore/MW809508].

Results and discussion

Morphology of strain CBS 554.65

The strain CBS 554.65 is the *A. niger* neotype, a reference strain for morphological and taxonomical analyses. The morphology of this strain grown on minimal medium and malt extract agar can be observed in Figure 4.1. On both media CBS 554.65 forms abundant conidia, black on minimal medium and dark brown on malt extract agar.

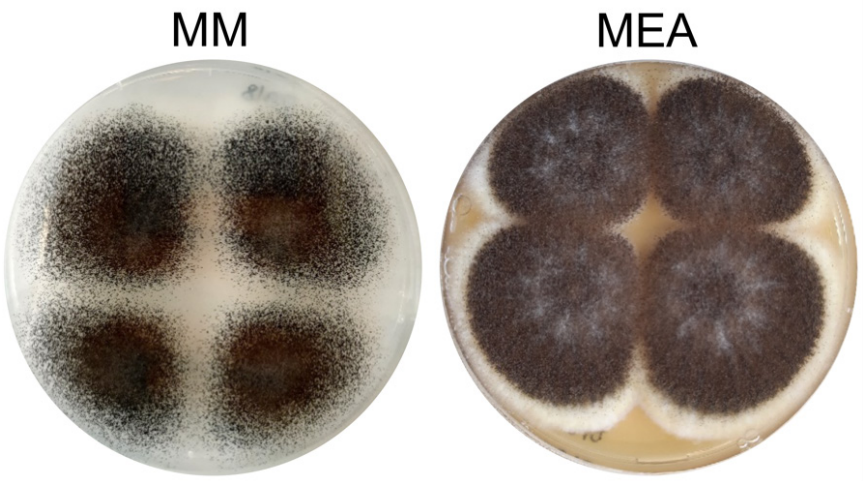

Figure 4.1. Morphology of the neotype strain CBS 554.65 on minimal medium (MM) and malt extract agar (MEA).

Genome sequence and analysis

The genome sequencing of the neotype strain CBS 554.65 yielded 5.3 Gbp in 287,000 subreads. The mean length was 18.4 Kbp for the longest subreads and half of the data was in reads longer than 29 Kbp. The assembly consisted of 17 contigs with a total of 40.4 Mbp and a 127-fold coverage. Half of the size of the genome is comprised in 4 scaffolds (L50) of which the smallest has a length of 4.07 Mbp (N50). The GC content is 49.57%. 100% complete BUSCOs (Benchmarking Universal Single-Copy Orthologs) with 2 duplicated and no fragmented BUSCOs were found. The repetitive regions were identified with RepeatMasker v4.0.9 [28]. Using this approach, we were able to recognize interspersed repeats, such as long interspaced nuclear repeats (LINEs) and long terminal repeats (LTR), short interspaced nuclear repeats (SINEs), transposable ele-

ment like repeats as well as small RNAs, tRNA genes, simple repeats and low complexity repeats. A total of 669,638 bp of the genome was flagged as repetitive, this represents 1.66% of the total genome. In addition, a tRNA prediction with tRNAscan-SE v1.3.1 was performed using the unmasked genome, because fungal specific SINEs were associated with tRNAs. Complete genome characteristics are reported in Tables 4.S3 and 4.S4 of Additional file 3.

The nuclear genome was annotated with Augustus, using the genome of strain ATCC 1015 as reference. Based on this automated annotation 12,240 protein coding genes were predicted. Table 4.1 shows some basic characteristics of the CBS 554.65 nuclear genome, calculated with Quast, in comparison to the characteristics of other three sequenced *A. niger* strains, CBS 513.88, ATCC 1015 and NRRL3, obtained from JGI.

Table 4.1. Comparison of the basic characteristics of the nuclear genomes of 4 different A. niger strains.

	CBS 554.65 (This study)	CBS 513.88 [4,5]	ATCC 1015 [5]	NRRL3 [41,42]
Genome size (Mb)	40.42	33.98	34.85	35.25
Coverage	127x	7.5x	8.9x	10x
Number of contigs	17	471	24	15
Number of scaffolds	17	19	24	15
Scaffold N50 (Mbp)	4.07	2.53	1.94	2.81
Scaffold L50	4	6	6	5
GC content (%)	49.57	50.4	50.3	49.92
Protein-coding genes	12,240	14,097	11,910	11,846

The CBS 554.65 genome assembly has an increased quality compared to the assemblies of the other strains, with a higher coverage, a higher N50 value and a lower L50 value. CBS 554.65 has a larger genome, while the GC content is similar in the 4 strains. For each of the 8 chromosomes, a putative centromeric region between 88 and 100 kb was identified, which is highlighted in Figure 4.2 with vertical black lines. These regions have a GC content between 17.1% and 18.4%, significantly lower than the GC content characterizing the total genome (49.57%) and do not contain any predicted ORF.

The only exception is a single ORF of 219 nucleotides in the centromere of chromosome 1. This is found in a 7 kb region of the centromere with a higher GC content compared to the GC content of the entire centromere, suggesting the presence of a mobile element. A conserved domain search [43] on this sequence gave as hits CHROMO and chromo shadow domains (accession: cd00024), ribonuclease H-like superfamily domain (accession: cl14782), integrase zinc binding domain (accession: pfam17921), reverse transcriptase domain (accession: cd01647), RNase H-like domain found in reverse transcriptase (accession: pfam17919) and a retropepsin-like domain (accession: cd00303). The presence of the last four domains suggests that the analyzed sequence has a retroviral or a retrotransposon origin. Similar sequences with domains for reverse transcriptase were also found in the centromeres of chromosomes 5, 6 and 7. Transposons and retrotransposons have been identified in the centromeres of other eukaryotes, including fungi [44,45]. Blast analyses of the single chromosomes of strain CBS 554.65 against the complete genome of strain NRRL3 and of strains CBS 513.88 showed that the putative centromeres are almost completely lacking from the genome assembly of NRRL3 (Figure 4.2, grey areas in the blast graph) and CBS 513.88 (Figure 4.S1, Additional file 4). Although difficult to identify, centromeric regions in filamentous fungi are composed of complex and heterogeneous AT rich sequences which can stretch up to 450 kb [45,46]. Due to the likely presence of near-identical long repeats, centromeres are difficult to sequence and assemble [46] which explains why they are lacking in strain NRRL3. The blast analyses against NRRL3 and CBS 513.88 showed that other large regions of the genome of CBS 554.65 do not find homology in NRRL3 or in CBS 513.88. To confirm that these unique regions are not artifacts, the sequencing reads of CBS 554.65 were remapped to the genome. 298,301 reads (90.38% of the total reads) were remapped to the nuclear genome yielding an average coverage calculated on scaffold level of 127x. Figure 4.S2 in the additional file 5 shows the coverage plots for each of the 17 contigs constituting the nuclear genome sequence. Continous coverage was also obtained for the CBS 554.65 regions not found in NRRL3 such as those present in chromosome 2 (chr2_00000F), chromosome 4 (chr4_000001F) and chromosome 5 (chr5_000008F)

(Figure 4.S2, Additional file 5). Moreover, two analytic PCR reactions were successfully performed on the non-homologous region on chromosome 5 (chr5_000008F, Figure 4.2). Sequencing of the PCR products confirmed the sequence obtained by genome assembly. The long reads and the high coverage characterizing this genome project allow to assemble sequences which are missing from previous genome assemblies obtained with other sequencing technologies. The number of protein-coding genes in CBS 554.65 is in line with what was found in ATCC 1015 and NRRL3. The large difference in the protein-coding genes in strain CBS 513.88 is likely caused by overpredictions, as previously suggested [5]. A comparison of the proteome of CBS 554.65 and NRRL3 by a blastp analysis showed that there are 694 unique protein sequences in the proteome of CBS 554.65 compared to NRRL3 (additional file 6, Table 4.S6) and 209 unique protein sequences in the proteome of NRRL3 compared to CBS 554.65 (additional file 6, Table 4.S7). GO terms were assigned to proteins and a GO term enrichment analysis was performed with agriGO [37,38]. 39 GO terms were significantly enriched in the set of unique CBS 554.65 GO terms when referenced to the entire CBS 554.65 GO term set (additional file 6, Table 4.S5, Figures 4.S3 and 4.S4). Interestingly, GO terms related to thiamine, cholesterol metabolic processes as well as RNA processing are enriched. Overall, this demonstrates that in this genome sequence novel protein sequences were detected, which are absent from previous reference genome projects and might yield novel insights into the biology of this fungus.

Mitochondrial DNA

The mitochondrial DNA is often neglected in genome projects, which tend to focus on the nuclear genome. In *A. niger* only one mitochondrial DNA (mtDNA) assembly was reported, for the strain N909 [48]. In this study, the mtDNA of strain CBS 554.65 was *de novo* assembled from PacBio reads as a circular DNA with a length of 31,363 bp. MtDNA is abundant in whole genome sequencing projects and the read coverage of the assembly (average: 1,220 x, min: 328 x, max: 1,674 x) is thus higher than that for the nuclear genome. In total 18 ORFs, 26 tRNA and 2 rRNA sequences were annotated (Figure 4.3).

All 15 core mitochondrial genes reported for *Aspergillus* species were identified with a similar gene organization [49]. In addition, three accessory genes *orf1L*, *orf3* and *endo1* were annotated. The gene *endo1* is located in the intron of *cox1* and encodes a putative homing endonuclease gene belonging to the LAGLIDADG family frequently found in the *cox1* intron of other filamentous fungi [49]. The gene *orf3* encodes a hypothetical protein of 191 residues, which is also present in the mtDNA of strain N909 but was not annotated there. Surprisingly this unknown protein has a good hit against an unknown protein of *Staphylococcus aureus* (99% identity, WP_117225298.1), however not against other proteins of *Aspergillus* species. In *A. niger* strain N909 two other unknown proteins are encoded in *orf1* and *orf2*. These two open reading frames are connected to *orf1L* in *A. niger* CBS 554.65 yielding a potential protein product with 739 amino acid residues. This is similar to an open reading frame located at the same position between *nad1* and *nad4* in the mtDNA of *A. flavus* NRRL 3357 (AFLA_m0040), with a size of 667 amino acid residues. In the N-terminal region of both putative proteins, transmembrane spanning regions can be predicted supposing a location in a mitochondrial membrane. However the C-terminal regions are not conserved between *A. niger* and *A. flavus* proteins. We suggest to use the mitochondrial assembly of CBS 554.65 as a reference sequence for *A. niger* mitochondria because it is known that strain N909 is resistant to oligomycin [50]. This resistance is typically linked to mutations in the mtDNA, either in *atp6* [51] or *atp9* [52], and indeed two mutations are found in *atp6* of strain N909 (L26W and S173L).

Discovery and sequencing of a MAT1-2 A. niger strain

The genome sequencing and analysis of strain CBS 554.65 allowed to determine the mating-type of this strain. The sequence of the putative MAT1-2-1 gene (g9041) was searched in the standard nucleotide collection database (nr/nt) using Blastn. This gave as hits the mating-type HMG-box protein MAT1-2-1 of other aspergilli, including *A. neoniger* (with an identity of 93.25%) and *A. tubingensis* (with an identity of 93.07%). As such, we consider gene g9041 to be homologous to the MAT1-2-1 gene of other *Aspergillus* species.



Figure 4.2. Assembly of the genome sequence of CBS 554.65 consisting of 17 contigs (in scale). For each contig (black horizontal lines) the annotated ORFs (first row), the GC content (second row) and the conservation compared to NRRL3 (third row) are schematically represented. The annotation was obtained with Augustus. The GC content was calculated using a window size of 25 bp. The upper and darker graph represents the maximum GC content value observed in that region, the middle graph represents the mean GC value and the lower graph represents the minimum GC value. The conservation graph (last row) was obtained by blasting each contig of

CBS 554.65 against the whole genome of strain NRRL3. The results shown here were additionally confirmed using Mauve [47] by performing progressive alignments of each CBS 554.65 scaffold with the complete genome sequence of NRRL3 (data not shown). Green areas indicate genomic regions conserved between the two strains, grey areas indicate regions only found in CBS 554.65 and not in NRRL3. Below the conservation graph lines representing the chromosomes of strain NRRL3 are reported, as a result of the blast analysis. Chr6_00005F, scaffold1_000010F, scaffold5_000015F and scaffold6_000016F contain the highly repetitive ribosomal DNA (rDNA) gene unit, indicated with a dashed line on top of the scaffolds. Notably, for each of the 8 identified chromosomes, a centromeric region of at least 80 kb could be identified where ORFs are not annotated (indicated with two parallel and vertical lines; the first and the last nucleotide after and before the annotated ORFs, respectively, are indicated). These regions correspond to a decrease in the GC content (as indicated in the GC graph) and are only partially present in the genome of strain NRRL3 (grey areas in the blast graph). Dots on chr5_000008F and on chr7_000002F indicate the region where the PCRs were performed. The MAT locus analyzed in the following paragraphs is indicated by a red box on chromosome 7. Figure 4.S1 in the additional file 4 reports the comparison of the CBS 554.65 genome to the one of strain CBS 513.88. Additional information on the length of the contigs and the coordinates of the alignments are reported in Table 4.S8 of Additional file 7.

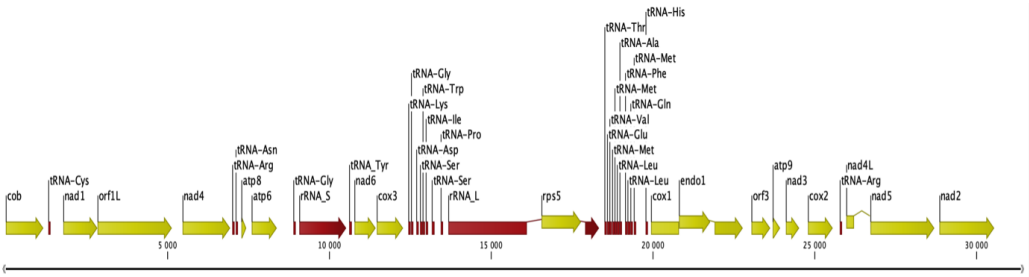

Figure 4.3. Annotation of the 31 kbp circular mtDNA sequence (displayed in a linear projection): ORF (yellow), rRNA, tRNA (red).

This is in line with a previous study that showed the presence of a MAT1-2-1 sequence in the CBS 554.65 strain through a PCR approach [12]. Here we report the complete genome sequence of an *A. niger* strain having a MAT1-2-1 gene. The availability of this genome sequence represents an important tool for further studies investigating the sexual potential of *A. niger*. The presence of both opposite mating-type genes in different strains belonging to the same species represents a strong hint of a sexual lifestyle [14].

MAT1-2 locus analysis and comparison to MAT1-1

The locus of strains CBS 554.65 containing the MAT1-2-1 gene was compared *in silico* to the locus of strain ATCC 1015 containing the MAT1-1-1 gene. This was done to determine whether the genes flanking the MAT1-1-1 gene are also present in the genome of the MAT1-2 strain and vice versa. A region of 40,517 bp, spanning from gene Aspni7|39467 (genomic position 2504615 in the v7 of the ATCC 1015 genome) to gene Aspni7|1128148 (genomic position 2545131) was aligned to the corresponding region of strain CBS 554.65 (Figure 4.4). In CBS 554.65 the two genes homologous to Aspni7|39467 (g9051) and Aspni7|1128148 (g9036) are comprised in a sequence of 43,891 bp, almost 4 kb longer than in ATCC 1015. The identifiers of the genes included in these regions are indicated in Figure 4.4 and additionally reported in Table 4.2, with their predicted function retrieved from FungiDB or blast analysis. The alignment shows that the MAT genes occupy the same genomic location at chromosome 7. The genes comprised in the analyzed loci are mostly conserved between the two strains, with the exception of genes Aspni7I1178859 (MAT1-1-1), Aspni7I1128137 and Aspni7I1160288, unique for ATCC 1015, and g9046, g9041 (MAT1-2-1) and g9040-2 (MAT1-2-4), unique for CBS 554.65. Aspni7I1128137 has predicted metal ion transport activity and it is found in other *Aspergillus* species, either heterothallic with a MAT1-1-1 or a MAT1-2-1 gene or homothallic. It is not found near the MAT gene, with the exception of *A. brasiliensis* and *A. ochraceoroseus*. Aspni7I1160288 has a domain with predicted role in proteolysis and its homolog in other aspergilli is present at another genomic locus, not in proximity to the MAT gene. A homolog of gene g9046 was found by Blastn search in *Aspergillus vadensis*, in a different location of the genome than the MAT locus. These results suggest that these unique genes are unlikely to be part of the “core” MAT locus. The gene g9040-2 is a putative homolog of the MAT1-2-4 gene in *A. fumigatus*, an additional mating-type gene required for mating and cleistothecia formation [53]. Another difference between ATCC 1015 and CBS 554.65 is represented by the gene putatively encoding for a HAD-like protein. While this gene is complete in CBS 554.65 (g9045), it appears disrupted in ATCC 1015 and, therefore, doubly annotated in this strain (Aspni7|1095364 and As-

pni7|1128138). The other genes present in the selected genomic region show a high level of conservation, with a higher synteny further away from the MAT genes (genes in the purple and blue boxes). Moreover, genes encoding for the DNA lyase a*pnB*, the cytoskeleton control assembly factor *slaB* and the anaphase promoting complex *apcE* are present in both MAT loci. These genes are normally found in the MAT loci of other fungi, including yeast [21]. Their presence in the MAT loci of *A. niger* further confirms the high level of conservation characterizing this locus. In heterothallic ascomycetes the MAT genes are commonly included between the genes *apnB* and *slaB* [21]. From the alignment in Figure 4.4 the relative position of the MAT genes to *apnB* and *slaB* can be analyzed. In CBS 554.65 the MAT1-2-1 gene (g9041) is flanked by *apnB* and *slaB* respectively upstream and seven genes downstream. In contrast, in the MAT1-1 locus of strain ATCC 1015 the MAT gene is flanked downstream by *apnB* and upstream by a conserved sequence including *adeA*, while *slaB* is found on the same side of *apnB*. The entire genomic locus, containing the MAT1-1-1 gene and eight other genes (23 kbp indicated by the red arrow in Figure 4.4), shows a flipped orientation compared to the corresponding locus in CBS 554.65 containing the MAT1-2-1 gene (indicated by an orange arrow in Figure 4.4). The ORF direction of the conserved genes *apnB*, *coxM* and *apcE* additionally confirms the different orientation of this locus in the two strains. In addition, PCRs performed with primers B150, B151 and B152 (Figure 4.4) yielded expected bands, confirming the orientation of the MAT loci of both ATCC 1015 and CBS 554.65. By sequence analysis, a repetitive 7 bp DNA motif (5´-TTACACT) was found in the MAT1-1 locus (orange triangles in Figure 4.4), where the homology between the MAT1-1 and MAT1-2 loci breaks (in proximity to *adeA* and *slaB*). An additional site of this motif was found in the gene encoding a HAD-like hydrolase (Aspni7I1128138). This motif is present at similar positions in at least two other sequenced MAT1-1 strains of *A. niger* (N402, CBS 513.88). Differently, the MAT1-2 strain presents this motif only at the site close to the *adeA* gene and in the putative HAD-like hydrolase gene (g9045), but not at the site close to the *slaB* gene.

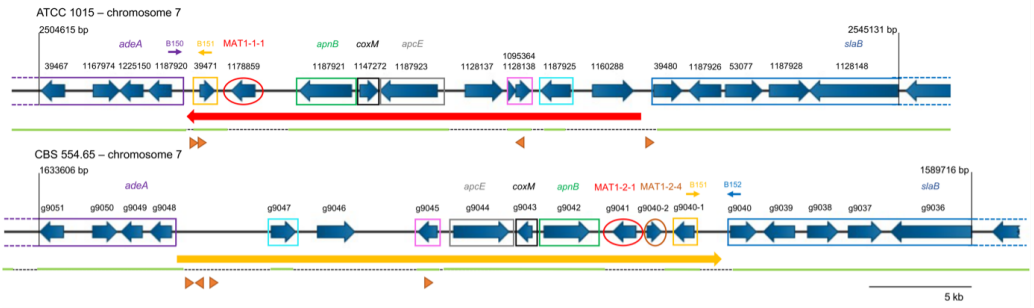

Figure 4.4. Nucleotide alignment between the same genomic region of ATCC 1015 (MAT1-1) and CBS 554.65 (MAT1-2). Genes found in both strains are indicated with a box of the same color, MAT genes are indicated with a circle and unmarked genes are unique in each strain. Below each genomic region, green lines indicate regions homologous in the two strains and dotted lines regions unique for each strain. A red arrow indicates the genomic region of ATCC 1015 which contains the MAT1-1-1 gene and appears flipped compared to the corresponding region in CBS 554.65 (yellow arrow). Small arrows with numbers B150, B151 and B152 indicate primers used for PCRs. Orange triangles indicate the presence of a 7 bp motif (5´-TTACACT).

Table 4.2. List of genes included in the genomic region comprising the MAT genes.

ATCC 1015	CBS 554.65	Predicted function retrieved from FungiDB or blast
Aspni7|39467	g9051	Hypothetical protein
Aspni7|1167974	g9050	CIA30-domain containing protein – Ortholog(s) have role in mitochondrial respiratory chain complex I assembly
Aspni7|1225150	g9049	SAICAR synthetase (*adeA*)
Aspni7|1187920	g9048	Homolog in CBS 513.88 has domain(s) with predicted catalytic activity, metal ion binding, phosphoric diester hydrolase activity
Aspni7|39471	g9040-1	Hypothetical protein
Aspni7|1178859	-	Mating-type protein MAT1-1-1
Aspni7|1187921	g9042	DNA lyase Apn2|Hypothetical protein
Aspni7|1147272	g9043	Hypothetical cytochrome C oxidase|Mitochondrial cytochrome c oxidase subunit VIa
Aspni7|1187923	g9044	Ortholog(s) are anaphase-promoting complex proteins
Aspni7|1128137	-	Homolog in CBS 513.88 has domain(s) with predicted metal ion transmembrane transporter activity, role in metal ion transport, transmembrane transport and membrane localization
Aspni7|1095364	g9045	HAD-like protein; Homolog in CBS 513.88 has domain(s) with predicted hydrolase activity
Aspni7|1128138	g9045	HAD-like protein; Homolog in CBS 513.88 has domain(s) with predicted hydrolase activity

ATCC 1015	CBS 554.65	Predicted function retrieved from FungiDB or blast
Aspni7|1187925	g9047	Glycosyltransferase Family 8 protein - Ortholog(s) have acetylglucosaminyltransferase activity, role in protein N-linked glycosylation and Golgi medial cisterna localization
Aspni7|1160288	-	Aspartic protease|Hypothetical aspartic protease
Aspni7|39480	g9040	WD40 repeat-like protein
Aspni7|1187926	g9039	Aldehyde dehydrogenase
Aspni7|53077	g9038	CoA-transferase family III
Aspni7|1187928	g9037	Salicylate hydroxylase
Aspni7|1128148	g9036	Cytoskeleton assembly control protein Sla2
-	g9046	Hypothetical protein
-	g9041	Mating-type HMG-box protein MAT1-2-1
-	g9040-2	Hypothetical protein – Putative homologue of MAT1-2-4 of *A. fumigatus*

Methods to identify the opposite mating-type in strains isolated from natural sources often rely on the use of primers designed to bind to *apnB* and *slaB*, since these are the genes that commonly flank the MAT gene itself [54,55]. In both mating-type *A. niger* strains, *slaB* is found more than 12 kbp away from the MAT gene. In addition, the relative orientation of *apnB* to *slaB* is different in strains having opposite mating types. This might explain why the MAT1-2 locus was only mentioned by one previous study [12] but never described in detail so far.

Both the particular orientation of the MAT locus and the presence of a repetitive motif in the MAT loci suggest that a genetic switch or a flipping event might have occurred or is still ongoing in *A. niger*, which might affect the expression of the MAT genes. Genetic switching events at the MAT locus are known for other ascomycetes, particularly yeasts. For instance, in *S. cerevisiae* a switching mechanism involving an endonuclease and two inactive but intact copies of the MAT genes allows to switch the MAT type of the cell [56]. Expression of the MAT gene is instead regulated in the methylotrophic yeasts *Komagataella phaffii* and *Ogataea polymorpha* via a flip/flop mechanism [57,58]. In these species, a 19 kbp sequence including both mating type genes is flipped so that a MAT gene will be close to the centromere (5 kbp from the centromere) and, therefore, silenced while the other will be transcribed. In CBS 554.65 the region comprising the

MAT1-2-1 gene is present at around 280 kbp downstream of the putative centromere, which is much further away of what observed for *K. phaffi* and *O. polymorpha*. However, in certain basidiomycetes, such as *Microbotryum saponariae* and *Microbotryum lagerheimii*, the mating-type locus HD (containing the homeodomain genes) is around 150 kbp distant from the centromere and linked to it [59]. It was proposed that the proximity to the centromere in these species might be enough to reduce recombination events [59]. The effect of the distance between the centromere and the MAT genes in *A. niger* merits further attention, especially in view of a potential sexual cycle characterizing this species.

Inversion at the MAT locus have been described for certain homothallic filamentous fungi such as *Sclerotinia sclerotiorum* and *Sclerotinia minor* [60,61]. Field analysis of a large number of isolates showed that strains belonging to these species can either present a non-inverted or an inverted MAT locus. In the inverted orientation two of the four MAT genes at the locus have the opposite orientation and one gene is truncated. In the case of *S. sclerotiorum*, differences in the gene expression were observed between inverted and non-inverted strains. This inversion, induced by crossing-over between two identical inverted repeat present in the locus, likely happens during the sexual cycle before meiosis [60]. The analysis of a larger number of *A. niger* isolates is required to investigate whether opposite orientations of both MAT loci exist for this species as well and what the implications of such inversions might be. Chromosomal inversions are considered to prevent recombination between sex determining genes in higher eukaryotes, such as animals and plants [62]. Further studies are required to investigate whether *A. niger* possesses a genetic switching mechanism controlling its sexual development.

Genetic comparison of MAT loci in different aspergilli and additional *A. niger* strains

This study revealed a particular configuration for the MAT1-1 locus of strain ATCC 1015. For this reason, the orientation of the MAT locus of additional *Aspergillus* species for which a genome sequence is available was analyzed. Firstly, the genes *adeA* and *slaB* were retrieved as they are conserved and often found at the right and left flank of the MAT gene, respectively (Figure 4.4). Subsequently, the position of the MAT gene was

compared to the three conserved genes *apnB*, *coxM* and *apcE*. The MAT gene could be either included between *adeA* and *apnB*, like in ATCC 1015 (flipped position), or between *apnB and slaB*, like in CBS 554.65 (conserved position). The results of this analysis are reported in Table 4.3. A complete table with the identifiers of all genes analyzed is reported in the Additional file 8.

Table 4.3. MAT gene identifiers of the analyzed Aspergillus strains and their position in the MAT locus. MAT genes which are found between apnB and slaB are considered to have a "conserved" position, while MAT genes identified between adeA and apnB are considered as "flipped". Aspergillus species are grouped in sections based on the most updated classification [71]. For each species it is indicated if a sexual cycle has been reported in the literature.

Section	Species	Strain	Mating-type gene MAT	Mating-type	MAT position	Sexual cycle described for the species
Nigri	*A. welwitschiae*	CBS 139.54	172181	MAT1-1	flipped	No
	A. kawachii (A. luchuensis)	IFO 4308	AKAW_03832	MAT1-2	conserved	No
	A. luchuensis	106.47	ASPFODRAFT_180958	MAT1-1	conserved	No
	A. tubingensis	G131	Not annotated	MAT1-2	conserved	Yes [63]
		CBS 134.48	ASPTUDRAFT_124452	MAT1-1	conserved	
	A. niger	CBS 554.65	g9041	MAT1-2	conserved	No
		ATCC 1015	ASPNIDRAFT2_1178859	MAT1-1	flipped	
	A. brasiliensis	CBS 101740	ASPBRDRAFT_167991	MAT1-2	flipped	No
	A. carbonarius	ITEM 5010	ASPCADRAFT_1991	MAT1-2	conserved	No
	A. aculeatus	ATCC 16872	ASPACDRAFT_1867751	MAT1-2	conserved	No
Nidulantes	*A. versicolor*	CBS 583.65	ASPVEDRAFT_82222	MAT1-2	conserved	No
	A. sydowii	CBS 593.65	ASPSYDRAFT_87884	MAT1-2	conserved	No
Ochraceorosei	*A. ochraceoroseus*	IBT 24754	P175DRAFT_0477739	MAT1-1	conserved	No
Flavi	*A. flavus*	NRRL 3357	AFLA_103210	MAT1-1	conserved	Yes [64]
	A. oryzae	BCC7051	OAory_01101300	MAT1-2	conserved	No
		RIB40	AO090020000089	MAT1-1	conserved	
Circumdati	*A. steynii*	IBT 23096	P170DRAFT_349471	MAT1-2	conserved	No
Candidi	*A. campestris*	IBT 28561	P168DRAFT_313902	MAT1-1	conserved	No
			P168DRAFT_285957	MAT1-2	conserved	
Terrei	*A. terreus*	NIH2624	ATEG_08812	MAT1-1	conserved	Yes [65]
Fumigati	*A. novofumigatus*	IBT 16806	P174DRAFT_462167	MAT1-2	conserved	No
	A. fischeri	NRRL 181	NFIA_071100	MAT1-1	conserved	Yes [66]
			NFIA_024390	MAT1-2	conserved	
	A. fumigatus	Af293	Afu3g06170	MAT1-2	conserved	Yes [67]
		A1163	AFUB_042900	MAT1-1	conserved	
			AFUB_042890	MAT1-2	conserved	
Clavati	*A. clavatus*	NRRL1	ACLA_034110	MAT1-1	conserved	Yes [68]
			ACLA_034120	MAT1-2	conserved	

Section	Species	Strain	Mating-type gene MAT	Mating-type	MAT position	Sexual cycle described for the species
Aspergillus	*A. glaucus*	CBS 516.65	ASPGLDRAFT_89185	MAT1-1	n.a.[1]	Yes [69,70]
Cremei	*A. wentii*	DTO 134E9	ASPWEDRAFT_184745	MAT1-2	conserved	No

[1] Conserved genes not in the MAT locus

In the analyzed *Aspergillus* sequences the MAT gene (either MAT1-1-1 or MAT1-2-1) was mostly found between the genes *apnB* and *slaB*, such as in CBS 554.65 (conserved). The only exceptions, showing a configuration similar to the MAT1-1 locus of ATCC 1015, were the MAT1-1-1 gene of *A. welwitschiae* and the MAT1-2-1 gene of *A. brasiliensis*. This analysis could not be performed on the MAT1-2 locus of *A. welwitschiae* nor on the MAT1-1 locus of *A. brasiliensis*, due to the unavailability of sequences for strains of the opposite mating type. Seven of the analyzed species, including the closely related *A. tubingensis*, were reported to have a sexual cycle. A conserved position of the MAT gene was observed for all of these species with the exception for *A. glaucus*, whose conserved genes were not found in the vicinity of the MAT gene. These observations suggest that the position of the MAT gene and the orientation of the locus might have an impact on the sexual development of the respective fungus.

Since the orientation observed for the MAT1-1 locus of ATCC 1015 might be peculiar for this *A. niger* strain only, additional genome sequences were analyzed to determine the orientation of the MAT locus of other sequenced strains of *A. niger* (Table 4.4). 18 out of 23 *A. niger* strain sequences deposited in GenBank contain a MAT1-1-1 gene and they all show the same orientation of the MAT locus as observed in ATCC 1015. The other 5 strains contain a MAT1-2 locus and they all show the same conserved orientation as observed in the strain CBS 554.65. The orientation could not be determined for one MAT1-2 strain, MOD1FUNGI2, since the different analyzed genes are present in different scaffolds in the available genome sequence. Overall, 80% of the sequenced strains contain a MAT1-1 locus. The selection procedure of strains for whole-genome sequencing might be biased by their industrial relevance and might not resemble the mating-type distribution in the environment. Therefore, 24 randomly picked isolates of *A. niger* were

sequenced and the MAT loci analyzed: 12 contain the MAT1-1 locus and 12 the MAT1-2 locus (Table 4.4).

Table 4.4. Mating-type and MAT gene position of the analyzed *A. niger* strains. 48 *A. niger* strains have been analyzed in respect to their MAT locus configuration. Newly sequenced *A. niger* isolates and CBS 554.65 are reported in green rows. Among these, 12 have a MAT1-1 and 13 a MAT1-2 locus. Previously sequenced *A. niger* strains are reported in blue rows. Among these, a bias towards MAT1-1 strains is present. All the MAT1-1 strain have a flipped orientation of the MAT locus and all the MAT1-2 strains a conserved one. *MAT locus distributed over multiple scaffolds which could not be combined.

MAT1-1				MAT1-2			
***A. niger* strain**	**Isolation source**	**MAT position**	**GenBank accession**	***A. niger* strain**	**Isolation source**	**MAT position**	**GenBank accession**
CBS 112.32	Unknown, Japan	flipped	MW809488	CBS 554.65	Tannin-gallic acid fermentation, USA	conserved	PRJ-NA715116
CBS 147371	Green coffee bean, India	flipped	MW809493	CBS 113.50	Leather, unknown	conserved	MW809487
CBS 147320	Grape, Australia	flipped	MW809494	CBS 124.48	Unknown	conserved	MW809489
CBS 147345	Unknown, USA	flipped	MW809501	CBS 118.52	Unknown	conserved	Incomplete coverage*
CBS 147347	Petridish, soft drink factory, The Netherlands	flipped	MW809503	CBS 147321	Arctic soil, Norway	conserved	MW809495
CBS 769.97	Leather, Unknown	flipped	MW809504	CBS 147322	Coffee, Brazil	conserved	MW809496
CBS 115989	Unknown	flipped	MW809505	CBS 147323	Raisin, Turkey	conserved	MW809497
CBS 147352	Air next to bottle blower, Mexico	flipped	MW809506	CBS 147324	Unknown	conserved	MW809498
CBS 147353	Food factory of Sanquinetto, Italy	flipped	MW809507	CBS 147482	Surface water, Portugal	conserved	Incomplete coverage*
CBS 115988	Unknown	flipped	MW809491	CBS 147344	Coffee beans, Thailand	conserved	MW809499
CBS 131.52	Leather, unknown	flipped	MW809490	CBS 133816	Black pepper, Denmark	conserved	MW809500
CBS 147343	Coffee bean, Thailand	flipped	MW809508	CBS 147346	CF patient material, The Netherlands	conserved	MW809502
H915-1	Soil, China	flipped	PRJ-NA288269	CBS 630.78	Army equipment, South Pacific Islands	conserved	MW809492

MAT1-1				MAT1-2			
***A. niger* strain**	**Isolation source**	**MAT position**	**GenBank accession**	***A. niger* strain**	**Isolation source**	**MAT position**	**GenBank accession**
L2	Soil, China	flipped	PRJ-NA288269	RAF106	Pu´er tea, China	conserved	PRJ-NA503751
LDM3	Industrial production, China	flipped	PRJ-NA562509	3.316	Laboratory, China	conserved	PRJ-NA597564
FDAAR-GOS_311	USA	flipped	PRJ-NA231221	An76	Soil, China	conserved	PRJDB4313
N402 (ATCC 64974)	Laboratory, The Netherlands	flipped	PR-JEB21769	JSC-093350089	ISS environmental surface, USA	conserved	PRJ-NA355122
ATCC 10864	Soil, Peru	flipped	PRJ-NA300350	MOD1-FUN-GI2	Red seedless grapes, USA	Genes in different scaffolds	PRJ-NA482816
F3_1F3_F	ISS environmental surface, USA	flipped	PRJ-NA667181				
F3_4F2_F	ISS environmental surface, USA	flipped	PRJ-NA667181				
F3_4F1_F	ISS environmental surface, USA	flipped	PRJ-NA667181				
DSM 1957	Soil, France	flipped	PRJ-NA566102				
FGSC A1279	Laboratory, The Netherlands	flipped	PRJ-NA255851				
A1	Soil, China	flipped	PRJ-NA288269				
ATCC 1015	USA	flipped	PRJ-NA15785				
ATCC 13496	Soil, USA	flipped	PRJ-NA209543				
CBS 101883 (*A. lacticoffeatus*)	Coffee beans, Sumatra	flipped	PRJ-NA479910				
CBS 513.88	Unknown	flipped	PRJ-NA19275				
SH-2	Soil, China	flipped	PRJ-NA196564				
ATCC 13157 (*A. phoenicis*)	Whole shelled corn	flipped	PRJ-NA209548				

The MAT locus configuration of these strains is similar to the configuration of strain ATCC 1015, in the case of the MAT1-1 strains, and to CBS 554.65, in the case of at least 10 out of 12 MAT1-2 strains. In the two remaining MAT1-2 strains (CBS 118.52 and CBS 147482) a gap between two genomic scaffolds could not be closed by PCR. This is likely due to the presence of a region with multiple G repeats. However, when the two separate scaffolds of these isolates were aligned to the MAT1-2 locus of CBS 554.65, they appeared to have the same locus configuration as the other 10 MAT1-2 isolates. Similarly to what was observed for ATCC 1015 and CBS 554.65, the HAD-like protein encoding gene appears disrupted in all the MAT1-1 isolates and complete in all the MAT1-2 isolates. Further studies are required to investigate whether the disruption of this gene in the MAT1-1 strains plays a role in the context of fungal development. Overall, the MAT1-1 configuration described in Figure 4.4 is a peculiar feature of *A. niger* and its close relative *A. welwitschiae*. Despite the unusual orientation, the presence of a 50:50 ratio of MAT1-1:MAT1-2 among 24 randomly selected *A. niger* isolates is remarkable and suggests that sexual reproduction is occurring in this species. Interestingly, MAT1-1 occurs at higher frequency in commonly used industrial and laboratory strains. This could be pure coincidence, but it could also indicate a phenotypic difference between strains with opposite mating types.

Conclusions

The *A. niger* neotype strain CBS 554.65 has now a high quality genome sequence, which covers all the 8 centromeres and includes a complete mtDNA sequence. This sequence represents an important tool for further studies. The analysis of this genome revealed the presence of a second mating-type locus (MAT1-2) in this strain, making it a suitable reference strain to investigate fungal development in *A. niger*. The position and the orientation of the MAT1-2-1 gene of all the 15 MAT1-2 *A. niger* strains analyzed was found to be similar to that of other aspergilli, with the MAT gene included between the genes *apnB* and *slaB*. The unusual orientation of the MAT1-1-1 locus found in the already sequenced *A. niger* strains and in other 12 newly sequenced isolates indicates that flipping or switching events have occurred at the MAT locus. Further research is required to investigate whether this difference in the position of the MAT genes in the opposite mating-type strains could have an effect on the expression of the genes included in this genomic region. These flipping events might have a direct impact on the sexual development in *A. niger*.

References

1.Schuster E, Dunn-Coleman N, Frisvad J, van Dijck P. On the safety of *Aspergillus niger* - a review. Appl Microbiol Biotechnol 2002;59:426–35. https://doi.org/10.1007/s00253-002-1032-6.

2. Currie JN. The citric acid fermentation of *Aspergillus niger*. J Biol Chem 1917:15–37.

3. Baker SE, Bennett J. The aspergilli. In: Goldman GH, Osmani SA, editors., CRC Press; 2007. https://doi.org/10.1201/9781420008517.

4. Pel HJ, de Winde JH, Archer DB, Dyer PS, Hofmann G, Schaap PJ, et al. Genome sequencing and analysis of the versatile cell factory *Aspergillus niger* CBS 513.88. Nat Biotechnol 2007;25:221–31. https://doi.org/10.1038/nbt1282.

5. Andersen MR, Salazar MP, Schaap PJ, van de Vondervoort PJI, Culley D, Thykaer J, et al. Comparative genomics of citric-acid-producing *Aspergillus niger* ATCC 1015 versus enzyme-producing CBS 513.88. Genome Res 2011;21:885–97. https://doi.org/10.1101/gr.112169.110.

6. Kozakiewicz Z, Frisvad JC, Hawksworth DL, Pitt JI, Samson RA, Stolk AC. Proposal for nomina specifica conservanda and rejicienda in *Aspergillus* and *Penicillium* (Fungi). Taxon 1992;41:109. https://doi.org/10.2307/1222500. https://www.jstor.org/stable/1222500

7. Turland NJ, Wiersema JH, Barrie FR, Greuter W, Hawksworth DL, Herendeen PS, et al. International Code of Nomenclature for algae, fungi and plants. vol. 159. Koeltz Botanical Books; 2018. https://doi.org/10.12705/Code.2018.

8. Jørgensen TR, Burggraaf A-M, Arentshorst M, Schutze T, Lamers G, Niu J, et al. Identification of SclB, a Zn(II)2Cys6 transcription factor involved in sclerotium formation in *Aspergillus niger*. Fungal Genet Biol 2020;139:103377. https://doi.org/10.1016/j.fgb.2020.103377.

9. Frisvad JC, Petersen LM, Lyhne EK, Larsen TO. Formation of sclerotia and production of indoloterpenes by *Aspergillus niger* and other species in section *Nigri*. PLoS One 2014;9:e94857. https://doi.org/10.1371/journal.pone.0094857.

10. Ellena V, Bucchieri D, Arcalis E, Sauer M, Steiger MG. Sclerotia formed by citric acid producing strains of *Aspergillus niger*: induction and morphological analysis. Fungal Biol 2021;125:485–94. https://doi.org/10.1016/j.funbio.2021.01.008.

11. Jørgensen TR, Nielsen KF, Arentshorst M, Park J, van den Hondel CA, Frisvad JC, et al. Submerged conidiation and product formation by *Aspergillus niger* at low specific growth rates are affected in aerial developmental mutants. Appl Environ Microbiol 2011;77:5270–7. https://doi.org/10.1128/AEM.00118-11.

12. Mageswari A, Kim J, Cheon K-H, Kwon S-W, Yamada O, Hong S-B. Analysis of the MAT1-1 and MAT1-2 gene ratio in black koji molds isolated from meju. Mycobiology 2016;44:269–76. https://doi.org/10.5941/MYCO.2016.44.4.269.

13. Debuchy R, Turgeon BG. Mating-type structure, evolution, and function in Euascomycetes. Growth, Differ. Sex. Growth, Di, Berlin/Heidelberg: Springer-Verlag; 2006, p. 293–323. https://doi.org/10.1007/3-540-28135-5_15.

14. Dyer PS, Kück U. Sex and the imperfect fungi. The Fungal Kingdom 2017:193–214. https://doi.org/10.1128/microbiolspec.funk-0043-2017.

15. Metzenberg RL, Glass NL. Mating type and mating strategies in *Neurospora*. BioEssays 1990;12:53–9. https://doi.org/10.1002/bies.950120202.

16. Lee SC, Ni M, Li W, Shertz C, Heitman J. The evolution of sex: a perspective from the fungal kingdom. Microbiol Mol Biol Rev 2010;74:298–340. https://doi.org/10.1128/MMBR.00005-10.

17. Coppin E, Debuchy R, Arnaise S, Picard M. Mating types and sexual development in filamentous ascomycetes. Microbiol Mol Biol Rev 1997;61:411–28. https://doi.org/10.5424/sjar/2014121-4340.

18. Kück U, Böhm J. Mating type genes and cryptic sexuality as tools for genetically manipulating industrial molds. Appl Microbiol Biotechnol 2013;97:9609–20. https://doi.org/10.1007/s00253-013-5268-0.

19. Pöggeler S. Mating-type genes for classical strain improvements of ascomycetes. Appl Microbiol Biotechnol 2001;56:589–601. https://doi.org/10.1007/s002530100721.

20. Galagan JE, Hynes M, Pain A, Machida M, Purcell S, Peñalva MÁ, et al. Sequencing of *Aspergillus nidulans* and comparative analysis with *A. fumigatus* and *A. oryzae*. Nature 2005;438:1105–15. https://doi.org/10.1038/nature04341.

21. Dyer PS. Sexual reproduction and significance of MAT in the Aspergilli. In: Heitman J, Kronstad J, Taylor J CL (ed), editor. Sex Fungi. ASM Press, American Society of Microbiology; 2007, p. 123–42. https://doi.org/10.1128/9781555815837.ch7.

22. Arentshorst M, Ram AFJ, Meyer V. Using non-homologous end-joining-deficient strains for functional gene analyses in filamentous fungi. In: Bolton MD, Thomma BPHJ, editors. Plant Fungal Pathog. Methods Protoc., vol. 835. Humana Pre, Totowa, NJ: Humana Press; 2012, p. 133–50. https://doi.org/https://doi.org/10.1007/978-1-61779-501-5_9.

23. Stanke M, Morgenstern B. AUGUSTUS: a web server for gene prediction in eukaryotes that allows user-defined constraints. Nucleic Acids Res 2005;33:W465–7. https://doi.org/10.1093/nar/gki458.

24. Bankevich A, Nurk S, Antipov D, Gurevich AA, Dvorkin M, Kulikov AS, et al. SPAdes: a new genome assembly algorithm and its applications to single-cell sequencing. J Comput Biol 2012;19:455–77. https://doi.org/10.1089/cmb.2012.0021.

25. Gurevich A, Saveliev V, Vyahhi N, Tesler G. QUAST: quality assessment tool for genome assemblies. Bioinformatics 2013;29:1072–5. https://doi.org/10.1093/bioinformatics/btt086.

26. Mikheenko A, Prjibelski A, Saveliev V, Antipov D, Gurevich A. Versatile genome assembly evaluation with QUAST-LG. Bioinformatics 2018;34:i142–50. https://doi.org/10.1093/bioinformatics/bty266.

27. Simão FA, Waterhouse RM, Ioannidis P, Kriventseva E V., Zdobnov EM. BUSCO: assessing genome assembly and annotation completeness with single-copy orthologs. Bioinformatics 2015;31:3210–2. https://doi.org/10.1093/bioinformatics/btv351.

28. Smit AFA, Hubley R, Green P. RepeatMasker Open-4.0. http://www.repeatmasker.org.

29. Lowe TM, Eddy SR. tRNAscan-SE: A program for improved detection of transfer RNA genes in genomic sequence. Nucleic Acids Res 1997;25:955–64. https://doi.org/10.1093/nar/25.5.955.

30. Li H, Durbin R. Fast and accurate short read alignment with Burrows-Wheeler transform. Bioinformatics 2009;25:1754–60. https://doi.org/10.1093/bioinformatics/btp324.

31. Li H, Durbin R. Fast and accurate long-read alignment with Burrows–Wheeler transform. Bioinformatics 2010;26:589–95. https://doi.org/10.1093/bioinformatics/btp698.

32. Li H, Handsaker B, Wysoker A, Fennell T, Ruan J, Homer N, et al. The Sequence Alignment/Map format and SAMtools. Bioinformatics 2009;25:2078–9. https://doi.org/10.1093/bioinformatics/btp352.

33. Team RC. R: A language and environment for statistical computing. 2019.

34. Buchfink B, Xie C, Huson DH. Fast and sensitive protein alignment using DIAMOND. Nat Methods 2015;12:59–60. https://doi.org/10.1038/nmeth.3176.

35. Camacho C, Coulouris G, Avagyan V, Ma N, Papadopoulos J, Bealer K, et al. BLAST+: architecture and applications. BMC Bioinformatics 2009;10:421. https://doi.org/10.1186/1471-2105-10-421.

36. Törönen P, Medlar A, Holm L. PANNZER2: a rapid functional annotation web server. Nucleic Acids Res 2018;46:W84–8. https://doi.org/10.1093/nar/gky350.

37. Du Z, Zhou X, Ling Y, Zhang Z, Su Z. agriGO: a GO analysis toolkit for the agricultural community. Nucleic Acids Res 2010;38:W64–70. https://doi.org/10.1093/nar/gkq310.

38. Tian T, Liu Y, Yan H, You Q, Yi X, Du Z, et al. agriGO v2.0: a GO analysis toolkit for the agricultural community, 2017 update. Nucleic Acids Res 2017;45:W122–9. https://doi.org/10.1093/

nar/gkx382.

39. Nordberg H, Cantor M, Dusheyko S, Hua S, Poliakov A, Shabalov I, et al. The genome portal of the Department of Energy Joint Genome Institute: 2014 updates. Nucleic Acids Res 2014;42:D26–31. https://doi.org/10.1093/nar/gkt1069.

40. Basenko E, Pulman J, Shanmugasundram A, Harb O, Crouch K, Starns D, et al. FungiDB: An Integrated Bioinformatic Resource for Fungi and Oomycetes. J Fungi 2018;4:39. https://doi.org/10.3390/jof4010039.

41. Aguilar-Pontes MV, Brandl J, McDonnell E, Strasser K, Nguyen TTM, Riley R, et al. The gold-standard genome of *Aspergillus niger* NRRL 3 enables a detailed view of the diversity of sugar catabolism in fungi. Stud Mycol 2018;91:61–78. https://doi.org/10.1016/j.simyco.2018.10.001.

42. Vesth TC, Nybo JL, Theobald S, Frisvad JC, Larsen TO, Nielsen KF, et al. Investigation of inter- and intraspecies variation through genome sequencing of *Aspergillus* section *Nigri*. Nat Genet 2018;50. https://doi.org/10.1038/s41588-018-0246-1.

43. Lu S, Wang J, Chitsaz F, Derbyshire MK, Geer RC, Gonzales NR, et al. CDD/SPARCLE: the conserved domain database in 2020. Nucleic Acids Res 2020;48:D265–8. https://doi.org/10.1093/nar/gkz991.

44. Talbert PB, Henikoff S. What makes a centromere? Exp Cell Res 2020;389:111895. https://doi.org/10.1016/j.yexcr.2020.111895.

45. Smith KM, Galazka JM, Phatale PA, Connolly LR, Freitag M. Centromeres of filamentous fungi. Chromosom Res 2012;20:635–56. https://doi.org/10.1007/s10577-012-9290-3.

46. Friedman S, Freitag M. Centrochromatin of Fungi. Prog Mol Subcell Biol 2017;56:85–109. https://doi.org/10.1007/978-3-319-58592-5_4.

47. Darling ACE, Mau B, Blattner FR, N.T. P. Mauve: multiple alignment of conserved genomic sequence with rearrangements. Genome Res 2004;14:1394–403. https://doi.org/10.1101/gr.2289704.

48. Juhász Á, Pfeiffer I, Keszthelyi A, Kucsera J, Vágvölgyi C, Hamari Z. Comparative analysis of the complete mitochondrial genomes of *Aspergillus niger* mtDNA type 1a and *Aspergillus tubingensis* mtDNA type 2b. FEMS Microbiol Lett 2008;281:51–7. https://doi.org/10.1111/j.1574-6968.2008.01077.x.

49. Joardar V, Abrams NF, Hostetler J, Paukstelis PJ, Pakala S, Pakala SB, et al. Sequencing of mitochondrial genomes of nine *Aspergillus* and *Penicillium* species identifies mobile introns and accessory genes as main sources of genome size variability. BMC Genomics 2012;13:698. https://doi.org/10.1186/1471-2164-13-698.

50. Juhász Á, Láday M, Gácser A, Kucsera J, Pfeiffer I, Kevei F, et al. Mitochondrial DNA organisation of the mtDNA type 2b of *Aspergillus tubingensis* compared to the *Aspergillus niger* mtDNA type 1a. FEMS Microbiol Lett 2004;241:119–26. https://doi.org/10.1016/j.femsle.2004.10.025.

51. Niedzwiecka K, Tisi R, Penna S, Lichocka M, Plochocka D, Kucharczyk R. Two mutations in mitochondrial ATP6 gene of ATP synthase, related to human cancer, affect ROS, calcium homeostasis and mitochondrial permeability transition in yeast. Biochim Biophys Acta - Mol Cell Res 2018;1865:117–31. https://doi.org/10.1016/j.bbamcr.2017.10.003.

52. Ward M, Wilkinson B, Turner G. Transformation of *Aspergillus nidulans* with a cloned, oligomycin-resistant ATP synthase subunit 9 gene. Mol Gen Genet MGG 1986;202:265–70. https://doi.org/10.1007/BF00331648.

53. Yu Y, Amich J, Will C, Eagle CE, Dyer PS, Krappmann S. The novel *Aspergillus fumigatus* MAT1-2-4 mating-type gene is required for mating and cleistothecia formation. Fungal Genet Biol 2017;108:1–12. https://doi.org/10.1016/j.fgb.2017.09.001.

54. Ramirez-Prado JH, Moore GG, Horn BW, Carbone I. Characterization and population analysis of the mating-type genes in *Aspergillus flavus* and *Aspergillus parasiticus*. Fungal Genet Biol 2008;45:1292–9. https://doi.org/10.1016/j.fgb.2008.06.007.

55. Houbraken J, Dyer PS. Induction of the sexual cycle in filamentous ascomycetes. In: van den Berg MA, Maruthachalam K, editors. Genet. Transform. Syst. Fungi, Vol. 2, vol. 2, Cham: Springer International Publishing; 2015, p. 23–46. https://doi.org/10.1007/978-3-319-10503-1_2.

56. Haber JE. Mating-Type Genes and MAT Switching in *Saccharomyces cerevisiae*. Genetics 2012;191:33–64. https://doi.org/10.1534/genetics.111.134577.

57. Hanson SJ, Byrne KP, Wolfe KH. Flip/flop mating-type switching in the methylotrophic yeast *Ogataea polymorpha* is regulated by an Efg1-Rme1-Ste12 pathway. PLoS Genet 2017;13:1–26. https://doi.org/10.1371/journal.pgen.1007092.

58. Hanson SJ, Byrne KP, Wolfe KH. Mating-type switching by chromosomal inversion in methylotrophic yeasts suggests an origin for the three-locus *Saccharomyces cerevisiae* system. Proc Natl Acad Sci U S A 2014;111:E4851–8. https://doi.org/10.1073/pnas.1416014111.

59. Carpentier F, Rodríguez De La Vega RC, Branco S, Snirc A, Coelho MA, Hood ME, et al. Convergent recombination cessation between mating-type genes and centromeres in selfing anther-smut fungi. Genome Res 2019;29:944–53. https://doi.org/10.1101/gr.242578.118.

60. Chitrampalam P, Inderbitzin P, Maruthachalam K, Wu BM, Subbarao K V. The *Sclerotinia sclerotiorum* Mating Type Locus (MAT) Contains a 3.6-kb Region That Is Inverted in Every Meiotic Generation. PLoS One 2013;8. https://doi.org/10.1371/journal.pone.0056895.

61. Chitrampalam P, Pryor BM. Characterization of mating type (MAT) alleles differentiated by a natural inversion in *Sclerotinia minor*. Plant Pathol 2015;64:911–20. https://doi.org/10.1111/ppa.12305.

62. Wright AE, Dean R, Zimmer F, Mank JE. How to make a sex chromosome. Nat Commun 2016;7:12087. https://doi.org/10.1038/ncomms12087.

63. Horn BW, Olarte RA, Peterson SW, Carbone I. Sexual reproduction in *Aspergillus tubingensis* from section *Nigri*. Mycologia 2013;105:1153–63. https://doi.org/10.3852/13-101.

64. Horn BW, Moore GG, Carbone I. Sexual reproduction in *Aspergillus flavus*. Mycologia 2009;101:423–9. https://doi.org/10.3852/09-011.

65. Arabatzis M. Sexual reproduction in the opportunistic human pathogen *Aspergillus terreus* 2013;105:71–9. https://doi.org/10.3852/11-426.

66. Raper KB, Fennell DI. The genus *Aspergillus*. 1965.

67. O'Gorman CM, Fuller HT, Dyer PS. Discovery of a sexual cycle in the opportunistic fungal pathogen *Aspergillus fumigatus*. Nature 2009;457:471–4. https://doi.org/10.1038/nature07528.

68. Ojeda-López M, Chen W, Eagle CE, Gutiérrez G, Jia WL, Swilaiman SS, et al. Evolution of asexual and sexual reproduction in the aspergilli. Stud Mycol 2018;91:37–59. https://doi.org/10.1016/j.simyco.2018.10.002.

69. Link HF. Observationes in ordines plantarum naturales. Dissertatio I. Mag Ges Naturf Freunde Berlin 3 1809;3–42.

70. Chen AJ, Hubka V, Frisvad JC, Visagie CM, Houbraken J, Meijer M, et al. Polyphasic taxonomy of *Aspergillus* section *Aspergillus* (formerly *Eurotium*), and its occurrence in indoor environments and food. Stud Mycol 2017;88:37–135. https://doi.org/10.1016/j.simyco.2017.07.001.

71. Houbraken J, Kocsubé S, Visagie CM, Yilmaz N, Wang XC, Meijer M, et al. Classification of *Aspergillus*, *Penicillium*, *Talaromyces* and related genera (*Eurotiales*): An overview of families, genera, subgenera, sections, series and species. Stud Mycol 2020;95:5–169. https://doi.org/10.1016/j.simyco.2020.05.002.

List of additional files

Additional files accompanying this chapter can be accessed through the following link:

https://doi.org/10.21203/rs.3.rs-256129/v1

Additional file 1. Table 4.S1.

Additional file 2. Table 4.S2.

Additional file 3. Table 4.S3. and Table 4.S4.

Additional file 4. Figure 4.S1.

Additional file 5. Figure 4.S2.

Additional file 6. Table 4.S5, 4.S6, and 4.S7 and Figures 4.S3 and 4.S4

Additional file 7. Table 4.S8

Additional file 8. Table 4.S9

CHAPTER 5

Genome sequences of 24 *Aspergillus niger sensu stricto* strains to study heterokaryon compatibility and sexual reproduction

Sjoerd J. Seekles, Maarten Punt, Niki Savelkoel, Jos Houbraken, Han A.B. Wösten, Robin A. Ohm, Arthur F.J. Ram

Submitted for publication

Abstract

Mating-type distribution, heterokaryon compatibility and subsequent diploid formation were studied in 24 *Aspergillus niger sensu stricto* strains. The genomes of the 24 strains were sequenced and analyzed revealing an average of 6.1 ± 2.0 SNPs/kb between *A. niger sensu stricto* strains. Mating-types were found to be equally distributed, as 12 *MAT1-1* loci and 12 *MAT1-2* loci were present. The genome sequences were used together with available genome data to generate a phylogenetic tree revealing three distinct clades within *A. niger sensu stricto*. The phylogenetic differences were used to select for strains to analyze heterokaryon compatibility. Conidial color markers (*fwnA* and *brnA*) and auxotrophic markers (*pyrG* and *nicB*) were introduced via CRISPR/Cas9 based genome editing in a selection of strains. Twenty-three parasexual crosses using eleven different strains were performed. Only a single parasexual cross between genetically highly similar strains resulted in successful formation of heterokaryotic mycelium, indicating widespread heterokaryon incompatibility as well as multiple active heterokaryon incompatibility systems between *A. niger sensu stricto* strains. The two vegetatively compatible strains were of two different mating-types and a stable diploid was isolated from this heterokaryon. Sclerotium formation was induced on agar media containing Triton X-100; however, the sclerotia remained sterile and no ascospores were observed. Nevertheless, this is the first report on a diploid *A. niger sensu stricto* strain with two different mating-types which offers the unique possibility to screen for conditions that might lead to ascospore formation in *A. niger.*

Introduction

Filamentous fungi, and more specifically *Aspergillus* species, are known to propagate mainly via asexual reproduction. For many *Aspergillus* species no sexual cycle is found [1]. In fact, researchers used to believe that meiosis was rendered impossible in certain strictly asexual *Aspergillus* species such as *Aspergillus fumigatus*, *Aspergillus flavus*, *Aspergillus terreus* and *Aspergillus niger* [2]. However, more recent studies and the rise of next generation sequencing revealed that *Aspergillus* species which are seemingly without a sexual cycle have the genetic information indicating that they could be able to propagate using meiosis [3]. Around 31% of all accepted Aspergilli have been proven to reproduce sexually, with 19 species being heterothallic [4]. The currently available (genomic) research data suggests that sexual reproduction within Aspergilli still occurs more often than is currently shown *in vitro* [5]. One such *Aspergillus* species with a rather elusive sexual cycle is *A. niger* [6].

The name *A. niger* has been used in a broad sense throughout literature to refer to species belonging to *Aspergillus* section *Nigri*, the '*A. niger* aggregate', the 'black Aspergilli', 'the *A. niger* clade' or the '*Aspergillus niger* group' [7–10]. However, *A. niger* is also referred to as a species within *Aspergillus* section *Nigri.* Therefore, it became a necessity to define strains strictly belonging to the species *A. niger* specifically as *A. niger sensu stricto* strains to inform the reader about the exclusion of other black Aspergilli part of *Aspergillus* section *Nigri*, such as *Aspergillus neoniger*, *Aspergillus welwitschiae* or *Aspergillus luchuensis.* The filamentous fungus *A. niger sensu stricto* is a well-known producer of enzymes and organic acids, and has been industrially and biotechnologically relevant for over 100 years [11–13]. Functional sexual reproduction in industrially relevant fungi can benefit industry greatly, as it can be a useful tool in strain improvement [14]. Genetic alterations resulting from sexual recombination are not considered genetic manipulation, making the methodology viable for strictly non-GMO strains [15]. Successful studies revealing *in vitro* sexual reproduction in industrially

important fungi, such as *Trichoderma reesei* and *Penicillium chrysogenum*, have been reported [16,17].

Research on vegetative heterokaryon incompatibility in ascomycetes and the involved *het* and *vic* genes has been mostly explored in *Neurospora crassa* and *Podospora anserina* [18]. All strains that show vegetative heterokaryon compatibility with each other are considered part of the same vegetative compatibility group (VCG). Heterokaryon incompatibility in *N. crassa* and *P. anserina* generally requires an interaction between two proteins of which at least one contains a HET domain [19]. The HET domain is defined as a region containing three conserved amino acid blocks [20]. In most cases, heterokaryon incompatibility occurs when different genetic versions exist within the fungus of the *het* gene or its partner, meaning the fungus is heteroallelic for this region, resulting in incompatibility and subsequently cell death [21]. The best studied heterokaryon incompatibility systems are regulated by two (or more) genes of which at least one contains a HET domain. This is true for the *het-c/pin-c* and *het-6/un-24* systems in *N. crassa* [20,22] as well as the *het-c/het-d* and *het-c/het-e* systems in *P. anserina* [23].

In *Aspergillus* section *Nigri*, anastomosis and subsequently plasmogamy leads to cell death in almost all cases when parasexual crosses are attempted, unless the nuclei are isogenic [24,25]. A hypothetical purpose for this phenomenon of vegetative incompatibility has been proposed and states that the organism could benefit by blocking transfer of viruses when the fungus is limited to self-mating [26]. The mechanisms behind self-recognition and subsequent heterokaryon compatibility or heterokaryon incompatibility are poorly understood in Aspergilli. Previous research concluded that vegetative heterokaryon incompatibility genes in *A. niger* differs from those observed in *N. crassa* and *P. anserina* [27]. The gene *het-C* is present in *A. niger*, but does not seem to vary between *A. niger* strains CBS513.88 and ATCC1015 even though these strains are vegetatively incompatible. Therefore, it is unlikely that the *het-C* gene functions as a heterokaryon incompatibility gene in *A. niger.* Consequently, heterokaryon incompatibility in *A. niger* seems to be mediated by different genes than in *N. crassa.*

Certain filamentous fungi are homothallic and therefore able to undergo a sexual cycle with itself, such as *Aspergillus nidulans* [28]. In contrast, sexual reproduction in heterothallic ascomycetes requires the crossing of strains with two different mating-types [29]. Screening natural isolates of a heterothallic species for the distribution of the MAT1-1 or the MAT1-2 locus would indicate whether sexual propagation still occurs in nature. MAT loci contain about 19 genes of which the presence of the MAT transcription factors (either the *MAT1-1-1* gene or the *MAT1-2-1* gene) define the mating-type (Figure 5.1). Sexual reproduction of ascomycetes is mediated by the mating-type genes and results in asci wherein ascospores are formed. The formation of asci and ascospores by Aspergilli occurs inside cleistothecia, and in some species these structures resemble sclerotia. It was inside sclerotia where the first products of sexual recombination have been found after prolonged incubation times for *A. tubingensis* [30], *Aspergillus parasiticus* [31] and *Aspergillus flavus* [32]. Therefore, identifying the appropriate environmental conditions needed for sclerotia formation is considered a first-step prerequisite for finding ascospore formation.

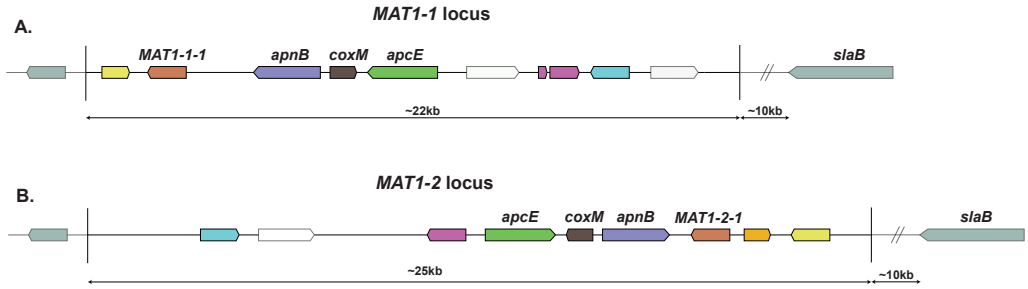

Figure 5.1. Schematical overview of the *MAT1-1* and *MAT1-2* loci in *Aspergillus niger*. Conserved genes between the two MAT loci have been color coded. White genes are not conserved between the two loci and grey genes are positioned outside of the two MAT loci. In red the mating type genes *MAT1-1-1* and *MAT1-2-1* respectively. These genes are transcription factors, where *MAT1-1-1* contains an 'alpha1 HMG-box' domain and *MAT1-2-1* contains a high mobility group (HMG) domain. In Aspergilli, these mating type genes are normally flanked by the DNA lyase *apnB* and a cytoskeleton assembly control factor *slaB*. However, in *A. niger* the *slaB* gene is located more than 10kb downstream of the MAT genes. **A.** Mating type locus *MAT1-1*. This mating type locus appears to have a flipped orientation when compared to the *MAT1-2* locus and when compared to *MAT1-1* and *MAT1-2* loci of other Aspergilli. **B.** Mating type locus *MAT1-2*.

Only recently described in the *A. niger* neotype strain CBS554.65, the orientation of the genes in this locus corresponds with expectations based on the *MAT1-1* and *MAT1-2* locus organization of other Aspergilli. The mating-type loci, the individual genes and their possible functions in *A. niger* have been discussed more extensively in a recent study [44].

Materials and Methods

Strains, media, cultivation conditions and conidia harvesting

The strains sequenced in this study are listed in Table 5.1. The mutant strains made in this study are listed in Table 5.2. Strains are cultivated on minimal medium (MM), prepared as described previously [33], for 7 days at 30°C unless noted otherwise. Conidia were harvested in physiological salt buffer containing Tween 80 (0.9% NaCl, 0.02% Tween 80 in demi water) and filtrated using sterile filters (Amplitude Ecocloth, CONTEC) to separate them from mycelium fragments.

Table 5.1. *Aspergillus niger sensu stricto* strains sequenced in this study

CBS number	Synonyms	DTO number	Country of Origin	Isolated from	Mating Type
CBS 112.32		DTO 028-I3	Japan	Unknown	MAT1-1
CBS 113.50	NRRL 334, ATCC 6275	DTO 008-C3	Unknown	Leather	MAT1-2
CBS 118.52		DTO 058-I1	Unknown	Unknown	MAT1-2
CBS 124.48		DTO 029-B1	Unknown	Unknown	MAT1-2
CBS 131.52	NRRL 334, ATCC 6275	DTO 029-C3	Unknown	Leather	MAT1-1
CBS 630.78	NRRL 1956	DTO 067-H7	South Pacific Islands	Army equipment	MAT1-2
CBS 769.97	NRRL 334, ATCC 6275	DTO 367-D1	Unknown	Leather	MAT1-1
CBS 115988	NRRL 3112	DTO 059-C7	Unknown	Unknown	MAT1-1
CBS 115989	NRRL 3122	DTO 367-D6	Unknown		MAT1-1
CBS 133816	IBT 24631	DTO 316-E3	Denmark	Black pepper	MAT1-2
CBS 147320		DTO 096-A7	Australia	Grape	MAT1-1
CBS 147321		DTO 096-A9	Norway	Arctic soil	MAT1-2
CBS 147322		DTO 096-C6	Brazil	Coffee	MAT1-2
CBS 147323		DTO 096-D7	Turkey	Raisin	MAT1-2
CBS 147324		DTO 096-E1	Unknown	Unknown	MAT1-2
CBS 147343		DTO 291-B7	Thailand	Coffee bean	MAT1-1
CBS 147344		DTO 293-G7	Thailand	Coffee beans (Robusta)	MAT1-2

CBS number	Synonyms	DTO number	Country of Origin	Isolated from	Mating type
CBS 147345		DTO 316-E4	United States	Unknown	MAT1-1
CBS 147346		DTO 321-E6	the Netherlands	CF patient material	MAT1-2
CBS 147347		DTO 326-A7	the Netherlands	Petridish; soft drink factory	MAT1-1
CBS 147352		DTO 368-I1	Mexico	Air next to bottle blower	MAT1-1
CBS 147353		DTO 368-I6	Italy	Foods factory of Sanquinetto	MAT1-1
CBS 147371		DTO 096-A5	India	Green coffee bean	MAT1-1
CBS 147482		DTO 175-I5	Portugal	Surface Water	MAT1-2

Table 5.2. Mutant *A. niger* strains made in this study

Strain name	Mutations	Description	Parental strain
NS1	*pyrG*$^-$, *fwnA*$^-$	fawn colored conidia, uridine deficient (needs supplement)	CBS 112.32
NS2	*pyrG*$^-$, *fwnA*$^-$	fawn colored conidia, uridine deficient (needs supplement)	CBS 118.52
NS3	*nicB*$^-$, *brnA*$^-$	brown colored conidia, nicotinamide deficient (needs supplement)	CBS 147371
NS4	*pyrG*$^-$, *fwnA*$^-$	fawn colored conidia, uridine deficient (needs supplement)	CBS 147323
NS5	*pyrG*$^-$, *fwnA*$^-$	fawn colored conidia, uridine deficient (needs supplement)	CBS 147324
NS6	*nicB*$^-$, *brnA*$^-$	brown colored conidia, nicotinamide deficient (needs supplement)	CBS 147482
NS7	*pyrG*$^-$, *fwnA*$^-$	fawn colored conidia, uridine deficient (needs supplement)	CBS 133816
NS8	*pyrG*$^-$, *fwnA*$^-$	fawn colored conidia, uridine deficient (needs supplement)	CBS 147347
NS9	*pyrG*$^-$, *fwnA*$^-$	fawn colored conidia, uridine deficient (needs supplement)	CBS 147352
NS10	*pyrG*$^-$, *fwnA*$^-$	fawn colored conidia, uridine deficient (needs supplement)	CBS 147353
NS11	*nicB*$^-$, *brnA*$^-$	brown colored conidia, nicotinamide deficient (needs supplement)	CBS 147343

Strain name	Mutations	Description	Parental strain
SJS111	*nicB*$^{-}$, *brnA*$^{-}$	brown colored conidia, nicotinamide deficient (needs supplement)	CBS 147323
SJS112	*nicB*$^{-}$, *brnA*$^{-}$	brown colored conidia, nicotinamide deficient (needs supplement)	CBS 118.52
SJS113	*nicB*$^{-}$, *brnA*$^{-}$	brown colored conidia, nicotinamide deficient (needs supplement)	CBS 112.32
SJS114	*nicB*$^{-}$, *brnA*$^{-}$	brown colored conidia, nicotinamide deficient (needs supplement)	CBS 147347
SJS150.1		Heterozygous diploid strain containing two mating type loci	SJS114 & NS4
SJS150.2		Heterozygous diploid strain containing two mating type loci	SJS114 & NS4
SJS150.3		Heterozygous diploid strain containing two mating type loci	SJS114 & NS4
SJS151.1		Heterozygous diploid strain containing two mating type loci	SJS111 & NS8
SJS151.2		Heterozygous diploid strain containing two mating type loci	SJS111 & NS8
SJS151.3		Heterozygous diploid strain containing two mating type loci	SJS111 & NS8

Whole genome sequencing

A total of 24 *Aspergillus niger* strains were obtained from the CBS culture collection housed at the Westerdijk Fungal Biodiversity Institute, Utrecht, the Netherlands. These strains were identified as *A. niger sensu stricto* based on partial calmodulin gene sequencing [34]. The strains were grown on malt extract agar (MEA, Oxoid) for 7 days and subsequently conidia were harvested. Liquid cultures containing complete medium (CM) [33] were inoculated with conidia suspension and grown overnight at 30 °C. Genomic DNA (gDNA) was isolated using a chloroform/phenol based genome extraction method [33]. The gDNA was subsequently purified using the DNA purification kit NucleoSpin Plant II (Macherey-Nagel). This gDNA was sequenced at the Utrecht Sequencing Facility (USEQ) using Illumina NextSeq 500 paired-end technology. Raw sequence files were trimmed on both ends when quality was lower than 15 using bbduk from the BBMap

tool suite (BBmap version 37.88; https://sourceforge.net/projects/bbmap/). The trimmed reads were assembled with SPAdes v3.11.1 applying kmer lengths of 21, 33, 55, 77, 99 and 127 (Bankevich et al., 2012). Sequences (scaffolds) shorter than 1000 bp were removed from the assembly. Genes were predicted with AUGUSTUS version 3.0.3 (Stanke et al., 2006) using the provided parameter set for *A. nidulans* and the publicly available *A. niger* ATCC1015 transcriptome reads (SRR6012879) were used as an aid in gene prediction. Functional annotation of the predicted genes was performed as previously described [35] to assign a putative function to the genes. The assemblies and gene predictions are available from NCBI GenBank under BioProject ID PRJNA743902 [to be released upon publication]. Furthermore, the annotated genomes can be analyzed interactively on https://fungalgenomics.science.uu.nl/.

Genomic differences between genomes

The genome comparisons were done using either the publicly available assembly of strain NRRL3 [36], or the assembly of the newly sequenced strain CBS147323 as reference. The reads of the other 23 or 24 strains were aligned to these references. Single nucleotide polymorphisms (SNPs) were identified and their impact on the predicted genes was determined. The reads were aligned to the reference assemblies using Bowtie 2 version 2.4.2. [37]. The resulting SAM files were provided with read groups and subsequently transformed to BAM files and sorted using SAMtools [38]. Duplicates were marked and subsequent variant calling was done using GATK HaploTypeCaller version 4.1.4.1. [39] resulting in VCF files describing the SNPs. Lastly, SnpEff and SnpSift [40,41] were used to determine the location of SNPs and their predicted impact in regard to the genes. Visualization and manual inspection of SNPs was done using the Integrative Genome Viewer [42].

Construction of phylogenetic tree based on conserved proteins

The sequences of the predicted proteins of the 24 strains were used to construct a phylogenetic tree. Additionally, we collected the protein files of nine other publicly available strains namely: *A. niger* ATCC1015 [12], *A. niger* NRRL3 [36], *A. niger* ATCC64974 [43],

A. niger CBS513.88 [11], *A. niger* CBS554.65 [44], *A. niger* CBS101883 [45], *A. niger* ATCC13496 [45], *A. niger* ATCC13157 [45] and outgroup *A. welwitschiae* CBS139.54b [45]. The complete proteome files were used by OrthoFinder [46] to identify the conserved proteins that are present exactly once in each of the 33 strains. The resulting proteins for each strain were concatenated which resulted in 33 files containing concatenated proteins. These sequences were aligned using MAFFT [47]. RAxML version 8 [48] was used to construct a phylogenetic tree from 1000 bootstrapping replicates. The resulting tree file was visualized using iTOL version 4 [49].

Plasmid construction

The primers used in this study are listed in Table 5.S1. The CRISPR/Cas9 plasmids were constructed as described previously [50]. In short, CRISPR/Cas9 target sequences were chosen based on ChopChop predictors [51] for the *fwnA* (An09g05730, NRRL3_00462), *pyrG* (An12g03570, NRRL3_03466) and *nicB* (An11g10910, NRRL3_09250) genes. Target sequences were tested with BLASTn for consistency within the 24 *A. niger sensu stricto* genomes sequenced in this study. Primers were designed to create CRISPR/Cas9 plasmids containing guide RNA targeting these genes. The resulting PCR products were digested with the restriction enzyme *Pac*I (Fermentas) and ligated into vector pFC332 [52]. Additionally we used a CRISPR/Cas9 plasmid targeting the *brnA* (An14g05370, NRRL3_01040) gene that has been made previously [50]. The complete list of plasmids used in this study can be found in Table 5.3.

Transformation of wild-type *A. niger sensu stricto* strains

PEG-mediated *A. niger* transformations and media preparations were carried out as previously described [33,50]. A total of 2 µg of each CRISPR/Cas9 plasmid was used per transformation. Auxotrophic markers (*pyrG* or *nicB*) and color markers (*fwnA* or *brnA*) were introduced via CRISRP/Cas9-based genome editing. Two genetic disruptions were performed in a single transformation experiment introducing either the disruption of *brnA* and *nicB* (Parent A) or the disruption of *fwnA* and *pyrG* (Parent B). Protoplasts were plated on minimal medium with sucrose (MMS), supplemented with the required compound for

the auxotrophic strains (20 µM nicotinamide for a *nicB*$^{-}$ mutants and 10 mM uridine for a *pyrG*$^{-}$ mutants). Transformants with a brown or fawn phenotype were selected and purified on supplemented MM plates containing 100 µg/mL hygromycin and the required supplementation. After purification on MM with supplement, the transformants were plated on MM with supplement and MM without supplement to test for the nicotinamide or uridine requirements. Transformants that had the correct conidia coloration and were unable to grow without supplement in the last purification round were harvested and used for parasexual crossings. The mutant strains generated in this study are listed in Table 5.2.

Table 5.3. Plasmids used in this study

Plasmid name	Description	Reference
pFC332	AMA1 sequence containing plasmid with *Aspergillus* optimized Cas9 and hygromycin selection marker	Nodvig, C.S. et al. "A CRISPR-Cas9 System for Genetic Engineering of Filamentous Fungi. PloS One. 2015
pFwnA1	pFC332 plasmid containing guide RNA targeting the *fwnA* gene of *A. Niger*	this study
pPyrG2	pFC332 plasmid containing guide RNA targeting the *pyrG* gene of *A. Niger*	this study
pNicB1	pFC332 plasmid containing guide RNA targeting the *nicB* gene of *A. Niger*	this study
pTLL40.9	pFC332 plasmid containing guide RNA targeting the *brnA* gene of *A. Niger*	van Leeuwe, T.M. et al. "Efficient marker free CRISPR/Cas9 genome editing for functional analysis of gene families in filamentous fungi" Fungal Biology and Biotechnology, 2019

Forced heterokaryon formation between *A. niger sensu stricto* strains

Heterokaryon formation was tested by mixing protoplasts of complementing parental strains and plating out the mixture of protoplasts on MM plates without supplement to select for heterokaryons. In short, protoplasts of both parents (Parent A and Parent B)

are mixed gently and subsequently incubated in 1 mL PEG buffer for five minutes similar to the PEG-mediated transformation protocol [33]. After PEG incubation, the suspension was diluted with 2 mL STC buffer and subsequently plated on MMS plates containing 500 µg/mL caffeine, but without supplementation of nicotinamide or uridine. Since both Parent A and Parent B are auxotroph for different compounds, only when protoplasts of the two parents fuse together to form a heterokaryotic mycelium can the fungus survive.

Diploid selection and purification

A stable diploid strain was isolated from the heterokaryotic mycelium (Figure 5.S1). A small piece of heterokaryotic mycelium was cut out from the MMS plates after 3 days of growth at 30°C and transferred to a new MM plate. This plate was incubated at 30°C for 7 days to maximize sporulation. During heterokaryotic growth, spontaneous diploid formation can take place (Shcherbakova and Rezvaia, 1977). In order to isolate diploids, the conidia from the heterokaryon were harvested, filtered and plated in high concentrations on fresh MM plates. These conidia will only survive the fresh MM plate if genotypes of both parents are present. After 5 days of incubation at 30°C colonies with normal (non-heterokaryotic) growth and black conidia were isolated, as these are the potentially diploid strains, and plated on MEA plates. These putative diploids strains were point inoculated on MM containing 0.4 µg/mL benomyl to show the true diploidy in these strains. The mating-type loci were amplified by performing diagnostic PCR and subsequently sequenced to confirm that these stable diploids contained both mating-types (Figure 5.2). The conidial size was measured by taking images and analyzing them by performing a threshold and subsequent particle analysis using Fiji (ImageJ) software (Figure 5.S2). This resulted in average conidium sizes based on pixels. Significance of the differences in conidium sizes was tested using a Student's t-test ($p<0.01$).

Sclerotia formation and investigating ascospore formation

Previous observations indicated that the addition of Triton X-100 stimulated sclerotia formation in *A. niger sensu stricto* strains (Seekles, unpublished data). This ability of Triton X-100 to induce sclerotium formation in *A. niger* was assessed in laboratory strain

N402. In these experiments, MEA plates with the addition of various concentrations of Triton X-100 (0%, 0.05%, 0.1%, 0.5% and 1%) were used to find optimal concentration of Triton X-100 to induce sclerotium formation. Conidia of N402 were diluted and approximately 100 conidia were subsequently plated and distributed over the ager plate to obtain colonies derived from a single conidium. Sclerotium formation was assessed after 6 days incubation at 30°C.

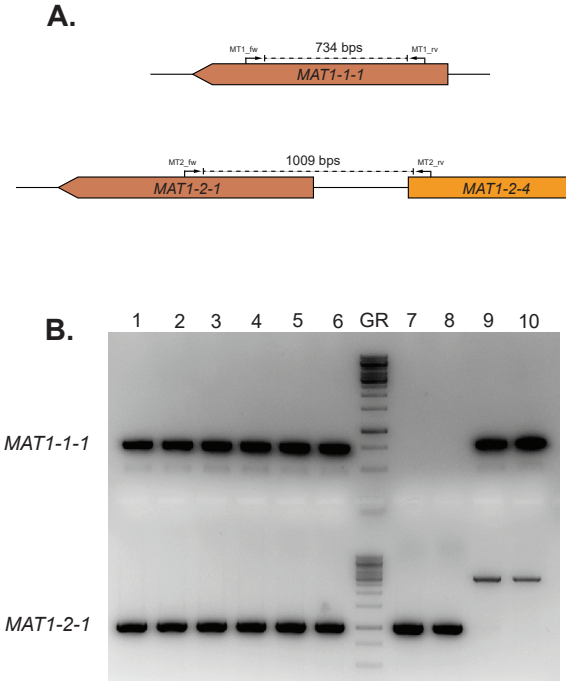

Figure 5.2. Diagnostic PCR for the presence of the mating-type genes. A. An *in silico* representation of the diagnostic PCRs performed to investigate presence of the mating-type genes. If the *MAT1-1-1* gene is present, amplification with the MT1_fw and MT1_rv primers will result in a 734 bps band on the gel. If the *MAT1-2-1* gene is present, amplification with the MT2_fw and MT2_rv primers will result in a 1009 bps band on the gel. **B.** This gel shows the diagnostic PCR results confirming the presence of both the *MAT1-1-1* gene and the *MAT1-2-1* gene in the six diploid strains. Column 1-6 are PCR products resulting from amplification on gDNA from individually obtained diploid strains SJS150.1, SJS150.2, SJS150.3, SJS151.1, SJS151.2 and SJS151.3, respectively. In the diploid strains, both PCR products are present confirming the presence of both mating-type genes. Column 7 contains the GeneRuler 1kb DNA ladder (Thermo Scientific). Column 8-9 are PCR products resulting from amplification on gDNA from *MAT1-2* containing CBS147323 parental strains (SJS111 and NS4, respectively). Column 10-11 are PCR

products resulting from amplification on gDNA from *MAT1-1* containing CBS147347 parental strains (SJS114 and NS8, respectively). In the haploid parental strains, only a single mating-type gene is present. Note that the CBS 147347 parental strains show off-target amplification, but do not contain the *MAT1-2-1* gene.

Sclerotia formation of the obtained diploid strains was induced by plating conidia on MEA, potato-dextrose agar (PDA, BD Difco) and oatmeal agar (OA, BD Difco) with the addition of 1% (v/v) Triton X-100 (Sigma). Additionally, sclerotia formation of both wild-type parental strains of the diploids, mixed together and plated, was assessed on MEA, OA, Czapek yeast agar (CYA), Czapek yeast agar / oatmeal agar (CYA/OA) and Wickerham's antibiotic test medium (WATM) with the addition of 1% (v/v) Triton X-100 (Sigma). Plating was performed by point inoculation or homogenous spread of ~100 or fewer conidia. The plates were covered in aluminum foil and left for 1 – 4 months at 30ºC after which sclerotia formation was assessed. Sclerotia were taken from the plate and rolled over a fresh agar plate to remove conidia attached to the outside of the sclerotium. The sclerotia were cracked on top of a microscope slide, 5 µL physiological salt buffer was added, and the presence of asci/ascospores was assessed using light microscopy.

Data availability

Strains and plasmids used are available upon request. Figure 5.S1 contains a detailed overview of the purification of the diploid strains. Figure 5.S2 shows the size differences between haploid and diploid conidia of *A. niger*. Figure 5.S3 shows the effectiveness of Triton X-100 as inducing agent for the formation of sclerotia in various wild-type *A. niger sensu stricto* strains. Table 5.S1 lists primers used in this study. Table 5.S2 lists the total parasexual crosses attempted in this study. The genome assemblies and predicted genes that were sequenced in this study are available in NCBI GenBank under BioProject ID PRJNA743902 [to be released upon publication]. The annotated genomes can be analyzed interactively on https://fungalgenomics.science.uu.nl/.

Results

Whole genome sequences of 24 *Aspergillus niger sensu stricto* strains

Twenty-four *A. niger sensu stricto* strains were studied in order to test for plasmogamy and subsequent vegetative heterokaryon compatibility. The *A. niger* strains originate from various sources from all over the world and include strains isolated from nature as well as from foods or from food-related industries (Table 5.1). These strains were all identified as *A. niger sensu stricto* based on partial sequencing of the calmodulin gene [1]. The genomes of these strains were sequenced, and genes were predicted and functionally annotated. Since the strains have been sequenced using Illumina technology, the assemblies are more fragmented than previously published assemblies. However, the gene count is comparable between the strains, and the assemblies and gene predictions are of high quality as indicated by their CEGMA and BUSCO completeness score (> 98%). A BLASTn search was performed in order to investigate the MAT1-1 and MAT1-2 distribution in the 24 *A. niger sensu stricto* strains. An equal distribution of mating-types (12:12) was found in these strains, as has been described before [44].

Genome-based phylogeny of 32 *A. niger* strains

To perform successful parasexual crossings, strains need to be heterokaryon compatible. The genetic similarity between strains has a direct effect on heterokaryon compatibility. To determine the similarities between the *A. niger sensu stricto* strains, a phylogenetic tree was made based on 7718 conserved proteins using the 24 strains sequenced in this study, as well as eight *A. niger sensu stricto* strains obtained from literature and an *A. welwitschiae* strain as an outgroup. The tree reveals that *A. niger sensu stricto* strains can be classified in three distinct clades (Figure 5.3).

Clade A consists of nine *A. niger sensu stricto* strains, most of which are known for their protein and enzyme production, such as *A. niger* CBS115989 (synonym NRRL3122) and its descendent *A. niger* CBS513.88 [54]. Strain *A. niger* CBS115989 has been well-studied for its enzyme production [55–58]. Additionally, the descendent strain

CBS513.88, industrially used as a glucoamylase producer, has been the first whole-genome sequenced *A. niger* strain chosen based on its importance as a cell factory [11]. Other strains in this clade are also known enzyme producers. Strain *A. niger* CBS115988 (synonym NRRL3112) has been used as an enzyme production platform in the past and present [59–61]. *A. niger* CBS101883 (formerly known as *A. lacticoffeatus*) has not been studied extensively, however it has been used for β-glucosidase production [62]. The type strain *A. niger* CBS554.65 has not been extensively studied either, although some examples of researched enzyme production exists [63,64]. Taken together, this clade contains most if not all *A. niger sensu stricto* strains available from literature used as protein and enzyme producers by industry.

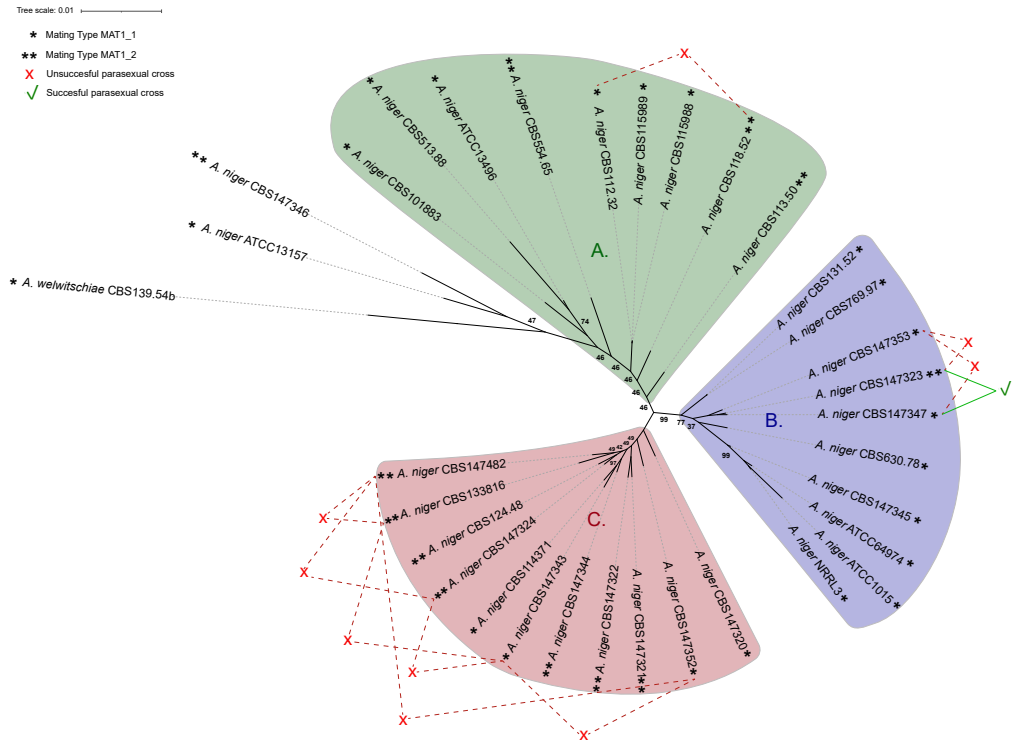

Figure 5.3. Phylogenetic tree of *Aspergillus niger sensu stricto*. The phylogenetic tree was based on 7718 single-copy orthologous proteins found in all 33 included strains. Most *A. niger sensu stricto* strains are part of three distinct clades, Clade A (green), Clade B (blue) or Clade C (red). Mating-types of each strain is visualized with * for the MAT1-1 locus containing genomes and ** for the MAT1-2 locus containing genomes. Heterokaryon formation via forced protoplast fusion was investigated; successful parasexual crosses are visualized by the green lines and

unsuccessful parasexual crosses are visualized by the red lines. A single parasexual crossing resulted in successful heterokaryon formation, between strain CBS147323 and CBS147347 located in Clade B, which are of different mating-type. Bootstrap values smaller than 100 were indicated. The tree was visualized using iTOL v4 [49].

Clade B consists of ten *A. niger sensu stricto* strains. Strains in this clade are best known for their organic acid production, such as the citric acid producer *A. niger* ATCC1015 [12] and strain CBS131.51 (synonym CBS769.97, ATCC6275), which was part of a patent from 1977 for citric acid production. Additionally this clade contains *A. niger* NRRL3 (synonym N400) and *A. niger* ATCC64974 (synonym N402) which have been initially selected for gluconic acid production, and thereafter have extensively been used in laboratory studies [65,66].

Clade C consists of eleven *A. niger sensu stricto* strains and none of the previously sequenced *A. niger* strains were classified in this clade. Therefore this clade consists solely of strains sequenced in this study, many of which are isolated from food or water sources (Table 5.1). The genomic diversity in this clade is relatively small when compared to the differences seen between strains part of clade A and B. Since strains in clade C are more similar to each other, most parasexual crossings between members of this clade were attempted to increase the chance of performing successful parasexual crossings.

The outgroup *A. welwitschiae* CBS139.54b as well as the two *A. niger* strains ATCC13157 and CBS147346 were considered outside of clade A. The exclusion of the two *A. niger* strains from clade A was based on the relatively high number of SNPs found between these two *A. niger* strains and the other *A. niger* strains (see below), as well as the relatively close approximation to the outgroup *A. welwitschiae*.

Quantification (in SNPs) and comparisons between *A. niger* strains

Variant calling was used to calculate the number of SNPs present between genomes sequenced in this study. When comparing the 24 strains to publicly available strain NRRL3, an average of 6.1 SNPs/kb ± 2.0 (standard deviation) was found. This

corresponds to an average of 213,665 SNPs ± 69,150 SNPs in total, when comparing all 24 strains to strain NRRL3 (Table 5.4). Similar results were obtained when using strain CBS147323 as a reference strain. The largest difference was found between NRRL3 and CBS147346 with SNP frequencies of 11.6 SNPs/kb, while the smallest difference was between NRRL3 and CBS147345 with only 112 variations found over the whole genome.

Table 5.4. SNPs between wild-type *A. niger sensu stricto* strains

Strain name	Clade	Compared to CBS 147323	Compared to NRRL3	Compared to *Aspergillus welwitschiae* CBS 139.54.b
CBS 147323	B	0	149612	
CBS 147347	B	40023	148179	
CBS 147353	B	83739	149538	
CBS 630.78	B	125385	157562	
CBS 147345	B	148229	114	
CBS 131.52	B	150536	181329	
CBS 769.97	B	151239	182108	
CBS 147352	C	233388	222760	
CBS 118.52	A	238414	245379	
CBS 124.48	C	239208	231794	
CBS 147321	C	239571	231095	
CBS 113.50	A	239627	232065	
CBS 112.32	A	239627	242061	
CBS 155988	A	240185	242510	
CBS 115989	A	241224	244163	
CBS 147482	C	242026	221875	
CBS 147322	C	242026	236220	
CBS 147343	C	244034	235889	
CBS 133816	C	244298	214050	
CBS 147324	C	244303	226295	
CBS 147344	C	244594	235091	
CBS 147371	C	247056	233945	
CBS 147320	C	248958	255113	
CBS 147346	-	408752	409208	615314
Median		239627	231445	
Average		216367	213665	
Stdev		73157	69150	

Heterokaryon formation between *A. niger sensu stricto* strains

Based on the phylogenetic distances between the *A. niger sensu stricto* strains, several strains were selected to perform parasexual crosses (Table 5.S2) and the parasexual crosses performed between strains within a single clade were visualized (Figure 5.3). To force heterokaryon formation and subsequent diploid formation, selected strains were genetically altered to have an auxotrophy (nicotinamide (*nicB*$^{-}$) or uracil (*pyrG*$^{-}$) requirement) and have conidia of altered coloration (fawn-colored (*fwnA*$^{-}$) or brown-colored (*brnA*$^{-}$) conidia). The genetic alterations were made by PEG-mediated protoplast transformations using CRISPR/Cas9 technology [50]. Since these wild-type strains contained an intact *kusA* gene, we did not include repair DNA in the transformation process, but instead selected for phenotype changes due to indels generated to escape from CRISPR/Cas9 endonuclease activity. A total of fifteen strains were made, being either Parent A (*brnA*$^{-}$, *nicB*$^{-}$) or Parent B (*fwnA*$^{-}$, *pyrG*$^{-}$). Six strains were genetically modified to be Parent A and nine strains were modified to be Parent B (Table 5.2). Notably, genetic alterations of strains CBS112.48 and CBS769.97 were also attempted and subsequently discontinued due to difficulties in protoplasting these strains. Heterokaryon formation was subsequently investigated using PEG-mediated protoplast fusion. Twenty-three parasexual crosses were attempted between eleven different strains. Additionally we performed three self-crosses between the same strain being both Parent A and Parent B. In short, all three attempted self-crosses between complementary marker strains were successful, where all 23 attempted crosses between different strains, except one, were unsuccessful (Table 5.S2). The single successful parasexual cross was between protoplasts of color and auxotrophic mutants of *A. niger* CBS147323 and *A. niger* CBS147347 which are located in clade B of the phylogenetic tree (Figure 5.3).

Possible heterokaryon incompatibility genes of *Aspergillus niger*

Interestingly, strains CBS147323 and CBS147347 were compatible and thus able to form heterokaryotic mycelium, but the closely related strain CBS147353 was incompatible with CBS147323 (Figure 5.3). Therefore, a genetic difference between CBS147347

(compatible with CBS147323) and CBS147353 (incompatible with CBS147323) likely causes the difference in observed heterokaryon compatibility. Strain CBS147353 has ~84,000 SNPs compared to CBS147323 (Table 5.4). From these ~84,000 SNPs, ~44,000 are shared with CBS147347 when compared to CBS147323, and therefore are left out of the analysis as these SNPs could not possibly explain the difference in heterokaryon (in)compatibility observed between these strains. Still ~40,000 SNPs are present in CBS147353 and absent in CBS147347 when compared to CBS147323, of which ~9,000 SNPs are inside exons of genes. Therefore, the comparison between these three strains was limited to differences in proteins containing a HET domain. The 34 HET domain containing proteins of *A. niger* NRRL3 [36] were used to perform BLASTp analyses to find the homologues in the three strains CBS147323, CBS147347 and CBS14753 (Table 5.5). In total, 10 out of the 34 HET domain containing proteins were identical between CBS147323 and CBS147347, but different from CBS147353 and therefore could explain the observed heterokaryon compatibility difference. Additionally, 7 out of the 34 HET domain containing proteins do not cause heterokaryon incompatibility, since differences in these proteins did not result in incompatibility between strains CBS147323 and CBS147347.

Table 5.5. Differences in amino acids (AAs) in HET domain containing proteins between three *A. niger* strains

Gene number	CBS 147323	CBS 147347	CBS 147353	Candidate *het* gene	Does not cause heterokaryon incompatibility
NRRL3_00449	0	0	0		
NRRL3_01616	1	1	17	NRRL3_01616	
NRRL3_01785	0	0	2	NRRL3_01785	
NRRL3_01816	9	9	9		
NRRL3_02842	0	0	0		
NRRL3_02917	1	**	**		NRRL3_02917
NRRL3_03302	3	2	2		
NRRL3_03291	0	0	0		
NRRL3_03392	*	0	*		NRRL3_03392
NRRL3_03956	4	4	2	NRRL3_03956	
NRRL3_03963	0	0	0		
NRRL3_03992	***	1	**		NRRL3_03992
NRRL3_04061	0	0	-1 G	NRRL3_04061	

Gene number	CBS 147323	CBS 147347	CBS 147353	Candidate *het* gene	Does not cause heterokaryon incompatibility
NRRL3_04562	0	0	*	NRRL3_04562	
NRRL3_04624	0	0	STOP	NRRL3_04624	
NRRL3_05224	0	0	6	NRRL3_05224	
NRRL3_05752	0	0	0		
NRRL3_06154	0	0	0		
NRRL3_06349	0	0	0		
NRRL3_07052	6	6	6		
NRRL3_07166	*	1	*		NRRL3_07166
NRRL3_07868	0	0	0		
NRRL3_08552	FRAME_SHIFT	FRAME_SHIFT	FRAME_SHIFT		
NRRL3_08556	*	*	*		
NRRL3_08963	8	8	2	NRRL3_08963	
NRRL3_08976	9	9	2	NRRL3_08976	
NRRL3_09099	*	5	0		NRRL3_09099
NRRL3_09410	4	4	4		
NRRL3_09458	16	*	16		NRRL3_09458
NRRL3_10072	0	0	0		
NRRL3_10361	1	1	1		
NRRL3_10454	**	0	**		NRRL3_10454
NRRL3_11116	0	0	1	NRRL3_11116	
NRRL3_11636	0	0	0		

*gene is absent

**a large gap inside this gene

***a big insertion inside this gene

Purification of a stable heterozygous diploid *A. niger* strain containing two mating-types

The crossing of *A. niger* CBS147323 and *A. niger* CBS147347 was performed in two ways: CBS147323 (*brnA*$^-$, *nicB*$^-$) x CBS147347 (*fwnA*$^-$, *pyrG*$^-$) resulting in three independently obtained diploid strains SJS150.1, SJS150.2, SJS150.3 and CBS147323 (*fwnA*$^-$, *pyrG*$^-$) x CBS147347 (*brnA*$^-$, *nicB*$^-$) resulting in three independently obtained diploid strains SJS151.1, SJS151.2 and SJS151.3 (Table 5.2). Three lines of evidence support that the SJS150.1-3 and SJS151.1-3 strains are true diploids.

First, the six independently obtained diploid strains were checked for sector

formation in the presence of benomyl, since growth in the presence of benomyl forces haploidization in diploids of *Aspergillus* species (Hastie, 1970). Indeed, haploïdization was observed in the presence of benomyl, as shown by the sectors that displayed the original color markers again (Figure 5.S1). Second, since the heterozygous diploid obtained was made between strains with different mating-types, the presence of both mating-type loci was analyzed in the six diploid strains SJS150.1-3 and SJS151.1-3. A diagnostic PCR was performed on the genomic DNA of the diploid strains and confirmed the presence of both the *MAT1-1-1* gene and the *MAT1-2-1* gene in all six independently obtained diploid strains (Figure 5.2). Third, conidia of diploid Aspergilli are known to have an increased size [68]. Therefore, we assessed average conidial sizes using light microscopy comparing the diploid strain SJS150.1 with both parental strains. On average, conidia from CBS147323 and CBS147347 were 19.4 ± 4.4 pixels and 17.7 ± 2.5 pixels in size (400x magnification). In contrast, conidia from diploid SJS150.1 were 32.4 ± 6.0 pixels in size. Indeed, conidia obtained from the diploid strain were significantly larger than conidia from either parent, confirmed statistically with a Student's t-test ($p<0.01$).

Sclerotia formation on medium supplemented with Triton X-100

Previous observations indicated that the addition of Triton X-100 stimulated sclerotia formation in *A. niger sensu stricto* strains (Seekles, unpublished data). The efficiency of Triton X-100 to induce sclerotium formation in *A. niger* was further assessed in laboratory strain N402. In these experiments, MEA plates with the addition of various concentrations of Triton X-100 (0%, 0.05%, 0.1%, 0.5% and 1%) All concentrations of Triton X-100 tested were able to induce sclerotium formation; however, growing *A. niger* N402 on MEA plates containing 1% Triton X-100 (v/v) was the most effective inducer and individual colonies formed sclerotia on all sides of the colony (Figure 5.4). The sclerotium induction by growth on MEA + 1% Triton X-100 plates was also assessed for various strains sequenced in this study (Figure 5.S3). We noted that sclerotium formation was observed in most strains, but the degree of induction varies between strains and experiments. Additionally we tested sclerotia induction by the addition of Triton X-100 to other media, namely: MM, CM, CYA, CYA+OA, OA, WATM and PDA. In short, sclerotia

induction was observed on all these media with the addition of 1% Triton X-100, with the exception of the two defined media MM and CM.

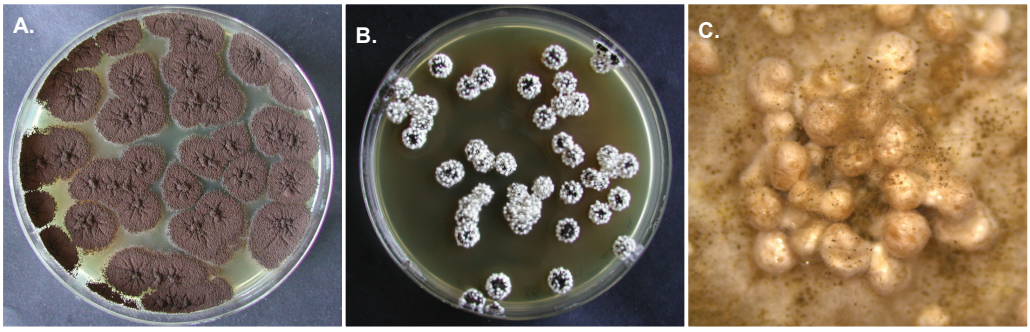

Figure 5.4. Sclerotia induction of *A. niger* N402 on MEA + Triton X-100 plates. Here the effect of Triton X-100 on sclerotium formation in *A. niger* N402 was assessed. Plates were inoculated by confluently plating ~25 conidia per plate. Pictures of plates were taken after 6 days of incubation at 30°C. **A.** Control plate *A. niger* colonies growing on MEA for 6 days at 30°C. **B.** Plate containing MEA + 1% Triton X-100 (v/v). Sclerotia formation is induced in *A. niger* N402 by the addition of Triton X-100. **C.** Pictures of colonies were taken after 14 days using a stereo microscope (Leica EZ4 D). The sclerotium formation in *A. niger* N402 colonies growing on MEA + 1% Triton X-100 is hyper-induced, as all individual colonies formed sclerotia on all sides of the colony.

Sclerotia formation was induced in the diploid strains SJS150.1 and SJS151.1 on MEA, PDA and OA containing 1% Triton X-100 (Figure 5.5A, B). The sclerotia obtained were studied using light microscopy; but no (empty) asci or ascospores were observed. We noted that on the backside of the plates the regions that showed sclerotium formation also produced a brown pigment released into the media, sclerotia of *A. niger* secreting liquid of brown pigmentation has been noted before [69].

Apart from inducing sclerotia formation of the diploid strain, sclerotia were also induced in parental strains CBS147323 and CBS147347 by mixing conidia and subsequently plating them on plates containing 1% Triton X-100 in an attempt to induce the sexual reproduction between these wild-type strains (Figure 5.5C, D). We observed hyper-induction of sclerotia when conidia of parental strains CBS147323 and CBS147347 were mixed and plated together on plates containing 1% Triton X-100.

Notably, the amount of sclerotia obtained after 4 months on the plates containing the mixed parental strains was considerably larger than for the plates containing the diploid strains. Unfortunately, when analyzing the sclerotia under the light microscope, no indicators of sexual reproduction (asci, ascospores) were found.

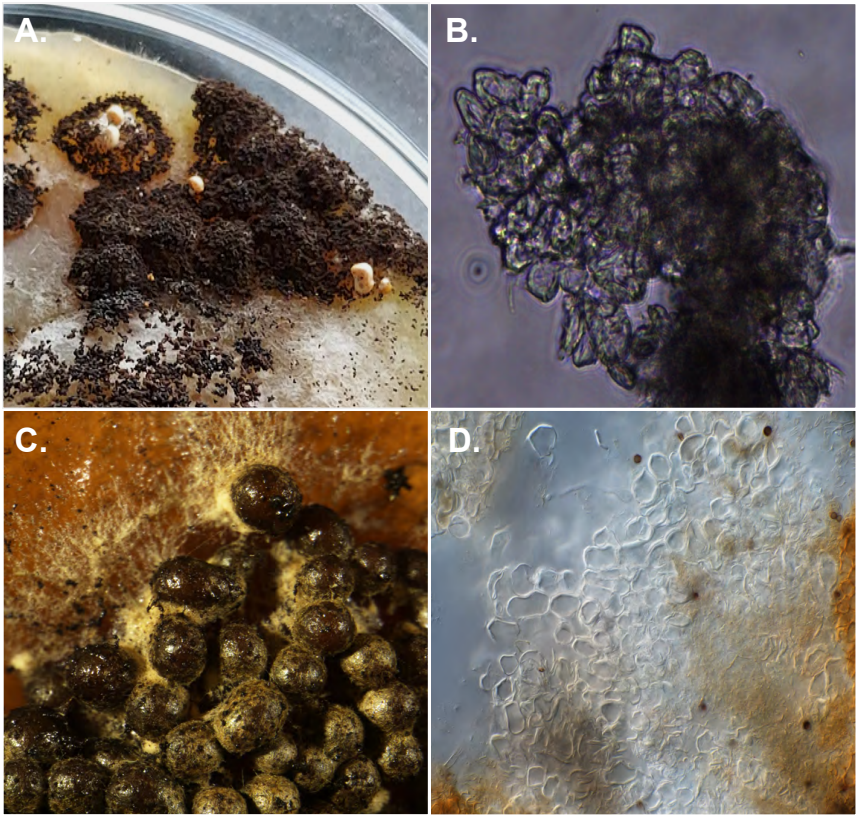

Figure 5.5. Sclerotia induction in diploid *A. niger* strains and its parental strains. Pictures were taken after 4 months of growth at 30°C in the dark in all cases. **A.** Diploid strains SJS150.1 and SJS151.1 were grown on sclerotia inducing media containing 1% Triton X-100. Only a single PDA and a single OA plate containing Triton X-100 showed sclerotia formation and this was limited to a small sector on the plate in both cases. **B.** Light microscopy was used to assess the cell structures of the obtained sclerotia obtained from the diploid strains. We found sclerotia composed of pseudoparenchymatous cells and these cells appeared to be empty, with no asci or ascospores present. **C.** Conidia of wild-type strains CBS147323 and CBS147347 were mixed and plated sclerotia inducing media containing 1% Triton X-100. Sclerotia formation visualized with a stereo microscope. Sclerotia formation in these two wild-type strains is hyper-induced as seen in N402 (Figure 5.4). **D.** Again, light microscopy was used to assess cell structures of the obtained sclerotia

from the mixed parental strains and only pseudoparenchymatous cells (of the sclerotia) without asci or ascospores were observed.

Discussion

The sequences obtained from 24 *A. niger sensu stricto* strains are a rich resource for future research on the strain diversity within the industrially relevant species *Aspergillus niger*. It is apparent that *A. niger* does not prefer to be diploid in nature as all 24 strains analyzed in this study are haploid strains. Further full genome comparisons between the 24 strains, focusing for example on the presence of unique genes or translocations could be a valuable future research line.

A 1:1 distribution of MAT1-1:MAT1-2 mating-type loci was found when analyzing the genomes of 24 *A. niger* strains. This finding is in agreement with an earlier report [70], but in contrast with various other reports that stated a skewed natural distribution in favor of the MAT1-1 locus [71,72]. The equal distribution of mating-types in wild-type strains analyzed in this study suggests, or otherwise increases the likelihood of, ongoing sexual reproduction. Additionally, both mating-types are found throughout the clades present in the phylogenetic tree (Figure 5.3), again emphasizing the likely ongoing (sexual) exchange of genetic material between strains of different mating-types. If sexual reproduction had been abolished in this species at a certain point during speciation, one would assume that within the branches observed in the phylogenetic tree, closely related strains would contain the same mating-type locus. The widespread heterokaryon incompatibility observed in this study and this species' supposed asexuality raises the question how exchange of genetic material can even occur within *A. niger*, if at all. Since heterokaryon incompatibility is widespread in *A. niger sensu stricto*, and sexual reproduction is known to be still possible between heterokaryon incompatible strains [18], it could suggest that the exchange of genetic material in *A. niger sensu stricto* occurs through sexual reproduction.

Previously, comparisons have been made between *A. niger* ATCC1015, which was selected as an optimal organic acid producing strain, and *A. niger* CBS513.88,

which is used for enzyme production [12,54]. Therefore, it is interesting to note that *A. niger* ATCC1015 and its closely related strains are part of clade A in the phylogenetic tree whereas *A. niger* CBS513.88 and its closely related strains are part of clade B (Figure 5.3). This suggests a (relatively large) genetic difference between the strains used for organic acid production and the strains used for protein production as they cluster distantly within this phylogenetic tree of *A. niger sensu stricto* strains. Previous research showed that there were potentially three clades within *A. niger sensu stricto* [12] and we could indeed confirm these three clades in this study. This previous study found an unexpectedly high number of SNPs (on average 8 ± 16 SNPs/kb) between CBS513.88 and ATCC1015. Based on these findings, Andersen and colleagues suggest that genomes within species *A. niger sensu stricto* contain a relatively large amount of variation when compared to genomes of other filamentous fungi such as *Fusarium graminearum*. Our current findings suggest that the strains CBS513.88 and ATCC1015 are on opposite sides of the phylogenetic tree within species *A. niger sensu stricto* (Figure 5.3), at least based on the 33 genomes analyzed in this study. Therefore, their genetic differences are among the highest observed within the species, and therefore relatively large compared to the average of 6.1 ± 2.0 SNPs/kb found between *A. niger sensu stricto* strains. These new insights suggest that *A. niger sensu stricto* stains, selected based on partial calmodulin gene sequencing results, do not have an abnormally high genetic diversity when compared to other filamentous ascomycete fungi.

Heterokaryon incompatibility was found to be widespread within species *A. niger sensu stricto*. However, the heterokaryon compatibility between strains CBS147323 and CBS147347 provided a unique opportunity to compare the genetic make-up of these two strains with closely related heterokaryon incompatible strain CBS147353. Ten possible candidate HET domain containing genes could explain the difference observed in heterokaryon incompatibility between these strains. However, none of these ten genes could explain all the heterokaryon incompatibility observed between the 23 parasexual crossings attempted in this study (Table 5.S2). Therefore, it is likely that multiple heterokaryon incompatibility systems are active within species *A. niger sensu stricto*.

The heterozygous diploid strain described here is the first stable diploid reported between distinct haploid strains containing both mating-type systems in the heterothallic fungus *A. niger sensu stricto*. Many heterothallic ascomycetes, especially heterothallic Aspergilli, show heterokaryon incompatibility between strains of different mating-type, such is the case for *N. crassa*, *A. flavus* and *Aspergillus heterothallicus* [73–75]. Perhaps the vegetative compatibility between strains of different mating-type found in *A. niger sensu stricto* suggests the absence of an active *tol* gene mediated incompatibility system in *A. niger*, which has been described as the mediator of mating-type associated heterokaryon incompatibility in *N. crassa* [76,77]. The availability of the diploid strain SJS150.1 opens up new possibilities to study mating-type driven interactions for example at the levels of gene expression to analyze whether genes related to sexual reproduction are activated. The diploid strains also enables the possibility to test for a broad range of environments that might trigger sexual reproduction.

References

1. Samson RA, Visagie CM, Houbraken J, Hong SB, Hubka V, Klaassen CHW, et al. Phylogeny, identification and nomenclature of the genus *Aspergillus*. Stud Mycol. 2014;78:141–73.

2. Geiser DM, Timberlake WE, Arnold ML. Loss of meiosis in *Aspergillus*. Mol Biol Evol. 1996;13:809–17.

3. Dyer PS, Paoletti M, Archer DB. Genomics reveals sexual secrets of *Aspergillus*. Microbiology. 2003;149:2301–3.

4. Houbraken J, Kocsubé S, Visagie CM, Yilmaz N, Wang XC, Meijer M, et al. Classification of *Aspergillus*, *Penicillium*, *Talaromyces* and related genera (Eurotiales): An overview of families, genera, subgenera, sections, series and species. Stud Mycol. 2020;95:5–169.

5. Ojeda-López M, Chen W, Eagle CE, Gutiérrez G, Jia WL, Swilaiman SS, et al. Evolution of asexual and sexual reproduction in the Aspergilli. Stud Mycol. 2018;91:37–59.

6. Houbraken J, Dyer PS. Induction of the sexual cycle in filamentous Ascomycetes. In: van den Berg M, Maruthachalam K, editors. Genet Transform Syst Fungi, Vol 2. Springer, Cham; 2015. p. 23–46.

7. Nielsen KF, Mogensen JM, Johansen M, Larsen TO, Frisvad JC. Review of secondary metabolites and mycotoxins from the *Aspergillus niger* group. Anal Bioanal Chem. 2009;395:1225–42.

8. da Silva JJ, Iamanaka BT, Ferranti LS, Massi FP, Taniwaki MH, Puel O, et al. Diversity within *Aspergillus niger* clade and description of a new species: *Aspergillus vinaceus* sp. nov. J Fungi. 2020;6:371.

9. Ferracin LM, Frisvad JC, Taniwaki MH, Iamanaka BT, Sartori D, Schapovaloff ME, et al. Genetic Relationships among strains of the *Aspergillus niger* aggregate. Brazilian Arch Biol Technol. 2009;52:241–8.

10. Abarca ML, Accensi F, Cano J, Cabañes FJ. Taxonomy and significance of black Aspergilli. Antonie van Leeuwenhoek, Int J Gen Mol Microbiol. 2004;86:33–49.

11. Pel HJ, De Winde JH, Archer DB, Dyer PS, Hofmann G, Schaap PJ, et al. Genome sequencing and analysis of the versatile cell factory *Aspergillus niger* CBS 513.88. Nat Biotechnol.

2007;25:221–31.

12. Andersen MR, Salazar MP, Schaap PJ, Van De Vondervoort PJI, Culley D, Thykaer J, et al. Comparative genomics of citric-acid-producing *Aspergillus niger* ATCC 1015 versus enzyme-producing CBS 513.88. Genome Res. 2011;21:885–97.

13. Cairns TC, Nai C, Meyer V. How a fungus shapes biotechnology: 100 years of *Aspergillus niger* research. Fungal Biol Biotechnol. 2018;5:1–14.

14. Kück U, Böhm J. Mating type genes and cryptic sexuality as tools for genetically manipulating industrial molds. Appl Microbiol Biotechnol. 2013;97:9609–20.

15. Garrigues S, Martínez-Reyes N, de Vries RP. Genetic engineering for strain improvement in filamentous fungi. In: de Vries R, Mäkelä M, editors. Encycl Mycol. Amsterdam: Elsevier; 2020. Available from: https://linkinghub.elsevier.com/retrieve/pii/B9780128199909000068

16. Seidl V, Seibel C, Kubicek CP, Schmoll M. Sexual development in the industrial workhorse *Trichoderma reesei*. Proc Natl Acad Sci. 2009;106:13909–14.

17. Böhm J, Hoff B, O'Gorman CM, Wolfers S, Klix V, Binger D, et al. Sexual reproduction and mating-type-mediated strain development in the penicillin-producing fungus *Penicillium chrysogenum*. Proc Natl Acad Sci U S A. 2013;110:1476–81.

18. Saupe SJ. Molecular genetics of heterokaryon incompatibility in filamentous ascomycetes. Microbiol Mol Biol Rev. 2000;64:489–502.

19. Paoletti M, Clavé C. The fungus-specific HET domain mediates programmed cell death in *Podosnora anserina*. Eukaryot Cell. 2007;6:2001–8.

20. Smith ML, Micali OC, Hubbard SP, Mir-Rashed N, Jacobson DJ, Glass NL. Vegetative incompatibility in the *het-6* region of *Neuospora crassa* is mediated by two linked genes. Genetics. 2000;155:1095–104.

21. Fedorova ND, Badger JH, Robson GD, Wortman JR, Nierman WC. Comparative analysis of programmed cell death pathways in filamentous fungi. BMC Genomics. 2005;6:177.

22. Kaneko I, Dementhon K, Xiang Q, Glass NL. Nonallelic interactions between *het-c* and a polymorphic locus, *pin-c*, are essential for nonself recognition and programmed cell death in *Neurospora crassa*. Genetics. 2006;172:1545–55.

23. Espagne E, Balhadère P, Penin ML, Barreau C, Turcq B. HET-E and HET-D belong to a new subfamily of WD40 proteins involved in vegetative incompatibility specificity in the fungus *Podospora anserina*. Genetics. 2002;161:71–81.

24. van Diepeningen AD, Debets AJM, Hoekstra RF. Heterokaryon incompatibility blocks virus transfer among natural isolates of black Aspergilli. Curr Genet. 1997;32:209–17.

25. Pál K, van Diepeningen AD, Varga J, Hoekstra RF, Dyer PS, Debets AJM. Sexual and vegetative compatibility genes in the Aspergilli. Stud Mycol. 2007;59:19–30.

26. van Diepeningen AD, Debets AJM, Hoekstra RF. Intra- and interspecies virus transfer in Aspergilli via protoplast fusion. Fungal Genet Biol. 1998;25:171–80.

27. van Diepeningen AD, Pál K, van der Lee TAJ, Hoekstra RF, Debets AJM. The *het-c* heterokaryon incompatibility gene in *Aspergillus niger*. Mycol Res. 2009;113:222–9.

28. Paoletti M, Seymour FA, Alcocer MJC, Kaur N, Calvo AM, Archer DB, et al. Mating type and the genetic basis of self-fertility in the model fungus *Aspergillus nidulans*. Curr Biol. 2007;17:1384–9.

29. Coppin E, Debuchy R, Arnaise S, Picard M. Mating types and sexual development in filamentous ascomycetes. Microbiol Mol Biol Rev. 1997;61:411–28.

30. Horn BW, Olarte RA, Peterson SW, Carbone I. Sexual reproduction in *Aspergillus tubingensis* from section Nigri. Mycologia. 2013;105:1153–63.

31. Horn BW, Ramirez-Prado JH, Carbone I. The sexual state of *Aspergillus parasiticus*. Mycologia. 2009;101:275–80.

32. Horn BW, Moore GG, Carbone I. Sexual reproduction in *Aspergillus flavus*. Mycologia. 2009;101:423–9.

33. Arentshorst M, Ram AFJ, Meyer V. Using non-homologous end-joining-deficient strains for functional gene analyses in filamentous fungi. Methods Mol Biol. 2012;835:133–50.

34. Samson RA, Noonim P, Meijer M, Houbraken J, Frisvad JC, Varga J. Diagnostic tools to identify black Aspergilli. Stud Mycol. 2007;59:129–45.

35. De Bekker C, Ohm RA, Evans HC, Brachmann A, Hughes DP. Ant-infecting *Ophiocordyceps* genomes reveal a high diversity of potential behavioral manipulation genes and a possible major

role for enterotoxins. Sci Rep. 2017;7:12508.

36. Aguilar-Pontes M V., Brandl J, McDonnell E, Strasser K, Nguyen TTM, Riley R, et al. The gold-standard genome of *Aspergillus niger* NRRL 3 enables a detailed view of the diversity of sugar catabolism in fungi. Stud Mycol. 2018;91:61–78.

37. Langmead B, Salzberg SL. Fast gapped-read alignment with Bowtie 2. Nat Methods. 2012;9:357–9.

38. Li H, Handsaker B, Wysoker A, Fennell T, Ruan J, Homer N, et al. The sequence alignment / map (SAM) format and SAMtools 1000 genome project data processing subgroup. Bioinformatics. 2009;25:2078–9.

39. Poplin R, Ruano-Rubio V, DePristo MA, Fennell TJ, Carneiro MO, Van der Auwera GA, et al. Scaling accurate genetic variant discovery to tens of thousands of samples. bioRxiv. 2017;

40. Cingolani P, Patel VM, Coon M, Nguyen T, Land SJ, Ruden DM, et al. Using *Drosophila melanogaster* as a model for genotoxic chemical mutational studies with a new program, SnpSift. Front Genet. 2012;3:35.

41. Cingolani P, Platts A, Wang LL, Coon M, Nguyen T, Wang L, et al. A program for annotating and predicting the effects of single nucleotide polymorphisms, SnpEff: SNPs in the genome of *Drosophila melanogaster* strain w1118; iso-2; iso-3. Fly (Austin). 2012;6:80–92.

42. Robinson JT, Thorvaldsdóttir H, Winckler W, Guttman M, Lander ES, Getz G, et al. Integrative Genome Viewer. Nat Biotechnol. 2011;29:24–6.

43. Laothanachareon T, Tamayo-Ramos JA, Nijsse B, Schaap PJ. Forward genetics by genome sequencing uncovers the central role of the *Aspergillus niger goxB* locus in hydrogen peroxide induced glucose oxidase expression. Front Microbiol. 2018;9:2269.

44. Ellena V, Seekles SJ, Ram AFJ, Steiger MG. Genome sequencing of the neotype strain CBS 554.65 reveals the *MAT1-2* locus of *Aspergillus niger*. Prepr (Version 1) available Res Sq. 2021;

45. Vesth TC, Nybo JL, Theobald S, Frisvad JC, Larsen TO, Nielsen KF, et al. Investigation of inter- and intraspecies variation through genome sequencing of *Aspergillus* section *Nigri*. Nat Genet. 2018;50:1688–95.

46. Emms DM, Kelly S. OrthoFinder: Phylogenetic orthology inference for comparative genomics.

Genome Biol. 2019;20:238.

47. Katoh K, Standley DM. MAFFT multiple sequence alignment software version 7: Improvements in performance and usability. Mol Biol Evol. 2013;30:772–80.

48. Stamatakis A. RAxML version 8: A tool for phylogenetic analysis and post-analysis of large phylogenies. Bioinformatics. 2014;30:1312–3.

49. Letunic I, Bork P. Interactive Tree of Life (iTOL) v4: Recent updates and new developments. Nucleic Acids Res. 2019;47:W256–9.

50. van Leeuwe TM, Arentshorst M, Ernst T, Alazi E, Punt PJ, Ram AFJ. Efficient marker free CRISPR/Cas9 genome editing for functional analysis of gene families in filamentous fungi. Fungal Biol Biotechnol. 2019;6:1–13.

51. Labun K, Montague TG, Krause M, Torres Cleuren YN, Tjeldnes H, Valen E. CHOPCHOP v3: expanding the CRISPR web toolbox beyond genome editing. Nucleic Acids Res. 2019;47:171–4.

52. Nødvig CS, Nielsen JB, Kogle ME, Mortensen UH. A CRISPR-Cas9 system for genetic engineering of filamentous fungi. PLoS One. 2015;10:e0133085.

53. Shcherbakova EI, Rezvaia MN. Formation of diploids by *Aspergillus niger* and their biosynthesis of citric acid. Mikrobiologiia. 1977;46:1064–9.

54. Schäfer D, Schmitz K, Weuster-Botz D, Benz JP. Comparative evaluation of *Aspergillus niger* strains for endogenous pectin-depolymerization capacity and suitability for d-galacturonic acid production. Bioprocess Biosyst Eng. 2020;43:1549–60.

55. Manera AP, Meinhardt S, Kalil SJ. Purificação de amiloglicosidase de *Aspergillus niger*. Semin Agrar. 2011;32:651–8.

56. Abdella A, El-Baz AF, Ibrahim IA, Mahrous EE, Yang ST. Biotransformation of soy flour isoflavones by *Aspergillus niger* NRRL 3122 β-glucosidase enzyme. Nat Prod Res. 2018;32:2382–91.

57. Sanzo AVL, Hasan SDM, Costa JAV, Bertolin TE. Enhanced glucoamylase production in semi-continuous solid state cultivation of *Aspergillus niger* NRRL 3122. Cienc Eng. 2001;10:59–62.

58. Manera AP, Kamimura ES, Brites LM, Kalill SJ. Adsorption of amyloglucosidase from *Aspergillus*

niger NRRL 3122 using ion exchange resin. Brazilian Arch Biol Technol. 2008;51:1015–24.

59. Abdella A, Mazeed TES, El-Baz AF, Yang ST. Production of β-glucosidase from wheat bran and glycerol by *Aspergillus niger* in stirred tank and rotating fibrous bed bioreactors. Process Biochem. 2016;51:1331–7.

60. Zaldivar-Aguero JM, Badino AC, Vilaca PR, Facciotti MCR, Schmidell W. Influence of phosphate concentrations on glucoamylase production by *Aspergillus awamori* in submerged culture. Brazilian J Chem Eng. 1997;14:4.

61. Dartora AB, Bertolin TE, Bilibio D, Silveira MM, Costa JAV. Evaluation of filamentous fungi and inducers for the production of endo-polygalacturonase by solid state fermentation. Zeitschrift fur Naturforsch - Sect C J Biosci. 2002;57c:666–70.

62. Cardoso BB, Silvério SC, Abrunhosa L, Teixeira JA, Rodrigues LR. β-galactosidase from *Aspergillus lacticoffeatus*: A promising biocatalyst for the synthesis of novel prebiotics. Int J Food Microbiol. 2017;257:67–74.

63. Chysirichote T. Cellulase production by *Aspergillus niger* ATCC 16888 on copra waste from coconut milk process in layered packed-bed bioreactor. Chem Biochem Eng Q. 2018;32:267–74.

64. Gera N, Uppaluri RVS, Sen S, Dasu VV. Growth kinetics and production of glucose oxidase using *Aspergillus niger* NRRL 326. Chem Biochem Eng Q. 2008;22:315–20.

65. Demirci E, Arentshorst M, Yilmaz B, Swinkels A, Reid ID, Visser J, et al. Genetic characterization of mutations related to conidiophore stalk length development in *Aspergillus niger* laboratory strain N402. Front Genet. 2021;12:581.

66. Bos CJ, Debets AJM, Swart K, Huybers A, Kobus G, Slakhorst SM. Genetic analysis and the construction of master strains for assignment of genes to six linkage groups in *Aspergillus niger*. Curr Genet. 1988;14:437–43.

67. Hastie AC. Benlate-induced instability of *Aspergillus* diploids. Nature. 1970;226:771.

68. de Lucas JR, Domínguez AI, Mendoza A, Laborda F. Use of flow-cytometry to distinguish between haploid and diploid strains of *Aspergillus fumigatus*. Fungal Genet Rep. 1998;45:2.

69. Frisvad JC, Petersen LM, Lyhne EK, Larsen TO. Formation of sclerotia and production of indoloterpenes by *Aspergillus niger* and other species in section *Nigri*. PLoS One. 2014;9:e94857.

70. Varga J, Szigeti G, Baranyi N, Kocsubé S, O'Gorman CM, Dyer PS. Aspergillus: Sex and Recombination. Mycopathologia. 2014;178:349–62.

71. Mageswari A, Kim JS, Cheon KH, Kwon SW, Yamada O, Hong SB. Analysis of the *MAT1-1* and *MAT1-2* gene ratio in black koji molds isolated from Meju. Mycobiology. 2016;44:269–76.

72. Pál K, Van Diepeningen AD, Varga J, Debets AJM, Hoekstra RF. Sexual genes in the asexual filamentous fungus *Aspergillus niger* and related Aspergilli. In: Samson R, Varga J, editors. Aspergillus Genomic Era. Wageningen: Wageningen Academic Publishers; 2008. p. 107–32.

73. Kwon KJ, Raper KB. Heterokaryon formation and genetic analyses of color mutants in *Aspergillus heterothallicus*. Am J Bot. 1967;54:49–60.

74. Olarte RA, Horn BW, Dorner JW, Monacell JT, Singh R, Stone EA, et al. Effect of sexual recombination on population diversity in aflatoxin production by *Aspergillus flavus* and evidence for cryptic heterokaryosis. Mol Ecol. 2012;21:1453–76.

75. Staben C. The mating-type locus of *Neurospora crassa*. J Genet. 1996;75:341.

76. Jacobson DJ. Control of mating type heterokaryon incompatibility by the *tol* gene in *Neurospora crassa* and *N. tetrasperma*. Genome. 1992;35:347–53.

77. Shiu PKT, Glass NL. Molecular characterization of *tol*, a mediator of mating-type-associated vegetative incompatibility in *Neurospora crassa*. Genetics. 1999;15:545–55.

Additional files

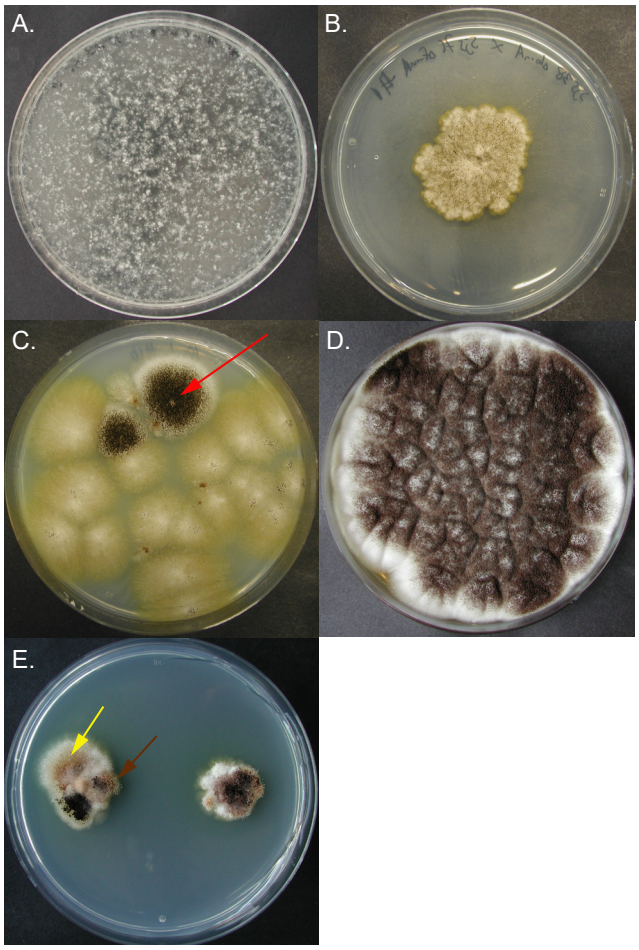

Figure 5.S1. The isolation of a heterozygous diploid of *A. niger* containing both mating-types. A. Heterokaryons grown on MMS without supplementation for 3 days at 30°C. Growth only occurs after successful protoplast fusion and heterokaryon formation. A slice of agar containing a single heterokaryon was transported to a new MM plate without supplement **B.** Heterokaryon grown on MM without supplementation for 7 days at 30°C. Conidia were harvested, filtered and subsequently plated on new MM plates without supplementation. **C.** Colonies formed after plating conidia obtained from heterokaryon. Diploid strain can be recognized by fast(er) growth and black conidia as shown by the red arrow. **D.** The Diploid colony was plated on MEA and grown for 5 days. Conidia were harvested. **E.** Diploid conidia were point inoculated on MM + 0.4 µg/ml benomyl. Haploidization is seen where sectors contain the original fawn colored conidia (yellow arrow) or brown colored conidia (brown arrow).

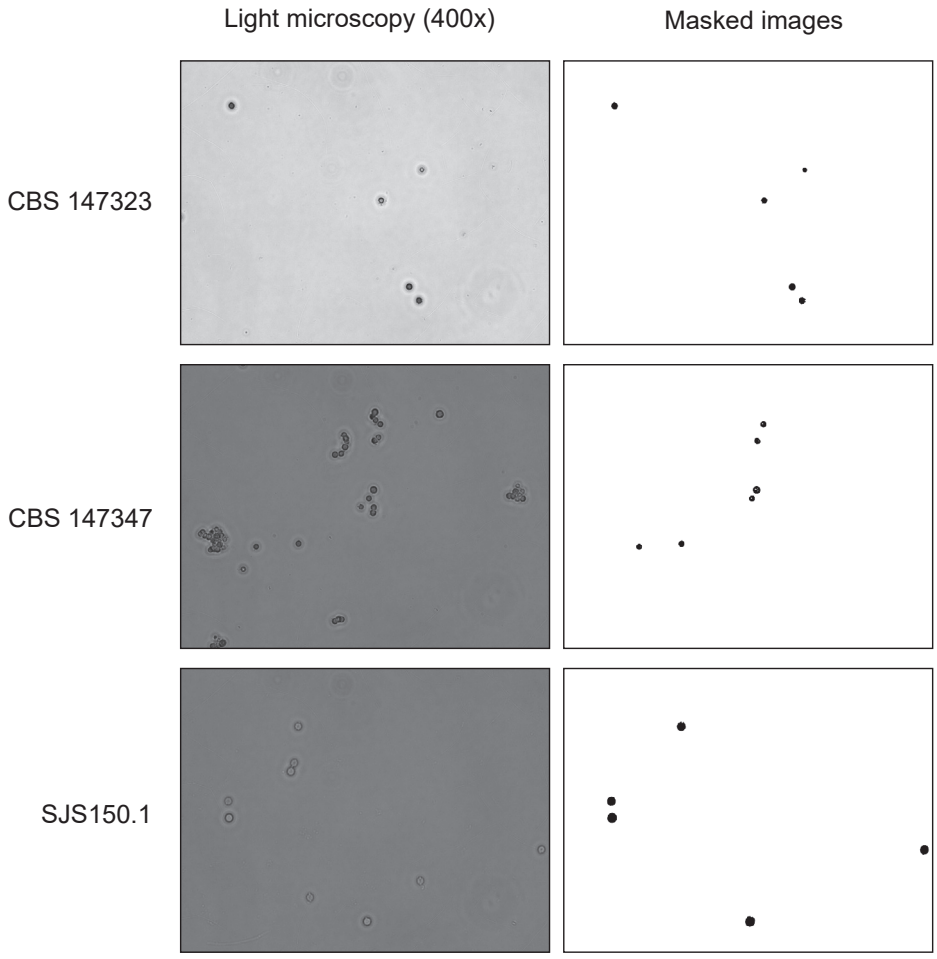

Figure 5.S2. Determination of size difference between diploid and haploid conidia of *A. niger sensu stricto*. Light microscopy images were taken while using a 400x magnification in all cases as seen in the left column. Images were processed using FIJI (ImageJ) software by manually adjusting thresholds until loose conidia were colored red. A mask was created of isolated conidia by manually adjusting the size and circularity of the particles to be analyzed. The black areas in the masked images on the right column represent the area of conidia measured. Sizes of the particles were measured based on pixel amounts. On average, conidia from CBS147323 and CBS147347 were 19.4 ± 4.4 pixels and 17.7 ± 2.5 pixels in size. In contrast, conidia from diploid SJS150.1 were 32.4 ± 6.0 pixels in size.

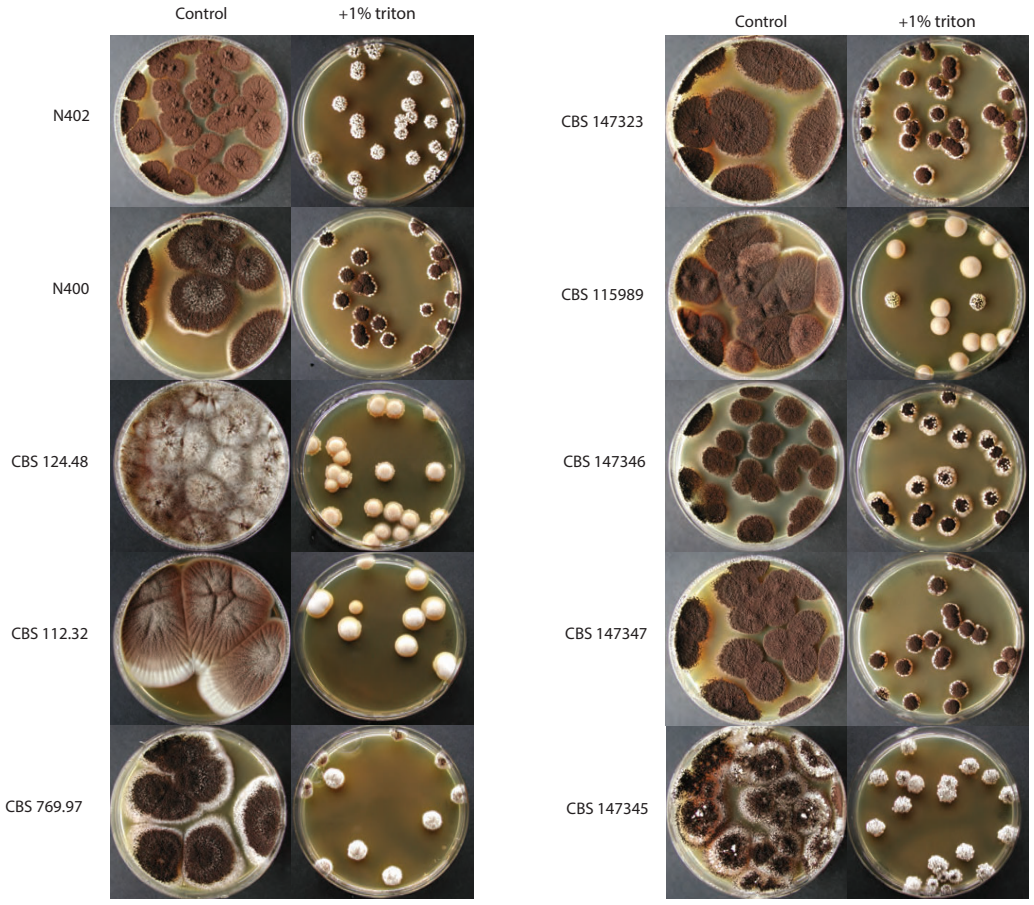

Figure 5.S3. The induction of sclerotia in *A. niger sensu stricto* strains on MEA + 1% Triton X-100. Approximately 25 conidia were plated per plate. Plates were incubated at 30°C for 5 days in a closed incubator (not opened throughout the experiment) for both conditions. Sclerotium formation was always more successful when Triton X-100 was added. Sclerotium formation was observed in the strains N402, N400 (synonym NRRL3, the parental strain of N402), CBS115989, CBS147323, CBS147345 and CBS147346.

Table 5.S1. Primers used in this study

Primer name	Bases	Description
pTE1_for	ccTTAATTAAactccgccgaacgtactg	Forward primer on promoter. Contains PacI site for ligation (upper case)
pTE1_rev	ccTTAATTAAaaaagcaaaaaaggaaggtacaaaaaagc	Reverse primer on terminator. Contains PacI site for ligation (upper case)
fwnA_1_fw	caagaattacaagccagtgagttttagagctagaaatagc	Crispr plasmid fwnA1
fwnA_1_rv	tcactggcttgtaattcttggacgagcttactcgtttcg	Crispr plasmid fwnA1
fwnA_2_fw	tttgttcacagtcctcaagagttttagagctagaaatagc	Crispr plasmid fwnA2
fwnA_2_rv	tcttgaggactgtgaacaaagacgagcttactcgtttcgt	Crispr plasmid fwnA2
pyrG_2_fw	gaggctgttcgagattgccggttttagagctagaaatagc	Crispr plasmid pyrG2
pyrG_2_rv	cggcaatctcgaacagcctcgacgagcttactcgtttcgt	Crispr plasmid pyrG2
f1_S_fwd	cccagcatagtcgtcgtaggag	Crispr check fwnA1 small deletions
f1_S_rev	cggttgtaattgcactgcgact	Crispr check fwnA1 small deletions
f1_L_fwd	ccagaagctctccgtaccatcc	Crispr check fwnA1 large deletions
f1_L_rev	tgcaattcgtcaagagatcgcg	Crispr check fwnA1 large deletions
f2_S_fwd	gttgatccagcaaccgtaagcc	Crispr check fwnA2 small deletions
f2_S_rev	ctctagaaggactgaccggctg	Crispr check fwnA2 small deletions
f2_L_fwd	aaatacccacacggtccctctg	Crispr check fwnA2 large deletions
p2_S_fwd	ggggctcgcgatgattttactg	Crispr check pyrG2 small deletions
p2_S_rev	ccgtgttgccgatgtcaatgaa	Crispr check pyrG2 small deletions
p2_L_fwd	gacgtcttttggagttgcgagg	Crispr check pyrG2 large deletions
p2_L_rev	gggcataatcgaccgaggaagt	Crispr check pyrG2 large deletions
MT1_fw	aggcccccgctcatagagttgg	Check for the presence of the *MAT1-1-1* gene.
MT1_rv	aacggcggccactgaacagttt	Check for the presence of the *MAT1-1-1* gene.
MT2_fw	tgcatttggcggacgaggaacc	Check for the presence of the *MAT1-2-1* gene.
MT2_rv	ctcgcgaaccacagcagcaaga	Check for the presence of the *MAT1-2-1* gene.

Table 5.S2. All parasexual crossings performed in this study

Parent A (brnA^{-}, nicB^{-})	Parent B (fwnA^{-}, pyrG^{-})	Parasexual cross	Self-cross	Diploid strain
CBS 112.32	CBS 118.52	unsuccessful	no	
CBS 112.32	CBS 112.32	successfull	yes	yes
CBS 147323	CBS 147347	successfull	no	SJS151
CBS 147323	CBS 112.32	unsuccessfull	no	
CBS 147323	CBS 118.52	unsuccessfull	no	
CBS 147323	CBS 147352	unsuccessfull	no	
CBS 147323	CBS 147353	unsuccessfull	no	
CBS 147323	CBS 147323	successfull	yes	(not tested)
CBS 147343	CBS 147352	unsuccessfull	no	
CBS 147343	CBS 147323	unsuccessfull	no	
CBS 147343	CBS 147347	unsuccessfull	no	
CBS 147343	CBS 1133816	unsuccessful	no	
CBS 147343	CBS 1447324	unsuccessfull	no	
CBS 147347	CBS 147323	successfull	no	SJS150
CBS 147347	CBS 147353	unsuccessfull	no	
CBS 147347	CBS 112.32	unsuccessfull	no	
CBS 147347	CBS 118.52	unsuccessfull	no	
CBS 147347	CBS 147352	unsuccessfull	no	
CBS 147347	CBS 147353	unsuccessfull	no	
CBS 147347	CBS 147347	successfull	yes	(not tested)
CBS 147371	CBS 147324	unsuccessfull	no	
CBS 147482	CBS 1133816	unsuccessfull	no	
CBS 147482	CBS 1447324	unsuccessfull	no	
CBS 147482	CBS 147352	unsuccessfull	no	
CBS 147482	CBS 147353	unsuccessfull	no	
CBS 147482	CBS 147323	unsuccessfull	no	
CBS 147482	CBS 147347	unsuccessfull	no	

CHAPTER 6

Preservation stress resistance of melanin deficient conidia from *Paecilomyces variotii* and *Penicillium roqueforti* mutants generated via CRISPR/Cas9 genome editing

Sjoerd J. Seekles, Pepijn P.P. Teunisse, Maarten Punt, Tom van den Brule, Jan Dijksterhuis, Jos Houbraken, Han A.B. Wösten, Arthur F.J. Ram

Published in: Fungal Biol Biotechnol (2021), 8, 4.

DOI: https://doi.org/10.1186/s40694-021-00111-w

Abstract

Background

The filamentous fungi *Paecilomyces variotii* and *Penicillium roqueforti* are prevalent food spoilers and are of interest as potential future cell factories. A functional CRISPR/Cas9 genome editing system would be beneficial for biotechnological advances as well as future (genetic) research in *P. variotii* and *P. roqueforti*.

Results

Here we describe the successful implementation of an efficient AMA1-based CRISPR/Cas9 genome editing system developed for *Aspergillus niger* in *P. variotii* and *P. roqueforti* in order to create melanin deficient strains. Additionally, *kusA*$^{-}$ mutant strains with a disrupted non-homologous end-joining repair mechanism were created to further optimize and facilitate efficient genome editing in these species. The effect of melanin on the resistance of conidia against the food preservation stressors heat and UV-C radiation was assessed by comparing wild-type and melanin deficient mutant conidia.

Conclusions

Our findings show the successful use of CRISPR/Cas9 genome editing and its high efficiency in *P. variotii* and *P. roqueforti* in both wild-type strains as well as *kusA*$^{-}$ mutant background strains. Additionally, we observed that melanin deficient conidia of three food spoiling fungi were not altered in their heat resistance. However, melanin deficient conidia had increased sensitivity towards UV-C radiation.

Introduction

The genome editing system by clustered regularly interspaced short palindromic repeats (CRISPR) and CRISPR-associated protein 9 (Cas9) has proven to be a powerful tool in filamentous fungi, providing new insights and opportunities within food, agricultural, clinical and biotechnological research [1–4]. Currently, the CRISPR/Cas9 gene editing tool has been introduced in over 40 species of filamentous fungi and oomycetes to date [5]. In this paper, we describe a functional CRISPR/Cas9 genome editing protocol for two food spoilage fungi *Paecilomyces variotii* and *Penicillium roqueforti*.

The CRISPR/Cas9 genome editing system introduces a double stranded break (DSB) on a specific genomic DNA site. Fungi have two main DNA repair mechanisms that can restore the DSB created by CRISPR/Cas9, namely the non-homologous end-joining repair mechanism (NHEJ) and the homology directed repair mechanism (HDR). For genome editing purposes, many studies rely on the HDR mechanism in order to control genomic editing (e.g. gene replacement studies), by providing the fungus with homologous DNA created *in vitro* [6]. This allows for precise DNA insertion, replacement or removal in the genome. However, many filamentous fungi prefer repair via NHEJ over HDR, which complicates this precise genome editing. In order to promote DNA repair by HDR in fungi, genes involved in the NHEJ repair mechanism can be deleted. A mutant fungus with a deleted *kusA* gene is defective in the NHEJ repair mechanism, therefore a DSB can only be repaired by HDR as shown in several filamentous fungi such including e.g. *Neurospora crassa* [7], *Aspergillus niger* [8].

The thermotolerant nature of *P. variotii* spores makes this fungus a relevant food spoiler [9–12]. *P. variotii* is a known spoiler of fruit juices, sauce, canned products and non-carbonized sodas [13,14]. Additionally, *P. variotii* strains have been reported to produce industrially interesting, often thermostable, enzymes such as tannases, amylases, β-glucosidases and a alcohol oxidase [15–21]. Recently, a genome of *P. variotii* has been published [22] in which the first method on targeted gene disruptions in this fungus

using *Agrobacterium tumefaciens* is described. Although *A. tumefaciens* mediated transformations are shown to be efficient and beneficial over other transformation methods in certain cases [23], it does require optimization of multiple factors and can be tedious compared to the relatively quick and easy to use PEG-mediated transformations [24].

The filamentous fungus *P. roqueforti* is best known as the 'blue cheese' fungus for its use in blue cheese production [25]. However, *P. roqueforti* is also a known food spoiler that can produce mycotoxins such as PR-toxin and roquefortine-C, which form potential health risks for humans [26–29]. As such, *P. roqueforti* has been intensively studied for its secondary metabolite production and specifically its mycotoxin production [30–33]. Additionally, *P. roqueforti* has biotechnological potential as a cell factory, as it produces proteolytic enzymes of interest to the cheese-making industry and high-value secondary metabolites such as mycophenolic acid [33–37]. A CRISPR/Cas9 genome editing system has been described for *Penicillium chrysogenum,* a closely related species to *P. roqueforti*, using a similar approach as has been used for *Aspergillus* species by providing a CRISPR/Cas9 plasmid during PEG-mediated transformation [38]. This has led to the possibility of large scale genome re-engineering making *P. chrysogenum* a useful platform organism as cell factory for production of natural products [39]. Taken together, a functional CRISPR/Cas9 targeted genome editing protocol based on PEG-mediated transformations of CRISPR/Cas9 plasmids would be beneficial for future research on food spoilage capabilities and potential biotechnological advances in both *P. variotii* and *P. roqueforti.*

Many food spoiling fungi, such as *P. variotii* and *P. roqueforti*, produce asexual derived spores (conidia) that can withstand commonly used preservation treatments such as UV radiation or heat [40,41]. Recently, the conidia of *P. variotii* have been reported to survive 60°C for 20 minutes, being the most heat resistant of this type of asexual spores [10]. Additionally, conidia of food spoilage fungi are able to survive UV radiation levels used for decontamination by food industry [42–45]. It is yet unclear if pigmentation provides stress resistance against these preservation techniques in food spoiling fungi. In many ascomycetes, disruption of a specific polyketide synthase (PKS) gene results in

loss of conidial pigmentation. As a consequence, these transformants produce lighter or white conidia [46–49]. Comparing the conidia of these mutants with their parental strain will lead to new insights into the potential roles of melanin in preservation stress resistance of conidia.

In this research, a functional CRISPR/Cas9 genome editing system for *P. variotii* and *P. roqueforti* is implemented to create melanin deficient mutants of both fungi, and subsequently comparing these mutants to their wild-type parental strains, using a recently described CRISPR/Cas9 deletion system developed for *A. niger* [50] with minor adaptations. This CRISPR/Cas9 genome editing system developed for *A. niger* is based on the expression of Cas9 driven from the *tef1* promoter [51]. The Cas9 expression cassette, together with the guide RNA expression cassette and the hygromycin selection marker are located on a plasmid that also contains the AMA1 sequence which enables autonomous replication in *Aspergillus* species, thereby making integration of the vector into the genome less likely [52]. This AMA1-based CRISPR/Cas9 genome editing system allows for the temporal presence of the CRISPR/Cas9 plasmid and therefore marker-free genome editing [50]. The CRISPR/Cas9 genome editing method is considerably faster than the already established marker-free genome editing method which relies on recyclable markers. The CRISPR/Cas9 based genome editing method allows for the creation of multiple mutations in a single transformation experiment, as demonstrated in *A. niger* [50], whereas the recycling method requires deletions to be performed one at a time.

Understanding the resistance mechanisms of conidia from food spoiling fungi will help us in designing novel targeted preservation techniques able to inactivate conidia without altering food flavor profiles. In order to investigate this, a working CRISPR/Cas9 genome editing system has been developed for *P. variotii* and *P. roqueforti*. These genome editing systems could enhance future research and provide a stepping stone towards creating novel biotechnologically relevant cell factories.

Results

Construction of melanin deficient mutants in *P. variotii* and *P. roqueforti* using CRISPR/Cas9 based genome editing.

In order to investigate the impact of melanin on stress resistance in *P. roqueforti* and *P. variotii*, melanin deficient strains in these species were made using a recently described CRISPR/Cas9 deletion system [50]. Polyketide synthase (PKS) homologues from *P. roqueforti* and *P. variotii* were identified as best bi-directional BLASTp hits with both the FwnA protein (gene ID: An09g05730) from *A. niger* [47] and the Pks17 protein (gene ID: Pc21g16000) from *P. chrysogenum* DS68530 [38]. The BLASTp searches identified Pro_LCP9604111_2|g6432.t1 as the bi-directional best hit in *P. roqueforti*. The *P. variotii* protein ID 456077, recently described as PvpP in [49], was identified as the bi-directional best hit in *P. variotii*. The *P. roqueforti* protein Pro_LCP9604111_2|g6432.t1 is 68% identical to FwnA from *A. niger* and 92% identical to Pks17 from *P. chrysogenum*. The *P. variotii* protein ID456077 (PvpP) is 67% identical to FwnA and 65% identical to Pks17.

Optimal guide RNAs for CRISPR/Cas9 genome editing for these genes were chosen based on CHOPCHOP predictors [53] (Additional file 1: Table 6.S1). The guide RNAs were chosen to target an exon near the start codon of the open reading frame (ORF). The guide RNAs targeting the PKS homologous were cloned into the autonomously replicating vector pFC332, expressing the Cas9 nuclease, creating the CRISPR/Cas9 plasmids pPT13.1 and pPT9.3 to use for transformation of *P. variotii* and *P. roqueforti* respectively (Additional file 1: Table 6.S1). The CRISPR/Cas9 plasmids were subsequently transformed to protoplasts of *P. variotii* CBS 101075 and *P. roqueforti* LCP96 04111. Transformants were obtained that produced white conidia, indicative of a disrupted melanin biosynthesis and subsequent loss of pigmentation, on the primary transformation plates for both fungi (Figure 6.1). The efficiency of obtaining transformants with white conidia on the primary transformation plates in *P. variotii* and *P. roqueforti* was 83% (728 colonies with white conidia from a total of 876 transformants) and 97% (56 colonies

with white conidia from a total of 58 transformants) respectively (Table 6.1).

Table 6.1. Gene editing efficiencies of *P. variotii* and *P. roqueforti* using CRISPR/Cas9.

	P. variotii		*P. roqueforti*	
	brown conidia	***white conidia***	***green conidia***	***white conidia***
Phenotype obtained on first transformation plate	148/876 (17%)	728/876 (83%)	2/58 (3%)	56/58 (97%)
Hygromycin resistance loss after one round of non-selective growth	32/40 (80%)	9/40 (23%)	1/2 (50%)	16/56 (29%)

Numbers represent transformants and were calculated over multiple transformation experiments. The average amount of transformants obtained per transformation using 2 µg of CRISPR/Cas9 plasmid was ± 100 colonies for *P. variotii* and ± 10 colonies for *P. roqueforti* depending on amounts of obtained protoplasts.

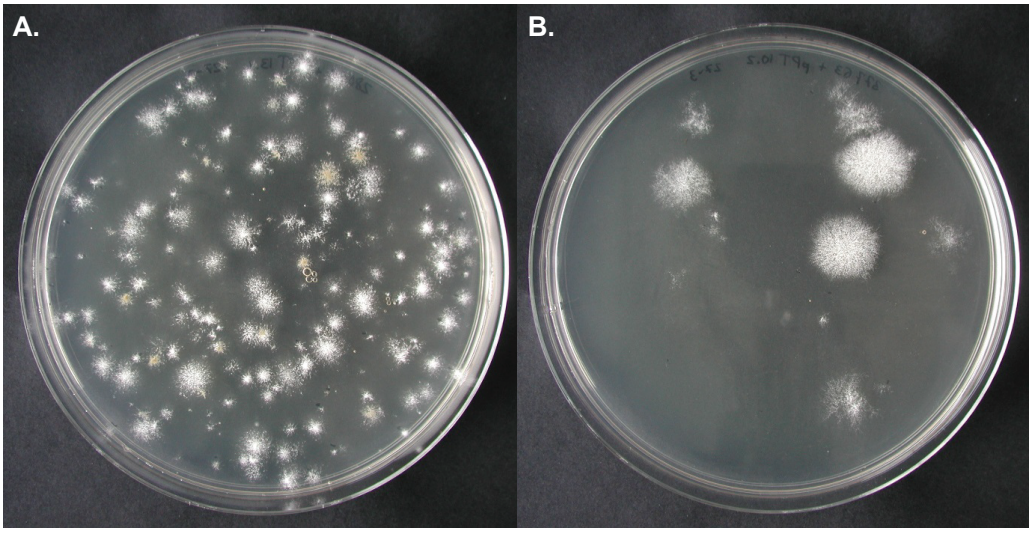

Figure 6.1. Transformation plates obtained when transforming *P. variotii* and *P. roqueforti* with PKS gene targeting CRISPR/Cas9 plasmids. A. Transformation plate of *P. variotii* CBS101075 transformed with AMA1-based CRISPR/Cas9 plasmid pPT13.1 targeting gene *pvpP* needed for melanin biosynthesis. Typically around 100 transformants are obtained when adding 2 µg of plasmid depending on the amount of protoplasts obtained. **B.** Transformation plate of *P. roqueforti* LCP96 04111 transformed with AMA1-based CRISPR/Cas9 plasmid pPT9.3 targeting gene *pksA*. Typically around 10 transformants are obtained when adding 2 µg of plasmid depending on the amount of protoplasts obtained.

The efficiency of a white-coloured mutant losing hygromycin resistance in *P. variotii* and *P. roqueforti* was 23% (9 out of 40) and 29% (15 out of 56), respectively. White sporulating mutants that lost their hygromycin resistance under non-selective growth conditions were purified further and subsequently checked for mutations in the PKS genes by performing diagnostic PCRs and DNA sequencing. Melanin deficient mutants *P. roqueforti* (PT34.2) and *P. variotii* (PT32.5) were chosen for further analysis (Figure 6.2). Both strains contain a 14 bps deletion in the *pksA* and *pvpP* gene respectively causing a frameshift and thus a probable genetic loss of function (Additional file 1: Figure 6.S1). These results show that CRISPR/Cas9 genome editing using the AMA1-based expression vectors are effectively disrupting target genes in both species.

The low efficiency of hygromycin loss after one round of non-selective growth in *P. variotii* transformants

The low efficiency of hygromycin loss in white-coloured transformants of 23% (9 out of 40) is lower compared to the efficiency of hygromycin loss in brown transformants of 80% (32 out of 40) in *P. variotii*. To investigate the low efficiency of hygromycin loss and its link with the phenotype, eleven white-coloured (of which two showed hygromcin loss) and six brown-coloured (of which four showed hygromycin loss) transformants of *P. variotii* CBS 101075 were analysed by diagnostic PCR and sequencing. When analyzing the *pvpP* locus of the eleven white-coloured *P. variotii* transformants, we discovered that only 3 out of 11 (27%) mutants had the expected small indel mutation of which 1 lost the hygromycin resistant phenotype after one round of non-selective growth (Table 6.2). Also, 4 out of the 11 (36%) transformants analysed had part of the pPT13.1 plasmid integrated in the *pvpP* locus at the site where the double stranded break (DSB) took place, of which one lost the hygromcin resistant phenotype. The sequence and size of parts of the integrated pPT13.1 plasmid were variable. We were unable to obtain PCR products for the remaining 4 out of 11 (36%) transformants, indicating a large insertion or deletion that hampered the PCR.

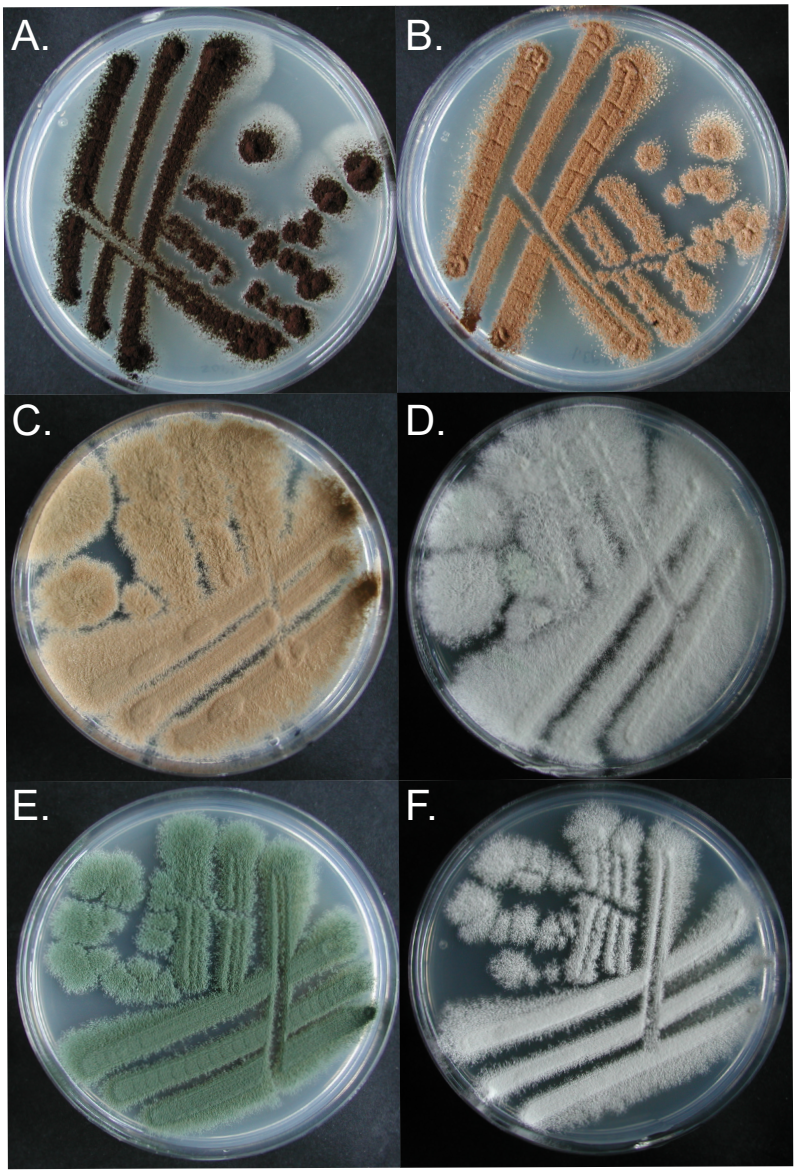

Figure 6.2. Phenotypes of parental strains and PKS mutants. A. Phenotype *A. niger* N402, it has black conidia. **B.** Phenotype *A. niger* MA93.1, it has fawn coloured / light brown conidia. **C.** Phenotype *P. variotii* CBS 101075 strain, it has fawn coloured conidia. **D.** Phenotype *P. variotii* pksA- strain PT32.5, it has white conidia. **E.** Phenotype *P. roqueforti* LCP96 04111, it has green conidia. **F.** Phenotype *P. roqueforti* pksA- strain PT34.2, it has white conidia.

Table 6.2. Plasmid integration in *P. variotii* CBS 101075 transformants that did not lose hygromycin resistance.

	Transformants with small indel	Transformants containing part of pPT13.1 plasmid at DBS site	No proper PCR product obtained
White conidia	3/11 (27%)	4/11 (36%)	4/11 (36%)
Brown conidia	6/6 (100%)	0/6 (0%)	0/6 (0%)

The six brown *P. variotii* transformants analysed, of which four showed hygromycin resistance loss after one round of non-selective growth, all contained an in-frame deletion in the *pvpP* locus at the DSB site (3 bps, 6 bps, 6 bps, 9 bps, 12 bps and 15 bps respectively). This indicates that the brown *P. variotii* transformants were modified by CRISPR/Cas9 gene editing, but had a functional PvpP enzyme despite the DSB and subsequent indel caused by CRISPR/Cas9.

Construction of NHEJ repair disrupted mutants in *P. variotii* and *P. roqueforti* using CRISPR-Cas9 genome editing.

In order to facilitate future genome editing in *P. variotii* and *P. roqueforti,* a *kusA*$^{-}$ strain was made for both *P. variotii* and *P. roqueforti*. When performing transformations of a *kusA*$^{-}$ mutant parental strain, the double stranded break caused by CRISPR/Cas9 cannot be repaired by non-homologous end-joining creating indels and instead relies on a homologous repair DNA fragment, which could be donor DNA provided by the user. This will enable targeted and complete gene knock-out or gene replacement studies. Gene deletion mutants in the *kusA* gene of *P. variotii* DTO 217-A2 and *P. roqueforti* DTO 013-F5 backgrounds were made, as these strains produce heat resistant conidia [10], a phenotype of interest for future food spoilage studies. The *kusA* homologous of *P. variotii* and *P. roqueforti* were identified by BLASTp analysis (best bi-directional hits) using the KusA protein from *A. niger* (An15g02700) as a query. Only a single homologous protein with significant identity score was found in *P. variotii* DTO 217-A2: Pva_DTO217A2_1|g5897.t1 (66% identity). Similarly, a single homologous protein was found in *P. roqueforti*: Pro_LCP9604111_2|g3395.t1 (67% identity). Plasmids pPT23.1

and pPT22.4, containing specific guide RNA and the Cas9 expression cassettes, were made for creating *kusA*$^{-}$ strains in *P. variotii* and *P. roqueforti* respectively (Additional file 1: Table 6.S1). The guide RNAs were chosen to target an exon near the start codon of the ORFs. The creation of the *kusA*$^{-}$ mutants of *P. variotii* and *P. roqueforti* relied on the creation of indels caused by NHEJ repair to disrupt the *kusA* homologous genes of these species. From 26 *P. variotii* transformants obtained only a single transformant lost the hygromycin resistant phenotype after one round of non-selective growth. In the case of *P. roqueforti* only 1 transformant was obtained and this single transformant lost the hygromycin resistance phenotype after one round of non-selective growth. Sequencing the *kusA* locus of transformants of strains *P. variotii* PT39.26 and *P. roqueforti* PT43.1 showed small indels in the *kusA* locus (7 bp deletion in the *kusA* gene of *P. variotii* and 22 bp deletion in *P. roqueforti*) resulting in frameshifts and thus potentially a disrupted *kusA* gene (Additional file 2: Figure 6.S2).

The impact of a disrupted NHEJ repair mechanism on the genome editing efficiency in *P. variotii* (*kusA*$^{-}$)

The *P. variotii* PT39.26 (*kusA*$^{-}$) strain was tested for its genome editing efficiency by transformation with the previously used pPT13.1 plasmid, which contains the *pvpP* specific guide RNA to create a double stranded break in the *pvpP* gene. A transformation of the PT39.26 strain with the pPT13.1 plasmid without providing a homologous repair DNA fragment did not give any transformants on the primary transformation plate, as expected. This indicates that indeed the NHEJ repair mechanism has been impaired in this strain and thus the strain cannot repair its double stranded break without the help of a homologous piece of DNA. Next, transformations were performed with the addition of donor DNA to allow the repair of the DSB created by the guide via homologous recombination. When donor DNA was added, putative transformants were obtained on the transformation plates. The donor DNA was a fused PCR product of both 5 and 3'untranslated flanks of the *pvpP* gene, which would theoretically result in the removal of the entire translated region of *pvpP* (6677 bps). In this transformation a total of fifteen transformants were obtained which all had the white-coloured phenotype. The transformants

were purified from the first transformation plate and 14 out of the 15 (93%) purified transformants lost their hygromycin resistant phenotype after one round of non-selective conditions. These efficiencies are similar to those observed in *A. niger* and a major improvement over the original ratio of 1 out of 26 (3.8%) for creating a *kusA*$^{-}$ strain observed in *P. variotii* DTO 217-A2 or the 9 out of 40 (23%) ratio observed in *P. variotii* CBS 101075. Genomic DNA was isolated for eight of these transformants. Diagnostic PCR revealed that all eight transformants were repaired using the homologous piece of DNA provided, making a full knock-out of the 6677 bps gene *pvpP* (Additional file 3: Figure 6.S3). The PCR products of two transformants were excised from gel and subsequently send for sequencing. This confirmed repair using the HDR mechanism, replacing the original *pvpP* gene with the provided donor DNA fragment that only contained the fused flanks. In this way, we obtained the *pvpP* knock-out strain *P. variotii* PT42.1 (*kusA*$^{-}$, *ΔpvpP*). All *kusA*$^{-}$ mutant strains described in this study have no visible alteration in morphology and no visible change in colony diameter or radial growth rate when compared to their parental strains (Additional file 4: Figure 6.S4).

Heat resistance of conidia from food spoiling fungi not affected in melanin deficient mutants

Heat inactivation assays were performed to determine the heat resistance of conidia from the *P. variotii* PT32.5 (*pvpP*$^{-}$) and *P. roqueforti* PT34.2 (*pksA*$^{-}$) deletion strains when compared to their parental strains. Additionally, we included the previously made Δ*fwnA* strain from *A. niger* (MA93.1) and its parental strain (N402) [47]. Note that the strains with intact *kusA* genes have been used for phenotyping, as the NHEJ disruption in the *kusA*$^{-}$ strains could potentially impact resistance against DNA damage caused by either UV radiation or heat. In order to observe at least a two log reduction in microbial load within 30 minutes, heating temperatures had to be adjusted per species. Conidia from *P. variotii* are more heat resistant than their *A. niger* and *P. roqueforti* counterparts [10,54] and thus heat inactivation was done in a 60°C water bath for *P. variotii* conidia instead of a 56°C water bath for *P. roqueforti* and *A. niger*. Heat inactivation curves of wild-type and melanin deficient conidia from *A. niger, P. variotii* and *P. roqueforti* are shown in Figure

6.3A, 6.3B and 6.3C respectively. Decimal reduction values were calculated based on these graphs and given in Table 6.3.

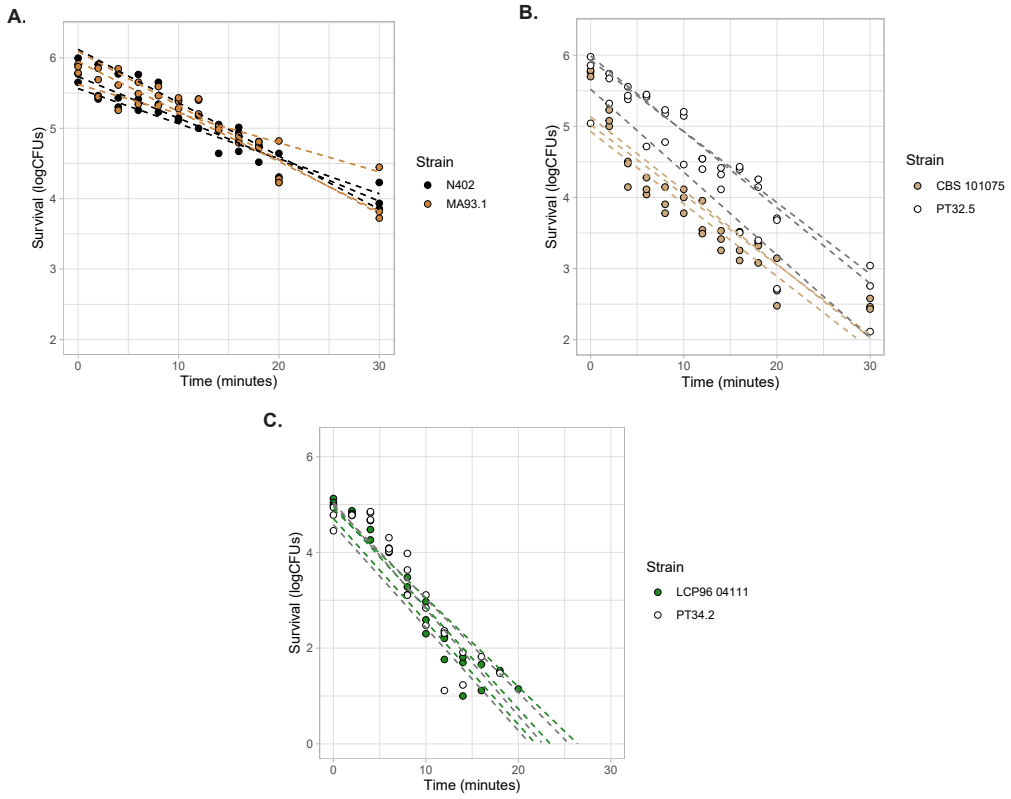

Figure 6.3. Heat resistance of three food spoiling fungi and their melanin deficient mutants. Colours used correspond with the phenotype of the conidia, see Figure 6.2 **A.** The heat inactivation curves of *A. niger* N402 wild-type conidia (black lines) and *A. niger* MA93.1 melanin deficient mutant conidia (brown lines). The *A. niger* strains were heat treated in a 56°C water bath. Heat inactivation shows only a 2-log reduction in microbial load for wild-type and mutant when treated for 30 minutes. **B.** The heat inactivation curves of *P. variotii* CBS 101075 wild-type conidia (light brown lines) and *P. variotii* PT32.5 melanin deficient mutant conidia (grey lines). The *P. variotii* strains were heat treated in a 60°C water bath. Heat inactivation shows a 3-log reduction in microbial load for wild-type and mutant when treated for 30 minutes. **C.** The heat inactivation curves of *P. roqueforti* LCP96 04111 wild-type conidia (green lines) and *P. roqueforti* PT 34.2 melanin deficient mutant conidia (grey lines). The *P. roqueforti* strains were heat treated in a 56°C water bath. Heat inactivation shows at least a 5-log reduction in microbial load for wild-type and mutant when treated for 30 minutes. Three biological triplicates were measured. Inactivation curves were drawn based on the linear regression model.

Table 6.3. D-values of heat inactivated conidia from three food spoiling fungi and their melanin mutants.

Species and strain names		D-value ± standard deviation in time (minutes)
A. niger	N402	16.8 ± 3.4
A. niger	MA93.1	17.1 ± 6.2
P. variotii	CBS 101075	9.3 ± 0.7
P. variotii	PT 32.5	9.9 ± 0.3
P. roqueforti	LCP96 04111	4.9 ± 0.4
P.roqueforti	PT 34.2	4.7 ± 0.3

D-values are measured at 60°C for *P. variotii* and 56°C for *A. niger* and *P. roqueforti.*

There were no significant differences in D-values based on Student's t-tests between wild-type and mutant (all p-values were $p > 0.05$). Therefore, no significant difference in heat resistance between wild-type conidia and their melanin deficient mutant conidia was observed.

UV-C radiation resistance of conidia from food spoiling fungi is affected in melanin deficient mutants

A UV-C radiation assay was performed to determine the UV resistance of the melanin deficient mutants *A. niger* MA93.1 (*ΔfwnA*), *P. variotii* PT32.5 (*pvpP*$^-$) and *P. roqueforti* PT34.2 (*pksA*$^-$). UV inactivation curves of conidia from *A. niger*, *P. variotii* and *P. roqueforti* are shown in Figure 6.4A, 6.4B and 6.4C respectively. The results show that conidia from all three food spoiling species have reduced UV resistance when melanin biosynthesis is disrupted. Decimal reduction values were calculated to quantify this difference and are listed in Table 6.4.

Student's t-tests revealed significant UV radiation reductions when wild-type is compared to the melanin mutant in *A. niger* ($p=0.01$), *P. roqueforti* ($p=0.01$), but not for *P. variotii* ($p=0.06$) although a similar trend is visible. The *A. niger* wild-type conidia are more resistant to UV radiation than the wild-type conidia from both *P. variotii* and *P. roqueforti* ($p<0.00$ and $p<0.00$ respectively). Interestingly, even the fawn coloured *A. niger* melanin mutant MA93.1 is significantly more resistant to UV than the *P. variotii*

and *P. roqueforti* wild-type conidia (p<0.00 and p<0.00 respectively). This suggests that other melanin types or pigments in the MA93.1 strain, produced independently from the FwnA enzyme, contribute significantly to the UV radiation resistance of *A. niger* conidia. Overall, the *pks*⁻ mutants were more sensitive to UV radiation than their parental strains, indicating that melanin contribute to UV resistance of conidia from food spoiling fungi.

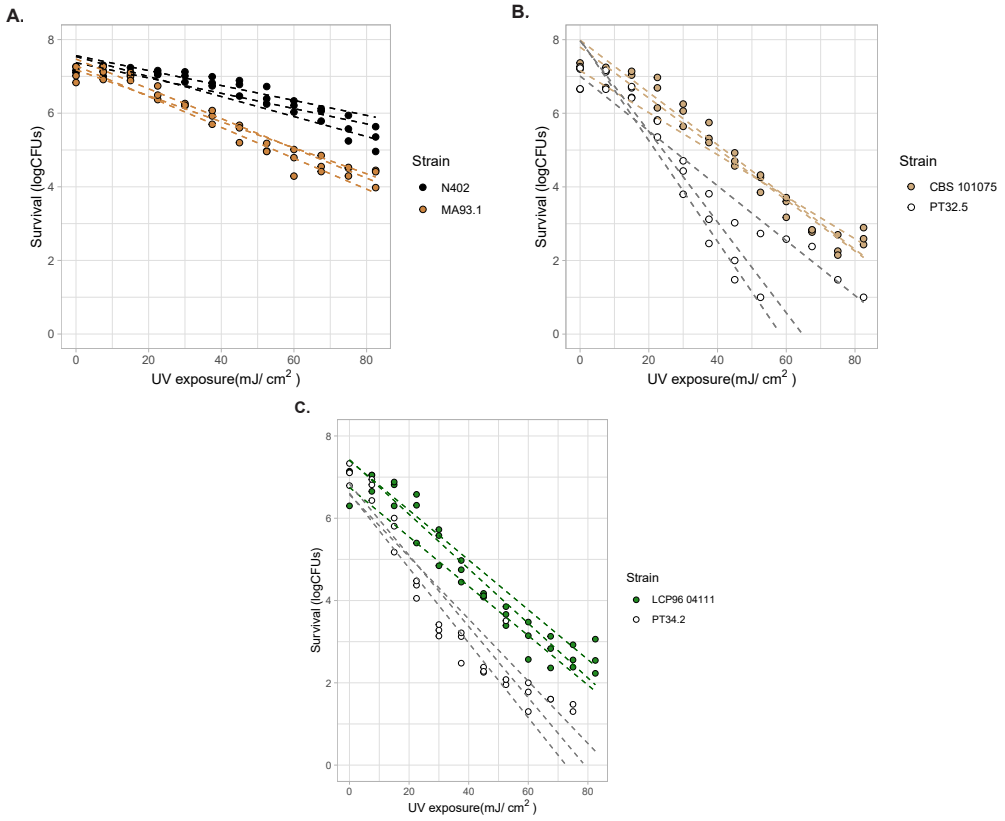

Figure 6.4. UV-C radiation resistance of melanin deficient mutants from food spoilage fungi. Colours used correspond with the phenotype of the conidia, see Figure 6.2. **A.** The UV inactivation curves of *A. niger* N402 wild-type conidia (black lines) and *A. niger* MA93.1 melanin deficient mutant conidia (brown lines). A maximum of 3-log reduction in microbial load was observed in the mutant after UV treatment. **B.** The UV inactivation curves of *P. variotii* CBS 101075 wild-type conidia (light brown lines) and *P. variotii* PT 32.5 melanin deficient mutant conidia (grey lines). A maximum of 7-log reduction in microbial load was observed in the mutant after UV treatment. **C.** The UV inactivation curves of *P. roqueforti* LCP96 04111 wild-type conidia (green lines) and *P. roqueforti* PT 34.2 melanin deficient mutant conidia (grey lines). A maximum of 7-log reduction in microbial load was observed in the mutant after UV treatment. Three biological triplicates were measured. Inactivation curves were drawn based on linear regression model.

Table 6.4. D-values of UV inactivated conidia from three food spoiling fungi and their melanin mutants.

Species and strain names		D-value ± standard deviation in dose (mJ/cm^2)
A. niger	N402	44.7 ± 5.6
A. niger	MA93.1	25.6 ± 1.9
P. variotii	CBS 101075	15.3 ± 1.5
P. variotii	PT 32.5	9.6 ± 2.7
P. roqueforti	LCP96 04111	16.1 ± 0.7
P.roqueforti	PT 34.2	11.9 ± 0.9

Discussion

CRISPR/Cas9 genome editing protocol for *P. variotii* and *P. roqueforti*

In this article a previously described CRISPR/Cas9 genome editing protocol for *A. niger* [50] was successfully implemented to perform genome editing in *P. roqueforti* and *P. variotii*. The efficiency of obtaining white-coloured transformants was 728 out of 876 (83%) in *P. variotii* CBS 101075 and 56 out of 58 (97%) in *P. roqueforti* LCP96 04111 (Table 6.1). This efficiency is comparable with previous findings in *A. niger* [50]. The total amount of transformants obtained per transformation experiment was consistently lower in *P. roqueforti* (n=10 per plate) when compared to *P. variotii* (n=100 per plate), which is probably due to less efficient protoplasting of *P. roqueforti* using adjusted *A. niger* protocols. As such, the protoplasting protocol for *P. roqueforti* should be further optimized.

The low efficiency of hygromycin loss after one round of non-selective growth in *P. variotii* transformants

When analyzing 40 *P. variotii* CBS101075 *pvpP*$^-$ transformants with white conidia, only 9 out of 40 (23%) lost the hygromycin resistance phenotype after one round of non-selective growth. This is in contrast to 40 *P. variotii* transformants with the wild-type brown conidia, where 32 out of 40 (80%) lost the hygromycin resistance phenotype after one

round of non-selective growth. Also, when transforming *P. variotii* CBS101075 with empty vector pFC332 a similar 17 out of 24 (71%) ratio of transformants that lose their hygromycin resistant phenotype after one round of non-selective growth is obtained. In *A. niger* the reported hygromycin loss efficiency is also around 80% [50]. This suggests that having a white-coloured phenotype in *P. variotii* transformants is tied to retaining the hygromycin resistant phenotype, which could be explained by integration of the hygromycin resistance marker on the *pvpP* locus itself where the double stranded break occurs. Indeed, further investigation of *P. variotii* transformants revealed that a significant portion of at least 4 out of 11 (36%) transformants with white conidia contained pieces of the pPT13.1 plasmid at the site where the double stranded break had occurred (Table 6.2). This observation suggests that the double stranded break in the genomic DNA of *P. variotii* is somehow repaired using the CRISPR/Cas9 containing vector itself. The integration of the AMA1-based vector containing the hygromycin selection marker explains the stability of the hygromycin marker even under non-selective conditions in *P. variotii*. Since the hygromycin loss efficiency in *P. roqueforti* is also low (29%, see Table 6.1), we speculate that the same plasmid integration is happening in *P.roqueforti* transformations.

Obtaining a transformant with a mutation in the targeted gene is highly efficient, thus this methodology suffices when a single gene disrupted mutant is made. However, the high stability of the hygromycin marker limits the possibility for sequential rounds of transformations. Additionally, this methodology does not allow for efficiently obtaining full knock-out mutants, nor the efficient targeted integration of new pieces of DNA (for example to produce heterologous proteins) as the NHEJ repair mechanism is the preferred DNA repair mechanism over HDR in most filamentous fungi [6]. Disrupting the NHEJ repair mechanism is therefore beneficial as it could potentially circumvents all these drawbacks. Therefore, the created *kusA*$^{-}$ mutants that are incapable of performing NHEJ are valuable tools for future genome editing in both *P. variotii* and *P. roqueforti*.

The impact of a disrupted NHEJ repair mechanism on the genome editing efficiency in *P. variotii* (*kusA*$^{-}$)

It was noticed that in the process of obtaining the *kusA*$^{-}$ mutant in *P. variotii* DTO 217-A2, only 1 out of 26 (3%) of transformants lost the hygromycin resistance phenotype after one round of non-selective growth. This again stresses the inefficiency of obtaining a marker free mutant after one round of growth on non-selective media when transforming a *kusA*$^{+}$ wild-type *P. variotii* strain with a AMA1-based CRISPR/Cas9 plasmid as previously seen when isolating melanin mutants (Table 6.1). After obtaining this single *P. variotii* PT39.26 (*kusA*$^{-}$) strain, we investigated its genome editing efficiency. *P. variotii* PT39.26 (*kusA*$^{-}$) was transformed using the pPT13.1 plasmid (pFC332 containing a *pvpP* targeting sgRNA) together with the addition of donor DNA consisting of the fused flanks of the *pvpP* gene. Obtaining white-coloured transformants in this transformation was highly efficient as 15 out of the 15 transformants produced white spores. The percentage of these transformants that lost their hygromycin resistant phenotype after one round of non-selective growth was also highly efficient, 14 out of 15 (93%). This is a major improvement over the 1 out of 26 (3%) ratio of hygromycin resistance loss mentioned earlier when creating the *kusA*$^{-}$ strain. Further analysis of eight of these white-coloured *P. variotii* transformants revealed that all eight transformants lost the complete *pvpP* gene (6677 bps) as checked by diagnostic PCR (Figure 6.S3), indicating that repair by HDR had taken place. This was further confirmed by sequencing 2 out of the 8 transformants which showed the knock-out of the complete 6677 bps as expected. Thus, eight knock-out mutants were obtained where no chunks of pPT13.1 plasmid were integrated into the *pvpP* locus. Taken together, the increased efficiency in hygromycin resistance loss and the absence of pPT13.1 chunks on the *pvpP* locus in transformants obtained from the *P. variotii* PT39.26 *kusA*$^{-}$ strain indicate that by disrupting the NHEJ repair mechanism in *P. variotii* DTO 217-A2 the integration of the AMA1 containing vector into the genome is prevented or severely reduced. Therefore, we conclude that the high degree of plasmid integration into the target site where DSB took place was due to repair facilitated by the NHEJ mechanism. Increasing overall efficiency of obtaining genetic alterations by HDR

will open up future research for generating full knock-out mutants as well as targeted integration of DNA (e.g. fluorescent proteins or non-native enzymes). The *kusA*$^{-}$ strains can be safely used for strain development as genome stability is not severely altered in NHEJ disrupted filamentous fungi [55].

In future research, it could be preferred to restore the *kusA* locus after complete knock-out of the target genes has been confirmed. For example, conidia of the ***ΔkusA*** mutant of *A. niger* show increased sensitivity to UV radiation resistance [8]. Thus, in order to investigate the impact of *pvpP* in the UV-C radiation resistance of conidia obtained from *P. variotii* PT42.1 (*kusA*$^{-}$, *ΔpvpP*) it would be desirable to restore the *kusA* gene back to wild-type. This can be done by performing the same CRISPR/Cas9 genome editing system described for the creation of the *ΔpvpP*, but changing the target sequence to target the disrupted *kusA* locus and provide donor DNA with the intact wild-type *kusA* gene and its flanks. However, the restored wild-type *kusA* gene should not be recognized by the guide RNA targeting the disrupted *kusA* locus. This can be achieved by either targeting the indel itself, or incorporating silent point mutations in the donor DNA.

The contribution of melanin on the heat resistance and UV radiation resistance of conidia in three food spoiling fungi

There have been reports on yeast species in which melanization correlates to heat resistance [56,57]. However, no altered heat resistance was observed in the conidia of the three food spoiling filamentous fungi with disrupted melanin biosynthesis. It has been previously shown that the conidia of *A. niger* strain MA93.1 have no altered heat inactivation resistance when compared to the parental strain N402 [58]. Here we similarly show no heat inactivation alterations for the mutant strains *P. roqueforti* PT34.2 and *P. variotii* PT32.5 when compared to their parental strains. These results suggests that melanin does not play a significant role in conidial heat resistance in these food spoiling fungi. In contrast, conidia disrupted in their melanin production showed increased susceptibility to UV-C radiation in all three food spoiling fungi. The UV-C radiation resistance of *A. niger* MA93.1 is lowered compared to the parental strain, as was previously shown [58].

Additionally, here we show that a gene disruption in the *pksA* homologue of *P. roqueforti* LCP96 04111 and the *pvpP* gene in *P. variotii* CBS 101075 also reduce UV-C radiation resistance of the conidia from these mutants. Interestingly, this result is in contrast to the polyketide synthase (*alb1*) knockdown mutant of *Penicillium marneffei,* which did not show altered UV-C radiation resistance [48]. It is apparent that the melanin deficient *A. niger* MA93.1 strain is more UV-C radiation resistant than either *P. roqueforti* or *P. variotii* wild-type strains ($p<0.00$ student's t-test). This suggests that the remaining pigmentation in the *A. niger* MA93.1 strain is a significant factor in UV-C radiation resistance, explaining the significant differences in resistance between *A. niger* and both the *P. roqueforti* and *P. variotii* strains (Figure 6.4). The *A. niger* conidia seem to have an additional type of pigmentation that does not require the functionality of the FwnA enzyme. Which type of pigmentation still remains in *A. niger* MA93.1 is currently unknown. There are reports of several *Aspergillus* species producing other melanin types besides DHN-melanin, such as DOPA-melanin or pyomelanin [59,60], which would make likely candidates. A total of eight different melanin types have been described for fungi alone, each with their own distinct biosynthesis pathway [61]. The relation between the type of fungal melanin and subsequent UV radiation and heat resistance is currently unknown. Additionally, we noted that UV radiation resistance of the three melanin deficient mutants is about two-thirds of their wild-type parental strains in each species. This finding suggests that the relative contribution of the PKS produced pigmentation to the UV radiation resistance of conidia is similar in each species.

Conclusions

We have shown the successful implementation of the AMA1-based CRISPR/Cas9 genome editing system in *P. variotii* and *P. roqueforti*, which is capable of creating indels in the targeted gene. However, we observed a large amount of plasmid integration events when using the AMA1-based plasmids in this way, resulting in mutant strains which are often no longer marker-free. We demonstrate that a *kusA*$^{-}$ background can be used

to prevent or otherwise severely reduce plasmid integration, which allows for efficient marker-free genome editing and additionally facilitates the creation of complete knock-outs by relying on the homology directed DNA repair mechanism.

We have used the AMA1-based CRISPR/Cas9 plasmids to create melanin deficient mutants of *P. variotii* and *P. roqueforti*, in order to analyse their preservation stress resistance. We show that the melanin-lacking conidia of food spoilers *P. variotii*, *P. roqueforti* and *A. niger* are not altered in their heat resistance compared to their parental strains. In contrast, mutant conidia of food spoilers *P. variotii*, *P. roqueforti* and *A. niger* have increased sensitivity towards UV-C radiation. As such, the presence of DHN-melanin in conidia of three food spoiling fungi does not contribute to their heat resistance, but does contribute to their UV-C radiation resistance.

Materials and Methods

Strains, growth conditions, spore harvesting, media and molecular techniques

The *A. niger*, *P. roqueforti* and *P. variotii* strains used in this study are listed in Table 6.5.

Table 6.5. Strains used in this study.

Strain name	Genotype	Reference
Aspergillus niger N402	*cspA1*	[62]
Aspergillus niger MA93.1	*cspA1, fwnA::hygB* in N402	[47]
Paecilomyces variotii CBS 101075	wild-type	[22]
Paecilomyces variotii PT32.5	*pvpP*$^-$ in CBS 101075	This study
Paecilomyces variotii DTO 217-A2	wild-type	[10]
Paecilomyces variotii PT39.26	*kusA*$^-$ in DTO 217-A2	This study
Paecilomyces variotii PT42.1	*kusA*$^-$, Δ*pvpP* in DTO 217-A2	This study
Penicillium roqueforti LCP96 04111	wild-type	[54]
Penicillium roqueforti PT34.2	*pksA*$^-$ in LCP96 04111	This study
Penicillium roqueforti DTO 013-F5	wild-type	Westerdijk Fungal Biodiversity Institute, CBS collection
Penicillium roqueforti PT43.1	*kusA*$^-$ in DTO 013-F5	This study

The *Escherichia coli* strain DH5α was used for cloning purposes. Fungal strains were grown for 7 days at 25°C on malt extract agar (MEA) unless noted otherwise. All media used and spore harvesting methods are described by Arentshorst et al. [63]. Standard PCR and *E. coli* cloning techniques were used according to Sambrook et al. [64]. Spore suspensions were made using physiological salt buffer (0.9% NaCl + 0.02% Tween 80 in demiwater) unless noted otherwise. The *P. roqueforti* strains were harvested and washed in ACES buffer (10 mM N-(2-Acetamido)-2-aminoethanesulfonic acid, 0.02% Tween 80, pH 6.8) according to van den Brule et al. [10].

CRISPR/Cas9 plasmids construction

All plasmids and primers used in this study are listed in the supplementary data (Additional file 5: Table 6.S1. Plasmids, Additional file 6: Table 6.S2. Primers). *In silico* work was performed on FASTA files obtained from JGI [65]. Plasmid construction was based on earlier work performed in *A. niger* [50]. A detailed protocol on the CRISPR/Cas9 plasmid construction and subsequent transformations in *P. variotii* and *P. roqueforti* can be found in the supplementary data (Additional file 7). Briefly, the plasmids pTLL108.1 and pTLL109.2 were used as templates for creating the 5' flank and 3' flank of the sgRNA respectively. After fusion PCR using the pTE1_for and pTE1_rv primers, a PacI (Fermentas, Thermo Scientific™) digestion on the purified PCR product was performed O/N. The PacI digested sgRNA was ligated into a PacI digested and dephosphorylated pFC332 plasmid and subsequently cloned into *E. coli* DH5α. The ampicillin resistant colonies were grown under selective pressure overnight and miniprepped (GeneJET Plasmid Miniprep Kit, Thermo Scientific™), after which restriction analysis was done with SacII (Fermentas, Thermo Scientific™) to check for correct insertion of the sgRNA. Lastly, sequencing was performed as a final check to ensure correct sgRNA is present in the newly constructed plasmid.

Transformation protocol and DNA isolation

Fungal transformations were performed according to van Leeuwe et al. [50] with a few adaptations. Hygromycin concentrations used for selection during transformation were adjusted per species, chosen based on the lowest concentration still preventing background growth. As such, the final concentrations used were 100 µg/ml hygromycin for *P. roqueforti* transformations and 200 µg/ml hygromycin for *P. variotii* transformations. Since these wild-type strains were *kusA*$^{+}$, gene disruptions relied on non-homologous end joining (NHEJ) for repair resulting in the creation of indels, see van Leeuwe et al. [50] for more information. In contrast, after the *P. variotii* PT39.26 (*kusA*$^{-}$) strain was obtained transformation with pPT13.1 was done with the addition of a repair DNA fragment to obtain *P. variotii* PT42.1 (*kusA*$^{-}$, *ΔpvpP*), see Results section. The mycelium for

protoplasting and subsequent transformation of *P. roqueforti* was pre-grown in CM for 2 days at 25 °C instead of 1 day at 30°C for *A. niger* and *P. variotii*. Protoplasting was done in SMC medium with Lysing enzymes (Sigma) essentially as described previously [63]. Protoplast formation was checked by light microscopy every 15 minutes for both *P. roqueforti* and *P. variotii*. The protoplasting process was commonly stopped after 45 minutes, when protoplasts were visually present. Genomic DNA isolations were done according to Arentshorst et al. 2012 [63].

Heat resistance assay

The heat inactivation assay was based on van den Brule et al. [10] with few exceptions. At t=0 a total of 200 µl spore suspension of 1 x 10^8 conidia/ml was added to pre-heated 19.8 mL ACES buffer (*P. roqueforti*) or 19.8 mL physiological salt buffer (*P. variotii* and *A. niger*). The temperatures of the water bath were adjusted per species (56°C *A. niger*, 56°C *P. roqueforti*, 60°C *P. variotii*). The *P. variotii* and *A. niger* conidia were treated in a static water bath with magnetic stirring (Julabo Corio C-BT19) at 180 rpm inside 50ml Erlenmeyers. The *P. roqueforti* conidia were treated in a shaking water bath (Grant OLS200) at 100 rpm. Samples were taken every 2 minutes until t = 20 min. Additionally t = 30 min was taken as a final sample. Heat inactivation curves and standard deviations were made based on three biological replicates. Dilutions were made in either ACES buffer (*P. roqueforti*) or physiological salt buffer (*P. variotii* and *A. niger*) corresponding with their heating menstruum. Spore suspensions were plated on MEA plates for colony counting. The colony forming units (CFUs) were counted after 7 days of growth at 25°C. Decimal reduction values (D-values) were calculated using the linear regression model.

UV-C radiation resistance assay

The UV-C radiation resistance assay was done in a UV crosslinker (Hoefer UVC 500 Ultraviolet Croslinker). A total of 2 x 10^7 conidia per mL were UV exposed inside open Petri dishes (total starting volume = 25 mL). After each UV dose, 1 mL of spore suspension was taken and subsequently serially diluted and plated on MEA plates. Survival was measured by CFUs scored after 7 days. The lowest dose applied was 7.5 mJ/cm^2 and

then increased by 7.5 mJ/cm^2 in a stepwise manner with a maximum dose of 82.5 mJ/cm^2. The UV radiation resistance assays were performed in biological triplicates. Decimal reduction values (D-values) were calculated based on the linear regression model. Significance was tested using an unpaired Student's *t*-test (significant if $p<0.05$).

References

1. Shi TQ, Liu GN, Ji RY, Shi K, Song P, Ren LJ, et al. CRISPR/Cas9-based genome editing of the filamentous fungi: the state of the art. Appl Microbiol Biotechnol. 2017;101:7435–7443.

2. Song R, Zhai Q, Sun L, Huang E, Zhang Y, Zhu Y, et al. CRISPR/Cas9 genome editing technology in filamentous fungi: progress and perspective. Appl Microbiol Biotechnol. 2019;103:6919–6932.

3. Ouedraogo JP, Tsang A. CRISPR_Cas systems for fungal research. Fungal Biol Rev. 2020;34:189–201.

4. Muñoz IV, Sarrocco S, Malfatti L, Baroncelli R, Vannacci G. CRISPR-CAS for fungal genome editing: A new tool for the management of plant diseases. Front Plant Sci. 2019;10:135.

5. Schuster M, Kahmann R. CRISPR-Cas9 genome editing approaches in filamentous fungi and oomycetes. Fungal Genet Biol. 2019;130:43–53.

6. Krappmann S. Gene targeting in filamentous fungi: the benefits of impaired repair. Fungal Biol Rev. 2007;21:25–9.

7. Ninomiya Y, Suzuki K, Ishii C, Inoue H. Highly efficient gene replacements in *Neurospora* strains deficient for nonhomologous end-joining. Proc Natl Acad Sci U S A. 2004;101:12248–53.

8. Meyer V, Arentshorst M, El-Ghezal A, Drews AC, Kooistra R, van den Hondel CAMJJ, et al. Highly efficient gene targeting in the *Aspergillus niger kusA* mutant. J Biotechnol. 2007;128:770–5.

9. Houbraken J, Samson RA, Frisvad JC. *Byssochlamys*: Significance of heat resistance and mycotoxin production. Adv Exp Med Biol. 2006;571:211–24.

10. van den Brule T, Punt M, Teertstra W, Houbraken J, Wösten H, Dijksterhuis J. The most heat resistant conidia observed to date are formed by distinct strains of *Paecilomyces variotii*. Environ Microbiol. 2019;22:986–99.

11. Houbraken J, Varga J, Rico-Munoz E, Johnson S, Samson RA. Sexual reproduction as the cause of heat resistance in the food spoilage fungus *Byssochlamys spectabilis* (anamorph *Paecilomyces variotii*). Appl Environ Microbiol. 2008;74:1613–9.

12. Dantigny P, Guilmart A, Radoi F, Bensoussan M, Zwietering M. Modelling the effect of ethanol on growth rate of food spoilage moulds. Int J Food Microbiol. 2005;98:261–9.

13. Piecková E, Samson RA. Heat resistance of *Paecilomyces variotii* in sauce and juice. J Ind Microbiol Biotechnol. 2000;24:227–30.

14. Pitt JI, Hocking AD. Fungi and food spoilage. 3rd ed. Fungi Food Spoilage. New York: Springer US; 2009.

15. Guimarães LHS, Peixoto-Nogueira SC, Michelin M, Rizzatti ACS, Sandrim VC, Zanoelo FF, et al. Screening of filamentous fungi for production of enzymes of biotechnological interest. Brazilian J Microbiol. 2006;37:474–80.

16. Battestin V, Macedo GA. Tannase production by *Paecilomyces variotii*. Bioresour Technol. 2007;98:1832–7.

17. Kondo T, Morikawa Y, Hayashi N. Purification and characterization of alcohol oxidase from *Paecilomyces variotii* isolated as a formaldehyde-resistant fungus. Appl Microbiol Biotechnol. 2008;77:995–1002.

18. Job J, Sukumaran RK, Jayachandran K. Production of a highly glucose tolerant β-glucosidase by *Paecilomyces variotii* MG3: Optimization of fermentation conditions using Plackett-Burman and Box-Behnken experimental designs. World J Microbiol Biotechnol. 2010;26:1385–1391.

19. Michelin M, Silva TM, Benassi VM, Peixoto-Nogueira SC, Moraes LAB, Leão JM, et al. Purification and characterization of a thermostable α-amylase produced by the fungus *Paecilomyces variotii*. Carbohydr Res. 2010;345:2348–53.

20. Herrera Bravo de Laguna I, Toledo Marante FJ, Mioso R. Enzymes and bioproducts produced by the ascomycete fungus *Paecilomyces variotii*. J Appl Microbiol. 2015;119:1455–66.

21. Battestin V, Macedo GA, De Freitas VAP. Hydrolysis of epigallocatechin gallate using a tannase from *Paecilomyces variotii*. Food Chem. 2008;108:228–33.

22. Urquhart AS, Mondo SJ, Mäkelä MR, Hane JK, Wiebenga A, He G, et al. Genomic and genetic insights into a cosmopolitan fungus, *Paecilomyces variotii* (Eurotiales). Front Microbiol. 2018;9:3058.

23. Idnurm A, Bailey AM, Cairns TC, Elliott CE, Foster GD, Ianiri G, et al. A silver bullet in a golden age of functional genomics: The impact of agrobacterium-mediated transformation of fungi. Fungal Biol Biotechnol. 2017;4:1–28.

24. Li D, Tang Y, Lin J, Cai W. Methods for genetic transformation of filamentous fungi. Microb Cell Fact. 2017;16:1–13.

25. Martín JF, Coton M. Blue Cheese: Microbiota and Fungal Metabolites. Fermented Foods Heal Dis Prev. 1st ed. Elsevier; 2017.

26. Dubey MK, Aamir M, Kaushik MS, Khare S, Meena M, Singh S, et al. PR Toxin - biosynthesis, genetic regulation, toxicological potential, prevention and control measures: Overview and challenges. Front Pharmacol. 2018;9:288.

27. Gallo A, Giuberti G, Bertuzzi T, Moschini M, Masoero F. Study of the effects of PR toxin, mycophenolic acid and roquefortine C on in vitro gas production parameters and their stability in the rumen environment. J Agric Sci. 2015;153:163–76.

28. Fernández-Bodega MA, Mauriz E, Gómez A, Martín JF. Proteolytic activity, mycotoxins and andrastin A in *Penicillium roqueforti* strains isolated from Cabrales, Valdeón and Bejes-Tresviso local varieties of blue-veined cheeses. Int J Food Microbiol. 2009;136:18–25.

29. Finoli C, Vecchio A, Galli A, Dragoni I. Roquefortine C occurrence in blue cheese. J Food Prot. 2001;64:246–51.

30. Larsen TO, Gareis M, Frisvad JC. Cell cytotoxicity and mycotoxin and secondary metabolite production by common penicillia on cheese agar. J Agric Food Chem. 2002;50:6148–52.

31. Ohmomo S, Sato T, Utagawa T, Abe M. Isolation of Festuclavine and Three New Indole Alkaloids, Roquefortine A, B and C from the Cultures of *Penicillium Roqueforti*. Nippon Någeikagaku Kaishi. 1975;39:1333–4.

32. Proctor RH, Hohn TM. Aristolochene synthase. Isolation, characterization, and bacterial expression of a sesquiterpenoid biosynthetic gene (*Ari1*) from *Penicillium roqueforti*. J Biol Chem. 1993;268:4543–8.

33. Kinsella JE, Hwang D. Biosynthesis of flavors by *Penicillium roqueforti*. Biotechnol Bioeng. 1976;18:927–38.

34. Mioso R, Toledo Marante FJ, Herrera Bravo de Laguna I. *Penicillium roqueforti*: A multifunc-

tional cell factory of high value-added molecules. J Appl Microbiol. 2015;118:781–91.

35. Ismaiel AA, Ahmed AS, El-Sayed ESR. Optimization of submerged fermentation conditions for immunosuppressant mycophenolic acid production by *Penicillium roqueforti* isolated from blue-molded cheeses: enhanced production by ultraviolet and gamma irradiation. World J Microbiol Biotechnol. 2014;30:2625–38.

36. García-Estrada C, Martín JF. Biosynthetic gene clusters for relevant secondary metabolites produced by *Penicillium roqueforti* in blue cheeses. Appl Microbiol Biotechnol. 2016;100:8303–8313.

37. Coton E, Coton M, Hymery N, Mounier J, Jany JL. *Penicillium roqueforti*: an overview of its genetics, physiology, metabolism and biotechnological applications. Fungal Biol Rev. 2020;34:59–73.

38. Pohl C, Kiel JAKW, Driessen AJM, Bovenberg RAL, Nygård Y. CRISPR/Cas9 Based Genome Editing of *Penicillium chrysogenum*. ACS Synth Biol. 2016;5:754–64.

39. Guzmán-Chávez F, Zwahlen RD, Bovenberg RAL, Driessen AJM. Engineering of the filamentous fungus *Penicillium chrysogenum* as cell factory for natural products. Front Microbiol. 2018;9:2768.

40. Guerrero-Beltrán JA, Barbosa-Cánovas G V. Review: Advantages and limitations on processing foods by UV light. Food Sci Technol Int. 2004;10:137–47.

41. Mañas P, Pagán R. Microbial inactivation by new technologies of food preservation. J Appl Microbiol. 2005;98:1387–99.

42. Can FO, Demirci A, Puri V, Gourama H. Decontamination of hard cheeses by pulsed UV-light. Am Soc Agric Biol Eng Annu Int Meet. 2014;77:1723–31.

43. Keklik NM, Krishnamurthy K, Demirci A. Microbial decontamination of food by ultraviolet (UV) and pulsed UV light. Microb Decontam Food Ind Nov Methods Appl. 1st ed. London: Elsevier Ltd; 2012. p. 344–69.

44. Begum M, Hocking AD, Miskelly D. Inactivation of food spoilage fungi by ultra violet (UVC) irradiation. Int J Food Microbiol. 2009;129:74–7.

45. Put HMC, Jong J De. The heat resistance of ascospores of four *Saccharomyces* spp. isolated from spoiled heat processed soft drinks and fruit products. J Appl Bacteriol. 1982;52:235–43.

46. Tsai HF, Wheeler MH, Chang YC, Kwon-Chung KJ. A developmentally regulated gene cluster involved in conidial pigment biosynthesis in *Aspergillus fumigatus*. J Bacteriol. 1999;181:6469–77.

47. Jørgensen TR, Park J, Arentshorst M, van Welzen AM, Lamers G, VanKuyk PA, et al. The molecular and genetic basis of conidial pigmentation in *Aspergillus niger*. Fungal Genet Biol. 2011;48:544–53.

48. Woo PCY, Tam EWT, Chong KTK, Cai JJ, Tung ETK, Ngan AHY, et al. High diversity of polyketide synthase genes and the melanin biosynthesis gene cluster in *Penicillium marneffei*. FEBS J. 2010;277:3750–8.

49. Urquhart AS, Hu J, Chooi YH, Idnurm A. The fungal gene cluster for biosynthesis of the antibacterial agent viriditoxin. Fungal Biol Biotechnol. 2019;6:1–13.

50. van Leeuwe TM, Arentshorst M, Ernst T, Alazi E, Punt PJ, Ram AFJ. Efficient marker free CRISPR/Cas9 genome editing for functional analysis of gene families in filamentous fungi. Fungal Biol Biotechnol. 2019;6:1–13.

51. Nødvig CS, Nielsen JB, Kogle ME, Mortensen UH. A CRISPR-Cas9 system for genetic engineering of filamentous fungi. PLoS One. 2015;10:e0133085.

52. Gems D, Johnstone IL, Clutterbuck AJ. An autonomously replicating plasmid transforms *Aspergillus nidulans* at high frequency. Gene. 1991;98:61–7.

53. Labun K, Montague TG, Krause M, Torres Cleuren YN, Tjeldnes H, Valen E. CHOPCHOP v3: expanding the CRISPR web toolbox beyond genome editing. Nucleic Acids Res. 2019;47:171–4.

54. Punt M, van den Brule T, Teertstra WR, Dijksterhuis J, den Besten HMW, Ohm RA, et al. Impact of maturation and growth temperature on cell-size distribution, heat-resistance, compatible solute composition and transcription profiles of *Penicillium roqueforti* conidia. Food Res Int. 2020;136:109287.

55. Álvarez-Escribano I, Sasse C, Bok JW, Na H, Amirebrahimi M, Lipzen A, et al. Genome sequencing of evolved aspergilli populations reveals robust genomes, transversions in *A. flavus*, and sexual aberrancy in non-homologous end-joining mutants. BMC Biol. 2019;17:1–17.

56. Rosas ÁL, Casadevall A. Melanization affects susceptibility of *Cryptococcus neoformans* to heat and cold. FEMS Microbiol Lett. 1997;153:265–72.

57. Jiang H, Liu NN, Liu GL, Chi Z, Wang JM, Zhang LL, et al. Melanin production by a yeast strain XJ5-1 of *Aureobasidium melanogenum* isolated from the Taklimakan desert and its role in the yeast survival in stress environments. Extremophiles. 2016;20:567–77.

58. Esbelin J, Mallea S, Ram AFJ, Carlin F. Role of pigmentation in protecting *Aspergillus niger* conidiospores against pulsed light radiation. Photochem Photobiol. 2013;89:758–61.

59. Schmaler-Ripcke J, Sugareva V, Gebhardt P, Winkler R, Kniemeyer O, Heinekamp T, et al. Production of pyomelanin, a second type of melanin, via the tyrosine degradation pathway in *Aspergillus fumigatus*. Appl Environ Microbiol. 2009;75:493–503.

60. Gonçalves RCR, Lisboa HCF, Pombeiro-Sponchiado SR. Characterization of melanin pigment produced by *Aspergillus nidulans*. World J Microbiol Biotechnol. 2012;28:1467–74.

61. Toledo AV, Franco MEE, Yanil Lopez SM, Troncozo MI, Saparrat MCN, Balatti PA. Melanins in fungi: Types, localization and putative biological roles. Physiol Mol Plant Pathol. 2017;99:2–6.

62. Bos CJ, Debets AJM, Swart K, Huybers A, Kobus G, Slakhorst SM. Genetic analysis and the construction of master strains for assignment of genes to six linkage groups in *Aspergillus niger*. Curr Genet. 1988;14:437–43.

63. Arentshorst M, Ram AFJ, Meyer V. Using non-homologous end-joining-deficient strains for functional gene analyses in filamentous fungi. Methods Mol Biol. 2012;835:133–50.

64. Sambrook J, Russell DW. Molecular Cloning: A Laboratory Manual. 3rd ed. New York: CSHL Press; 2001.

65. Nordberg H, Cantor M, Dusheyko S, Hua S, Poliakov A, Shabalov I, et al. The genome portal of the Department of Energy Joint Genome Institute: 2014 updates. Nucleic Acids Res. 2014;42:26–31.

Additional files

Additional file 1.

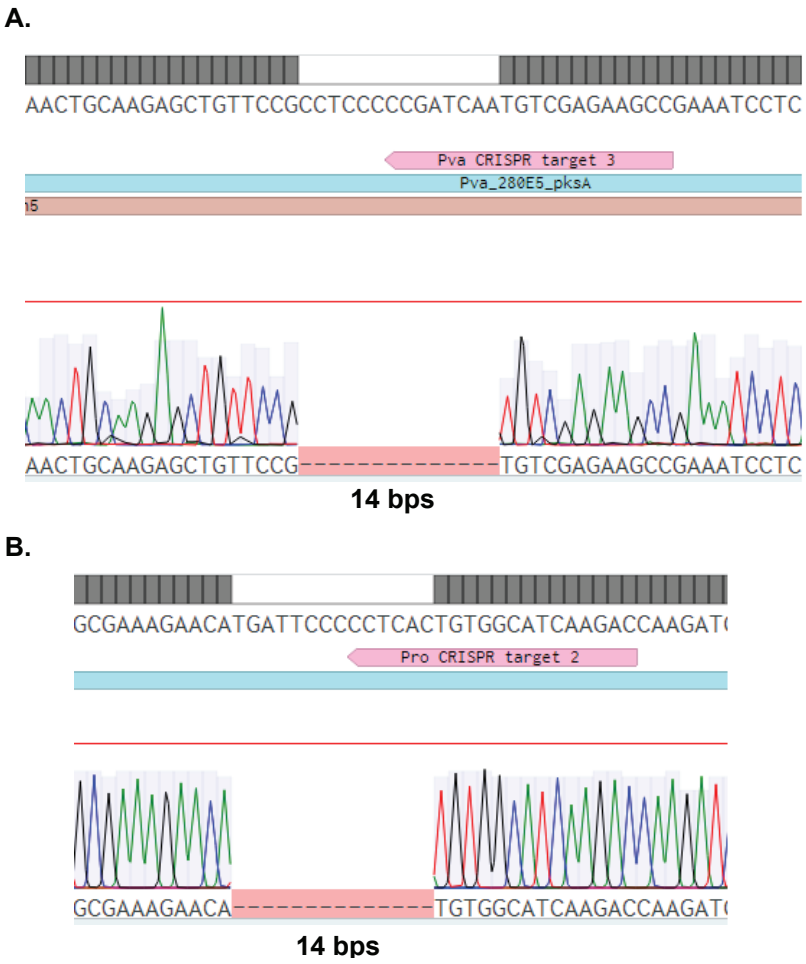

Figure 6.S1. Indels found in *P. variotii* PT32.5 and *P. roqueforti* PT34.2. Sequencing results of *pksA* genes after mutation caused by CRISPR/Cas9 double stranded break and subsequently repair with the NHEJ repair machinery. **A.** Indel of 14 bps in the *pvpP* gene in *P. variotii* causing a frameshift soon after the start codon. This frameshift likely disrupts gene function**. B.** Indel of 14 bps in the *pksA* gene of *P.* roqueforti causing a frameshift soon after the start codon. This frameshift likely disrupts gene function. Pictures were made using Benchling [Biology Software] (2020). Retrieved from https://benchling.com.

Additional file 2.

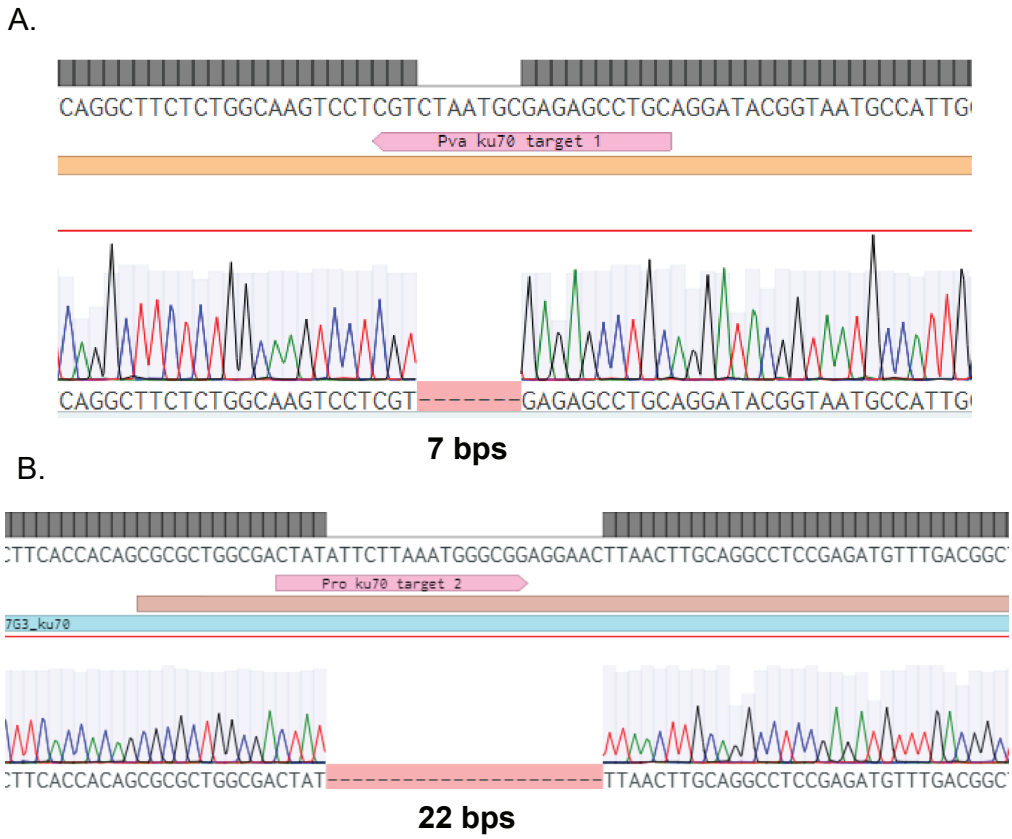

Figure 6.S2. Indels found in *kusA*⁻ strains *P. variotii* PT39.26 and *P. roqueforti* PT43.1. Sequencing results of *kusA* genes after mutation caused by CRISPR/Cas9 double stranded break and subsequently repair with the NHEJ repair machinery. **A.** Indel of 7 bps in the *kusA* gene in *P. variotii* PT39.26 causing a frameshift soon after the start codon. This frameshift likely disrupts gene function**. B.** Indel of 22 bps in the *kusA* gene of *P. roqueforti* PT43.1 causing a frameshift soon after the start codon. This frameshift likely disrupts gene function. Pictures were made using Benchling [Biology Software] (2020). Retrieved from https://benchling.com.

Additional file 3.

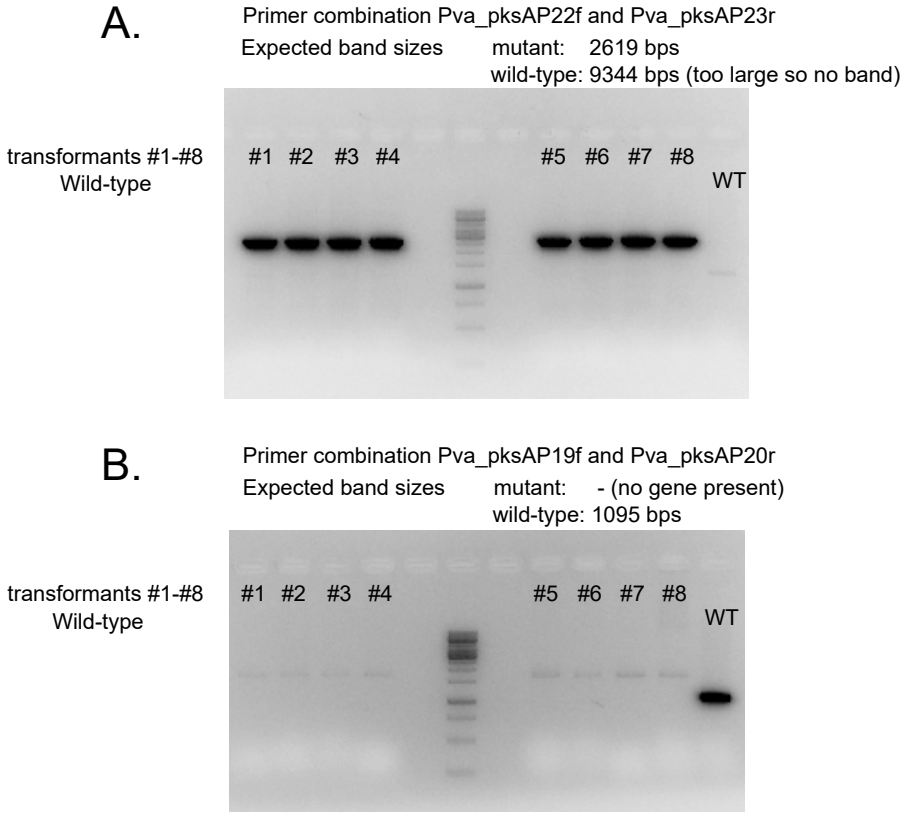

Figure 6.S3. Diagnostic PCR on eight transformants in *P. variotii* PT39.26 missing the *pvpP* gene.

A. Diagnostic PCR to investigate the presence of the *pvpP* gene by amplifying outside the used flanks**.** If the gene is absent a band size of 2619 bps is expected. If the gene *pvpP* is still present, a band size of 9344 bps is present. The eight transformants all have lost the *pvpP* gene. The PCR fragments loaded on #6 and #7 were purified and subsequently send for sequencing. **B.** Diagnostic PCR to investigate the presence of the *pvpP* gene by amplifying inside the gene**.** If the gene is absent, no band is expected. In wild-type situation, a PCR fragment of 1095 bps is expected. No transformants show the presence of *pvpP* gene. Taken together, these results show that 8/8 transformants had a full knock-out of the *pvpP* gene. Both contained the expected sequence for the repair DNA fragment, indicating repair by HDR.

Additional file 4.

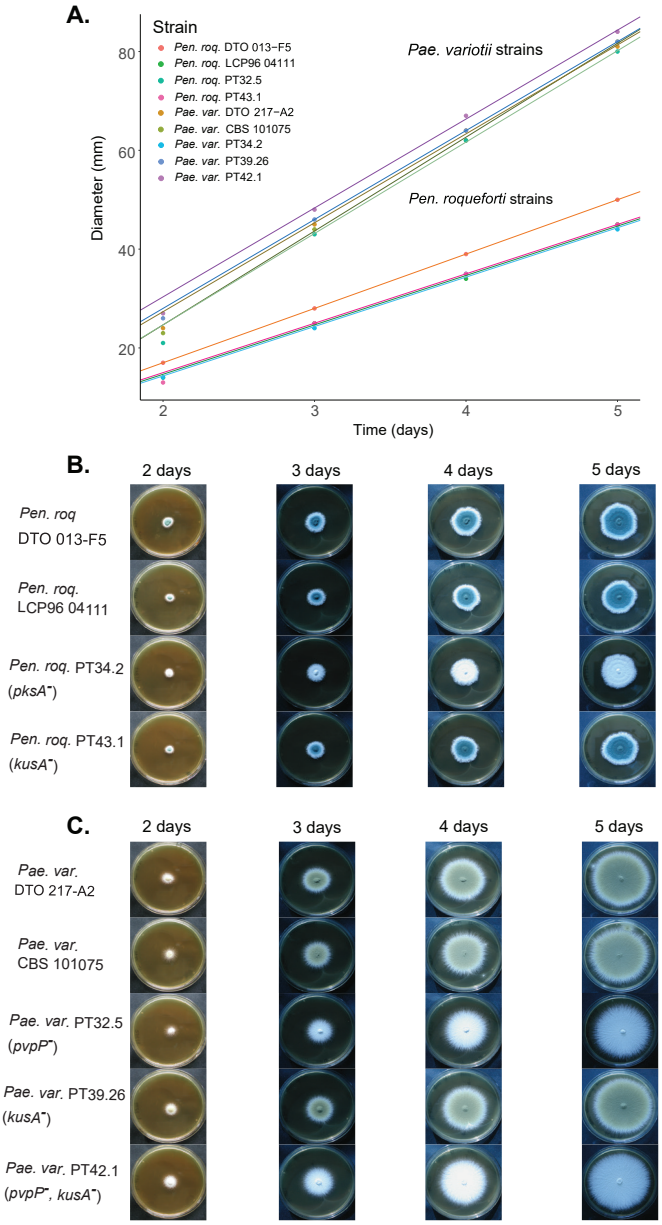

Figure 6.S4. Growth rate of *P. variotii* and *P. roqueforti* strains.

Colony diameters were measured of *P. variotii* and *P. roqueforti* strains growing 2-5 days at 25°C point-inoculated on MEA plates. **A.** Colony diameters of strains plotted against time. The average growth rate in millimeters was estimated by performing a best fit using linear regression. The slope

represents the average millimeter increase in diameter per day. On average, all *P. variotii* strains increased 18-19 mm in diameter per day and all *P. roqueforti* strains increased 10-11 mm in diameter per day. No differences were observed between mutant strains and their parental strains. **B.** Morphology of *P. roqueforti* strains growing on MEA plates. No differences are visible between mutant strains and their parental strains except for the expected change in spore coloration. **C.** Morphology of *P. variotii* strains growing on MEA plates. No differences are visible between mutant strains and their parental strains except for the expected change in spore coloration.

Additional file 5.

Table 6.S1. Plasmids used in this chapter

Plasmid name	Parental plasmid	Gene number of target gene	Gene name	Target sequence	Reference
pFC332	-	-	-	-	[41]
pPT9.3	pFC332	Pro_LCP9604111_2|g6432.t1	*pksA*	GTCTTGATGCCACAGTGAGG	This study
pPT13.1	pFC332	ID456077	*pvpP*	GGCTTCTCGACATTGATCGG	This study
pPT22.4	pFC332	Pro_LCP9604111_2|g3395.t1	*kusA*	CTATATTCTTAAATGGGCGG	This study
pPT23.1	pFC332	ID464258	*kusA*	GCAGGCTCTCGCATTAGACG	This study

Additional file 6.

Table 6.S2. Primers used in this chapter

Primer name	Sequence	Used for
pTE1_for	CCTTAATTAAACTCCGCCGAACGTACTG	Creating new CRISPR gRNAs
pTE1_rev	CCTTAATTAAAAAAGCAAAAAAGGAAGGTA-CAAAAAAGC	Creating new CRISPR gRNAs
Pro_pks1P9r	CCTCACTGTGGCATCAAGACGACGAGCT-TACTCGTTTCG	Creating CRISPR/Cas9 target for *pksA* gene in *P. roqueforti*
Pro_pks1P10f	GTCTTGATGCCACAGTGAGGGTTTTA-GAGCTAGAAATAGCAAG	Creating CRISPR/Cas9 target for *pksA* gene in *P. roqueforti*
Pro_pks1P13f	TTCCAGGGGACAGCTTCAGATG	Diagnostic PCR to confirm mutation on *pksA* locus in *P. roqueforti*
Pro_pks1P14r	TCACCTCGGTTCAGCAAAGTCA	Diagnostic PCR to confirm mutation on *pksA* locus in *P. roqueforti*
Pro_ku70P11f	CTGCTCGGTTAATCTTACTAGACGAGCT-TACTCGTTTCG	Creating CRISPR/Cas9 target for *kusA* gene in *P. roqueforti*
Pro_ku70P12r	TAGTAAGATTAACCGAGCAGGTTTTA-GAGCTAGAAATAGCAAG	Creating CRISPR/Cas9 target for *kusA* gene in *P. roqueforti*
Pro_ku70P15f	TGCCTCACCGGTCTTAGCTGCT	Diagnostic PCR *kusA* mutation in *P. roqueforti*
Pro_ku70P16r	GCCTTGGGAAGCTGCAATTGGC	Diagnostic PCR *kusA* mutation in *P. roqueforti*
Pva_pksAP11r	CCGATCAATGTCGAGAAGCCGACGAGCT-TACTCGTTTCG	Creating CRISPR/Cas9 target for *pvpP* gene in *P. variotii*
Pva_pksAP12f	GGCTTCTCGACATTGATCGGGTTTTA-GAGCTAGAAATAGCAAG	Creating CRISPR/Cas9 target for *pvpP* gene in *P. variotii*
Pva_ku70P11f	CGTCTAATGCGAGAGCCTGCGACGAGCT-TACTCGTTTCG	Creating CRISPR/Cas9 target for *kusA* gene in *P. variotii*
Pva_ku70P12r	GCAGGCTCTCGCATTAGACGGTTTTA-GAGCTAGAAATAGCAAG	Creating CRISPR/Cas9 target for *kusA* gene in *P. variotii*

Primer name	Sequence	Used for
Pva_pksAP17f	ACATTCTCTTGGGCACGGAGAA	Diagnostic PCR to confirm mutation on *pvpP* locus in *P. variotii*
Pva_pksAP18r	ACGCTTGGTCCTGCTGACTTTA	Diagnostic PCR to confirm mutation on *pvpP* locus in *P. variotii*
Pva_pksAP19f	AAGCCTCTGATCGCCAAGAACT	Diagnostic PCR to check presence of *pvpP*
Pva_pksAP20r	AAGGTCCTTGACAGTCGGATGG	Diagnostic PCR to check presence of *pvpP*
Pva_pksAP22f	TCTCCGATCAACTGCGGGCAGA	Diagnostic PCR outside of flanks to see 'clean' knock-out of *pvpP*
Pva_pksAP23r	AACTTGTTCGAGCACGCGAGGG	Diagnostic PCR outside of flanks to see 'clean' knock-out of *pvpP*
Pva_ku70P15f	TCGCTTCTCAGCTTTGCAATGG	Diagnostic PCR *kusA* mutation in *P. variotii*
Pva_ku70P16r	TTCGATTTTCCGGTACTGGGCT	Diagnostic PCR *kusA* mutation in *P. variotii*

Additional file 7.

Protocol for CRISPR Cas9 mediated gene knock-out in *Penicillium roqueforti* and *Paecilomyces variotii* can be accessed through this link:

https://static-content.springer.com/esm/art%3A10.1186%2Fs40694-021-00111-w/MediaObjects/40694_2021_111_MOESM7_ESM.pdf

CHAPTER 7

Dissecting the pivotal role of mannitol and trehalose as compatible solutes in heat resistance of conidia, germination, and population heterogeneity in the filamentous fungus *Aspergillus niger*

Sjoerd J. Seekles, Maryam Ijadpanahsaravi, Tom van den Brule, Maarten Punt, Gwendolin Meuken, Véronique Ongenae, Mark Arentshorst, Jan Dijksterhuis, Johannes H. de Winde, Han A.B. Wösten, and Arthur F.J. Ram

Manuscript in preparation

Abstract

Populations of conidia are naturally heterogeneous, which is a challenge for food preservation strategies. Variation in maturation and thereby spore age of conidia causes heterogeneity within a conidial population. In this research, we investigate the impact of spore age and compatible solutes on the heat stress resistance of *A. niger* conidia. Young conidia from *A. niger* were found to contain reduced amounts of compatible solutes, were more heat sensitive and had altered germination kinetics. To further investigate the impact of compatible solutes on the heat resistance and germination of *A. niger* conidia, knock-out strains were made of trehalose biosynthesis genes (*tpsABC*) as well as the genes putatively involved in the mannitol cycle (*mpdA, mtdAB*) using CRISPR/Cas9 genome editing. A total of twenty-five knock-out strains and five complemented strains containing most of the potential combinations of these six genes were made. Conidia of these knock-out strains were tested for their relative heat resistance, compatible solute profiles and germination capacity. The strain in which four genes (*tpsABC* and *mpdA*) were deleted, contained no measurable amount of trehalose and limited left-over mannitol in its conidia and were found to be sensitive to heat treatments. Conidia lacking compatible solutes, either because they are young or from this four-fold knock-out strain, have higher germination percentages in 10 mM arginine and 0.1 mM proline when compared to wild-type conidia, but lower germination percentages in 10 mM glucose. Taken together, it is concluded that differences in intracellular concentration of compatible solutes within a clonal spore population can affect heterogeneity in heat resistance and germination of *A. niger* conidia.

Introduction

A population of asexual fungal spores (conidia) can be highly heterogeneous, which poses a challenge for food preservation strategies [1]. The conidia are a constant concern in relation to food spoilage, impacting food production [2,3]. Many fungal species produce numerous conidia that are dispersed by air. Every cubic meter of air contains conidia of genera *Cladosporium*, *Penicillium* and *Aspergillus* [4], and this aerial population of conidia varies with the season [5,6]. Apart from species variation, conidia within a population can differ from each other even though they belong to the same species or even strain [1]. This is due to the history of the conidium, and specifically the growth conditions of the mycelium from which the conidia originate. Conidiation during increased cultivation temperature is known to decrease melanin concentrations as well as increase internal compatible solute concentrations, thereby impacting heat stress resistance of the conidia of *Paecilomyces variotii*, *Penicillium roqueforti* and *Aspergillus fumigatus* [7–10]. Additionally, the composition of the medium on which the mycelium feeds during conidiation impacts internal compatible solute concentrations, germination kinetics and conidial stress resistance [11–13]. Yet another source of heterogeneity is introduced by the difference in age of conidia. Culture age is reported to affect the transcription profile and physical properties of conidia, such melanin and compatible solute composition [9,14,15]. Therefore, the change in physical properties and compatible solute compositions due to spore age differences could impact stress resistance to various (preservation) stressors.

An important parameter in stress resistance of fungal cells is the amount and composition of internal compatible solutes [16,17]. These compounds can be quickly accumulated and degraded in the cytoplasm of vegetative cells in response to stress conditions. Compatible solutes like glycerol, erythritol and arabitol are suggested to protect fungal cells against osmotic stress, whereas trehalose and mannitol are shown to be important for protection against heat, cold and drought [17,18]. The biosynthesis routes of trehalose and mannitol in Aspergilli are tightly linked to glycolysis and have been

largely described [19,20], see Figure 7.1.

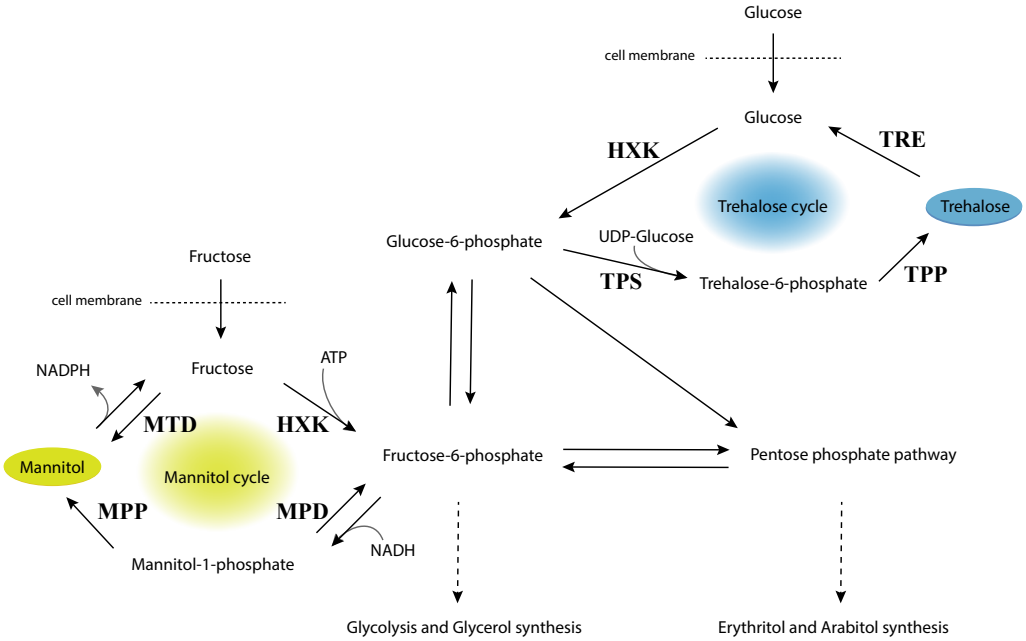

Figure 7.1. Mannitol and trehalose cycles in Aspergilli. The biosynthesis of trehalose in Aspergilli, as depicted in blue, starts with the phosphorylation of glucose to glucose-6-phosphate by hexokinase activity (HXK). Glucose-6-phosphate is converted to trehalose-6-phosphate by trehalose-6-phosphate synthase (TPS). Trehalose-6-phosphate phosphatase (TPP) is able to dephosphorylate trehalose-6-phosphate, yielding trehalose. The catabolism of trehalose is catalyzed by trehalase (TRE) yielding glucose. As represented by the yellow mannitol cycle, mannitol in Aspergilli is mainly synthesized from fructose, which is converted to fructose-6-phosphate by HXK activity. Subsequently, fructose-6-phosphate may be reduced to mannitol-1-phosphate by mannitol-1-phosphate dehydrogenase (MPD). Finally, the dephosphorylation of mannitol-1-phosphate is catalyzed by mannitol-1-phosphate phosphatase (MPP), thereby yielding mannitol. The catabolic conversion of mannitol to fructose by mannitol dehydrogenase (MTD) completes the cycle. Both cycles are connected to glycolysis. Additionally, there is a connection with the pentose phosphate pathway and subsequently erythritol and arabitol synthesis. This figure was adapted from figures shown by Svanström *et al.* (2003) and Ruijter *et al.* (2003).

The role of both mannitol and trehalose in stress resistance of conidia of *A. niger* has been studied previously. Trehalose is responsible for about 4-5% of the conidial dry weight of *A. niger* conidia [21]. Three trehalose-6-phosphate synthase genes (*tpsABC*) and three trehalose-6-phosphate phosphatase genes (*tppABC*) have been

identified in *A. niger* [22]. For the catabolism of trehalose during germination, the *treB* gene was identified, encoding a neutral trehalase [21]. Additionally, *treA* encodes an acid trehalase, presumably involved in the extracellular degradation of trehalose during vegetative growth [23,24]. Deletion of the *tpsA* gene in *A. niger* leads to a 56% reduction of the mycelial trehalose content, compared to wild-type [25]. In addition, *A. niger* ΔtpsA conidia show reduced heat tolerance and a 50% decrease in conidial trehalose content, whereas *tpsB* and *tpsC* deletions showed less effect on both the trehalose content and heat resistance.

Besides trehalose, mannitol is involved in determining stress resistance of *A. niger* conidia. Mannitol is the predominant compatible solute present in *A. niger* conidia and responsible for about 10-15% of the conidial dry weight [26]. The mannitol dehydrogenase gene A (*mtdA)* is suggested to be responsible for the mannitol dehydrogenase activity in *A. niger* [27], whereas the mannitol-6-phosphate dehydrogenase (MPD) enzyme is encoded by *mpdA* [20]. In the *A. niger ΔmpdA* strain, only 30% of the original mannitol concentration is present inside conidia. Furthermore, ΔmpdA conidia show increased sensitivity to stressors like heat and oxidative stress.

The role of trehalose and mannitol in relation to germination has not been well studied so far. In *A. niger*, the concentrations of both trehalose and mannitol drops drastically during the first hours of germination [26,28] suggesting that these two compatible solutes could play a role in the energy household of the mould during early germination. However, whether there is an actual requirement for the presence of the compatible solutes trehalose and mannitol as storage sugars for efficient germination of conidia has not yet been investigated.

Here we describe the impact of conidial age on heat resistance of *A. niger* conidia. We found that young conidia are heat sensitive and contain low concentrations of compatible solutes. A gradual increase in heat resistance and compatible solute concentrations is observed that correlates with an increase in spore age. In order to further investigate the role of compatible solutes, knock-out strains deleted in genes involved in

the trehalose and mannitol cycle were constructed in order to investigate the role of both trehalose and mannitol in the heat resistance. We found that young conidia and conidia from knock-out strain SJS128 (*ΔmpdA, ΔtpsABC*) both lacked most compatible solutes. Conidia lacking most compatible solutes were heat sensitive and were found to significantly differ in germination kinetics when compared to wild-type conidia. Conidia with limited internal compatible solutes show higher germination percentages and speeds in 10 mM arginine, 0.1 mM proline and 1 mM alanine, but lower germination percentages and speeds in 10 mM glucose. Taken together, conidia of *A. niger* show heterogeneity in heat stress resistance and germination kinetics based on internal compatible solute composition.

Results

The impact of culture age on heat resistance and germination of *A. niger* conidia

Previous reports have focussed on the comparison between conidia with age differences of several days [9,14,15]. However, most conidia are formed during the first three days following inoculation after which many spore chains reach their maximum capacity of approximately 20 conidia per chain [15]. In this study, we compared conidia harvested from plates that were inoculated for different amounts of time in hours rather than days. Conidia harvested from plate cultures incubated for 39 hours, will be referred to as 39h conidia.

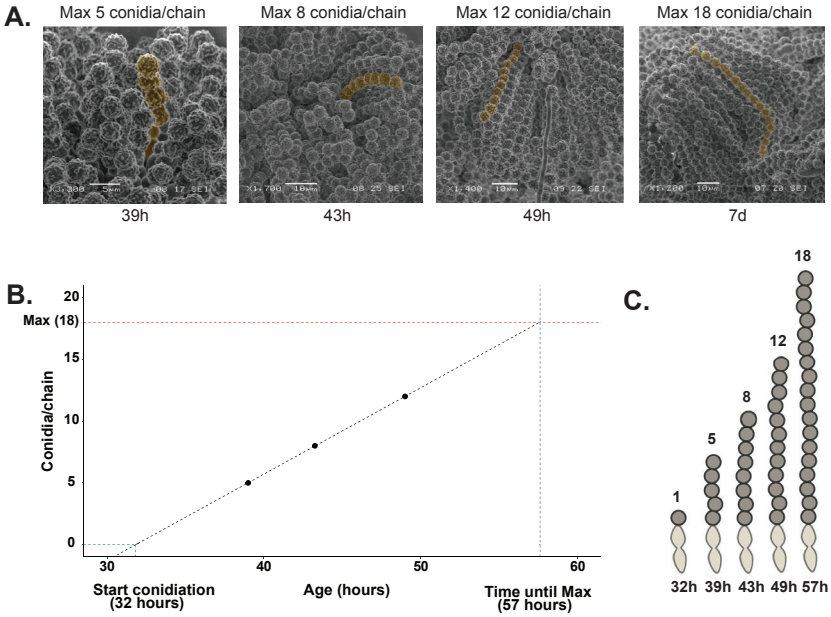

Figure 7.2. Maximum spore chain length of *Aspergillus niger* followed through time. Scanning electron microscopy pictures were analyzed taken from conidiophores of *A. niger* taken from MEA plates (in hours after inoculation). Additionally, a 7 days old plate was taken as a control. **A.** Spore chain lengths were manually counted for at least 15 conidiophores per sample and scanned for the longest chain. The longest possible chain per plate was noted for each time point and highlighted in the picture. **B.** The maximum chain lengths found suggests a constant conidiation speed, calculated to be around ~80 minutes/conidium. Assuming conidiation speed is constant, the first conidium was formed ~32 hours after inoculation and the first spore chain reached its maximum ~57 hours after inoculation. **C.** A representation of the maximum chain lengths found for each time point. A single spore chain takes ~25 hours to reach maximum capacity.

Scanning electron microscopy (SEM) pictures were taken of conidiophores from confluently plated MEA plates incubated for 39h, 43h, 49h and 7 days to see how many conidia are formed during these incubation times (Figure 7.2). The largest spore chain length found from plates incubated for 7 days contained 18 conidia, which is similar to the 20 conidia per chain reported for *A. niger* before [15]. Based on the maximum number of conidia on the chain at the different time points, conidial formation on the spore chain seemed of consistent speed under these conditions (MEA plates, incubated at 28°C) and was found to be around 1 conidium per 80 minutes (Figure 7.2B). From these results it was extrapolated that the first conidium on the first phialide was formed ~32 hours after inoculation and the spore chain hits maximum capacity at ~57 hours after inoculation, which suggests that the formation of a full spore chain takes ~25 hours under these conditions.

In an additional experiment using the exact same conditions as a above but with a slightly different timing, internal compatible solute concentrations and the heat resistance of conidia harvested at 38h, 43h, 46h, 53h and 64h were determined (Figure 7.3). A correlation is seen between the absence of compatible solutes and the heat sensitivity of young conidia. The 38h conidia were significantly more heat sensitive and contained very limited amounts of compatible solutes when compared to older conidia. The heat resistance and compatible solute concentrations of the conidial population increased gradually when conidia were harvested after longer times of growth. The maximum number of conidia found on the largest spore chain at each time point (Figure 7.2) was compared to the heat resistance (Figure 7.3). On plates where the largest spore chain contained eight conidia (as found for 43h conidia), conidia were still considered heat sensitive, since no colony forming units (CFUs) were found when plating 10^6 43h conidia after a heat treatment of 57°C for 10 minutes (Figure 7.3B). Therefore, the heat resistance of conidia is still increasing on plates where a maximum spore chain length of eight conidia was found. These results indicate that compatible solute concentrations, and therefore the heat resistance of conidia, are still increasing during conidial maturation. The maturation, in terms of heat resistance, only occurs while conidia are attached

to the spore chain, since dry harvested 43h conidia no longer show increased heat resistance when incubation times are extended (Figure 7.S1).

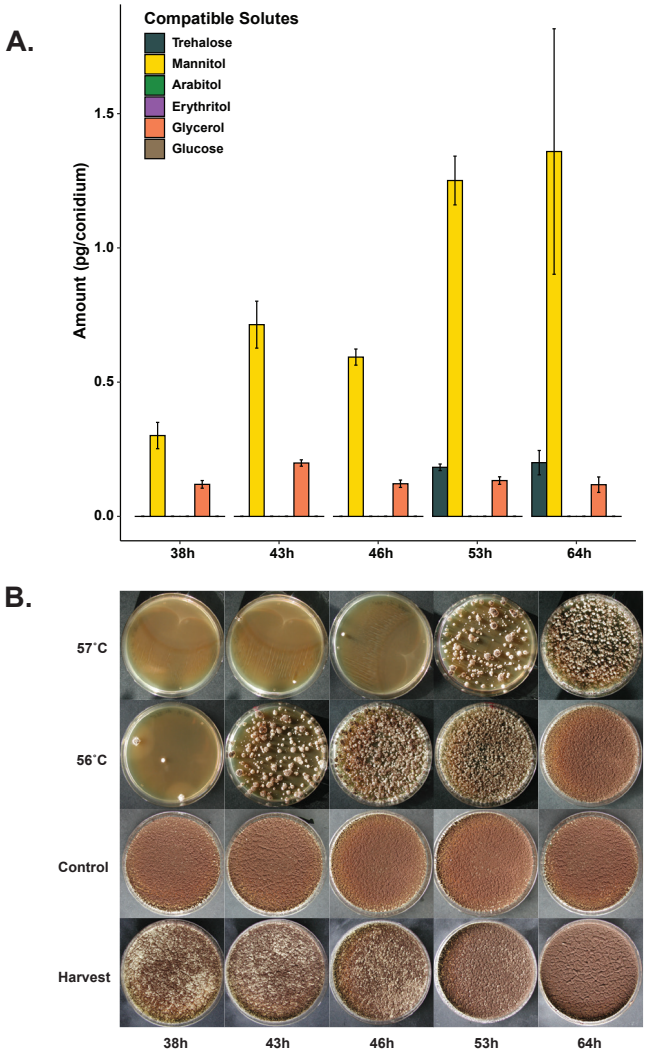

Figure 7.3. Young conidia are sensitive to heat and contain very little compatible solutes. **A.** HPLC analysis of $1*10^8$ cracked conidia revealed only limited amounts of compatible solutes are present inside young conidia. The level of compatible solutes increases when the age of the conidia increases. **B.** Heat treatment assay (Figure 7.S5) results, showing that young spores are sensitive to heat stress. 10^6 conidia were heat treated for 10 minutes at either 56°C, 57°C or room temperature (control) and subsequently plated confluently. After 5 days pictures are taken and visualized here, the amount of colony forming units observed gives an indication of the amount of conidia that survived the heat treatment. A picture of the harvesting plates has been included to show the level of conidiation present on the initial plates from which the conidia were harvested to perform the heat treatment assay.

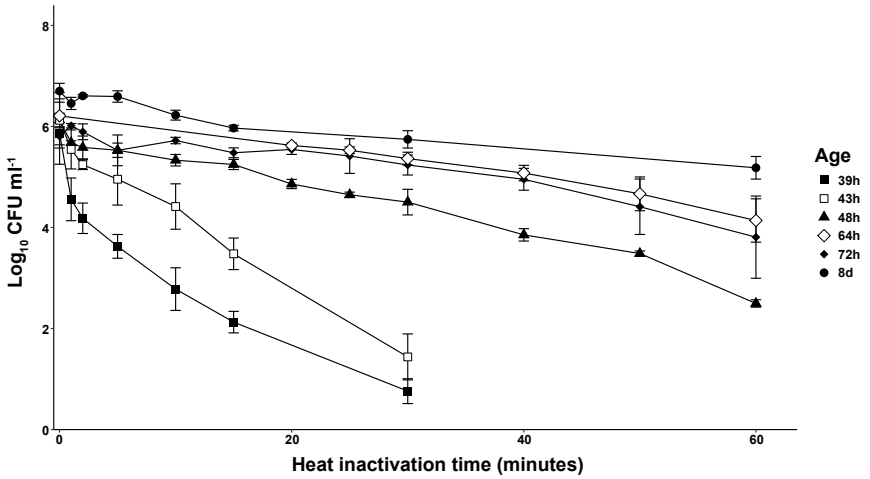

Figure 7.4. Heat inactivation curves of *Aspergillus niger* N402 conidia of different ages. Here the inactivation curves of N402 conidia from different ages 39h (■), 43h (□), 48h (▲), 64h (◊), 72h (♦) and 8d (●) are visualized. Heat treatments were done in a water bath at 54°C. Samples were taken for each time point, put directly on ice and subsequently serially diluted and plated. CFUs were counted after 5 days of growth. Measurements were done in biological triplicates. Linear regression lines were drawn from these curves in order to calculate decimal reduction values (Table 7.1). Heat resistance of conidial populations gradually increases when the age increases, which is in agreement with the heat treatment assay as shown in Figure 7.3.

Table 7.1. Decimal reduction values of *Aspergillus niger* conidia heat treated at 54°C.

Strain	Age	D_{54} value ± SD (minutes)
N402	8d	41.4 ± 7.3
N402	72h	36.8 ± 13.9
N402	64h	30.8 ± 7.2
N402	48h	16.4 ± 2.2
N402	43h	7.1 ± 1.0
N402	39h	5.3 ± 0.6
MA234.1	8d	52.3 ± 25.8
SJS126	8d	22.1 ± 7.7
SJS128	8d	3.3 ± 1.0
SJS132	8d	22.9 ± 5.4
SJS134	8d	22.4 ± 3.5

In this table the quantified results of the heat inactivation curve experiments are summarized as decimal reduction values (D-values). D-values are listed in minutes: average ± the standard deviation. The D-values were based on a log-linear model, calculated from heat inactivation curves shown in Figure 7.4 (N402 conidia of various ages) and shown in Figure 7.7 (conidia of various knock-out strains).

In addition to determining the sensitivity of conidia to a 10 min heat shock at 56° C and 57° C (Figure 7.3B), heat inactivation curves at 54° C of conidia were made to further quantify the heat resistance of young vs older conidia (Figure 7.4). From these graphs, D-values were calculated based on the linear regression model (Table 7.1). The 39h conidia were significantly more sensitive to heat stress ($D_{54°C}$ = 5.3 ± 0.6 minutes) when compared to 8d conidia ($D_{54°C}$ = 41.4 ± 7.3 minutes) and, in agreement with Figure 7.3, heat resistance of conidial populations gradually increased with conidial age.

Compatible solute profiles and heat stress resistance of conidia of knock-out strains

To address the role of mannitol and trehalose as compatible solutes in relation to heat sensitivity of conidia, *A. niger* strains were constructed in which the genes involved in mannitol and trehalose cycles were deleted. Strains lacking compatible solutes, in which multiple genes were deleted simultaneously, were constructed using a recently described CRISPR/Cas9 genome editing system [29]. Single knock-out strains were made in which putative mannitol dehydrogenases were deleted *(*Δ*mtdA*, Δ*mtdB*), the mannitol-phosphate dehydrogenase was deleted *(*Δ*mpdA*) and in which the trehalose-6-phosphate synthase encoding genes were deleted *(*Δ*tpsA*, Δ*tpsB* and Δ*tpsC*). Additional knock-out strains lacking any of these six genes were made in several combinations (Table 7.2). Additionally, complemented strains of a subset of knock-out strains with interesting phenotypes were constructed. Correct deletion and complementation of all transformants was confirmed by diagnostic PCR (Figure 7.5).

Ruijter *et al.* have shown that a *ΔmpdA* strain in *A. niger*, lacking the main mannitol biosynthesis enzyme MpdA, produces conidia containing ~70% less mannitol which are heat sensitive when compared to wild-type conidia [20]. Ruijter *et al.* postulate that the residual mannitol in this strain could be produced by a dual function of the mannitol dehydrogenases, which are thought to mainly catalyse the conversion from mannitol back to fructose, but could also catalyse the conversion from fructose to mannitol [30]. We confirmed that conidia from a Δ*mpdA* strain, as described by Ruijter *et al.*, contain

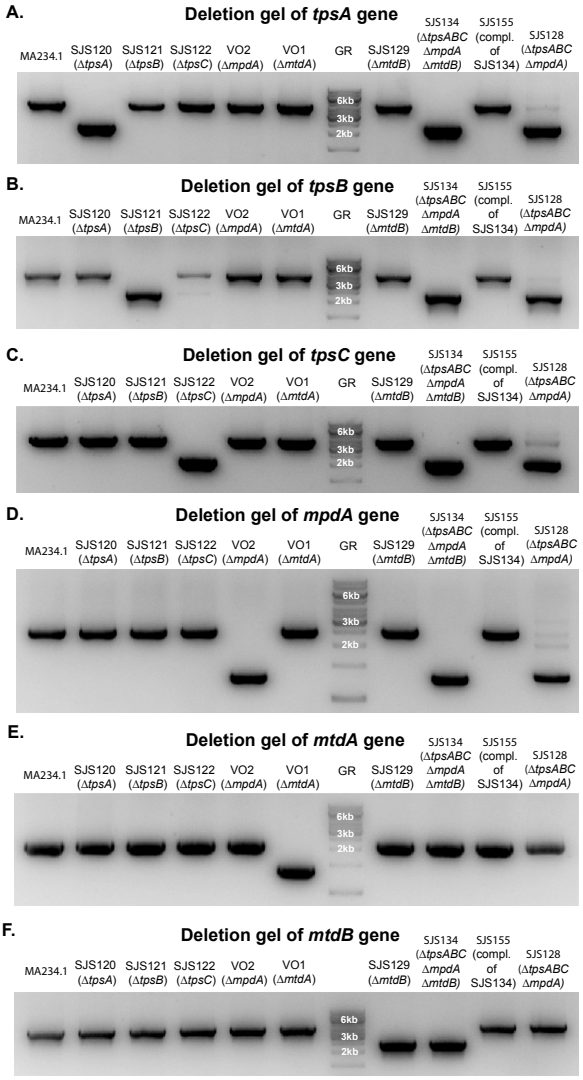

Figure 7.5. Diagnostic PCR confirming deletions in knock-out strains. Each column on the gel represents a knock-out strain. Each individual gel amplified one gene. The GeneRuler lane (GR) contains the ladder. **A.** Deletion of the *tpsA* gene. If the gene is present, a band size of 4118 bps is expected. If the gene is absent a band size of 2189 bps is expected. **B.** Deletion of the *tpsB* gene. If the gene is present, a band size of 3994 bps is expected. If the gene is absent a band size of 2281 bps is expected. **C.** Deletion of the *tpsC* gene. If the gene is present, a band size of 3894 bps is expected. If the gene is absent a band size of 2196 bps is expected. **D.** Deletion of the *mpdA* gene. If the gene is present, a band size of 2499 bps is expected. If the gene is absent a band size of 1345 bps is expected. **E.** Deletion of the *mtdA* gene. If the gene is present, a band size of 2176 bps is expected. If the gene is absent a band size of 1387 bps is expected. **F.** Deletion of the mtd*B* gene. If the gene is present, a band size of 4233 bps is expected. If the gene is absent a band size of 2347 bps is expected.

less mannitol (~65% compared to wild type), more trehalose (~300% compared to wild type) and are heat sensitive compared to conidia of the parental strain (Figure 7.S2). Conidia of the triple knock-out strain lacking *mtdAB* (two putative mannitol dehydrogenases) and *mpdA* were similar to the Δ*mpdA* strain in heat resistance and internal compatible solute profile. These results suggest that only the *mpdA* gene has a direct effect on the internal compatible solute composition of conidia. Surprisingly, all obtained knock-out strains lacking genes involved in the mannitol cycle were still able to produce some amount of mannitol indicating that additional (currently unknown) genes are involved in the mannitol biosynthesis in *A. niger*.

Additionally, the HPLC analysis on conidia of strains lacking *tps* genes revealed that the Δ*tpsAB* and Δ*tpsABC* strains were devoid of (measurable) internal trehalose and were heat sensitive (Figure 7.S3). Therefore, both *tpsA* and *tpsB* are essential for trehalose biosynthesis under standard laboratory conditions. Taken together, we show that the reduction of internal mannitol or trehalose concentrations both lead to heat sensitive conidia compared to wild type, indicating that both mannitol and trehalose are important for the heat stress resistance of *A. niger* conidia.

Conidia from strains deleted in both trehalose and mannitol cycle genes had the largest changes in compatible solute profiles (Figure 7.6A). Specifically, the ΔmpdA and Δ*tpsABC* four-fold knock-out strain (named strain SJS128) resulted in conidia with a drastically changed compatible solute profile. No trehalose and only very little mannitol was detected, which are normally the two most pre-dominant compatible solutes inside *A. niger* conidia. Deletion of the *mtdB* gene in the four-fold knock-out strain SJS128 (*ΔtpsABC*, *ΔmpdA*), creating the five-fold knock-out strain SJS134 (*ΔtpsABC*, *ΔmpdA*, *ΔmtdB*), restored mannitol concentrations to wild-type level. This indicates that the *mtdB* gene encodes for a mannitol dehydrogenase being able to catalyse the conversion of mannitol to fructose, as removing this dehydrogenase results in accumulation of mannitol in these conidia. Additionally, the five-fold knock-out strain SJS134 (*ΔtpsABC*, *Δmpda*, *ΔmtdB*) accumulates a large amount of arabitol, indicating that if genes in both the trehalose and mannitol cycle are being deleted, the conidia accumulate arabitol. All com-

binations in which the deletion of the *mtdA* gene was added did not result in a change in compatible solute composition inside the conidia, and therefore strains in which *mtdA* had been additionally deleted were left out of any further experiments (Figure 7.S4).

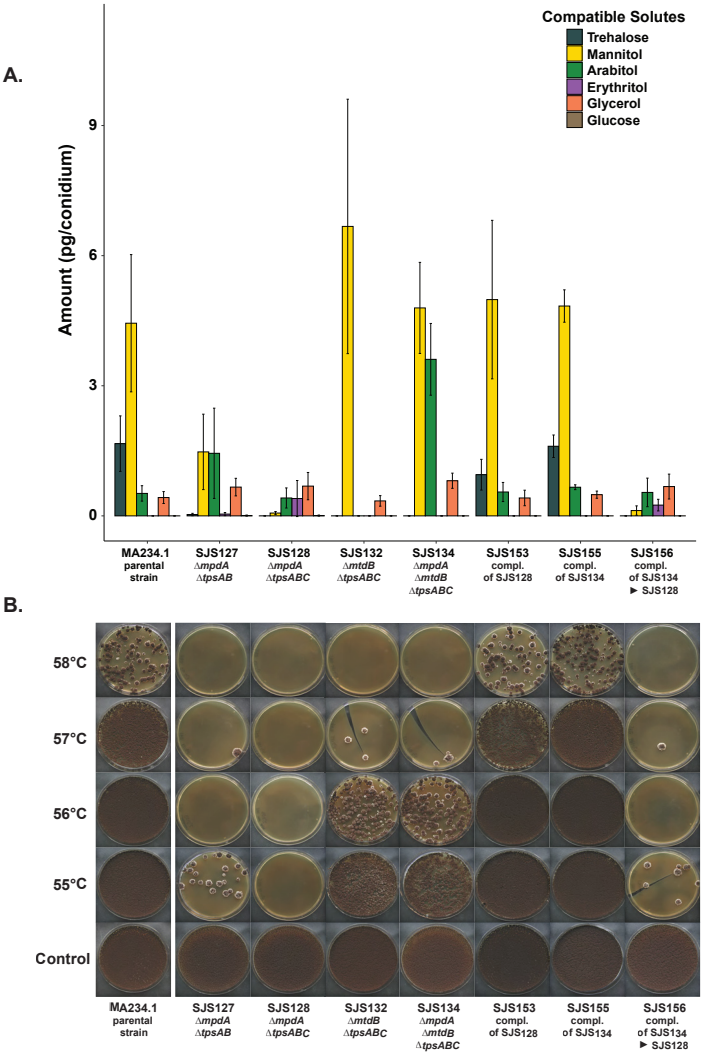

Figure 7.6. Internal compatible solute composition and heat resistance of conidia from *A. niger* trehalose and mannitol knock-out strains. Conidia were freshly harvested from MEA plates grown for 8 days at 28°C. Measurements were performed in biological triplicates. **A.** Internal compatible solute composition of conidia from knock-out strains as determined by HPLC analysis. The conidia from strain SJS128 were most impacted in their trehalose and mannitol concentrations. The SJS127 strain still produces a sliver of trehalose when compared to SJS128, which shows that the *tpsC* gene has impact on trehalose production and overall compatible solute profile of the conidia. Addition of an extra *mtdB* mutation in SJS128 restores mannitol back to wild-type

level and the knock-out strain SJS134 and this strain additionally accumulates arabitol. Complementation strains SJS153 and SJS155 show restoration of the compatible solute profile back to wild type. Strain SJS156 in which only the *mtdB* gene is restored in the SJS134 background re-introduces the SJS128-like compatible solute composition in the conidia. **B.** Heat treatments were applied to 10^6 conidia for 10 minutes in a thermocycler (Figure 7.S5). After heat treatments conidia were plated on plates containing MEA+0.05% triton x-100. Plates were grown for 5 days after which the pictures were made as shown above. The Δ*mpdA*, Δ*tpsABC* mutations (strain SJS128) has the largest effect on the heat resistance of *A. niger* conidia as zero colonies were found after a relatively mild heat stress of 55°C was applied. This correlates with a change in internal compatible solute composition in this strain, showing no trehalose and almost completely abolished mannitol concentrations. When introducing an extra *mtdB* deletion (creating SJS134), the heat resistance of the conidia is partially restored. Conidia of the complementation strains have restored heat resistance as the conidia survive 58°C similarly to parental strain MA234.1. Additionally, when complementing the five-fold knock-out strain SJS134 back to the four-fold knock-out strain SJS128 the heat sensitive phenotype returns.

Heat resistance of the knock-out strains lacking multiple genes in the trehalose biosynthesis route and the mannitol cycle was assessed using a heat treatment assay (Figure 7.6B). The largest impact on heat resistance was found in the four-fold knock-out strain SJS128 (Δ*tpsABC*, Δ*mpdA*). The HPLC analysis showed that this strain lacked detectable levels of trehalose and contained limited levels of mannitol indicating that the low level of compatible solutes is correlated with heat sensitivity. None of the 10^6 conidia from strain SJS128 survived 10 minutes at 55°C, indicating enhanced heat sensitivity when compared to the other knock-out strains and the parental strain, again emphasizing that both mannitol and trehalose contribute to the heat resistance of *A. niger* conidia. Conidia of strain SJS127 (Δ*tpsAB*, Δ*mpdA*), which still contains the *tpsC* gene in comparison to strain SJS128, were more heat sensitive as wild-type conidia but not as heat sensitive as conidia from strain SJS128. The presence of the gene *tpsC* in SJS127 has a major impact on the compatible solute profile, in contrast to the previous comparison between the Δ*tpsAB* and Δ*tpsABC* strains (Figure 7.S3), since the conidia from strain SJS127 (Δ*tpsAB*, Δ*mpdA*) still contain mannitol, arabitol and a small but measurable amount of trehalose when compared to SJS128 (Δ*tpsABC*, Δ*mpdA*). The heat sensitivity of conidia from strains SJS132 (Δ*tpsABC*, Δ*mtdB*) and SJS134 (Δ*tpsABC*, Δ*mpdA,*

Δ*mtdB*), containing mostly mannitol and arabitol, is comparable to that of the trehalose null strain SJS126 (Δ*tpsABC*) (Figure 7.S3).

All complementation strains (SJS149.2, SJS152.3 – SJS155) restored both the compatible solute profile and the heat resistance of conidia back to wild type concentrations. As an extra control, the five-fold knock-out strain SJS134 (*ΔtpsABC*, *Δmpda*, *ΔmtdB*) was complemented with only the *mtdB* gene re-creating the genotype of four-fold knock-out strain SJS128 (this complemented strain is named SJS156). The conidia of this strain SJS156 were again lacking in compatible solutes and showed the heat sensitive phenotype similar to that of the original four-fold knock-out strain SJS128 (Figure 7.6).

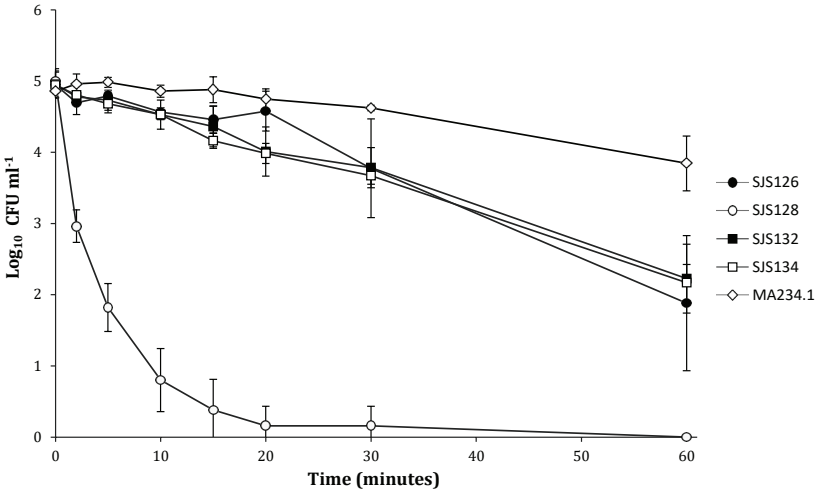

Figure 7.7. Inactivation curves of conidia from *A. niger* knock-out strains altered in their compatible solute concentrations. Here the inactivation curves of conidia from strains MA234.1 (ΔkusA, ◊) parental strain, SJS126 (ΔtpsABC, ●), SJS128 (ΔmpdA ΔtpsABC, ○), SJS132 (ΔmtdB ΔtpsABC, ■) and SJS134 (ΔmpdA ΔmtdB ΔtpsABC, □) are visualized. Conidia of these strains were subjected to heat stress in a heat bath at 54 °C and sampled for up to 60 minutes. Mean values of three biological replicates are shown; standard deviations are indicated by error bars. The conidia of the three knock-out strains SJS126, SJS132 and SJS134 were all similarly affected in their heat resistance, while the conidia of knock-out strain SJS128 were very heat sensitive. D-values were calculated based on linear regression (Table 7.1). During 1 hour of 54°C heat stress wild-type conidia showed ~1 log reduction (1 in 10^1 conidia survive), knock-out strains SJS126, SJS132 and SJS134 showed ~3 log reduction (1 in 10^3 conidia survive) while knock-out strain SJS128 showed, based on linear regression, ~15 log reduction (1 in 10^{15} conidia survive).

After assessing the heat resistance of the conidia from the knock-out strains, additional heat inactivation experiments, that followed heat inactivation in time, were performed to further quantify conidial heat resistance of a subset of heat sensitive strains. Strains SJS126 (Δ*tpsABC*), SJS128 (Δ*tpsABC*, Δ*mpdA*), SJS132 (Δ*tpsABC*, Δ*mtdB*) and SJS134 (Δ*tpsABC*, Δ*mpdA*, Δ*mtdB*) as well as their parental strain MA234.1 were analysed. Survival of conidia during a 54°C heat exposure was followed in time (Figure 7.7) and D-values were calculated from linear regression lines based on this data (Table 7.1). All four knock-out strains have a decreased conidial heat resistance when compared to their parental strain (MA234.1), confirming the earlier findings shown in Figure 7.6 and Figure 7.S3. The conidia of strains SJS126, SJS132 and SJS134 were all similarly sensitive to heat, with D_{54}-values of 22.1 ± 7.7, 22.9 ± 5.4 and 22.4 ± 3.5 minutes respectively when compared to the parental strain MA234.1, which had a D_{54}-value of 52.3 ± 25.8 minutes. To put this in perspective in terms of spore survival; these three knock-out strains display a 3-log reduction after 60 minutes (1 in 10^3 conidia survives the heat treatment) when compared to 1-log reduction (1 in 10^1 conidia survive the heat treatment) observed in the parental strain. The conidia of strain SJS128 (Δ*tpsABC*, Δ*mpdA*) were the most heat sensitive with a decimal reduction value of D_{54} = 3.9 ± 1.0 min when compared to their parental strain D_{54} = 52.3 ± 25.8 min. Therefore, a 60 minutes heat stress of 54°C would result in a ~1 log reduction in the amount of viable conidia in the parental strain (1 in 10^1 conidia survives the heat stress), and a ~13 log reduction in the four-fold knock-out strain SJS128 (1 in 10^{13} conidia survives the heat stress). These results in combination with the obtained compatible solute profiles (Figure 7.6A) suggest that both mannitol and trehalose play a pivotal role in the heat resistance of *A. niger* conidia.

Conidia lacking compatible solutes germinate different from wild-type conidia

Compatible solutes are often referred to as storage sugars, required for the early stages of germination [26,31–33]. Germination efficiency of knock-out strains lacking compatible solutes was tested by plating ~100 conidia (counted using a Bio-Rad TC20™ automated cell counter) on MEA plates in triplicates to get an initial indication of germination and CFUs (Table 7.S1). These results suggest a near 100% germination on MEA plates

for wild-type conidia, as well as for all compatible solute lacking knock-out strains created in this study. From this result it was concluded that all conidia lacking compatible solutes are viable and are capable of germinating under nutrient-rich conditions on MEA plates.

To further investigate if there is any effect on the swelling and germ tube formation of conidia with altered compatible solutes concentrations, germination experiments were performed following germination on defined NaPS medium (25 mM Na_2HPO_4/NaH_2PO_4 (pH 6.0), 2 mM $MgSO_4$) testing four germination triggering molecules; glucose, alanine, proline and arginine. The swelling and germination of conidia was tracked using oCelloscope imaging, based on previous work [34]. The asymmetric model [35] was used to describe germination of conidia. The maximum germination percentage after 24 hours (P_{max}) and the time in hours until 50% of the observed germination was reached (τ) were calculated from this model, and all germination characteristics are summarized in Table 7.S2. Strains tested included lab strain N402, parental strain MA234.1 (*ΔkusA*), compatible solutes lacking four-fold knock-out strain SJS128 (*ΔtpsABC*, *ΔmpdA*), complemented knock-out strain SJS153 and 38h conidia from lab strain N402. The P_{max} values were used to compare the germination percentages after 24 hours of conidia that have wild-type levels of compatible solutes (N402, MA234.1, SJS153) versus conidia with altered compatible solute composition (SJS128 and 38h N402 conidia) (Figure 7.8).

All conditions with higher germination percentages (P_{max} = the maximum germination percentage, determined at t = 24 hours) also showed significantly higher germination speeds (theta = time until 0.5, or half, of P_{max} is reached), as is seen in Table 7.S2. Additionally, the swelling and germ tube formation percentages follow the same trend. Therefore, conidia that were triggered for germination and showed swelling, also formed germ tubes given time in the conditions tested. Conidia of MA234.1 and SJS153 germinated the same in all tested conditions. A slight difference in germination percentage was found between wild-type strain N402 and the *ΔkusA* strains MA234.1 and SJS153 in the 10 mM glucose condition, where N402 germinated slightly better (~35%) than the two *ΔkusA* strains (~26%). However, the largest differences in germination percentages

were seen when comparing 38h conidia and SJS128 conidia to the other three strains. In conditions with relatively high glucose and high amino acid concentrations, 8d N402 wild-type conidia showed relatively high germination percentages (93% in 10 mM proline, 60% in 10 mM alanine and 35% in 10 mM glucose). In these conditions, the 38h N402 conidia have significantly lower germination percentages (49% in 10 mM proline, 48% in 10 mM alanine and 7% in 10 mM glucose) than the 8 days N402 conidia. Interestingly, the 38h conidia show significantly higher germination percentages (26% instead of 11% in 10 mM arginine and 18% instead of 8% in 0.1 mM proline) than 8d conidia when germinating in 10 mM arginine and 0.1 mM proline. Overall, the results show that 38h conidia have higher germination percentages in 10 mM arginine and 0.1 mM proline, but lower germination percentages in 10 mM glucose and 10 mM alanine compared to 8d conidia.

Conidia from strain SJS128 (*ΔmpdA*, *ΔtpsABC*), containing no trehalose and very limited mannitol (Figure 7.6A), showed significantly higher germination percentages than parental strain in 10 mM arginine, 0.1 mM proline and 1 mM alanine (22% versus 14%, 29% versus 7% and 27% versus 13%, respectively), but a significantly lower germination percentage than the parental strain in 10 mM glucose (12% versus 27%, respectively). Therefore, similar to the observations for young conidia, the conidia from strain SJS128 showed significantly different germination on all four germination triggers. In both 38h conidia and SJS128 conidia germination percentages were higher than wild-type conidia in 10 mM arginine and 0.1 mM proline, and lower than wild-type conidia in 10 mM glucose. In conclusion these data indicate that although young conidia do not show identical germination kinetics to conidia from strain SJS128, they do show similar trends.

Additional experiments are needed to fully elucidate the effect of compatible solutes on the germination kinetics of *A. niger* conidia. However, it is safe to conclude that young conidia germinated differently from old(er) conidia in all four conditions tested. Additionally, conidia from four-fold knock-out strain SJS128 (containing no trehalose and limited mannitol) also germinated significantly differently from wild-type conidia in all four

conditions tested. Therefore, the results indicate that internal compatible solutes have an impact on the germination kinetics of *A. niger* conidia.

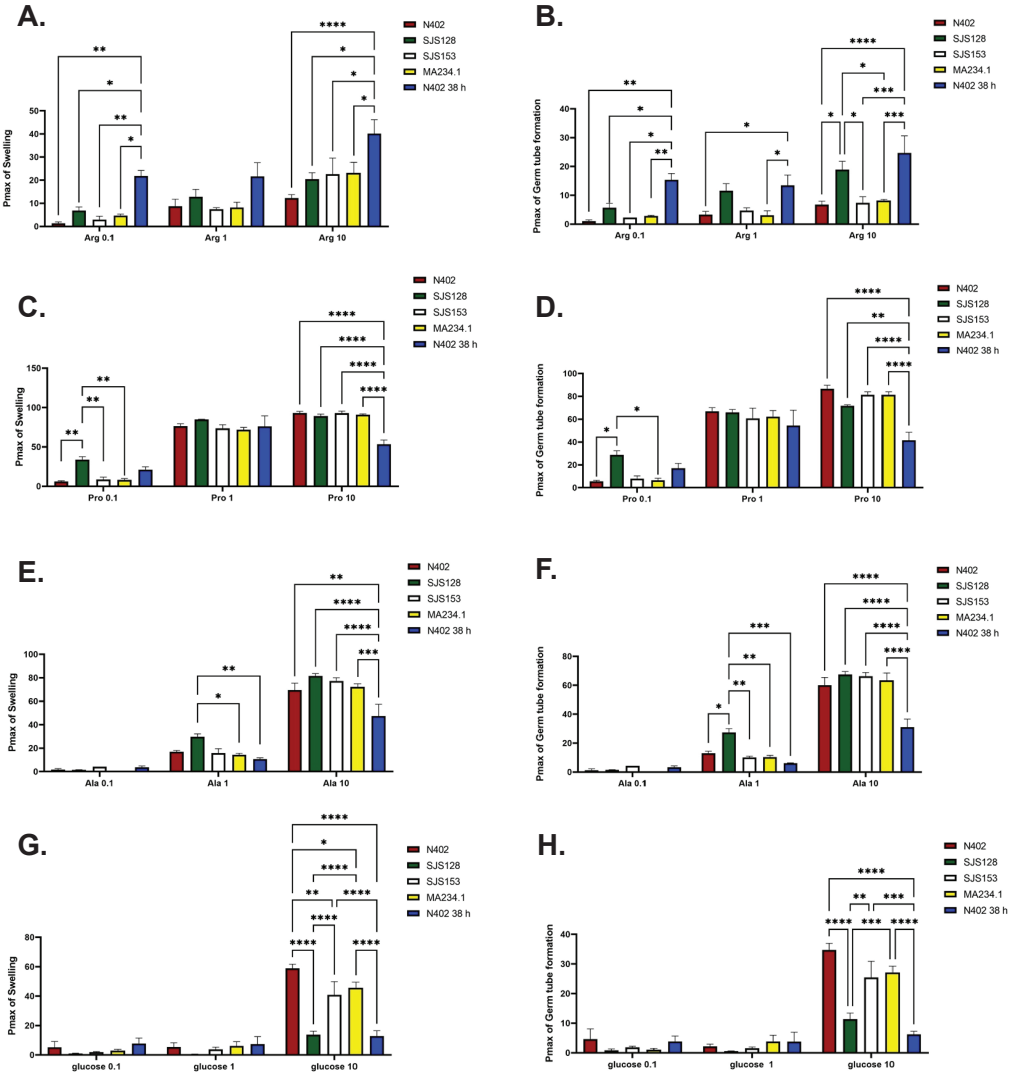

Figure 7.8. Swelling and germ tube formation percentages (P_{max}) after 24 hours on NaPS with glucose, alanine, proline and arginine. All four molecules (arginine, proline, alanine and glucose) were added as 0.1 mM, 1 mM and 10 mM. Conidia were harvested from MEA plates incubated for 8 days or 38 hours at 28°C. Germination experiments were done in triplicates and grouped, a Two-way ANOVA and subsequently Tukey's test for multiple comparisons were performed to calculate significant differences between the strains ($p<0.05$). All significantly higher germination percentages are accompanied by significantly higher germination speeds (theta), see Table 7.S2. The germination percentages follow the pattern seen in the swelling germination per-

centages, indicating that no strain or conditions causes swelling without subsequently germination. Germination percentages of conidia of compatible solute mutant SJS128 (*ΔmpdA*, *ΔtpsABC*) were higher than parental strain MA234.1 or wild-type strain N402 in NaPS medium with 10 mM arginine, 0.1 mM proline and 1 mM alanine. Similarly, young conidia had higher germination percentages than 8d old conidia (N402) in 10 mM arginine and 0.1 mM proline (but not alanine). Both young conidia and SJS128 conidia had lower germination percentages in glucose when compared to the controls. Swelling percentages on arginine (**A**), proline (**C**), alanine (**E**) and glucose (**G**) were visualized. Similarly, germ tube formation percentages on arginine (**B**), proline (**D**), alanine (**F**) and glucose (**H**) were visualized.

Discussion

Filamentous fungi grow as colonies, where young conidia are located on conidiophores at the edge of the colony, and matured conidia reside in the middle of the colony [15]. Therefore, the conidial population from a single fungal colony is highly heterogeneous with respect to their age. In this study, we show that young *A. niger* conidia harvested from MEA plates 38 hours after confluent inoculation have significantly less internal compatible solutes and are sensitive to heat stress compared to their older counterparts (Figure 7.3). The heat resistance and compatible solute concentrations of the conidia increased gradually when strains were grown for longer times. This indicates that during the early hours of conidiation, *A. niger* conidia do not contain the expected high concentrations of compatible solutes (yet), even though conidia harvested from these plates are viable and the spore chains already contain multiple conidia (Figure 7.2 & Figure 7.3). Therefore, we conclude that compatible solute accumulation and the observed heat resistance increase are part of the conidial maturation process in *A. niger*.

A recent study showed that conidia are still subject to change and mature after their formation, while being attached to the spore chain [36]. In agreement with Wang and colleagues, our findings suggest the accumulation of internal compatible solutes, and subsequently heat resistance increase, occurs after conidia are formed. When 43h conidia were dry harvested and kept for further incubation, a heat resistance increase was no longer observed, indicating that attachment to the spore chain is crucial for proper heat resistance maturation of *A. niger* conidia. Several pre-culturing conditions are known to impact conidial compatible solute concentrations and even germination kinetics. A recent study in *A. fumigatus* showed that conidia from a single strain can differ in germination kinetics, depending on the growth medium the mycelium was feeding on during conidiation [37]. Moreover, conidia harvested from plates cultivated at a high(er) temperature have high(er) heat resistance in both *A. fumigatus* and *P. roqueforti*, and this heat resistance increase correlates with an increase in the amount of internal trehalose in both species [7,9]. Here we show for the first time that compatible solute accumulation occurs after conidial formation, suggesting that the increased accumulation

of trehalose inside conidia due to high cultivation temperature also occurs after conidial formation when the conidia are still attached to the chain.

We propose that the compatible solute composition of any given conidium is dependent on the amount of time that has passed since its formation, and the environmental cues received during this time. Moreover, this difference in compatible solute composition has a direct effect on the germination kinetics of the conidium (Figure 7.8). Conidia from knock-out strain SJS128 (*ΔmpdA*, *ΔtpsABC*), containing limited compatible solutes, have a different germination profile from wild type in all tested conditions, showing higher germination percentages than wild type in 10 mM arginine, 0.1 mM proline and 1 mM alanine, and lower germination percentages than wild type in 10 mM glucose. This is in agreement with a study done on *A. nidulans*, where conidia of a *ΔtpsA* strain, lacking all internal trehalose, were shown to have a reduced germ tube formation speed during carbon (glucose) limiting conditions [38]. These authors conclude that internal trehalose concentration of conidia impacts germination, but that trehalose is not essential for the overall germination process. Indeed, in our study we show that strain SJS128 (*ΔmpdA*, *ΔtpsABC*), lacking all trehalose and most mannitol, is still able to germinate with 10 mM glucose, 1 mM alanine and even in nutrient limited NaPS medium containing 0.1 mM proline and arginine, suggesting that both internal trehalose and mannitol pools are not essential for germ tube formation of *A. niger* conidia.

Conidia of *A. niger* show differences in internal compatible solute composition based on age, but also based on environmental cues received during conidiation, such as cultivation temperature (see Chapter 7). This suggests that the fungus employs a form of bet-hedging, where conidial populations from a single fungal colony are diverse in their compatible solute composition, based on age and environmental cues received during conidiation, which has a direct impact on germination kinetics of conidia (Figure 7.8). This heterogeneity among *A. niger* conidia form a single colony could be considered a survival strategy and an ecological advantage, since there is a natural distribution of conidia from the same colony with different germination kinetics. It is interesting to hypothesize about the possibility that the fungus can shift between these types of conidia,

depending on the environmental cues it has experienced during conidiation.

The compatible solutes trehalose and mannitol both significantly contribute to the heat resistance of *A. niger* conidia. The impact of trehalose on heat resistance is best illustrated by the conidia of strain SJS126 (Δ*tpsABC*), which are devoid of trehalose and are more sensitive to heat stress than wild-type conidia (Figure 7.S3), while no significant increase in any other compatible solute is observed. The impact of mannitol on heat resistance is best illustrated by the four-fold knock-out strain SJS128 (Δ*tpsABC*, Δ*mpdA*), which lacks most compatible solutes including most mannitol and is very heat sensitive, compared to the four-fold knock-out SJS132 (Δ*tpsABC*, Δ*mtdB*) that contains mainly a large amount of mannitol (Figure 7.6). Conidia of knock-out strains SJS132 (Δ*tpsABC*, Δ*mtdB*) and SJS134 (Δ*tpsABC*, Δ*mpdA,* Δ*mtdB*) each have comparable heat resistance (Table 7.1), but have different compatible solute profiles (Figure 7.6). This suggests that arabitol and glycerol, which are the only significant compatible solute differences between SJS132 and SJS134 ($p = 0.02$ and $p = 0.02$, respectively based on a Student's t-test), do not significantly impact heat resistance of *A. niger* conidia.

The D-value (54°C) of 39h conidia, lacking most compatible solutes (Figure 7.3A), and the D-value of strain SJS128 (*ΔmpdA*, *ΔtpsABC*), lacking all trehalose and most mannitol (Figure 7.6A), were 5.3 ± 0.6 minutes and 3.3 ± 1.0 minutes, respectively. The 39h conidia are not identical to 8d conidia of knock-out strain SJS128 in terms of compatible solute composition and heat resistance, but do show similar trends. Both contain low concentrations of compatible solutes, are relatively heat sensitive with comparable D-values, and both germinate significantly different compared to wild-type conidia (Figure 7.8).

It would be informative to create conidia containing wild-type levels of trehalose but no mannitol, however deletion of the genes *mpdA*, *mtdA* and *mtdB* did not result in conidia unable to produce any mannitol (conidia of triple knock-out strain SJS139 contained ~80% of wild-type mannitol concentration) (Figure 7.S2). Previously, it was suggested that the mannitol dehydrogenases can act to either synthesize and/or metabolize mannitol, which would explain the remaining ~30% mannitol observed in the

ΔmpdA strain when compared to wild type [20]. However, the conidia of a strain where the two putative mannitol dehydrogenases (*mtdA*, *mtdB*) have been additionally deleted (SJS139) still contain mannitol, suggesting that either additional mannitol dehydrogenases are present, or an alternative biosynthesis route is producing the leftover mannitol in these strains.

The *mtdA* deletion did not alter mannitol concentrations whereas the *mtdB* deletion did (Figure 7.S4), this suggests that *mtdB* rather than *mtdA* codes for the main mannitol dehydrogenase in *A. niger*. This also suggests that a mannitol cycle could still be active in *A. niger,* contrasting a previous report stating that such cycle does not exist in *A. niger* based on the spatial differentiation of the MpdA and MtdA enzymes [27]. Additionally, we noted that HPLC data and heat resistance data of strains only deleted in genes that are part of the trehalose cycle (*tpsABC*), suggested that *tpsC* is not important for trehalose biosynthesis (Figure 7.S3). However, the presence of the *tpsC* gene did have a significant impact on the internal compatible solute composition and heat resistance when a *ΔtpsAB, ΔmpdA* strain was compared with a *ΔtpsABC, ΔmpdA* strain (Figure 7.6). Therefore, only when genes were deleted in both the trehalose and mannitol cycles was the importance of *tpsC* for the biosynthesis of trehalose observed. Similarly, the importance of *mtdB* for the metabolism of mannitol was only observed in a strain deleted in genes from both the trehalose and mannitol cycles (Figure 7.S4B).

Additional experiments are needed to fully understand the impact of internal compatible solutes on the germination of *A. niger* conidia. Future research could focus on the molecular mechanisms behind the observed changes in germination of conidia with limited internal compatible solutes. Dijksterhuis and colleagues have shown that the microviscosity inside conidia decreases during the germination process and that compatible solutes play an important role in the internal microviscosity of conidia [39,40]. Perhaps the conidia of the *ΔtpsAB, ΔmpdA* strain and the young conidia have decreased internal microviscosity, thereby impacting the germination process or trigger, which would be an interesting topic for future studies.

Materials and Methods

Standard growth media and conditions used

The strains used in this study are listed in Table 7.2. Media were prepared as described previously [41]. Minimal medium (MM) contained 1% (w/v) glucose and 1.5% agar, supplemented with hygromycin (100 µg ml^{-1}) when needed. Transformation plates contained minimal medium + sucrose (MMS) 32.5% (w/v) sucrose and 1.5% agar, supplemented with hygromycin (200 µg ml^{-1}) and caffeine (500 µg ml^{-1}). Malt extract agar (MEA, Oxoid) contained 3% (w/v) malt extract, 0.5% (w/v) mycological peptone and 1.5% agar. In order to harvest conidia, strains were first inoculated on MEA plates and grown for 8 days at 28 °C. Conidia were harvested by adding 13 mL of physiological salt buffer (PS, 0.9% (w/v) NaCl and 0.02% (v/v) Tween-80 in demi water), after which the conidia were carefully scraped from the plate using a cotton swab. The resulting spore solution was filtrated through a sterilized filter (Amplitude™ Ecocloth™ Wipes, Contec Inc., Spartanburg, SC, USA) in order to remove mycelial debris.

Table 7.2. List of strains used in this study

Name	Genotype	Parental strain	Reference
N402	*cspA1, amdS-*		[45]
MA234.1	*cspA1, ΔkusA::DR-amdS-DR*	N402	[42]
VO1	*cspA1, ΔkusA::DR-amdS-DR, ΔmtdA*	MA234.1	This study
VO2	*cspA1, ΔkusA::DR-amdS-DR, ΔmpdA*	MA234.1	This study
VO3	*cspA1, ΔkusA::DR-amdS-DR, ΔmtdA, ΔmpdA*	MA234.1	This study
SJS120	*cspA1, ΔkusA::DR-amdS-DR, ΔtpsA*	MA234.1	This study
SJS121	*cspA1, ΔkusA::DR-amdS-DR, ΔtpsB*	MA234.1	This study
SJS122	*cspA1, ΔkusA::DR-amdS-DR, ΔtpsC*	MA234.1	This study
SJS123	*cspA1, ΔkusA::DR-amdS-DR, ΔtpsAB*	SJS121	This study
SJS124	*cspA1, ΔkusA::DR-amdS-DR, ΔtpsAC*	MA234.1	This study
SJS125	*cspA1, ΔkusA::DR-amdS-DR, ΔtpsBC*	SJS121	This study
SJS126	*cspA1, ΔkusA::DR-amdS-DR, ΔtpsABC*	SJS121	This study
SJS127	*cspA1, ΔkusA::DR-amdS-DR, ΔmpdA, ΔtpsAB*	SJS123	This study
SJS128	*cspA1, ΔkusA::DR-amdS-DR, ΔmpdA, ΔtpsABC*	SJS126	This study
SJS129	*cspA1, ΔkusA::DR-amdS-DR, ΔmtdB*	MA234.1	This study
SJS130	*cspA1, ΔkusA::DR-amdS-DR, ΔmtdB, ΔmpdA*	VO2	This study
SJS131	*cspA1, ΔkusA::DR-amdS-DR, ΔmtdB, ΔtpsAB*	SJS123	This study

Name	Genotype	Parental strain	Reference
SJS132	*cspA1, ΔkusA::DR-amdS-DR, ΔmtdB, ΔtpsABC*	SJS126	This study
SJS133	*cspA1, ΔkusA::DR-amdS-DR, ΔmtdB, ΔmpdA, ΔtpsAB*	SJS127	This study
SJS134	*cspA1, ΔkusA::DR-amdS-DR, ΔmtdB, ΔmpdA, ΔtpsABC*	SJS128	This study
SJS135	*cspA1, ΔkusA::DR-amdS-DR, ΔtpsAB, ΔmtdA*	SJS123	This study
SJS136	*cspA1, ΔkusA::DR-amdS-DR, ΔtpsABC, ΔmtdA*	SJS126	This study
SJS137	*cspA1, ΔkusA::DR-amdS-DR ΔtpsABC, ΔmpdA, ΔmtdA*	SJS128	This study
SJS138	*cspA1, ΔkusA::DR-amdS-DR, ΔmtdAB*	SJS129	This study
SJS139	*cspA1, ΔkusA::DR-amdS-DR, ΔmtdAB, ΔmpdA*	SJS130	This study
SJS141	*cspA1, ΔkusA::DR-amdS-DR, ΔmtdAB, ΔtpsABC*	SJS132	This study
SJS142	*cspA1, ΔkusA::DR-amdS-DR, ΔmtdAB, ΔmpdA, ΔtpsABC*	SJS134	This study
SJS149.2	*cspA1, ΔkusA::DR-amdS-DR, mpdA* T669A, T672G	VO2	This study
SJS152.3	*cspA1, ΔkusA::DR-amdS-DR, tpsC* T93A, A96T	SJS126	This study
SJS153	*cspA1, ΔkusA::DR-amdS-DR, tpsA* T258C, G273A	SJS128	This study
SJS154	*cspA1, ΔkusA::DR-amdS-DR, tpsB* G267A, G270A	SJS132	This study
SJS155	*cspA1, ΔkusA::DR-amdS-DR, tpsA* T258C, G273A, *tpsB* G267A, G270A	SJS134	This study
SJS156	*cspA1, ΔkusA::DR-amdS-DR, ΔmpdA, ΔtpsABC*	SJS134	This study

Conidial age experiments

The age of conidia was defined as the amount of time passed since inoculation. Hence, conidia harvested from a plate that had been incubated for 38 hours are referred to as 38h conidia. The precise amount of time passed may vary a maximum of 15 minutes from their designated age. To prevent heterogeneity in the spore population, conidia were plated out confluently. All plates were inoculated confluently using sterilized glass beads. All plates were incubated at 28°C. All conidial age experiments were done using MEA plates.

CRISPR/Cas9 mediated genome editing approach

Using marker-free CRISPR/Cas9 mediated gene editing [29], ORFs were deleted from the non-homologous end-joining (NHEJ)-deficient *A. niger* strain MA234.1 [42]. All primers used in this study are listed in Table 7.3. The sgRNA targeting the gene of interest (GOI) was created essentially as described previously [29]. All plasmids used in this study are listed in Table 7.4. The DNA repair fragments were obtained by amplifying both the 5' and the 3' flanks of the GOI from the parental strain MA234.1, followed by fusion

PCR. Primers contained an overhang creating a novel 23 base pairs region replacing the original open reading frame (ORF). This 23 base pairs overhang was identical for all deletions and resulted in the replacement of the original gene by a new unique artificially created CRISPR/Cas9 target sequence named KORE1 (sequence: CCGGCTTATATTG-GTACCACTCC). Complementation of the knock-out strains was done by re-inserting the original gene on the original locus, using a CRISPR/Cas9 containing vector targeting the KORE1 sequence to cut open the original loci. In this case, repair DNA was a PCR product amplified from the original gene including both 5' and 3' flanks with the following alteration; In order to show that the correct complementation was obtained, two silent mutations were introduced into the original gene (created during amplification by using primers with overhangs containing these point mutations) before re-insertion the original gene into the genome. In this way, sequencing of the gene confirms that the obtained strain is indeed a complemented, and not a contamination of the genetically identical original parental strain MA234.1.

Table 7.3. List of primers used in this study.

Primer	Sequence	Purpose
pTE1_for	CCTTAATTAAACTCCGCCGAACGTACTG	Creation sgRNA on plasmids
pTE1_rev	CCTTAATTAAAAAAGCAAAAAAGGAAGGTACAAAAAAGC	Creation sgRNA on plasmids
tpsA_2_fw	CAGCTGTCGCTTCTCCCATCGTTTTAGAGCTAGAAATAGCAAG	3' *tpsA* gRNA (target)
tpsA_2_rv	GATGGGAGAAGCGACAGCTGGACGAGCTTACTCGTTTCG	5' *tpsA* gRNA (target)
TS1_tpsA_fw	GTTGTTGCTCGTTAAGTCGGGG	5' tpsA flank (repair DNA fragment)
TS1_tpsA_rv	ATAAGCCAGTCTCGCCCTTTGTGATTGTTCAACGGCCGAGGATC	5' tpsA flank (repair DNA fragment)
TS2_tpsA_fw	GATCCTCGGCCGTTGAACAATCACAAAGGGCGAGACTGGCTTAT	3' tpsA flank (repair DNA fragment)
TS2_tpsA_rv	GCCGGAACTACTCTTGTCCCTT	3' tpsA flank (repair DNA fragment)
DIAG_tpsA_5'_fw	TTGGTCTTGTAGGGGTAGCTGC	Diagnostic PCR tpsA deletion
DIAG_tpsA_3'_rv	GGTGGTTTTTACTGCTGGGGTG	Diagnostic PCR tpsA deletion
tpsB_fw	TTTGTCGTCCATGAACACCGGTTTTAGAGCTAGAAATAGCAAG	3' tpsB gRNA (target)
tpsB_rv	CGGTGTTCATGGACGACAAAGACGAGCTTACTCGTTTCG	5' tpsB gRNA (target)
TS1_tpsB_fw	CCATCTGTCTGCCTGTCCTTCA	5' tpsB flank (repair DNA fragment)
TS1_tpsB_rv	CTCCTTTCGCTCTGCTCTCCATTCTCTTTGGCGAACACAAGCAC	5' tpsB flank (repair DNA fragment)
TS2_tpsB_fw	GTGCTTGTGTTCGCCAAAGAGAATGGAGAGCAGAGCGAAAGGAG	3' tpsB flank (repair DNA fragment)

Primer	Sequence	Purpose
TS2_tpsB_rv	TAGACACCCGAACCAGCAGATG	3' tpsB flank (repair DNA fragment)
DIAG_tpsB_5'_fw	CAACCGCAACCGCTACTACTTC	Diagnostic PCR tpsB deletion
DIAG_tpsB_3'_rv	CCGGACCAAGGGATGCTAAAGA	Diagnostic PCR tpsB deletion
tpsC_2_fw	TCGCTGAAAAAGGTCGACGGGTTTTAGAGCTAGAAATAGCAAG	3' *tpsC* gRNA (target)
tpsC_2_rv	CCGTCGACCTTTTTCAGCGAGACGAGCTTACTCGTTTCG	5' *tpsC* gRNA (target)
TS1_tpsC_fw	TGCTCGAGTCTGAGTCTGAAGC	5' tpsC flank (repair DNA fragment)
TS1_tpsC_rv	GCAGCTCGAAGCATTGCAATTGAGAGACCGTTGGAAGGCTGAAC	5' tpsC flank (repair DNA fragment)
TS2_tpsC_fw	GTTCAGCCTTCCAACGGTCTCTCAATTGCAATGCTTCGAGCTGC	3' tpsC flank (repair DNA fragment)
TS2_tpsC_rv	AGCTGGAAGGCGATTGTAGGTT	3' tpsC flank (repair DNA fragment)
DIAG_tpsC_5'_fw	AATGAATGTGTGTGGGTGCTGC	Diagnostic PCR tpsC deletion
DIAG_tpsC_3'_rv	AAACTGGGAGCGATGCATGAAC	Diagnostic PCR tpsC deletion
mtdA_fw	GCTGGCAAGACAGCCAGCAGGTTTTAGAGCTAGAAATAGCAAG	3' mtdA gRNA (target)
mtdA_rv	CTGCTGGCTGTCTTGCCAGCGACGAGCTTACTCGTTTCG	5' mtdA gRNA (target)
GOI5_mtdA_fw	CGGTTTGTTTCGGTCTTACGGG	5' mtdA flank (repair DNA fragment)
XXGOI5_mtdA_rv	GGAGTGGTACCAATATAAGCCGGCGCGGTCGGATAGAAAATAATGT	5' mtdA flank (repair DNA fragment)
XXGOI3_mtdA_fw	CCGGCTTATATTGGTACCACTCCTGATTGAGGTAGAGATGAGTTTGGT	3' mtdA flank (repair DNA fragment)
GOI3_mtdA_rv	CTGCAACGTCACTTAGTGGCTG	3' mtdA flank (repair DNA fragment)
DIAG_mtdA_3'_rv	GCATGCTTGACGTACGGATTGT	Diagnostic PCR mtdA deletion
DIAG_mtdA_5'_fw	CCCCTTGATTTCTCTCCAGCCA	Diagnostic PCR mtdA deletion
mtdB1_fw	GAATTTGTCGCAAATCGTGGGTTTTAGAGCTAGAAATAGCAAG	3' mtdB gRNA (target)
mtdB1_rv	CCACGATTTGCGACAAATTCGACGAGCTTACTCGTTTCG	5' mtdB gRNA (target)
5_mtdB_fw	ATCAAGGGATGGAAGGGGTTGG	5' mtdB flank (repair DNA fragment)
5_ mtdB _rv	GGAGTGGTACCAATATAAGCCGGGCGGTGTAATTTACCTCTTTGTCGG	5' mtdB flank (repair DNA fragment)
3_ mtdB _fw	CCGGCTTATATTGGTACCACTCCTGGGAGGATGAAGGAGGAAGGA	3' mtdB flank (repair DNA fragment)
3_ mtdB _rv	AGGTGGCACATGTTCGGTATCA	3' mtdB flank (repair DNA fragment)
DIAG_MtdB_3'_rv	CGACCAGATCCTCGAAGGGCCA	Diagnostic PCR mtdB deletion
DIAG_MtdB_5'_fw	CTTGCGGAATTTGCGTGGCCAC	Diagnostic PCR mtdB deletion
mpdA_fw	CGATGAACTTGAGAATGTGGGTTTTAGAGCTAGAAATAGC	3' mpdA gRNA (target)
mpdA_rv	CCACATTCTCAAGTTCATCGGACGAGCTTACTCGTTTCGT	5' mpdA gRNA (target)
GOI5_mpdA_fw	TAGTCGCGAGGGAGTCAAGTTG	5' mpdA flank (repair DNA fragment)
NEW_GOI5_mpdA_rv	GGAGTGGTACCAATATAAGCCGGATTCCGAGTCGATCACCTGCAT	5' mpdA flank (repair DNA fragment)
XXGOI3_mpdA_fw	CCGGCTTATATTGGTACCACTCCAGTGGAAGTCTGATAGTAGAAGGGA	3' mpdA flank (repair DNA fragment)
GOI3_mpdA_rv	TTTGGATTGGCTTGGATTGGGC	3' mpdA flank (repair DNA fragment)

Primer	Sequence	Purpose
DIAG_mpdA_3'_rv	AATCAACCGGGACCATGACTGT	Diagnostic PCR mpdA deletion
DIAG_mpdA_5'_fw	CCGACATGGTGATTGCGTCTTC	Diagnostic PCR mpdA deletion
tpsA_KORE2_fw	CAAGAATTACATACCTATGAAGGACAAAGGGCGAGACTGGCTT	Complementation with different KORE (no repair) for SJS156
tpsA_KORE2_rv	CCTTCATAGGTATGTAATTCTTGGATTGTTCAACGGCCGAGGA	Complementation with different KORE (no repair) for SJS156
tpsB_KORE3_fw	TTTGTTCACAGTCCTCATTAAGGATGGAGAGCAGAGCGAAAGG	Complementation with different KORE (no repair) for SJS156
tpsB_KORE3_rv	CCTTAATGAGGACTGTGAACAAATGACTGCAGCTTTTTCCTTG	Complementation with different KORE (no repair) for SJS156
tpsC_KORE4_fw	AACACCGTTTACCCCCTTAAGGGCAATTGCAATGCTTCGAGCT	Complementation with different KORE (no repair) for SJS156
tpsC_KORE4_rv	CCCTTAAGGGGGTAAACGGTGTTAGAGACCGTTGGAAGGCTGA	Complementation with different KORE (no repair) for SJS156
mpdA_KORE5_fw	TCAGTCTATCCGTTTCTTGACGGAGTGGAAGTCTGATAGTAGA	Complementation with different KORE (no repair) for SJS156
mpdA_KORE5_rv	CCGTCAAGAAACGGATAGACTGATTGCTACTGTCGCAAACTGT	Complementation with different KORE (no repair) for SJS156
SJS_compl_tpsC_seq_rv	ACGTATTGCCATTCCGTCGGAG	sequence silent mutations tpsC gene
compl_tpsA_fw	CTCATCATCAATGAACACCGGCACG	Create complementation with 2 silent mutations in tpsA gene
compl_tpsA_rv	CGTGCCGGTGTTCATTGATGATGAG	Create complementation with 2 silent mutations in tpsA gene
seq_tpsA_fw	GCCGATCTCCTCACGCAGCATC	sequence silent mutations tpsA gene
seq_tpsA_rv	CGGTGGCCTGGTCAGTGGACTA	sequence silent mutations tpsA gene
compl_tpsB_fw	CAGTTTATCATCCATGAACACCGGG	Create complementation with 2 silent mutations in tpsB gene
compl_tpsB_rv	CCCGGTGTTCATGGATGATAAACTG	Create complementation with 2 silent mutations in tpsB gene
seq_tpsB_fw	AGACAAGGTCTCCTTCCCGGGC	sequence silent mutations tpsB gene
seq_tpsB_rv	TCCATGTCCTCTGGTGGCCTGG	sequence silent mutations tpsB gene
seq_mtdB_fw	ACCCGCATCGTGTCTCTCACCA	sequence silent mutations mtdB gene
seq_mtdB_rv	GTGACGACAGGCCAGGAGTCCT	sequence silent mutations mtdB gene
seq_mpdA_fw	CTCGTCGTCACCAGGCACGTTC	Create complementation with 2 silent mutations in mpdA gene
seq_mpdA_rv	CTCAGCAAGCCCCCAACAGTGG	Create complementation with 2 silent mutations in mpdA gene
mpdA_comsil_fw	CCAAAGTAGGCCGTTGTAGCATGGCTGGTGTTGACAGTGA	sequence silent mutations mpdA gene
mpdA_comsil_rv	CTACAACGGCCTACTTTGGACACTTCCGGGGCAAGAAGAT	sequence silent mutations mpdA gene
SJS_tpsC_complementationSilent_fw	GTGACTAGTCCACCACTGGAGAGGGAAGATTCGTATCCCC	Create complementation with 2 silent mutations in tpsC gene
SJS_tpsC_complementationSilent_rv	CTCCAGTGGTGGACTAGTCACATCTTTATCGGGATTGACT	Create complementation with 2 silent mutations in tpsC gene
compl3_mtdB_rv	GCGAGGGCAGCGTAGAGGAAACCGAAAGTGGTACGGGGGG	Create complementation with 2 silent mutations in mpdA gene
compl2_mtdB_fw	CCCCCCGTACCACTTTCGGTTTCCTCTACGCTGCCCTCGC	Create complementation with 2 silent mutations in mpdA gene

Table 7.4. Plasmids used in this study

Plasmid	Technical name	Gene	An# (gene)	Gene name	Target sequence	Reference
pFC332	pFC332	-	-	-	-	[46]
pTLL108.1	pTLL108.1	-	-	-	-	[29]
pTLL109.2	pTLL109.2	-	-	-	-	[29]
pFC332_*mtdA*-sgRNA	pVO1	NRRL3_04005	An15g05450	*mtdA*	GCTGGCAAGACAGCCAGCAG	This study
pFC332_*mtdB*-sgRNA	pSJS4	NRRL3_08606	An03g02430	*mtdB*	GAATTTGTCGCAAATCGTGG	This study
pFC332_*mpdA*-sgRNA	pVO2	NRRL3_05796	An02g05830	*mpdA*	CGATGAACTTGAGAATGTGG	This study
pFC332_*tpsA*-sgRNA	pSJS2	NRRL3_11571	An08g10510	*tpsA*	TCGCGGGTTGACGAAACAAT	This study
pFC332_*tpsB*-sgRNA	pSJS3	NRRL3_04893	An07g08710	*tpsB*	TTTGTCGTCCATGAACACCG	This study
pFC332_*tpsC*-sgRNA	pSJS4	NRRL3_00777	An14g02180	*tpsC*	TCGCTGAAAAAGGTCGACGG	This study
pFC332_KORE1-sgRNA	pTL71.1	-	-	KORE1	CCGGCTTATATTGGTACCACTCC	This study

Transformation techniques for the creation of compatible solute deficient knock-out strains

Protoplastation and subsequent transformation of fungal cells was performed according to a previously described PEG-mediated transformation protocol [41]. CRISPR/Cas9 mediated transformation was done essentially as described previously [29]. In short, each transformation used 2 µg of Cas9-sgRNA plasmid together with 0.5 µg of repair DNA. Transformed cells were incubated at 30 °C on selective MMS containing 200 µg ml^{-1} hygromycin for approximately 3 days (until colonies are visible). Transformants were inoculated on MM selection plates containing 100 µg ml^{-1} hygromycin. To allow loss of the Cas9-sgRNA plasmid, transformants were subsequently grown on MM without selection pressure. Finally, each transformant was grown on both MM and MM containing 100 µg ml^{-1} hygromycin, in order to verify whether the Cas9-sgRNA plasmid was lost when selection pressure was removed. Genomic DNA of transformants was subsequently isolated with a phenol-chloroform based protocol as described previously [41]. Diagnostic PCR was used to confirm deletion of the targeted genes. The presence of the silent point mutations in the complemented strains was confirmed by sequencing the PCR fragments.

The internal compatible solutes investigated with HPLC analyses

Conidia were harvested using PS buffer. All knock-out strains were analysed in biological triplicates. Spore suspension concentrations were determined with a Bio-Rad TC20 Cell Counter. A total of $2*10^8$ cracked conidia per sample were used for HPLC analysis. Conidial suspensions were centrifuged at 13000 rpm at 4°C for 15 minutes after which supernatant was removed. The pellet was immediately frozen in liquid nitrogen. Two metal beads (QIAGEN, 3 mm diameter) were added to the pellets and the tubes were subsequently loaded into a Tissuelyser II (QIAGEN). The cracking of the conidia was performed for 1 minute at 30 Hz. A total of 1 mL of miliQ was added to the crushed samples and subsequently heated in a water bath at ~95°C for 30 minutes. Samples were then centrifuged for 15 minutes at 13.000 rpm. Supernatant was filtered through a 0.2 µm Acrodisc filter and stored in -20°C for a maximum of one week. Samples were thawed and transferred to HPLC tubes and subsequently analysed by HPLC. Two sugar pack columns (Waters), installed in series, were used to analyse the samples. Pure compounds of trehalose, mannitol, glycerol, glucose, erythritol and arabitol were serially diluted and measured as a reference for each HPLC analysis. Compatible solute amounts were calculated by taking the area under the corresponding retention peak and comparing this area to the references.

Germination analyses of *A. niger* conidia using the oCelloScope

Conidia were used directly after harvesting. Spore solutions were counted and diluted to obtain $2 \cdot 10^4$ per well of a 96 wells suspension culture plate (Greiner bio-one, Cellstar 655185, www.gbo.com) in 150 µl NaPS (25 mM Na_2HPO_4/NaH_2PO_4 (pH 6.0), 2 mM $MgSO_4$) with 0.1 mM, 1 mM or 10 mM glucose, alanine, proline or argenine. All experiments were done using three biological replicates. Germination of the conidia was monitored at 28 °C using an oCelloScope imager (Biosense Solutions, www.biosense-solutions.dk) with UniExplorer software version 8.1.0.7682-RI2 as described in [34]. In short, objects were scanned every hour for 24 hours, starting 1 hour after inoculation to allow settling of the conidia. Conidial aggregates, and non-conidial objects at t = 1 h were manually removed from the data set and conidia were followed in time based on

their X and Y coordinates using the fast k-nearest neighbour (KNN) searching algorithm from the R package 'FNN'[43]. This was done from t = x to t = x+1 and vice versa. In addition, neighbour distance of an object was not allowed to exceed 27.5 µm (i.e. 50 pixels) between 2 adjacent time points. The lineage was discontinued if these conditions were no longer met. The objects were classified as resting or germinating conidia at t = 1 h, resting conidia had a surface area of < 150 pixels and circularity > 0.93. Germinating conidia had circularity ≤ 0.93 and had a surface are of > 150. Each sample followed 229-478 conidia, an average was calculated for each condition and listed as part of Table 7.S2. Two-way ANOVA and Tukey's multiple comparison tests were used for statistical analysis and were deemed significant if $p \leq 0.05$.

Modelling of germination kinetics

The asymmetric model [35] was used to describe germination (P) and germination time τ (h) as a function of time, (Eq. 1).

$$P = P_{max}\left(1 - \frac{1}{1+\left(\frac{t}{\tau}\right)^{d}}\right) \qquad \text{(Eq. 1).}$$

P_{max} is the maximal percentage of conidia that germinate (the asymptotic value of P at $t \rightarrow +\alpha$). Germination time τ (h) is the time at which $P = 0.5 \cdot P_{max}$, while d is a shape parameter that can be correlated to the heterogeneity of the population. A low d reflects a population where conidia have more variable individual germination times. To estimate the model parameters of the asymmetric model, three biological replicates (≥ 200 conidia per condition) were fitted together with the R package GrowthRates [44] using the Levenberg-Marquardt algorithm. Parameters were limited to P ≥ 0 and ≤ 120 %, τ ≥ 1 and ≤ 16, d ≥1 and ≤30 when fitting the model. Objects that had an object area > 300 pixels and that had decreased in size were excluded from the data set. Missing objects represent resting spores (R) that are lost during the analysis (i.e. that were no longer detected at t ≥ 2 h because the object had moved or was obscured for instance by germlings of other spores) before they germinated. Size and circularity data of all objects were used for the parameter estimation until the time point when hyphal growth started to obscure resting spores.

Heat treatment assays using a thermo cycler

Heat treatment assays were applied to test for changes in the heat resistance of conidia, see Figure 7.S5 for a detailed overview. The strains were confluently plated on MEA plates and subsequently grown for 8 days at 28°C unless noted otherwise. Measurements were done in biological triplicates. Freshly harvested conidia were diluted in PS buffer and spore suspension concentrations were measured using a Bio-Rad TC20™ automated cell counter. A total of $1*10^6$ conidia inside a volume of 100 µl PS buffer was used for each heat treatment assay. The heat treatment was applied in a thermocycler for 10 minutes at 55 °C, 56 °C, 57 °C or 58 °C. Controls were taken which were subjected to room temperature for 10 minutes. After heat treatment, the conidia were confluently plated on MEA containing 0.05% (v/v) Triton® X-100. Plates were incubated for five days at 28°C, after which pictures were taken. The number of colony forming units (CFUs) per plate is considered a readout of the amount of conidia that survived the heat treatment.

Heat inactivation experiments using a water bath

In order to further quantify the heat resistance, heat inactivation curves of selected knock-out strains were made. These measurements were done in biological triplicates. Freshly harvested conidia were diluted in PS and spore concentrations were measured using a Bio-Rad TC20™ automated cell counter. A volume of 19.8 mL of PS buffer inside an Erlenmeyer was pre-heated in a water bath (Julabo Corio c-bt27) to 54°C. A total volume of 200 µl spore suspension was added to obtain a final concentration of $1x10^7$ spores ml^{-1} inside each Erlenmeyer for the heat inactivation experiment. Samples were taken after 0, 2, 5, 10, 15, 20, 30 and 60 minutes of exposure to heat stress. The samples were serially diluted into 10^6, 10^5, 10^4 and 10^3 spores ml^{-1}, after which 100 µl of each dilution was inoculated on MEA containing 0.05% (v/v) Triton® X-100. Plates were incubated for seven days at 30 °C, after which the number of colony forming units (CFUs) per plate was counted. The results were used to calculate and subsequently plot inactivation curves based on a log-linear fit. The linear regression line in turn was used to calculate a decimal reduction value (D-value).

References

1. Dijksterhuis J. The fungal spore and food spoilage. Curr Opin Food Sci. 2017;17:68–74.

2. Snyder AB, Churey JJ, Worobo RW. Association of fungal genera from spoiled processed foods with physicochemical food properties and processing conditions. Food Microbiol. 2019;83:211–8.

3. Rico-Munoz E, Samson RA, Houbraken J. Mould spoilage of foods and beverages: Using the right methodology. Food Microbiol. 2019;81:51–62.

4. Wyatt TT, Wösten HAB, Dijksterhuis J. Fungal spores for dispersion in space and time. Adv Appl Microbiol. 2013;85:43–91.

5. Abu-Dieyeh MH, Barham R, Abu-Elteen K, Al-Rashidi R, Shaheen I. Seasonal variation of fungal spore populations in the atmosphere of Zarqa area, Jordan. Aerobiologia (Bologna). 2010;26:263–76.

6. Guinea J, Peláez T, Alcalá L, Bouza E. Outdoor environmental levels of *Aspergillus* spp. conidia over a wide geographical area. Med Mycol. 2006;44:349–56.

7. Hagiwara D, Sakai K, Suzuki S, Umemura M, Nogawa T, Kato N, et al. Temperature during conidiation affects stress tolerance, pigmentation, and trypacidin accumulation in the conidia of the airborne pathogen *Aspergillus fumigatus*. PLoS One. 2017;12:e0177050.

8. van den Brule T, Punt M, Teertstra W, Houbraken J, Wösten H, Dijksterhuis J. The most heat-resistant conidia observed to date are formed by distinct strains of *Paecilomyces variotii*. Environ Microbiol. 2019;22:986–99.

9. Punt M, van den Brule T, Teertstra WR, Dijksterhuis J, den Besten HMW, Ohm RA, et al. Impact of maturation and growth temperature on cell-size distribution, heat-resistance, compatible solute composition and transcription profiles of *Penicillium roqueforti* conidia. Food Res Int. 2020;136:109287.

10. Nguyen Van Long N, Vasseur V, Coroller L, Dantigny P, Le Panse S, Weill A, et al. Temperature, water activity and pH during conidia production affect the physiological state and germination time of *Penicillium* species. Int J Food Microbiol. 2017;241:151–60.

11. Chin JP, Megaw J, Magill CL, Nowotarski K, Williams JP, Bhaganna P, et al. Solutes determine the temperature windows for microbial survival and growth. Proc Natl Acad Sci U S A. 2010;107:7834–40.

12. Rangel DEN, Braga GUL, Fernandes ÉKK, Keyser CA, Hallsworth JE, Roberts DW. Stress tolerance and virulence of insect-pathogenic fungi are determined by environmental conditions during conidial formation. Curr Genet. 2015;61:383–404.

13. Earl Kang S, Celia BN, Bensasson D, Momany M. Sporulation environment drives phenotypic variation in the pathogen *Aspergillus fumigatus*. G3 Genes|Genomes|Genetics. 2021;11:jkab208.

14. Hallsworth JE, Magan N. Culture age, temperature, and pH affect the polyol and trehalose contents of

fungal propagules. Appl Environ Microbiol. 1996;62:2435–42.

15. Teertstra WR, Tegelaar M, Dijksterhuis J, Golovina EA, Ohm RA, Wösten HAB. Maturation of conidia on conidiophores of *Aspergillus niger*. Fungal Genet Biol. 2017;98:61–70.

16. Dijksterhuis J. Fungal spores : Highly variable and stress-resistant vehicles for distribution and spoilage. J Food Microbiol. 2019;81:2–11.

17. Dijksterhuis J, de Vries RP. Compatible solutes and fungal development. Biochem J. 2006;399:e3-5.

18. Ruijter GJG, Visser J, Rinzema A. Polyol accumulation by *Aspergillus oryzae* at low water activity in solid-state fermentation. Microbiology. 2004;150:1095–101.

19. Fillinger S, Chaveroche MK, van Dijck P, de Vries R, Ruijter G, Thevelein J, et al. Trehalose is required for the acquisition of tolerance to a variety of stresses in the filamentous fungus *Aspergillus nidulans*. Microbiology. 2001;147:1851–62.

20. Ruijter GJG, Bax M, Patel H, Flitter SJ, Van De Vondervoort PJI, De Vries RP, et al. Mannitol is required for stress tolerance in *Aspergillus niger* conidiospores. Eukaryot Cell. 2003;2:690–8.

21. Svanström A, Melin P. Intracellular trehalase activity is required for development, germination and heat-stress resistance of *Aspergillus niger* conidia. Res Microbiol. 2013;164:91–9.

22. Svanström Å, Van Leeuwen MR, Dijksterhuis J, Melin P. Trehalose synthesis in *Aspergillus niger*: Characterization of six homologous genes, all with conserved orthologs in related species. BMC Microbiol. 2014;14:1–16.

23. D'Enfert C, Fontaine T. Molecular characterization of the *Aspergillus nidulans treA* gene encoding an acid trehalase required for growth on trehalose. Mol Microbiol. 1997;24:203–16.

24. van Leeuwen MR, Krijgsheld P, Bleichrodt R, Menke H, Stam H, Stark J, et al. Germination of conidia of *Aspergillus niger* is accompanied by major changes in RNA profiles. Stud Mycol. 2013;74:59–70.

25. Wolschek MF, Kubicek CP. The filamentous fungus *Aspergillus niger* contains two "differentially regulated" trehalose-6-phosphate synthase-encoding genes, *tpsA* and *tpsB*. J Biol Chem. 1997;272:2729–35.

26. Witteveen CFB, Visser J. Polyol pools in *Aspergillus niger*. FEMS Microbiol Lett. 1995;134:57–62.

27. Aguilar-Osorio G, van Kuyk PA, Seiboth B, Blom D, Solomon PS, Vinck A, et al. Spatial and developmental differentiation of Mannitol dehydrogenase and Mannitol-1-phosphate dehydrogenase in *Aspergillus niger*. Eukaryot Cell. 2010;9:1398–402.

28. Hayer K, Stratford M, Archer DB. Structural features of sugars that trigger or support conidial germination in the filamentous fungus *Aspergillus niger*. Appl Environ Microbiol. 2013;79:6924–31.

29. van Leeuwe TM, Arentshorst M, Ernst T, Alazi E, Punt PJ, Ram AFJ. Efficient marker free CRISPR/Cas9

genome editing for functional analysis of gene families in filamentous fungi. Fungal Biol Biotechnol. 2019;6:1–13.

30. Hult K, Veide A, Gatenbeck S. The distribution of the NADPH regenerating mannitol cycle among fungal species. Arch Microbiol. Germany; 1980;128:253–5.

31. Argüelles C. Physiological roles of trehalose in bacteria and yeasts: a comparative analysis. Arch Microbiol. 2000;174:217–24.

32. Krijgsheld P, Bleichrodt R, van Veluw GJ, Wang F, Müller WH, Dijksterhuis J, et al. Development in *Aspergillus*. Stud Mycol. 2013;74:1–29.

33. Thevelein JM. Regulation of trehalose mobilization in fungi. Microbiol Rev. 1984;48:42–59.

34. Ijadpanahsaravi M, Punt M, Wösten HAB, Teertstra WR. Minimal nutrient requirements for induction of germination of *Aspergillus niger* conidia. Fungal Biol. 2021;125:231–8.

35. Dantigny P, Nanguy SPM, Judet-Correia D, Bensoussan M. A new model for germination of fungi. Int J Food Microbiol. 2011;146:176–81.

36. Wang F, Sethiya P, Hu X, Guo S, Chen Y, Li A, et al. Transcription in fungal conidia before dormancy produces phenotypically variable conidia that maximize survival in different environments. Nat Microbiol. 2021;6:1066–81.

37. Earl Kang S, Celia BN, Bensasson D, Momany M. Sporulation environment drives phenotypic variation in the pathogen *Aspergillus fumigatus*. G3 Genes|Genomes|Genetics. 2021;

38. D'Enfert C, Bonini BM, Zapella PDA, Fontalne T, Da Silva AM, Terenzi HF. Neutral trehalases catalyse intracellular trehalose breakdown in the filamentous fungi *Aspergillus nidulans* and *Neurospora crassa*. Mol Microbiol. 1999;32:471–83.

39. Van Leeuwen MR, Van Doorn TM, Golovina EA, Stark J, Dijksterhuis J. Water- and air-distributed conidia differ in sterol content and cytoplasmic microviscosity. Appl Environ Microbiol. 2010;76:366–9.

40. Dijksterhuis J, Nijsse J, Hoekstra FA, Golovina EA. High viscosity and anisotropy characterize the cytoplasm of fungal dormant stress-resistant spores. Eukaryot Cell. 2007;6:157–70.

41. Arentshorst M, Ram AFJ, Meyer V. Using non-homologous end-joining-deficient strains for functional gene analyses in filamentous fungi. Methods Mol Biol. 2012;835:133–50.

42. Park J, Hulsman M, Arentshorst M, Breeman M, Alazi E, Lagendijk EL, et al. Transcriptomic and molecular genetic analysis of the cell wall salvage response of *Aspergillus niger* to the absence of galactofuranose synthesis. Cell Microbiol. 2016;18:1268–84.

43. Beygelzimer A, Kakadet S, Langford J, Arya S, Mount D, Li S. FNN, R Package Version 1.1.3. 2019;

44. Petzoldt T. GrowtRates, R package version 0.8.1. 2019.

45. Bos CJ, Debets AJM, Swart K, Huybers A, Kobus G, Slakhorst SM. Genetic analysis and the construction of master strains for assignment of genes to six linkage groups in *Aspergillus niger*. Curr Genet. 1988;14:437–43.

46. Nødvig CS, Nielsen JB, Kogle ME, Mortensen UH. A CRISPR-Cas9 system for genetic engineering of filamentous fungi. PLoS One. 2015;10:e0133085.

Additional files

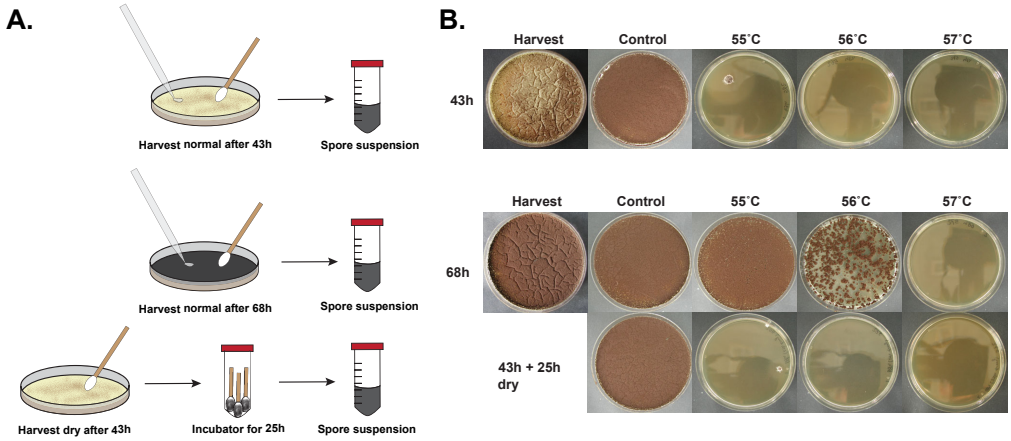

Figure 7.S1. Heat resistance increase no longer observed after 43h conidia detached from the mycelium. Three types of conidia were tested for their heat resistance: 43h conidia, 68h conidia and 43h conidia harvested dry and subsequently incubated for an additional 25 hours. **A.** The methodology of the experiment. The 43h and 68h conidia were harvested in PS buffer as normal. However, some 43h conidia were harvested dry using sterilized cotton buds and subsequently stored inside falcon tubes, and returned to the 28°C incubator for another 25 hours. After 25 hours PS buffer was added and the heat resistance assay was performed as normal. **B.** The heat resistance results, tested with the heat treatment assay (Figure 7.S5). The 43h conidia do not survive 10 minutes at 55 °C or 56 °C, whereas 68h conidia do. When 43h conidia are dry harvested and kept inside a falcon tube, returned to the incubator for another 25h and subsequently tested for heat resistance. No increase in heat resistance is observed for dry harvested conidia if compared to the 43h conidia. These results show that maturation, at least in heat resistance, does no longer occur after conidia are detached, by dry harvesting, from the mycelium.

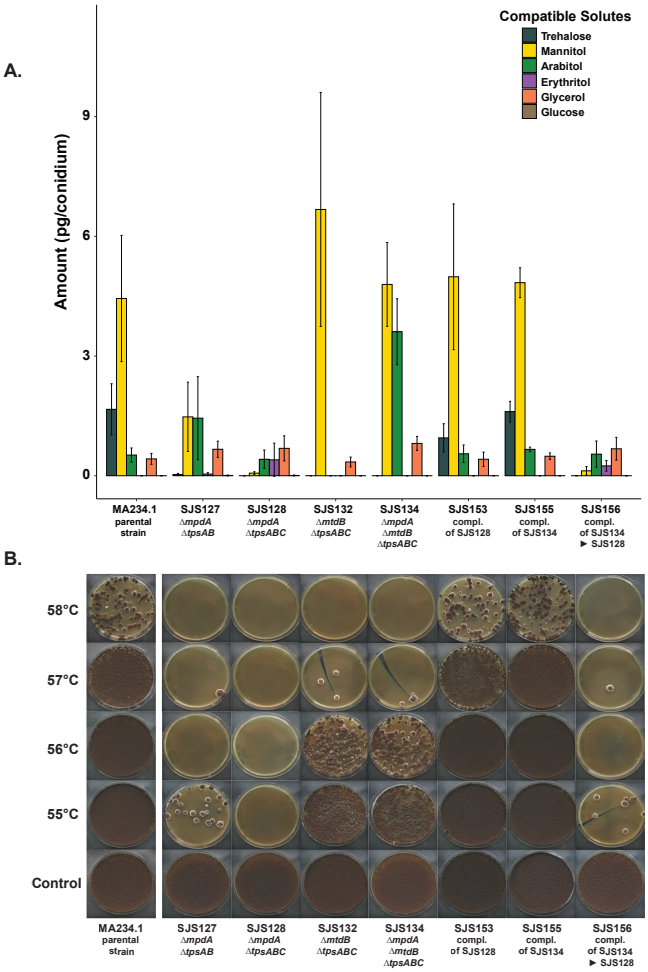

Figure 7.S2. Internal compatible solute composition and heat resistance of conidia from *A. niger* mannitol knock-out strains. Conidia were freshly harvested from MEA plates grown for 8 days at 28°C. Measurements were performed in biological triplicates. **A.** Internal compatible solute composition of conidia from mannitol knock-out strains lacking genes in the mannitol cycle. Only the deletion of the *mpdA* gene resulted in a change of internal sugar composition inside conidia of *A. niger*. Strain VO2 (***Δ****mpdA*) contains less mannitol and more trehalose as has been observed before [20]. The internal compatible solute composition of the strain SJS139 (*mpdA, mtdAB*) was the same as VO2 (*mpdA*). As such, no effect of both *mtdA* or *mtdB* deletion on compatible solute composition of conidia was seen in these knock-out strains. **B.** Heat treatments were applied for 10 minutes to 10^6 conidia (Figure 7.S5). After heat treatment, conidia were plated on plates containing MEA+0.05% triton x-100. Plates were grown for 5 days after which the pictures were made as shown above. The Δ*mpdA* mutation has the largest effect on the heat resistance of *A. niger* conidia as the CFUs is less than 100 when heat stress of 57°C is applied. The strain SJS139, in which *mpdA* and both mannitol dehydrogenases *mtdA* and *mtdB* have been knocked out, is comparable in heat resistance to the Δ*mpdA* single knock-out strain, suggesting that *mtdA* and *mtdB* do not significantly contribute to the heat resistance of *A. niger* conidia.

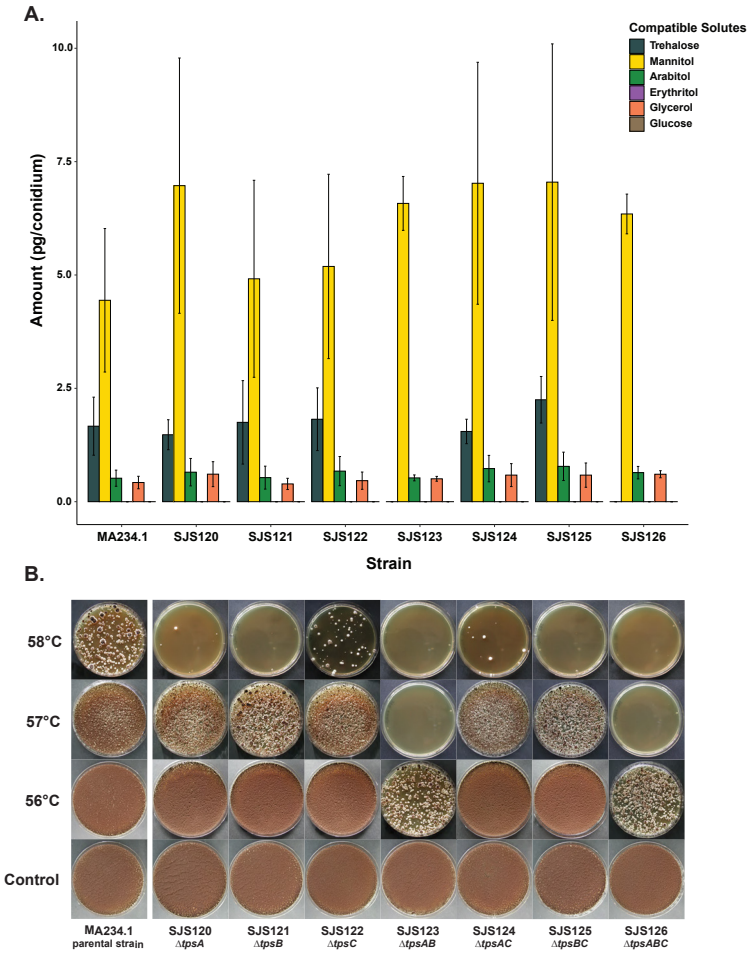

Figure 7.S3. Internal compatible solute composition and heat resistance of conidia from *A. niger* trehalose knock-out strains. Conidia were freshly harvested from MEA plates grown for 8 days at 28°C. Measurements were performed in biological triplicates. **A.** Internal compatible solute composition of conidia from trehalose knock-out strains as determined by HPLC analysis. Conidia from strains SJS123 (***Δ**tpsAB*) and SJS126 (***Δ**tpsABC*) were significantly impacted in their internal compatible solute composition, as they produced no measurable amount of trehalose. No significant increase in another type of sugar was measured in these two strains. **B.** Heat treatments were applied for 10 minutes to 10^6 conidia (Figure 7.S5). After heat treatments conidia were plated on plates containing MEA+0.05% triton x-100. Plates were grown for 5 days after which the pictures were made as shown above. All conidia from knock-out strains lacking *tps* genes showed at least a slight decrease in heat resistance. However, the largest drop in heat resistance was observed in strains SJS123 (***Δ**tpsAB*) and SJS126 (***Δ**tpsABC*). This drop in conidial heat resistance corresponds with the decrease and overall absence of trehalose inside these conidia. Overall, a clear link is seen between internal trehalose concentration and conidial heat resistance.

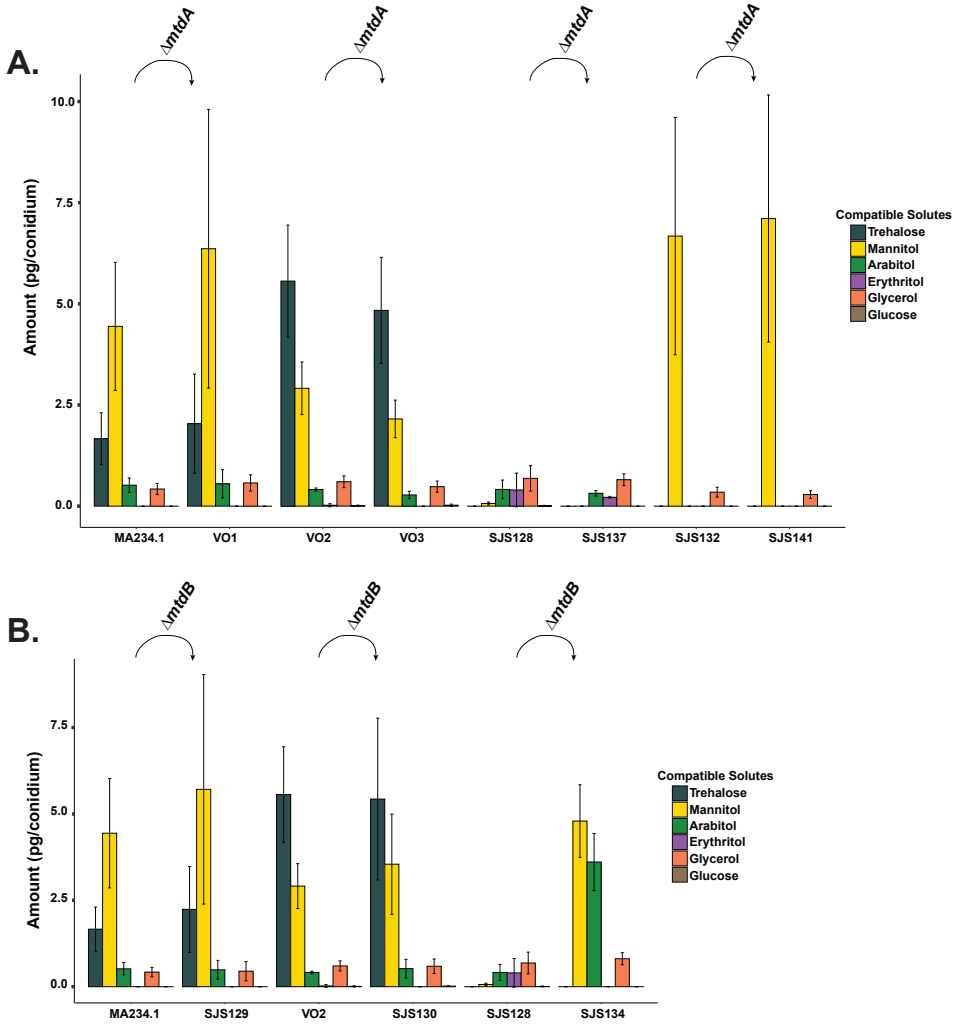

Figure 7.S4. The *mtdA* gene does not have an impact on internal compatible solute composition of conidia. The genes *mtdA* and *mtdB* have been deleted in many different backgrounds. Here we give an overview of the effect of the individual mutations on the internal compatible solute profiles of conidia. In all cases, the parental strain without the *mtdA* or *mtdB* mutation is given first, followed by the strain in which the *mtdA* or *mtdB* gene is additionally knocked-out. **A.** Here the effect of the *mtdA* deletion is visualized. When comparing *ΔmtdA* strains with their respective parental strains, no significant changes in compatible solute profiles were found in any of the knock-out strains where an extra *ΔmtdA* deletion was made. **B.** Here the effect of the *mtdB* deletion is visualized. Initially, in single double or triple knock-out strains the absence of the *mtdB* gene does not show any significant impact on the compatible solute profiles. However, when adding the *ΔmtdB* deletion to the strain SJS128 (*ΔmpdA*, *ΔtpsABC*) therefore becoming strain SJS134 (*ΔmpdA, ΔmtdB, ΔtpsABC*) a clear change in compatible solute profile is seen.

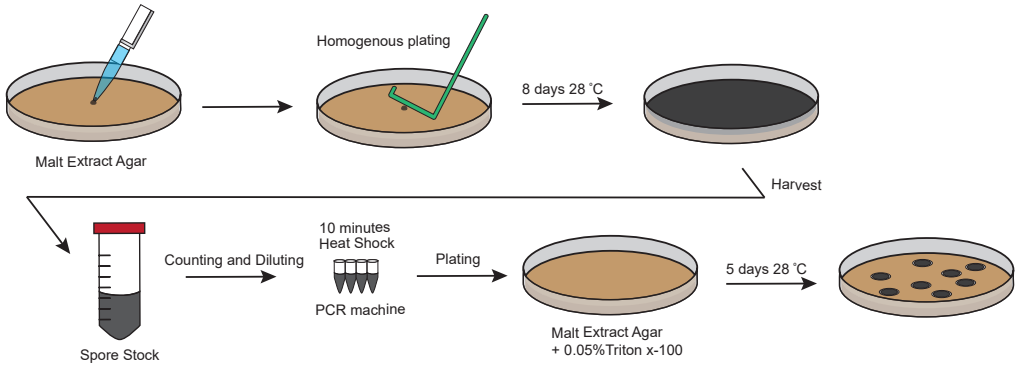

Figure 7.S5. Heat treatment assay protocol. All strains were plated homogenously and subsequently grown on MEA for 8 days (or other amounts of time in days/hours depending on the experiment) at 28°C. Conidia were harvested in PS buffer and subsequently counted using a Bio-Rad Automated Cell Counter. A total volume of 100 µl with $1*10^6$ conidia were heat treated per PCR tube in a thermocycler for 10 minutes. After heat treatment the 100 µl is plated homogenously on MEA + 0.05% Triton X-100 and grown for 5 days at 28°C after which CFUs are counted and pictures were taken.

Table 7.S1. Colony forming units of *A. niger* conidia from knock-out strains plated on MEA.

Strain	Average (CFUs)	Stdev (CFUs)
N402	107	±19
SJS126 (*ΔtpsABC*)	107	±19
SJS128 (*ΔmpdA, ΔtpsABC*)	88	±8
SJS132 (*ΔmtdB, ΔtpsABC*)	92	±11
SJS134 (*ΔmpdA, ΔmtdB, ΔtpsABC*)	73	±17

Conidia were counted with a Bio-Rad TC20™ automated cell counter and diluted until 100 conidia/100µl and subsequently confluently plated. This experiment was done in biological triplicates. No significantly lower amount ($p<0.05$ student t-test) of colonies were formed when conidia from knock-out strains were plated and compared to wild-type conidia of strain N402.

Table 7.S2. Germination kinetics of conidia of *Aspergillus niger* strains with altered internal compatible solute compositions. Maximum germination or swelling percentage after 24 hours (P_{max}), the time in hours until 50% germination/swelling (theta) and the heterogeneity parameter between conidia (d) are given with their corresponding confidence interval in between brackets.

Swelling							
Strain name	**Genotype**	**Treatment**	**Pmax (%)**	**Theta (hours)**	**d**	**Missing**	**Total**
MA234.1	*ΔkusA*	0.1 mM Ala	NA	NA	NA	8	309
N402	Wild type	0.1 mM Ala	2.22 [-1.65;6.08]	15.92 [-14.99;46.8]	2 [-0.79;4.79]	5	326
N402 38h	Young conidia of wild type	0.1 mM Ala	6.08 [-1.45;13.61]	20 [7.81; 32.19]	4.55 [-0.17; 9.28]	12	370
SJS128	*ΔmpdA*, *ΔtpsABC*	0.1 mM Ala	1.88 [-2.78;6.54]	20 [-12.56; 52.56]	3.24 [-2.34; 8.82]	7	497
SJS153	Complementation of SJS128 to MA234.1 (*tpsA* T258C, G273A)	0.1 mM Ala	1.37 [-0.08;2.81]	5.06 [-3.54; 13.67]	2 [-4.53; 8.53]	8	329
MA234.1	*ΔkusA*	0.1 mM Arg	4.23 [3.06;5.39]	5.83 [3.37; 8.29]	2 [0.5; 3.5]	7	359
N402	Wild type	0.1 mM Arg	2.5 [-2.58;7.58]	20 [-0.95; 40.95]	4.31 [-2.79; 11.4]	9	396
N402 38h	Young conidia of wild type	0.1 mM Arg	32.62 [3.31;61.93]	20 [2.07; 37.92]	2.03 [0.99; 3.08]	29	362
SJS128	*ΔmpdA*, *ΔtpsABC*	0.1 mM Arg	6.36 [5.18;7.54]	13.16 [11.56; 14.76]	5.6 [2.5; 8.71]	28	500
SJS153	Complementation of SJS128 to MA234.1 (*tpsA* T258C, G273A)	0.1 mM Arg	3.48 [0.18;6.77]	14.81 [4.19; 25.43]	3.44 [-1.03; 7.91]	12	353
MA234.1	*ΔkusA*	0.1 mM Glucose	3.65 [0.88;6.41]	13.84 [1.52; 26.15]	2 [0.53; 3.47]	16	356
N402	Wild type	0.1 mM Glucose	5.28 [0.38;10.17]	5.81 [-2.42; 14.04]	2 [-3.06; 7.06]	24	348
N402 38h	Young conidia of wild type	0.1 mM Glucose	8.37 [2.96;13.78]	11.77 [3.58; 19.96]	2.48 [0.17; 4.8]	10	353
SJS128	*ΔmpdA*, *ΔtpsABC*	0.1 mM Glucose	0.99 [-0.1;2.09]	17.65 [8.44; 26.86]	5.54 [-3.33; 14.41]	10	464
SJS153	Complementation of SJS128 to MA234.1 (*tpsA* T258C, G273A)	0.1 mM Glucose	2.96 [0.13;5.78]	13.39 [-1.84; 28.63]	2 [0.06; 3.94]	16	396
MA234.1	*ΔkusA*	0.1 mM Pro	7.98 [6.06;9.9]	12.86 [10.68; 15.04]	4.86 [1.79; 7.93]	21	361
N402	Wild type	0.1 mM Pro	6.59 [3.58;9.61]	13.22 [5.99; 20.44]	2 [1.05; 2.95]	9	374
N402 38h	Young conidia of wild type	0.1 mM Pro	20.75 [15.15;26.36]	13.23 [10.56; 15.9]	4.04 [1.85; 6.23]	43	344
SJS128	*ΔmpdA*, *ΔtpsABC*	0.1 mM Pro	34.48 [30.54;38.43]	9.22 [8.12; 10.31]	4.4 [2.57; 6.22]	66	445
SJS153	Complementation of SJS128 to MA234.1 (*tpsA* T258C, G273A)	0.1 mM Pro	10.49 [1.84;19.14]	14.28 [2.99; 25.56]	2.56 [0.22; 4.91]	20	340

Strain name	Genotype	Treatment	Pmax (%)	Theta (hours)	d	Missing	Total
MA234.1	*ΔkusA*	1 mM Ala	13.8 [12.14;15.46]	10.86 [9.62; 12.1]	3.51 [2.54; 4.48]	19	324
N402	Wild type	1 mM Ala	17.52 [13.59;21.45]	10.91 [8.23; 13.6]	2.55 [1.61; 3.49]	27	388
N402 38h	Young conidia of wild type	1 mM Ala	16.35 [3.88;28.82]	20 [9; 30.99]	2.91 [1.45; 4.37]	23	349
SJS128	*ΔmpdA*, *ΔtpsABC*	1 mM Ala	29.9 [27.88;31.93]	10.12 [9.48; 10.77]	4.93 [3.72; 6.15]	56	477
SJS153	Complementation of SJS128 to MA234.1 (*tpsA* T258C, G273A)	1 mM Ala	16.06 [11.64;20.47]	13 [9.57; 16.44]	2.73 [1.71; 3.75]	28	353
MA234.1	*ΔkusA*	1 mM Arg	11.03 [3.85;18.21]	16.09 [8.33; 23.84]	3.29 [0.89; 5.7]	9	272
N402	Wild type	1 mM Arg	12.88 [-5.44;31.19]	20 [-2.06; 42.06]	2.68 [0.27; 5.1]	11	386
N402 38h	Young conidia of wild type	1 mM Arg	21.3 [13.48;29.12]	12.09 [8.3; 15.88]	3.64 [0.9; 6.37]	37	292
SJS128	*ΔmpdA*, *ΔtpsABC*	1 mM Arg	13.18 [9.95;16.41]	12.56 [10.29; 14.83]	4.66 [1.7; 7.63]	51	510
SJS153	Complementation of SJS128 to MA234.1 (*tpsA* T258C, G273A)	1 mM Arg	11.25 [4.82;17.67]	20 [11.16; 28.84]	2.69 [1.72; 3.66]	8	356
MA234.1	*ΔkusA*	1 mM Glucose	5.97 [2.93;9.01]	7.07 [2.13; 12]	2.25 [-0.65; 5.16]	8	322
N402	Wild type	1 mM Glucose	5.49 [1.65;9.32]	7.83 [0.49; 15.17]	2.2 [-1.16; 5.56]	7	311
N402 38h	Young conidia of wild type	1 mM Glucose	4.89 [0.47;9.31]	6.39 [-2.17; 14.94]	2 [-2.49; 6.49]	4	344
SJS128	*ΔmpdA*, *ΔtpsABC*	1 mM Glucose	0.54 [0.34;0.74]	3.49 [0.93; 6.05]	2 [-1.03; 5.03]	12	487
SJS153	Complementation of SJS128 to MA234.1 (*tpsA* T258C, G273A)	1 mM Glucose	3.77 [2.84;4.7]	5.31 [3.37; 7.25]	3.23 [-0.51; 6.96]	7	370
MA234.1	*ΔkusA*	1 mM Pro	71.89 [69.84;73.95]	5.69 [5.47; 5.91]	4.27 [3.59; 4.94]	20	321
N402	Wild type	1 mM Pro	76.37 [73.18;79.55]	6.24 [5.91; 6.56]	4.67 [3.58; 5.77]	22	280
N402 38h	Young conidia of wild type	1 mM Pro	80.63 [59.95;101.31]	13.72 [10.67; 16.77]	3.04 [1.96; 4.12]	37	267
SJS128	*ΔmpdA*, *ΔtpsABC*	1 mM Pro	85.13 [80.44;89.82]	6.97 [6.52; 7.43]	4.57 [3.28; 5.86]	14	427
SJS153	Complementation of SJS128 to MA234.1 (*tpsA* T258C, G273A)	1 mM Pro	73.76 [70.71;76.8]	6.23 [5.91; 6.55]	4.68 [3.59; 5.77]	21	315
MA234.1	*ΔkusA*	10 mM Ala	72.81 [69.25;76.37]	4.83 [4.46; 5.21]	3.37 [2.52; 4.22]	22	250
N402	Wild type	10 mM Ala	69.55 [66.12;72.98]	6.25 [5.85; 6.65]	4.07 [3.05; 5.09]	23	266
N402 38h	Young conidia of wild type	10 mM Ala	56.62 [16.74;96.5]	10.37 [0.89; 19.85]	2 [0; 4]	21	183
SJS128	*ΔmpdA*, *ΔtpsABC*	10 mM Ala	82.29 [77.12;87.46]	8.54 [7.94; 9.13]	3.83 [2.99; 4.66]	25	353
SJS153	Complementation of SJS128 to MA234.1 (*tpsA* T258C, G273A)	10 mM Ala	77.32 [75.56;79.07]	5.82 [5.64; 6]	3.82 [3.38; 4.26]	23	271

Strain name	Genotype	Treatment	Pmax (%)	Theta (hours)	d	Missing	Total
MA234.1	*ΔkusA*	10 mM Arg	32.95 [4.39;61.5]	20 [5.79; 34.21]	2.52 [1.17; 3.87]	11	277
N402	Wild type	10 mM Arg	20.02 [9.17;30.88]	20 [13.9; 26.1]	3.87 [2.27; 5.47]	12	276
N402 38h	Young conidia of wild type	10 mM Arg	40.33 [33.06;47.61]	14.12 [12.29; 15.95]	3.91 [2.7; 5.13]	33	245
SJS128	*ΔmpdA*, *ΔtpsABC*	10 mM Arg	23.68 [17.43;29.94]	16.41 [14.13; 18.7]	5.19 [2.9; 7.49]	6	219
SJS153	Complementation of SJS128 to MA234.1 (*tpsA* T258C, G273A)	10 mM Arg	32.47 [-17.83;82.77]	20 [-8.36; 48.36]	2.23 [0.19; 4.27]	10	289
MA234.1	*ΔkusA*	10 mM Glucose	46.11 [42.82;49.4]	4.35 [3.81; 4.89]	3.18 [1.98; 4.38]	25	313
N402	Wild type	10 mM Glucose	59.06 [56.76;61.36]	4.75 [4.47; 5.04]	4.21 [3.22; 5.19]	21	286
N402 38h	Young conidia of wild type	10 mM Glucose	12.58 [7.37;17.79]	5.49 [1.95; 9.03]	2 [-0.38; 4.38]	32	281
SJS128	*ΔmpdA*, *ΔtpsABC*	10 mM Glucose	14.91 [9.43;20.38]	9.75 [5.11; 14.39]	2.06 [0.87; 3.26]	38	458
SJS153	Complementation of SJS128 to MA234.1 (*tpsA* T258C, G273A)	10 mM Glucose	40.98 [36.26;45.7]	4.67 [3.82; 5.52]	4.06 [1.27; 6.84]	26	229
MA234.1	*ΔkusA*	10 mM Pro	91.97 [85.26;98.69]	5.31 [4.74; 5.89]	3.33 [2.16; 4.5]	16	288
N402	Wild type	10 mM Pro	98.02 [82.39;113.64]	4.14 [2.96; 5.32]	2 [0.84; 3.16]	10	237
N402 38h	Young conidia of wild type	10 mM Pro	54.93 [46.94;62.92]	9.6 [8.17; 11.03]	3.82 [2.16; 5.49]	51	270
SJS128	*ΔmpdA*, *ΔtpsABC*	10 mM Pro	89.86 [83.88;95.84]	6.67 [6.12; 7.23]	3.91 [2.69; 5.12]	18	472
SJS153	Complementation of SJS128 to MA234.1 (*tpsA* T258C, G273A)	10 mM Pro	93.45 [88.98;97.93]	5.28 [4.91; 5.64]	3.85 [2.86; 4.84]	17	298
MA234.1	*ΔkusA*	NaPS	0.17 [-0.08;0.41]	19.96 [13.6; 26.31]	15.73 [-44.8; 76.26]	6	325
N402	Wild type	NaPS	3.99 [-2.07;10.04]	10.41 [-10.08; 30.91]	2 [-2.29; 6.29]	3	252
N402 38h	Young conidia of wild type	NaPS	8.51 [0.58;16.44]	20 [6.1; 33.9]	2.8 [1.12; 4.49]	5	349
SJS128	*ΔmpdA*, *ΔtpsABC*	NaPS	0.18 [0.1;0.27]	10.97 [5.91; 16.03]	29.97 [-120.49; 180.44]	10	492
SJS153	Complementation of SJS128 to MA234.1 (*tpsA* T258C, G273A)	NaPS	1.69 [-0.72;4.1]	11.64 [-6.81; 30.09]	2.38 [-2.4; 7.17]	5	331
Germ tube formation							
Strain name	**Genotype**	**treatment**	**Pmax (%)**	**Theta (hours)**	**d**	**Missing**	**Total**
MA234.1	*ΔkusA*	0.1 mM Ala	NA	NA	NA	8	309
N402	Wild type	0.1 mM Ala	1.75 [-3.29; 6.79]	20 [-10.99; 50.99]	4.1 [-5.2; 13.39]	5	326
N402 38h	Young conidia of wild type	0.1 mM Ala	5.52 [-0.79; 11.82]	20 [9.44; 30.56]	4.91 [-0.02;9.85]	12	370

Strain name	Genotype	treatment	Pmax (%)	Theta (hours)	d	Missing	Total
SJS128	*ΔmpdA*, *ΔtpsABC*	0.1 mM Ala	1.88 [-2.78; 6.54]	20 [-12.56; 52.56]	3.24 [-2.34; 8.82]	7	497
SJS153	Complementation of SJS128 to MA234.1 (*tpsA* T258C, G273A)	0.1 mM Ala	1.45 [-0.41; 3.31]	6.39 [-5.75; 18.53]	2 [-4.36;8.36]	8	329
MA234.1	*ΔkusA*	0.1 mM Arg	2.31 [1.79; 2.84]	3.27 [1.72; 4.83]	2 [0.04; 3.96]	7	359
N402	Wild type	0.1 mM Arg	1.89 [-4.19; 7.98]	20 [-43.91; 83.91]	2.04 [-1.71; 5.79]	9	396
N402 38h	Young conidia of wild type	0.1 mM Arg	16.4 [10.64; 22.16]	14.23 [10.55; 17.92]	3.73 [1.62; 5.84]	29	362
SJS128	*ΔmpdA*, *ΔtpsABC*	0.1 mM Arg	5.84 [4.51; 7.16]	14.33 [12.54; 16.13]	6.68 [2.04;11.32]	28	500
SJS153	Complementation of SJS128 to MA234.1 (*tpsA* T258C, G273A)	0.1 mM Arg	3.08 [-4.42; 10.58]	20 [-11.87; 51.87]	3.25 [-2.25; 8.76]	12	353
MA234.1	*ΔkusA*	0.1 mM Glucose	1.14 [0.75; 1.53]	11.09 [7.94; 14.23]	5.77 [-1.99; 13.53]	16	356
N402	Wild type	0.1 mM Glucose	4.94 [-1.28; 11.16]	8.24 [-6.14; 22.62]	2 [-2.73; 6.73]	24	348
N402 38h	Young conidia of wild type	0.1 mM Glucose	4.07 [2.29; 5.85]	12.31 [8.3; 16.32]	4.85 [-1.09; 10.79]	10	353
SJS128	*ΔmpdA*, *ΔtpsABC*	0.1 mM Glucose	0.91 [-1.57; 3.38]	20 [-8.09; 48.09]	4.31 [-5.23; 13.85]	10	464
SJS153	Complementation of SJS128 to MA234.1 (*tpsA* T258C, G273A)	0.1 mM Glucose	2.83 [-0.79; 6.46]	17.61 [-6.45; 41.67]	2 [0.24; 3.76]	16	396
MA234.1	*ΔkusA*	0.1 mM Pro	7.47 [4.44; 10.49]	16.22 [12.73; 19.72]	5.23 [1.55; 8.91]	21	361
N402	Wild type	0.1 mM Pro	7.91 [-0.03; 15.86]	20 [2.81; 37.19]	2.4 [0.94; 3.86]	9	374
N402 38h	Young conidia of wild type	0.1 mM Pro	17.84 [11.47; 24.2]	14.42 [11.14; 17.7]	4.63 [1.33; 7.93]	43	344
SJS128	*ΔmpdA*, *ΔtpsABC*	0.1 mM Pro	28.56 [25.96; 31.16]	12.22 [11.42; 13.02]	5.86 [3.97; 7.75]	66	445
SJS153	Complementation of SJS128 to MA234.1 (*tpsA* T258C, G273A)	0.1 mM Pro	10.91 [-1.53; 23.34]	18.48 [3.56; 33.41]	3.14 [0.24; 6.04]	20	340
MA234.1	*ΔkusA*	1 mM Ala	12.62 [10.3; 14.95]	16.61 [15.19; 18.02]	6.35 [4.02; 8.69]	19	324

Strain name	Genotype	treatment	Pmax (%)	Theta (hours)	d	Missing	Total
N402	Wild type	1 mM Ala	13.78 [12.02; 15.53]	14.55 [13.54; 15.55]	6.63 [4.15; 9.12]	27	388
N402 38h	Young conidia of wild type	1 mM Ala	7.35 [5.33; 9.37]	16.7 [14.04; 19.37]	4.41 [2.77; 6.04]	23	349
SJS128	*ΔmpdA*, *ΔtpsABC*	1 mM Ala	27.11 [25.48; 28.74]	13.88 [13.38; 14.38]	5.96 [4.93; 7]	56	477
SJS153	Complementation of SJS128 to MA234.1 (*tpsA* T258C, G273A)	1 mM Ala	9.98 [8.85; 11.1]	14.74 [13.85; 15.62]	6.57 [4.47; 8.67]	28	353
MA234.1	*ΔkusA*	1 mM Arg	4.38 [2.34; 6.42]	18.56 [15.99; 21.13]	11.28 [-2.05; 24.61]	9	272
N402	Wild type	1 mM Arg	4.4 [1.6; 7.21]	17.97 [12.71; 23.23]	5.63 [0.64; 10.63]	11	386
N402 38h	Young conidia of wild type	1 mM Arg	13.6 [10.11; 17.09]	12.2 [9.77; 14.62]	4.48 [1.51; 7.46]	37	292
SJS128	*ΔmpdA*, *ΔtpsABC*	1 mM Arg	11.59 [9.71; 13.47]	13.71 [12.42; 15.01]	7.16 [2.98; 11.33]	51	510
SJS153	Complementation of SJS128 to MA234.1 (*tpsA* T258C, G273A)	1 mM Arg	6.36 [-2.54; 15.26]	20 [-6.27; 46.27]	2.17 [0.4; 3.95]	8	356
MA234.1	*ΔkusA*	1 mM Glucose	4.09 [1.25; 6.93]	8.36 [0.34; 16.39]	2 [-0.56; 4.56]	8	322
N402	Wild type	1 mM Glucose	2.19 [1.73; 2.65]	8.68 [6.76; 10.61]	5.69 [-0.14; 11.51]	7	311
N402 38h	Young conidia of wild type	1 mM Glucose	3.69 [-0.25; 7.64]	7.12 [-3.83; 18.07]	2 [-2.73; 6.73]	4	344
SJS128	*ΔmpdA*, *ΔtpsABC*	1 mM Glucose	0.49 [0.4; 0.57]	4.65 [1.83; 7.48]	30 [-216.74; 276.73]	12	487
SJS153	Complementation of SJS128 to MA234.1 (*tpsA* T258C, G273A)	1 mM Glucose	1.02 [0.56; 1.48]	4.56 [1.1; 8.03]	2.21 [-1.51; 5.93]	7	370
MA234.1	*ΔkusA*	1 mM Pro	75.58 [56.6; 94.56]	16.12 [13.1; 19.14]	3.26 [2.36; 4.17]	20	321
N402	Wild type	1 mM Pro	68.09 [63.27; 72.9]	12.05 [11.39; 12.7]	4.79 [3.82; 5.75]	22	280
N402 38h	Young conidia of wild type	1 mM Pro	73.4 [35.86; 110.95]	17.82 [13.35; 22.29]	5.19 [1.67; 8.71]	37	267
SJS128	*ΔmpdA*, *ΔtpsABC*	1 mM Pro	105.01 [70.83;139.19]	19.79 [16.02; 23.57]	3.73 [2.8; 4.66]	14	427
SJS153	Complementation of SJS128 to MA234.1 (*tpsA* T258C, G273A)	1 mM Pro	60.37 [50.32; 70.42]	11.88 [10.29; 13.46]	4.43 [2.47; 6.39]	21	315

Strain name	Genotype	treatment	Pmax (%)	Theta (hours)	d	Missing	Total
MA234.1	*ΔkusA*	10 mM Ala	61.98 [58.54; 65.42]	13.46 [13.01; 13.92]	6.6 [5.35; 7.86]	22	250
N402	Wild type	10 mM Ala	60.05 [55.18; 64.92]	12.65 [11.96; 13.33]	6.56 [4.54; 8.58]	23	266
N402 38h	Young conidia of wild type	10 mM Ala	47.95 [-6.93; 102.83]	20 [0.75; 39.25]	2.45 [0.74; 4.16]	21	183
SJS128	*ΔmpdA*, *ΔtpsABC*	10 mM Ala	67.65 [65.14; 70.16]	12.87 [12.56; 13.18]	6.54 [5.65; 7.43]	25	353
SJS153	Complementation of SJS128 to MA234.1 (*tpsA* T258C, G273A)	10 mM Ala	65.62 [61.85; 69.39]	12.91 [12.43; 13.38]	6.88 [5.35; 8.4]	23	271
MA234.1	*ΔkusA*	10 mM Arg	13.63 [7.17; 20.09]	20 [16; 24]	5.51 [3.03; 7.98]	11	277
N402	Wild type	10 mM Arg	11.12 [4.49; 17.75]	20 [15.21; 24.79]	5.87 [2.39; 9.34]	12	276
N402 38h	Young conidia of wild type	10 mM Arg	25.72 [18.54; 32.9]	14.95 [12.47; 17.43]	4.93 [2.2; 7.66]	33	245
SJS128	*ΔmpdA*, *ΔtpsABC*	10 mM Arg	21.92 [16.45; 27.39]	16.42 [14.38; 18.46]	5.71 [3.08; 8.34]	6	219
SJS153	Complementation of SJS128 to MA234.1 (*tpsA* T258C, G273A)	10 mM Arg	12.75 [4.55; 20.95]	20 [15.67; 24.33]	7.4 [1.7; 13.1]	10	289
MA234.1	*ΔkusA*	10 mM Glucose	27.25 [25.88; 28.62]	7.2 [6.78; 7.61]	5.08 [3.69; 6.48]	25	313
N402	Wild type	10 mM Glucose	34.58 [33.38; 35.78]	7.01 [6.74; 7.28]	5.57 [4.42; 6.71]	21	286
N402 38h	Young conidia of wild type	10 mM Glucose	6.73 [3.78; 9.69]	14.23 [7.96; 20.49]	2.42 [1.29; 3.55]	32	281
SJS128	*ΔmpdA*, *ΔtpsABC*	10 mM Glucose	11.77 [7.92; 15.62]	12.13 [8.59; 15.67]	3.32 [1.32; 5.32]	38	458
SJS153	Complementation of SJS128 to MA234.1 (*tpsA* T258C,G273A)	10 mM Glucose	25.49 [22.85; 28.14]	6.67 [5.95; 7.39]	6.91 [1.99; 11.83]	26	229
MA234.1	*ΔkusA*	10 mM Pro	80.97 [78.63; 83.3]	11.75 [11.49; 12.01]	5.95 [5.3; 6.6]	16	288
N402	Wild type	10 mM Pro	93.16 [75.27; 111.06]	9.94 [7.89; 11.99]	2.95 [1.72; 4.17]	10	237
N402 38h	Young conidia of wild type	10 mM Pro	48.99 [35.06; 62.92]	16.59 [13.98; 19.2]	4.77 [2.75; 6.8]	51	270
SJS128	*ΔmpdA*, *ΔtpsABC*	10 mM Pro	74.37 [71.07; 77.68]	14.91 [14.57; 15.26]	6.76 [5.91; 7.62]	18	472
SJS153	Complementation of SJS128 to MA234.1 (*tpsA* T258C, G273A)	10 mM Pro	81.13 [78.57; 83.69]	11.54 [11.26; 11.81]	6.87 [5.89; 7.85]	17	298

Strain name	Genotype	treatment	Pmax (%)	Theta (hours)	d	Missing	Total
MA234.1	*ΔkusA*	NaPS	NA	NA	NA	6	325
N402	Wild type	NaPS	1.72 [0.57; 2.87]	4.81 [-0.48; 10.09]	2 [-2.32; 6.32]	3	252
N402 38h	Young conidia of wild type	NaPS	7.26 [1.81; 12.72]	20 [10.01; 29.99]	3.19 [1.54; 4.84]	5	349
SJS128	*ΔmpdA*, *ΔtpsABC*	NaPS	0.18 [0.1; 0.27]	10.97 [5.91; 16.03]	29.97 [-120.49; 180.44]	10	492
SJS153	Complementation of SJS128 to MA234.1 (*tpsA* T258C, G273A)	NaPS	0.82 [0.61; 1.04]	12.98 [10.71; 15.25]	30 [-37.23; 97.23]	5	331

CHAPTER 8

The impact of cultivation temperature on the transcriptome, proteome and heat resistance of *Aspergillus niger* conidia

Sjoerd J. Seekles, Maarten Punt, Tom van den Brule, Mark Arentshorst, Gertjan Kramer, Winfried Roseboom, Gwen Meuken, Véronique Ongenae, Jordy Zwerus, Stanley Brul, Jan Dijksterhuis, Han A. B. Wosten, Robin A. Ohm, Arthur F.J. Ram

Manuscript in preparation

Abstract

Asexual spores (conidia) of filamentous fungi are reported to have increased heat resistance when cultivated at higher temperatures, which is shown to be associated with trehalose accumulation. In this study, we show that the heat resistance of conidia from food spoiler *Aspergillus niger* also increases when cultivated at increased temperatures. Phenotypic analysis of *A. niger* mutants devoid from any trehalose due to the deletion of all three trehalose 6-phosphate synthase genes (Δ*tpsABC*) showed that the observed increase in heat resistance was not solely due to trehalose accumulation inside conidia. We investigated the possibility that protective proteins could cause the observed increase in conidial heat resistance. Several strains lacking putative protective proteins were created, and subsequently investigated for their role in conidial heat resistance. The conidia an *A. niger* strain lacking NRRL3_02725, a Hsp104 homologue, was found to be in general more heat sensitive compared to the parental strain, but none of the knock-out strains in genes encoding putative protective proteins, including Δ*NRRL3_02725*, could explain the heat resistance increase seen in conidia due to cultivation at increased temperatures. Therefore, transcriptome and proteome studies were conducted on dormant conidia cultivated at 28°C, 32°C and 37°C in order to find possible candidate protective proteins. We show that only two genes encoding putative *hsp26/42*-type heat shock proteins, NRRL3_04002 and NRRL3_10215, are upregulated in both the transcriptome and proteome datasets. These two genes are promising candidates for the observed heat resistance increase in conidia when cultivated at increased temperature.

Introduction

Filamentous fungi are among the most common food spoilage microbes found across food sectors, and are known spoilers of highly processed food products [1,2]. Food spoiling filamentous fungi can be classified in five different groups [3]: Xerophilic fungi that can grow on water activities below 0.85 [4], anaerobic fungi that can grow without oxygen [5], psychrophilic/psychrotolerant fungi that can grow or survive at or below 0 °C [6], preservative resistant fungi that can grow in the presence of preservatives [7] and heat resistant fungi capable of surviving high temperature treatments up to 90°C for 25 minutes [8]. The group of heat resistant molds (HRM) produce heat resistant sexual spores (ascospores) known to survive pasteurization treatments of 65°C to 70°C [8–10]. These ascospores are generally regarded as the most heat resistant fungal structure and have therefore been studied more than asexual fungal spores (conidia) with regards to food spoilage [11]. However, conidia, in contrast to ascospores, are survival structures that are airborne and produced in huge amounts. Virtually every cubic meter of air contains these asexual fungal spores [12–15]. Therefore, food spoilage by conidia is more prevalent and thus seen in many food sectors, such as in the production of animal feed, dairy products and fruit juices [16–19]. Recently, the most heat resistant conidia to date were described as produced by *Paecilomyces variotii* DTO 217-A2 which survive up to 22 minutes at 60 °C which is within the margins of common milk thermization protocols [20,21].

Previous research has shown the impact of conidial age, cultivation medium as well as cultivation temperature on the stress resistance of resulting conidia [22–26] (and Chapter 7). Conidial populations of *Aspergillus fumigatus* and *Penicillium roqueforti* harvested from plates incubated at a high temperature were more heat resistant than conidial populations harvested from plates incubated at a low temperature [23,25].

The heat resistance of conidia is at least partially due to its high intracellular concentrations of compatible solutes [21,25,27–29]. Recently, we have shown that *A. niger* conidia lacking both trehalose and most mannitol are comparable to young conidia, and

survive up to ~5 minutes at 54°C (Chapter 7). Additionally, other protective molecules, such as heat shock proteins (HSPs) and dehydrins, accumulate inside conidia of *A. niger* and *A. fumigatus* as found in transcriptomic and proteomic data, which are speculated to impact conidial stress resistance [30–33]. Indeed, expression of heat shock proteins is induced in conidia when heat treated for 4 hours during conidiation, suggesting that these protective proteins play a role in the increased heat resistance of conidia as an adaptive response to the shift towards a high temperature environment [34].

In this research, we show the impact of cultivation temperature during conidiation on the heat resistance of the resulting conidia of *A. niger*. We show that cultivation at higher temperatures increases the heat resistance of conidia. This correlates with an increase in trehalose content, which has also has been observed in other filamentous fungi [23,25]. However, conidia of a deletion strain incapable of producing trehalose still increased in heat resistance when cultivated at higher temperatures, suggesting involvement of other molecules. Deletion mutants lacking candidate protective proteins were made, however all knock-out mutants analysed showed conidia with increased heat resistance when cultivated at higher temperatures. Therefore, we compared the transcriptome and proteome data of dormant conidia cultivated at 28°C, 32°C and 37°C to find potential proteins involved in conidial heat resistance. The possible role of two potential candidate heat shock proteins, NRRL3_04002 and NRRL3_10215, which are most likely involved in the heat resistance increase of conidia when cultivated at higher temperatures is discussed.

Results

Conidia cultivated at higher temperatures show increased heat resistance

The impact of cultivation temperature, meaning the temperature at which conidiation takes place, on the heat resistance of conidia of *A. niger* was investigated. Previous reports have shown that an increase in heat resistance of conidia cultivated at higher temperatures correlates with increased trehalose concentrations [23,25]. In order to investigate this correlation, conidia from strains N402 (parental) and SJS126 (*ΔtpsABC*) unable to produce trehalose (Chapter 7) were harvested from plates that had been incubated at either 28°C or 37°C for 8 days and subsequently analysed for internal compatible solute composition and heat resistance (Figure 8.1). Additionally, heat resistance changes due to cultivation temperature (28°C, 32°C and 37°C) of conidia from *A. niger* N402 were further quantified in a heat inactivation experiment to determine decimal reduction values (D-values), by following conidial heat inactivation through time (Figure 8.2). The D_{57}-values of N402 conidia cultivated at 28°C, 32°C and 37°C were 6.5 ± 1.9 minutes, 9.7 ± 0.5 minutes and 17.0 ± 0.4 minutes, respectively (Table 8.1). Statistical analysis confirmed that *A. niger* conidia cultivated at 37°C are significantly more heat stress resistant than those cultivated at 28°C and 32°C ($p<0.05$). No significant difference was detected between D_{57}-values of *A. niger* conidia cultivated at 28 °C and 32 °C ($p=0.45$). Taken together, both experiments show that conidia of *A. niger* N402 harvested from plates cultivated at 37°C, are more heat resistant than conidia harvested from plates cultivated at 28°C. This increase in heat resistance due to increased cultivation temperature was also not specific for the N402 *A. niger* strain that is often used in lab studies [35,36] and also observed in two randomly picked wild-type *A. niger* strains CBS112.32 and CBS147347 (Figure 8.S1), showing the consistency of the increase in heat resistance due to increased cultivation temperature among *A. niger* strains. An increase in intracellular trehalose levels was measured in conidia of lab strain N402 when cultivated at higher temperatures (Figure 8.1B), suggesting that the accumulation of trehalose upon cultivation at higher temperatures is conserved among *A. niger*,

A. fumigatus and *P. roqueforti* [23,25]. As shown earlier and confirmed here, trehalose levels are undetectable in the *ΔtpsABC* strain (SJS126) and its conidia have lower heat resistance than wild type N402, but interestingly still produced conidia with increased heat resistance upon cultivation at higher temperatures (Figure 8.1). Therefore, the observed increase in conidial heat resistance due to higher cultivation temperature is not solely due to an increase in the amount of intracellular trehalose. We hypothesized that the observed change in heat resistance is instead due to the accumulation of currently unknown protective proteins.

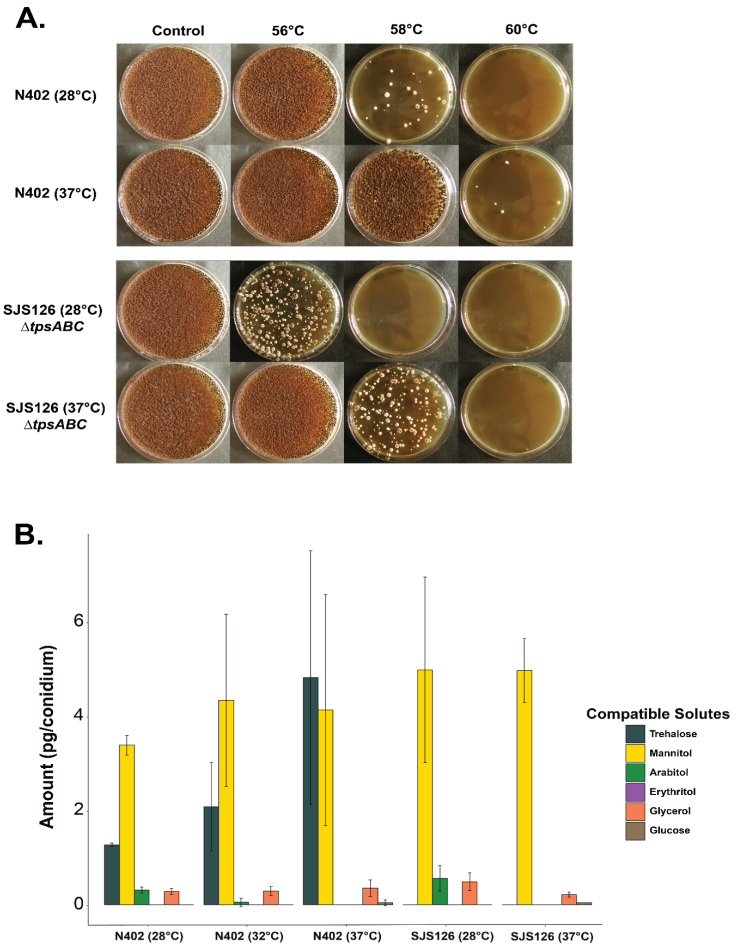

Figure 8.1. Heat resistance increase due to increased cultivation temperature of N402 and the trehalose deficient mutant SJS126. A. Conidia were harvested from mycelium cultivated at 28°C or 37°C. Heat resistance of lab strain N402 is higher than trehalose deficient mutant SJS126 (ΔtpsABC) as was shown previously (Chapter 7). Conidia harvested from mycelium cultivated at

37°C are more heat resistant than conidia harvested from mycelium cultivated at 28°C in both the lab strain N402 and the trehalose deficient mutant SJS126. B. The heat resistance increase in the lab strain N402 correlates with an increase observed in the amount of trehalose accumulated in the conidia. However, the conidia of trehalose deficient mutant SJS126 do not accumulate extra compatible solutes (the strain is incapable of biosynthesizing trehalose) when cultivated at 37°C, while these conidia still have an increased heat resistance. Therefore, the heat resistance increase observed of conidia cultivated at higher temperatures is not solely due to accumulation of trehalose.

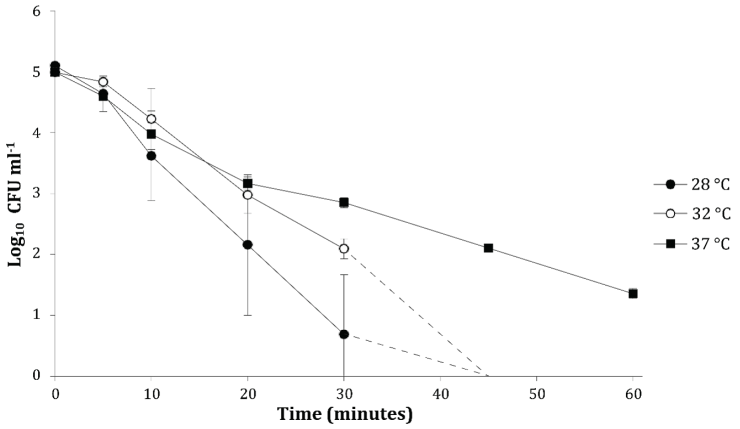

Figure 8.2. Heat inactivation curves of A. niger N402 conidia cultivated at 28°C, 32°C and 37°C. The heat inactivation experiment was performed in a 57°C water bath. Data is based on biological duplicates. After 45 minutes, none of the conidia harvested from plates cultivated at 28°C or 32°C survived the heat treatment, a 5-log reduction in microbial load was observed (less than 1 in 105 conidia survive). In contrast, conidia harvested from plates that were incubated at 37°C survived up till 60 minutes of heat treatment, a 3-log reduction in microbial load was observed (1 in 103 conidia survive). These data indicate that a population of A. niger conidia harvested from mycelium that was incubated at a high(er) temperature has a high(er) heat resistance. D-values were calculated based on linear regression lines and given in Table 8.1.

Table 8.1. D_{57}-values of *A. niger* N402 conidia cultivated at 28°C, 32°C or 37°C. These D-values were calculated based on the log-linear regression model and is based on two biological replicates.

Cultivation temperature	D_{57}-value ± SD (minutes)
28 °C	6.5 ± 1.9
32 °C	9.7 ± 0.5
37 °C	17.0 ± 0.4

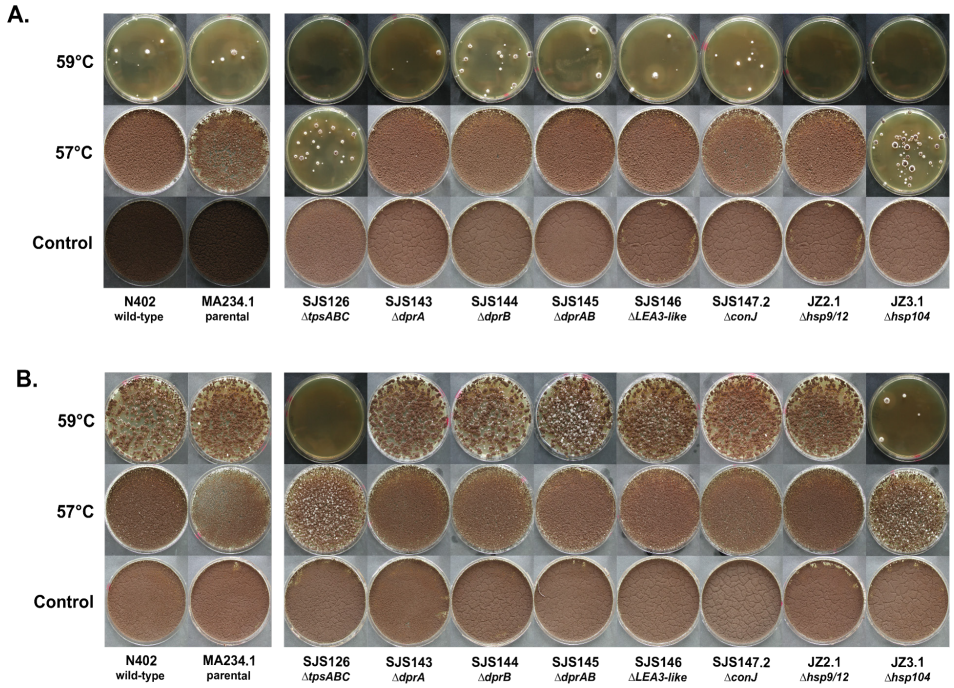

Figure 8.3. Heat resistance of knock-out mutants lacking protective proteins. Knock-out strains were grown for 8 days at 28°C or 37°C on MEA plates. Conidia were harvested and subsequently 106 conidia were heat treated and plated to count colony forming units (CFUs). Heat treatment was done for 10 minutes at either room temperature (control), 57°C or 59°C. All samples were measured in biological triplicates. A. heat treatment of conidia harvested from mycelium cultivated at 28°C. Knock-out mutants lacking protective proteins are comparable in heat resistance to their parental strain MA234.1, except for the Δhsp104 mutant JZ3.1. Conidia of strain SJS126 that lacks trehalose are sensitive to heat, as was shown before (Chapter 7). B. Heat treatment of conidia harvested from mycelium cultivated at 37°C. Heat resistance of conidia from all knock-out strains increased when compared to those cultivated at 28°C as seen by the increased amount of colony forming units after a 10 minutes 59°C heat treatment.

8

Conidia from deletion mutant *Δhsp104* are more sensitive to heat stress, but still show increased heat resistance upon cultivation at higher temperatures

Deletion mutant strains of *A. niger* were made lacking genes coding for putative protective proteins. The gene selection was based on putative protective proteins shown to accumulate high amount of mRNA inside dormant conidia of *A. niger* based on previous transcriptomic data [30], and the details on the six target genes can be found in Table 8.2. The heat resistance of conidia of strains SJS143 (*ΔNRRL3_01479*; *ΔdprA*), SJS144

(*ΔNRRL3_01479*; *ΔdprB*), SJS145 (*ΔNRRL3_01479, ΔNRRL3_01479*; *ΔdprA*B), SJS146 (*ΔNRRL3_05684*; *ΔLEA3-like*), SJS147.2 (*ΔNRRL3_02511*, *ΔconJ*), JZ2.1 (*ΔNRRL3_11620*; *Δhsp9/12*) and JZ3.1 (*ΔNRRL3_02725*; *Δhsp104*) was compared to that of the parental strain MA234.1 (*ΔkusA*), lab strain N402 and the trehalose deficient knock-out strain SJS126 (*ΔtpsABC*) (Figure 8.3). Strain JZ3.1 (*Δhsp104*) produced conidia with reduced heat resistance, with no observed change in internal compatible solutes when compared to its parental strain (Figure 8.S2). Therefore, the putative Hsp104 homologue was found to contribute to conidial heat resistance. However, all knock-out strains, including JZ3.1 (*Δhsp104*), continued to show an increased heat resistance when conidia were cultivated at 37°C (Figure 8.3B) versus 28°C (Figure 8.3A). None of these six putative protective proteins could explain the observed increase in heat resistance due to increased cultivation temperature.

Table 8.2. Six target genes coding for putative protective proteins. These six putative protective proteins were all highly expressed in dormant *A. niger* conidia in a previous study by van Leeuwen et al. [30]. The putative gene names were used throughout the manuscript instead of gene numbers to help guide the reader.

Gene name used	NRRL3-number	An-number	Description	Additional information
dprA	NRRL3_01017	An14g05070	Dehydrin-like protective proteins, homologoues DprA & DprB, found in conidia of *Aspergillus fumigatus*, are involved in multiple stress responses including osmotic, pH and oxidative stress[62].	BLASTp reveals DprA from *A. fumigatus* has 71.8% and 56.8% homology with NRRL3_01017 and NRRL3_01479, respectively. Similarly, DprB from *A. fumigatus* has 74.4% and 61.4% homology with NRRL3_01017 and NRRL3_01479, respectively.
dprB	NRRL3_01479	An13g01110	Dehydrin-like protective proteins, homologoues DprA & DprB, found in conidia of *Aspergillus fumigatus*, are involved in multiple stress responses including osmotic, pH and oxidative stress [62].	BLASTp reveals DprA from *A. fumigatus* has 71.8% and 56.8% homology with NRRL3_01017 and NRRL3_01479, respectively. Similarly, DprB from *A. fumigatus* has 74.4% and 61.4% homology with NRRL3_01017 and NRRL3_01479, respectively.

Gene name used	NRRL3-number	An-number	Description	Additional Information
LEA3-like	NRRL3_05684	An02g07350	Described as a LEA3-like protein, LEA3 proteins are known to protect plants against desiccation [30,63] which coincided with one round of mitosis.	Has a 'CsbD-like protein' domain which are thought to be stress response proteins in bacteria.
conJ	NRRL3_02511	An01g10790	Name derived from conidiation specific factor 10. Highly expressed in dormant conidia of *A. niger* and known in *A. nidulans* and *A. fumigatus* to be important for spore viability [64]. Deletion mutants lacking multiple *con* genes accumulate more of the compatible solutes erythritol and glycerol.	In *Neurospora crassa*, *A. nidulans* and *A. fumigatus* no phenotype is observed in single knock-out deletion mutants. Only when multiple *con* genes are deleted are spore viability and compatible solute levels affected.
hsp9/12	NRRL3_11620	An06g01610	Best homologue to Hsp9 and Hsp12 known from yeast species. This heat shock protein is known to stabilize the plasma membrane in yeast [46,65].	
hsp104	NRRL3_02725	An01g13350	Best homologue to Hsp104 known from yeast. This heat shock protein is important for thermotolerance in yeast [37, 48, 66].	This protein is known to have interplay with trehalose, meaning that if the protein is deleted, trehalose is accumulated inside the yeast cell as compensation. Only when both trehalose and Hsp104 are abolished is the cell sensitive to heat stress.

Transcriptome and proteome analysis reveals the upregulation of two *hsp26/42* type heat shock proteins

In order to investigate which proteins are potentially involved in the observed change in heat resistance between conidia cultivated at different temperatures, a transcriptome and proteome study was conducted comparing the contents of dormant conidia cultivated for 8 days at 28°C, 32°C and 37°C. A principal component analysis was done on both the transcriptome and proteome datasets, showing in both cases that the largest differences were caused by the 37°C condition, and that the data belonging to the 28°C and 32°C conditions were fairly similar (Figure 8.S3). Therefore, the main comparison discussed in this study are the transcriptome and proteome differences between conidia

cultivated at 28°C versus 37°C. In total, 666 genes and 26 proteins were found significantly upregulated, while 783 genes and 34 proteins were found significantly downregulated in the transcriptome dataset when comparing 37°C conidia versus 28°C conidia. Log_2 fold changes (Log_2FC) were calculated for both the transcriptome and proteome datasets and subsequently plotted against each other (Figure 8.4). Genes located in the top-right corner are upregulated in the 37°C cultivated conidia in both the transcriptome and proteome dataset. Only two genes are significantly upregulated in both the transcriptome and proteome dataset, NRRL3_04002 and NRRL3_10215, which are both putative small heat shock proteins of the *hsp26/42* type. All 60 proteins that were significantly more, or less, present in conidia cultivated at 37°C (represented by blue, pink and red dots in Figure 8.4) are listed in Table 8.S1. Additionally, an enrichment study was performed investigating the annotation terms that were over- and under-represented in the 666 genes that were upregulated and the 783 genes that were downregulated. Overall, no clear biologically relevant changes could be distilled from these over- and under-represented annotation terms.

We investigated the transcriptome and proteome changes of all putative chaperones, as well as some other putative protective proteins such as hydrophobins, catalases and superoxide dismutases as these genes/proteins are most likely responsible for the increased heat resistance of conidia described above (Table 8.S2). At the top of Table 8.S2 the genes that were deleted in this study based on previously found high expression inside conidia by van Leeuwen *et al.* [30] (Figure 8.3 & Table 8.2) are listed. Indeed, the newly obtained transcriptome dataset of dormant conidia confirms that these genes are highly expressed as seen by the high baseMean DESeq2 values of these six genes. Additionally, we show that these six genes have high LFQ intensity values, indicating that the dormant conidia also contain a high amount of these proteins. Even though they are present in relatively high amounts, none of these six proteins show a significant fold change in the proteome dataset between 28°C cultivated conidia and 37°C cultivated conidia. As described above (Figure 8.4), there were only two chaperones that showed both significantly more transcript and protein in the conidia cultivated

at a high temperature (37°C) versus conidia cultivated at a low temperature (28°C). Therefore, NRRL3_04002 and NRRL3_10215, make likely candidates for the observed differences in heat resistance between conidia cultivated at a high temperature (37°C) versus a low temperature (28°C).

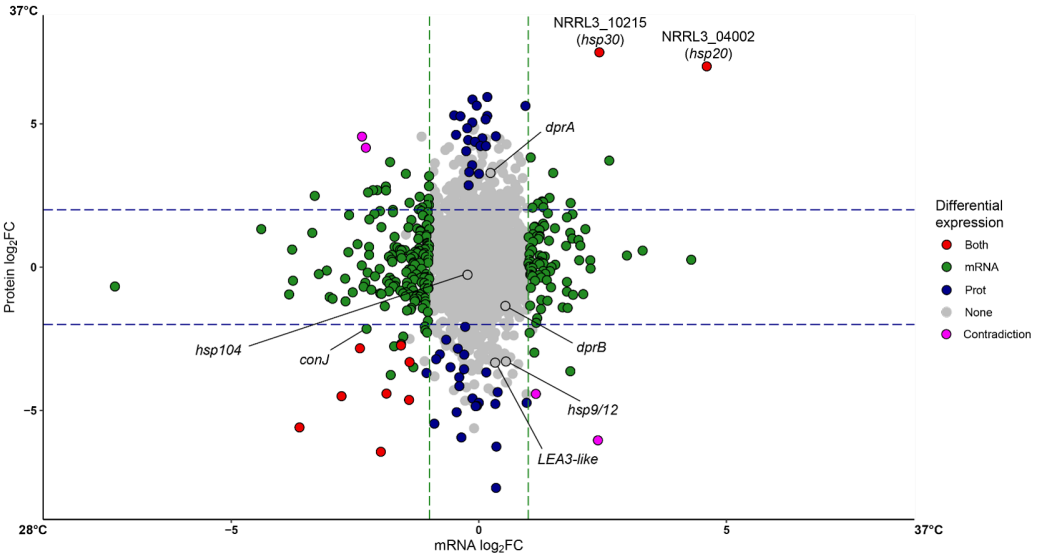

Figure 8.4. Comparison of both transcriptome and proteome fold changes of genes between conidia (37°C) and conidia (28°C). Genes having significant changes in expression (green), significant changes in protein amounts (blue) or both (red) between dormant conidia harvested from a plate cultivated at 37°C and 28°C are listed here. This graph contains only information of 2381 genes, of which proteome data was obtained, out of in total 11846 genes present on the A. niger NRRL3 genome. Only two genes and their corresponding proteins are significantly more present in the form of transcript and protein in 37°C cultivated conidia versus 28°C (NRRL3_04002 and NRRL3_10215). Therefore, these two putative heat shock proteins make excellent candidates for the observed difference in heat resistance between these two types of conidia.

Discussion

In this study we show that cultivation temperature during conidiation increases the heat resistance of the resulting conidia of *A. niger*. This phenomenon has also been observed in other filamentous fungi, including pathogenic (*A. fumigatus* [23]) and food spoilage fungi (*A. nidulans* and *P. roqueforti* [25,34]), indicating an evolutionary conserved trait of these fungi. The increase in heat resistance of conidia due to cultivation at increased temperatures has been shown to additionally correlate with an increase of internal trehalose in *A. fumigatus* and *P. roqueforti* [23,25] and was also found this study, indicating a conserved response of conidia of filamentous fungi. However, a trehalose deficient knock-out strain SJS126 (constructed previously Chapter 7) still produced conidia with increased heat resistance despite having no increased amount of internal trehalose. This indicates that molecules or proteins other than trehalose play a role in this observed increase in conidial heat resistance.

Previous reports indicated that various protective proteins accumulate inside conidia, which can potentially influence conidial stress resistance [30,31]. Therefore, deletion mutants of six putative protective proteins were constructed to investigate whether these protective proteins impact conidial heat resistance and could explain the increase in heat resistance of conidia when cultivated at higher temperatures. The deletion of a gene coding for a Hsp104 homologue resulted in conidia with lowered heat resistance (Figure 8.2). Heat shock protein 104 has been best described in *S. cerevisiae* and is a known factor in heat tolerance in this species [37]. In *S. cerevisiae*, both trehalose and protein chaperones, such as Hsp12 and Hsp104, are important for protecting against protein aggregation and are involved in proper protein refolding after damage [38,39]. It is interesting to note that Hsp104 is known to be regulated by master regulator Heat Shock Factor 1 (HSF1), a transcription factor which is key in *S. cerevisiae* for the stress response against heat [40]. The mRNA and the encoded protein of the best homologue of this transcription factor in *A. niger* (NRRL3_07278) are also present in dormant conidia of *A. niger* according to our transcriptome and proteome data (Table 8.S2). Attempts

to create a knock-out strain lacking NRRL3_07278were unsuccessful and transformants grew only as heterokaryons and were very sickly (data not shown), which suggests that deletion of this gene is lethal. Indeed, transcription factor HSF1 is known to regulate many heat shock proteins, such as Hsp70 and Hsp90, some of which are required for cell viability, and deletion mutants of HSF1 were also not viable in *S. cerevisiae*, *Candida albicans* and *A. fumigatus* [41–44]. To circumvent the lethality in *A. fumigatus*, a mutant strain was constructed in which the HsfA transcription factor was expressed from a inducible promoter. Under low-inducing conditions several genes encoding heat shock proteins were found to be downregulated including Hsp104. Interestingly, *hsp30/42* (Afu3g14540) and *hsp20/26* (Afu5g10270), best homologues of NRRL3_04002 (putative *hsp20*) and NRRL3_10215 (putative *hsp30*), were also regulated by HsfA in *A. fumigatus*.

Both trehalose and protein chaperones, like heat shock proteins, have been shown to contribute to the heat resistance of *S. cerevisiae* cells. Interestingly, researchers have suggested that trehalose might be a better chaperone than many of the protein chaperones, giving better protection against protein aggregation when studying long-term survival [45]. The yeast cell responds when faced with a lack of the protein chaperones by accumulating additional trehalose and vice versa, suggesting that the loss of one of these heat resistance elements is compensated by increasing another [46–48]. However, in our study the *Δhsp104 A. niger* strain showed altered heat resistance of conidia (Figure 8.2), but no change in internal trehalose concentration (Figure 8.S3) indicating no compensatory mechanism. Other strains lacking putative protective proteins such as Hsp9/12 also did not show an increased accumulation of trehalose inside conidia. This indicates that some protective proteins do protect against heat stressors in conidia, such as Hsp104, but do not show this interplay with trehalose, at least when analyzed inside dormant conidia. Unfortunately, although conidia of the *Δhsp104* strain show increased sensitivity towards heat stress, all conidia of deletion strains analysed in this study still showed increased heat resistance when cultivated at higher temperatures. Therefore, Hsp104 is not responsible for the increased resistance of conidia in response

to cultivation at higher growth temperatures.

To identify possible candidate proteins involved in the acquired heat resistance by cultivation at higher temperatures, we performed both transcriptome and proteome studies on dormant conidia of *A. niger* cultivated at 28°C, 32°C or 37°C. When comparing conidia cultivated at 37°C with conidia cultivated at 28°C only two genes were more prevalent in both transcriptome and proteome data, NRRL3_04002 and NRRL3_10215, which both putatively code for heat shock proteins. Gene NRRL3_04002 is the best homologue of the *hsp20* gene (AN10507) and NRRL3_10215 is the best homologue of three *hsp30/hsp26* genes (AN2530, AN3555 and AN7892) of *A. nidulans* FGSC A4. Recently, conidia of *A. nidulans* have been described as responsive to their environment while still attached to the spore chain, thereby potentially creating individual differences between conidia dependent on environmental cues during the conidiation process [34]. Wang et al. describe how multiple heat shock proteins, but mainly two genes, *hsp26* (AN7892) and *hsp30* (AN2530), are significantly upregulated when conidia attached to the spore chain are heat treated for 4 hours in *A. nidulans*. This again emphasizes the potential role of these two small heat shock proteins in the heat resistance of conidia as a response to the high temperatures of the environment. Additionally, this finding suggests that these two heat shock proteins could potentially be accumulated after conidial formation, as is also seen with compatible solute accumulation in *A. niger* (Chapter 7).

Materials and Methods

Strains, cultivation conditions and media used

The *A. niger* strains were cultivated on malt extract agar plates (MEA, Oxoid) for 8 days unless noted otherwise. The cultivation temperature experiments were done on lab strain *A. niger* N402. Plates were inoculated homogenously using sterilized glass beads. For every experiment, conidia were freshly harvested using sterilized physiological salt buffer (PS; 0.9% NaCl, 0.02% Tween 80 in demi water). A sterilized cottonbud was used to scrape the conidia off the plate, and the spore suspension was subsequently filtered using a sterilized filter (Amplitude Ecocloth, Contec) to filter out mycelial fragments.

Heat treatment assays

Heat treatment assays were performed to investigate the heat resistance of dormant conidia. Conidia were freshly harvested, counted in a cell counter (BioRad) and subsequently diluted until 10^6 conidia / 100 µL. PCR tubes were filled with 100 µL conidial suspension and heat treated for 10 minutes in a thermocycler, the lid temperature was fixed at 60°C. After heat treatment, the 100 µL conidial suspensions were plated on MEA plates with 0.05% Triton X-100 (Sigma). Pictures were taken after 5 days of growth at 28°C.

Heat inactivation experiments using a water bath (Julabo) were done inside Erlenmeyer flasks at 54°C. In short, each Erlenmeyer contained 19.8 mL PS buffer with a sterilized stirring bean which was spinning at 180 rpm inside the heated water bath. Temperatures were checked inside an extra testing Erlenmeyer by using thermometers, and care was taken to ensure the PS buffer temperature was at 54 °C +- 0.1 °C. At t = 0 the Erenmeyers were inoculated with 200 uL of conidial suspension (10^8 conidia / mL). At pre-determined time points 1.5 mL samples were taken, transferred to 2 mL Eppendorf tubes and instantly put on ice. These samples were diluted to be able to plate 10^2, 10^3, 10^4 and 10^5 conidia per plate. Plates were incubated for 7 days after which colony forming units (CFUs) were counted for each time point. D-values were calculated using

a log-linear fit.

Sample preparation and HPLC analysis

HPLC analysis was done following a previously established protocol [21]. In short, 10^8 conidia inside a 2 mL Eppendorf safe-lock tube were centrifuged and supernatant was removed. The pellets were flash frozen in liquid nitrogen, and two stainless steel beads (diameter 3.2 mm) were added per tube. The tubes were loaded into a TissueLyser II adapter (pre-cooled in -80 °C) and cracked using a TissueLyser II (QIAGEN) shaking at 30 Hz for 6 minutes. After cracking 1 mL Milli-Q water was added and samples were heated in a 95 °C water bath for 30 minutes. Samples were centrifuged for 30 minutes and the supernatant was filtered (0.2 µm Acrodisc). Samples were stored at -20°C until HPLC analysis.

HPLC analysis was done using two Sugar-Pak I columns (Waters) placed in line in order to get good separation between polyols. A sample volume of 20 µl was injected in the mobile phase consisting of 0.1 mM Ca EDTA in ultrapure water and samples were followed for 30 min. A mixture of trehalose, glucose, glycerol, erythritol, mannitol and arabitol (0.002% – 0.10% w/v) was used as reference. All calibration curves showed an R2 > 0.999 with a limit of detection

Creation of knock-out strains lacking protective proteins

Strains lacking putative protective proteins were made using a CRISPR/Cas9 genome editing protocol described previously [49]. In sort, a target sequence was designed *in silico* using ChopChop predictors [50]. The guide RNA targeting the gene coding for the protective proteins was constructed by PCR and inserted into vector pFC332 using PacI (Fermentas, Thermo Fisher) digestion and subsequent ligation. The newly created plasmids were used for PEG-mediated protoplast transformation, using strain MA234.1 (*ΔkusA*) as the parental strain. Selection was based on hygromycin, and transformants were purified in multiple rounds to lose the CRISPR/Cas9 containing plasmid (see [49] for more details). Genomic DNA was extracted from purified transformants using a phe-

nol-chloroform based protocol [51]. Diagnostic PCR amplifying the deleted region was performed to check for correct deletion of the target gene. All strains created this way are listed in Table 8.3. Primers and plasmids used to create the knock-out strains are listed in Table 8.4 and Table 8.5, respectively.

Table 8.3. Strains used in this study

Strain name	Genotype	Description	Parental strain	Origin
MA234.1	*ΔkusA*	Parental strain for CRISPR/Cas9 genome editing, lacking *kusA* gene.	N402	[69]
SJS143	*ΔNRRL3_01479; 'ΔdprA'*	Strain lacking a gene coding for a putative dehydrin-like protein [62]	MA234.1	This study
SJS144	*ΔNRRL3_01479; 'ΔdprB'*	Strain lacking a gene coding for a putative dehydrin-like protein [62]	MA234.1	This study
SJS145	*ΔNRRL3_01479, ΔNRRL3_01479; 'ΔdprAB'*	Strain lacking both dehydrin-like proteins [62]	MA234.1	This study
SJS146	*ΔNRRL3_05684; 'ΔLEA3-like'*	Strain lacking a LEA3-like protein thought to be involved in the cell stress response [30,63]	MA234.1	This study
SJS147.2	*ΔNRRL3_02511, 'ΔconJ'*	Strain lacking a homologue of *conJ* described in *A. nidulans* involved in stress response [64]	MA234.1	This study
JZ2.1	*ΔNRRL3_11620; 'Δhsp9/12'*	Strain lacking putative Hsp12, important for plasma membrane stability in *S. cerevisiae* [46,65]	MA234.1	This study
JZ3.1	*ΔNRRL3_02725; 'Δhsp104'*	Strain lacking putative Hsp104, important for heat resistance in *S. cerevisiae* [37,48,66]	MA234.1	This study

Table 8.4. Primers used in this study.

Primer name	Sequence	Use
pTE1_for	CCttaattaaACTCCGCCGAACGTACTG	5' gRNA constructs (promotor). Lower-case letters represent PacI cut site.
pTE1_rev	CCttaattaaAAAAGCAAAAAAGGAAGGTACAAAAAAGC	3' gRNA constructs (terminator). Lower-case letters represent PacI cut site.
Con10_fw	AGTGTCGAATATCGCCAAGAGTTTTAGAGCTAGAAATAGC	3' *conJ* gRNA
Con10_rv	TCTTGGCGATATTCGACACTGACGAGCTTACTCGTTTCGT	5' *conJ* gRNA
5_Con10_fw	CCCTGCCATGTAAGTTCCCGCG	5' *conJ* flank (repair DNA fragment)
5_Con10_KORE_rv	GGAGTGGTACCAATATAAGCCGGTGATTCTGATCCAATTCCAAACCTCA	5' *conJ* flank (repair DNA fragment)

Primer name	Sequence	Use
3_Con10_KORE_fw	CCGGCTTATATTGGTACCACTCCTTGAGT-GAAGGTACCGCTGGGA	3' *conJ* flank (repair DNA fragment)
3_Con10_rv	CGTCGAGTTGAAGCGACCGGAA	3' *conJ* flank (repair DNA fragment)
DIAG_Con10_5_fw	TAGCCTAGGCTCCCCTTCCCCA	Diagnostic PCR *conJ* deletion
DIAG_Con10_3_rv	ACGCTGCCGCTTACTGTAGCAC	Diagnostic PCR *conJ* deletion
Lea3_fw	GCCACTGCCCGTCGTGACAAGTTTTA-GAGCTAGAAATAGC	3' *LEA3-like* gRNA
Lea3_rv	TTGTCACGACGGGCAGTGGCGACGAGCT-TACTCGTTTCGT	5' *LEA3-like* gRNA
5_Lea3_fw	GGCAGTTGGACTGGGTTTGGGG	5' *LEA3-like* flank (repair DNA fragment)
5_Lea3_KORE_rv	GGAGTGGTACCAATATAAGCCGGTCAAGTT-GATGGGATTGAGGATGGA	5' *LEA3-like* flank (repair DNA fragment)
3_Lea3_KORE_fw	CCGGCTTATATTGGTACCACTCCGCACGCTT-GACGACCTGCATGA	3' *LEA3-like* flank (repair DNA fragment)
3_Lea3_rv	CCCGGACACTGGCAATTCCGTC	3' *LEA3-like* flank (repair DNA fragment)
DIAG_Lea3_5_fw	TCACCGACCAGGGGAAGGATGC	Diagnostic PCR *LEA3-like* deletion
DIAG_Lea3_3_rv	TGGAGACGATGGGTCCGCATGA	Diagnostic PCR *LEA3-like* deletion
DehydrinA_fw	TGGTCCCCACTCCTCCAACAGTTTTA-GAGCTAGAAATAGC	3' *dprA* gRNA
DehydrinA_rv	TGTTGGAGGAGTGGGGACCAGACGAGCT-TACTCGTTTCGT	5' *dprA* gRNA
5_DehydrinA_fw	ACCCCAGACTTGGACTCGAGGC	5' *dprA* flank (repair DNA fragment)
5_DehydrinA_KORE_rv	GGAGTGGTACCAATATAAGCCGGTGGG-CAATTGTATGTGTGTTTGGT	5' *dprA* flank (repair DNA fragment)
3_DehydrinA_KORE_fw	CCGGCTTATATTGGTACCACTCCGCGGG-CAAACATAAATGCTTGCGT	3' *dprA* flank (repair DNA fragment)
3_DehydrinA_rv	ACGTTCCCGCACACATATGCAT	3' *dprA* flank (repair DNA fragment)
DIAG_DehydrinA_5_fw	GACATCGACGGCACTGGCTGAG	Diagnostic PCR *dprA* deletion
DIAG_DehydrinA_3_rv	CGGAAGGGCTGTTCAACCCACC	Diagnostic PCR *dprA* deletion
DehydrinB_fw	CCAGCGCAACCACTGCAACAGTTTTA-GAGCTAGAAATAGC	3' *dprB* gRNA
DehydrinB_rv	TGTTGCAGTGGTTGCGCTGGGACGAGCT-TACTCGTTTCGT	5' *dprB* gRNA
5_DehydrinB_fw	CCGCAATCCACACTAGGCCGTC	5' *dprB* flank (repair DNA fragment)
5_DehydrinB_KORE_rv	GGAGTGGTACCAATATAAGCCGGAGGTAG-TATCCATTCCCCACCGT	5' *dprB* flank (repair DNA fragment)
3_DehydrinB_KORE_fw	CCGGCTTATATTGGTACCACTCCCGCTATGG-GAATGAACCCCGCC	3' *dprB* flank (repair DNA fragment)

Primer name	Sequence	Use
3_DehydrinB_rv	GAAGATGGAGCACCTCAGGCGC	3' *dprB* flank (repair DNA fragment)
DIAG_DehydrinB_5_fw	GGCGATCGTGGTGCTCTTGAGG	Diagnostic PCR *dprB* deletion
DIAG_DehydrinB_3_rv	AGAGGATTGGGTGCGCTGGAGT	Diagnostic PCR *dprB* deletion
HSF1_fw_1	ACTGGAACTGGAGAAAACGGGTTTTA-GAGCTAGAAATAGCAAG	PCR target 3'flank
HSF1_rv_1	CCGTTTTCTCCAGTTCCAGTGACGAGCT-TACTCGTTTCG	PCR target 5' flank
HSP12_fw_2	CAGCAAGTCCGGTCCCCAGGGTTTTA-GAGCTAGAAATAGCAAG	PCR target 3'flank
HSP12_rv_2	CCTGGGGACCGGACTTGCTGGACGAGCT-TACTCGTTTCG	PCR target 5' flank
HSP104_fw_2	GGATCGAGAAGGGCCGTCGGGTTTTA-GAGCTAGAAATAGCAAG	PCR target 3'flank
HSP104_rv_2	CCGACGGCCCTTCTCGATCCGACGAGCT-TACTCGTTTCG	PCR target 5' flank
NRRL3-02725-5'-fw	ACGTGCTGGTCAAGTGTATCGA	Donor DNA Hsp104 deletion; Diagnostic PCR
NRRL3-02725-5'-rv	GGAGTGGTACCAATATAAGCCGGGGTGGTT-GATGGGTAGATGGAA	Donor DNA Hsp104 deletion
NRRL3-02725-3'-fw	CCGGCTTATATTGGTACCACTCCGGCGGAAT-GTGAGGGAAGAATG	Donor DNA Hsp104 deletion
NRRL3-02725-3'-rv	GCTTGAGCATCCCAAGGAGAGA	Donor DNA Hsp104 deletion; Diagnostic PCR
NRRL3-07278-5'-fw	GAAATCAGGCTTTGGGACAGGC	Donor DNA Hsf1 deletion
NRRL3-07278-5'-rv	GGAGTGGTACCAATATAAGCCGGCGGTCGG-TAAAGAGCAAAGACG	Donor DNA Hsf1 deletion
NRRL3-07278-3'-fw	CCGGCTTATATTGGTACCACTCCTGTGTCCG-CGGAAGGCAATATA	Donor DNA Hsf1 deletion
NRRL3-07278-3'-rv	TAGGCGATGACACAGACCAAGG	Donor DNA Hsf1 deletion
NRRL3-11620-5'-fw	ATGATACTGCGGATGAGGAGGC	Donor DNA Hsp9/12 deletion; Diagnostic PCR
NRRL3-11620-5'-rv	GGAGTGGTACCAATATAAGCCGGCGCCA-CACCCTGATTACAATCG	Donor DNA Hsp9/12 deletion
NRRL3-11620-3'-fw	CCGGCTTATATTGGTACCACTC-CCAAGTTGCTCCATGACGTCGAC	Donor DNA Hsp9/12 deletion
NRRL3-11620-3'-rv	TTTGTCTCCCAAGTAGGCCGAG	Donor DNA Hsp9/12 deletion; Diagnostic PCR

Table 8.5. Plasmids used in this study

Plasmid	Target gene	An# (gene)	Gene name	CRISPR/Cas9 target sequence	Ref.
pTLL108.1	-	-	-	-	[49]
pTLL109.2	-	-	-	-	[49]
pFC332	-	-	-	-	[70]
pFC332_ *con10*-sgRNA	NRRL3_02511	An01g10790	*conJ*	AGTGTCGAATATCGCCAAGA	This study
pFC332_ *lea3*-sgRNA	NRRL3_05684	An02g07350	*LEA3-like*	GCCACTGCCCGTCGTGACAA	This study
pFC332_*dehydrinA*-sgRNA	NRRL3_01017	An14g05070	*dprA*	TGGTCCCCACTCCTCCAACA	This study
pFC332_*dehydrinB*-sgRNA	NRRL3_01479	An13g01110	*dprB*	CCAGCGCAACCACTGCAACA	This study
pHSF1_1	NRRL3_07278	An16g01760	*hsfA*	ACTGGAACTGGAGAAAACGG	This study
pHSP12_2	NRRL3_11620	An06g01610	*hsp9/12*	CAGCAAGTCCGGTCCCCAGG	This study
pHSP104_2	NRRL3_02725	An01g13350	*hsp104*	GGATCGAGAAGGGCCGTCGG	This study

RNA isolation and protein isolation

To obtain dormant conidia, MEA plates were inoculated confluently using sterilized glass beads and incubated at 28°C, 32°C and 37°C for 8 days. Temperatures of the incubators were double-checked with multiple thermometers and settings were adjusted if needed to obtain cultivation temperatures as close as possible to absolute temperatures. Conidia were harvested in cold PS + 0.02% Tween 80 buffer and filtered using sterile filters (Amplitude Ecocloth, CONTEC) into a falcon tube and put directly on ice. In the case of plates cultivated at 37°C, conidia from three plates were pooled (forming 1 pellet) in order to get enough conidia per sample. Samples were centrifuged for 5 minutes at 3000 rpm and 4°C, after which supernatant was removed from the pellets. The pellets were resuspended in 100µL RNAlater (Sigma) and subsequently flash frozen in liquid nitrogen. Stainless steel grinding jars for Tissuelyzer use (QIAGEN) were pre-cooled in a -80°C freezer and kept cold with liquid nitrogen inside a mortar until the flash frozen pellets were added. Cells were broken using a Tissuelyzer II (QIAGEN) shaking for 1 minute at 30 Hz. Crushed samples, while still cold and powdery, were divided between two safe-lock Eppendorf tubes; one meant for proteome analysis (kept in liquid nitrogen

and subsequent -80°C until further analysis) and one for RNA extraction already containing 450 µL RLC buffer from the RNeasy Plant Mini Kit (QIAGEN). RNA extraction and purification was continued following the manual supplied by the manufacturer including the on-column DNA digestion step. RNA quality was assessed on gel and the quantity was determined using Qubit (ThermoFisher). The RNA samples were handed over to the Utrecht Sequencing facility for Illumina NextSeq2000 2x50 paired-end sequencing.

Protein sample preparation

Powdered samples were extracted using an extraction buffer of 1% (w/v) sodium dodecyl sulfate (SDS, Sigma-Aldrich) in 100 mM ammonium bicarbonate (AMBIC, Sigma-Aldrich), by vigorous vortexing and sonication followed by 10 minutes of centrifugation at 10,000 x g to clear the extract. Supernatants were transferred to a fresh tube and their protein content was determined by bicinchoninic acid assay (BCA assay, Thermo Scientific, Etten-Leur, the Netherlands), according to the manufacturer's protocol.

Subsequently, 20 µg of protein for each sample was reduced and alkylated by the addition of 10 mM Tris carboxyethyl phosphine (TCEP, Sigma-Aldrich) and 40 mM chloroacetamide (CAA, Sigma Aldrich) and incubation at 60°C for 30 minutes. Samples were cooled at room temperature and cleaned up using protein aggregation capture on microparticles to remove interfering contaminants such as SDS by protein precipitation [52] on carboxyl modified magnetic beads (1:1 mixture Sera-Mag A and Sera-Mag B Thermo Scientific, Etten-Leur), also called SP3 [53] using improvements described by Sielaff, M *et al.* [54].

In short 20 µg of protein lysate (20 µl) was added to 2 µl (100 µg/µl beads suspension) of carboxyl modified magnetic bead mixture. The mixture was brought to 50% (v/v) acetonitrile (ULC-MS grade, Biosolve) concentration vortex mixed and incubated for 20 minutes at room temperature, after which samples were placed on a magnetic rack. Supernatants were removed and beads were washed twice with 200 µl 70% (v/v) ethanol (HPLC-Grade, Biosolve) on the magnetic rack. Subsequently beads are washed with 180 µl of acetonitrile on the magnetic rack and following removal, air dried. Beads

were resuspended in 20 ul of digestion buffer (100 mM AMBIC), and following addition of 1 µg of trypsin (sequencing grade, Promega, 1:20 enzyme to substrate ratio by weight) and incubation overnight at 37° C. Following digestion, supernatants were acidified by addition of 1% (v/v) formic acid (ULC-MS Biosolve) and careful transfer of peptide containing supernatants to a clean tube after placing samples on a magnetic rack. Cleaned samples were ready for LC-MS analysis.

Mass spectrometry (proteome)

200 ng of peptides were injected onto a 75 µm × 250 mm column (C18, 1.6 µm particle size, Aurora, IonOpticks, Australia) kept at 50 °C at 400 nL/min for 15 min with 3% acetonitrile, 0.1% formic acid in water using an Ultimate 3000 RSLCnano UHPLC system (Thermo Scientific, Germering, Germany). Peptides were subsequently separated by a multi-step gradient to 40% acetonitrile at 90 minutes, 99% acetonitrile at 92 min held until 102 min returning to initial conditions at 105 min and kept there until 120 min to re-equilibrate the column. Eluting peptides were sprayed into a captive spray source (Bruker, Bremen, Germany) with a capillary voltage of 1.5 kV, a source gas flow of 3 L/min of pure nitrogen and a dry temperature setting of 180 °C, attached to a timsTOF pro (Bruker, Bremen, Germany) trapped ion mobility, quadrupole, time of flight mass spectrometer. The timsTOF was operated in PASEF mode of acquisition. The TOF scan range was 100–1700 m/z with a tims range of 0.6–1.6 V·s/cm2. In PASEF mode a filter was applied to the m/z and ion mobility plane to select features most likely representing peptide precursors, the quad isolation width was 2 Th at 700 m/z and 3 Th at 800 m/z, and the collision energy was ramped from 20–59 eV over the tims scan range to generate fragmentation spectra. A total number of 10 PASEF MS/MS scans scheduled with a total cycle time of 1.16 s, scheduling target intensity 2 × 104 and intensity threshold of 2.5 × 103 and a charge state range of 0–5 were used. Active exclusion was on (release after 0.4 min), reconsidering precursors if ratio current/previous intensity >4.

Data analysis (proteome)

Generated mass spectral data were processed using MaxQuant (Version 1.6.10.43),

searching a proteome database of *Aspergillus niger* (Uniprot downloaded September 2019). The proteolytic enzyme was set to trypsin allowing for a maximum of two missed cleavages. Carbamidomethyl (C) was set as a fixed modification Oxidation (M) as a variable modification. Group specific settings was set to timsDDA, and LFQ and iBAQ for quantitation were enabled. Matched between runs was also enabled using the standard settings for matching. Significantly differentially expressed proteins (DEPs) were calculated using the DEP package in R [55] using the user defined cut-offs alpha = 0.05 and lfc = $\log_2(2)$.

Data analysis (transcriptome)

Raw transcriptome data was obtained from the Utrecht Sequencing facility. The fastq files were mapped to the publicly available *A. niger* NRRL3 genome [56] using HISAT2 [57] with setting intron lengths between 20 and 1000 and suppressing SAM records for reads that failed to align. SAM files were turned into BAM files using the view and sort functions of SAMtools [58]. The htseq-count option of the tool HTSEQ [59] was used to create count text files. The count files served as input for the DESeq2 R package [60] using the DEseqDataSetFromHTSeqCount option. Shrunken log fold changes are calculated using the apeglm package [61].

The $\log_2$ fold changes ($\log_2$FC) in transcriptome and proteome data were compared using only 2381 genes (out of the 11863 genes present on the *A. niger* NRRL3 genome) of which both transcriptome and proteome data was available. Enrichment studies were done on the transcriptome dataset. Custom scripts were developed in Python and implemented in a web interface (https://fungalgenomics.science.uu.nl) to analyze over- and under-representation of functional annotation terms in sets of differentially regulated genes using the Fisher Exact test. The Benjamin-Hochberg correction was used to correct for multiple testing using a p-value < 0.05.

References

1. Criado MV, Fernández Pinto VE, Badessari A, Cabral D. Conditions that regulate the growth of moulds inoculated into bottled mineral water. Int J Food Microbiol. 2005;

2. Snyder AB, Churey JJ, Worobo RW. Association of fungal genera from spoiled processed foods with physicochemical food properties and processing conditions. Food Microbiol. 2019;83:211–8.

3. Rico-Munoz E, Samson RA, Houbraken J. Mould spoilage of foods and beverages: Using the right methodology. Food Microbiol. 2019;81:51–62.

4. Pitt JI. Xerophilic fungi and the spoilage of foods of plant origin. In: Duckworth L, editor. Water relations of foods. Elsevier; 1975. p. 273–307.

5. Hess M, Paul SS, Puniya AK, van der Giezen M, Shaw C, Edwards JE, et al. Anaerobic fungi: past, present, and future. Front Microbiol. 2020;11:1–18.

6. Wang M, Jiang X, Wu W, Hao Y, Su Y, Cai L, et al. Psychrophilic fungi from the world's roof. Persoonia Mol Phylogeny Evol Fungi. 2015;34:100–12.

7. Davies CR, Wohlgemuth F, Young T, Violet J, Dickinson M, Sanders JW, et al. Evolving challenges and strategies for fungal control in the food supply chain. Fungal Biol Rev. 2021;36:15–26.

8. Bayne HG, Michener HD. Heat resistance of *Byssochlamys* ascospores. Appl Environ Microbiol. 1979;37:449–53.

9. Rico-Munoz E. Heat resistant molds in foods and beverages: recent advances on assessment and prevention. Curr Opin Food Sci. 2017;17:75–83.

10. Dijksterhuis J. Heat-resistant ascospores. In: Dijksterhuis J, Samson RA, editors. Food Mycol A Multifaceted Approach to Fungi Food. CRC Press; 2007. p. 101–18.

11. Dijksterhuis J. Fungal spores : Highly variable and stress-resistant vehicles for distribution and spoilage. J Food Microbiol. 2019;81:2–11.

12. Wyatt TT, Wösten HAB, Dijksterhuis J. Fungal spores for dispersion in space and time. Adv Appl Microbiol. 2013;85:43–91.

13. Jara D, Portnoy J, Dhar M, Barnes C. Relation of indoor and outdoor airborne fungal spore levels in the Kansas City metropolitan area. Allergy asthma Proc. United States; 2017;38:130–5.

14. Guinea J, Peláez T, Alcalá L, Bouza E. Outdoor environmental levels of *Aspergillus* spp. conidia over a wide geographical area. Med Mycol. 2006;44:349–56.

15. Abu-Dieyeh MH, Barham R, Abu-Elteen K, Al-Rashidi R, Shaheen I. Seasonal variation of fungal spore populations in the atmosphere of Zarqa area, Jordan. Aerobiologia (Bologna).

2010;26:263–76.

16. Kure CF, Skaar I, Brendehaug J. Mould contamination in production of semi-hard cheese. Int J Food Microbiol. 2004;

17. Groot MN, Abee T, van Bokhorst-van de Veen H. Inactivation of conidia from three *Penicillium* spp. isolated from fruit juices by conventional and alternative mild preservation technologies and disinfection treatments. Food Microbiol. 2019;

18. Dijksterhuis J, Meijer M, van Doorn T, Houbraken J, Bruinenberg P. The preservative propionic acid differentially affects survival of conidia and germ tubes of feed spoilage fungi. Int J Food Microbiol. 2019;306:108258.

19. Samson RA, Houbraken J, Thrane U, Frisvad JC, Andersen B. Food and Indoor Fungi. 2nd ed. Samson RA, Houbraken J, Thrane U, Frisvad JC, Andersen B, editors. Utrecht: Centraalbureau voor Schimmelcultures; 2019.

20. Rukke EO, Sørhaug T, Stepaniak L. Heat treatment of milk: Thermization of milk. In: Fuquay JW, Fox PF, McSweeny PLH, editors. Encycl Dairy Sci. 2nd ed. Elsevier Ltd; 2011. p. 693–8.

21. van den Brule T, Punt M, Teertstra W, Houbraken J, Wösten H, Dijksterhuis J. The most heat-resistant conidia observed to date are formed by distinct strains of *Paecilomyces variotii*. Environ Microbiol. 2019;22:986–99.

22. Hallsworth JE, Magan N. Culture Age, temperature, and pH affect the polyol and trehalose contents of fungal propagules. Appl Environ Microbiol. 1996;62:2435–42.

23. Hagiwara D, Sakai K, Suzuki S, Umemura M, Nogawa T, Kato N, et al. Temperature during conidiation affects stress tolerance, pigmentation, and trypacidin accumulation in the conidia of the airborne pathogen *Aspergillus fumigatus*. PLoS One. 2017;12:e0177050.

24. Teertstra WR, Tegelaar M, Dijksterhuis J, Golovina EA, Ohm RA, Wösten HAB. Maturation of conidia on conidiophores of *Aspergillus niger*. Fungal Genet Biol. 2017;98:61–70.

25. Punt M, van den Brule T, Teertstra WR, Dijksterhuis J, den Besten HMW, Ohm RA, et al. Impact of maturation and growth temperature on cell-size distribution, heat-resistance, compatible solute composition and transcription profiles of *Penicillium roqueforti* conidia. Food Res Int. 2020;136:109287.

26. Earl Kang S, Celia BN, Bensasson D, Momany M. Sporulation environment drives phenotypic variation in the pathogen *Aspergillus fumigatus*. G3 Genes|Genomes|Genetics. 2021;11:jkab208.

27. Ruijter GJG, Bax M, Patel H, Flitter SJ, Van De Vondervoort PJI, De Vries RP, et al. Mannitol is required for stress tolerance in *Aspergillus niger* conidiospores. Eukaryot Cell. 2003;2:690–8.

28. Wolschek MF, Kubicek CP. The filamentous fungus *Aspergillus niger* contains two “differentially regulated” trehalose-6-phosphate synthase-encoding genes, *tpsA* and *tpsB*. J Biol Chem. 1997;272:2729–35.

29. Svanström Å, Van Leeuwen MR, Dijksterhuis J, Melin P. Trehalose synthesis in *Aspergillus niger*: Characterization of six homologous genes, all with conserved orthologs in related species. BMC Microbiol. 2014;14:1–16.

30. van Leeuwen MR, Krijgsheld P, Bleichrodt R, Menke H, Stam H, Stark J, et al. Germination of conidia of *Aspergillus niger* is accompanied by major changes in RNA profiles. Stud Mycol. 2013;74:59–70.

31. Suh MJ, Fedorova ND, Cagas SE, Hastings S, Fleischmann RD, Peterson SN, et al. Development stage-specific proteomic profiling uncovers small, lineage specific proteins most abundant in the *Aspergillus fumigatus* conidial proteome. Proteome Sci. 2012;10:30.

32. Hagiwara D, Suzuki S, Kamei K, Gonoi T, Kawamoto S. The role of AtfA and HOG MAPK pathway in stress tolerance in conidia of *Aspergillus fumigatus*. Fungal Genet Biol. 2014;73:138–49.

33. Baltussen TJH, Zoll J, Verweij PE, Melchers WJG. Molecular mechanisms of conidial germination in *Aspergillus* spp. Microbiol Mol Biol Rev. 2019;84:e00049-19.

34. Wang F, Sethiya P, Hu X, Guo S, Chen Y, Li A, et al. Transcription in fungal conidia before dormancy produces phenotypically variable conidia that maximize survival in different environments. Nat Microbiol. 2021;6:1066–81.

35. Bos CJ, Debets AJM, Swart K, Huybers A, Kobus G, Slakhorst SM. Genetic analysis and the construction of master strains for assignment of genes to six linkage groups in *Aspergillus niger*. Curr Genet. 1988;14:437–43.

36. Demirci E, Arentshorst M, Yilmaz B, Swinkels A, Reid ID, Visser J, et al. Genetic characterization of mutations related to conidiophore stalk length development in *Aspergillus niger* laboratory strain N402. Front Genet. 2021;12:581.

37. Sanchez Y, Lindquist S. HSP104 required for induced thermotolerance. Science. 1990;248:1112–5.

38. Singer M, Lindquist S. Thermotolerance in *Saccharomyces cerevisiae*: the Yin and Yang of trehalose. Trends Biotechnol. 1998;16:460–8.

39. Glover J, Lindquist S. Hsp104, Hsp70, and Hsp40: a novel chaperone system that rescues previously aggregated proteins. Cell. 1998;94:73–82.

40. Chowdhary S, Kainth AS, Pincus D, Gross DS. Heat Shock Factor 1 drives intergenic association of its target gene loci upon heat shock. Cell Rep. 2019;26:18.

41. Nicholls S, Leach MD, Priest CL, Brown AJP. Role of the heat shock transcription factor, Hsf1, in a major fungal pathogen that is obligately associated with warm-blooded animals. Mol Microbiol. 2009;74:844.

42. Sorger PK, Pelham HRB. Yeast heat shock factor is an essential DNA-binding protein that exhibits temperature-dependent phosphorylation. Cell. 1988;54:855–64.

43. Solís EJ, Pandey JP, Zheng X, Jin DX, Gupta PB, Airoldi EM, et al. Defining the essential function of yeast Hsf1 reveals a compact transcriptional program for maintaining eukaryotic proteostasis. Mol Cell. 2016;63:60–71.

44. Fabri JHTM, Rocha MC, Fernandes CM, Persinoti GF, Ries LNA, Cunha AF da, et al. The heat shock transcription factor HsfA is essential for thermotolerance and regulates cell wall integrity in *Aspergillus fumigatus*. Front Microbiol. 2021;12:656548.

45. Tapia H, Koshland DE. Trehalose is a versatile and long-lived chaperone for desiccation tolerance. Curr Biol. 2014;24:2758–66.

46. Pacheco A, Pereira C, Almeida M, Sousa M. Small heat-shock protein Hsp12 contributes to yeast tolerance to freezing stress. Microbiology. 2009;155:2021–8.

47. Saleh AA, Gune US, Chaudhary RK, Turakhiya AP, Roy I. Roles of Hsp104 and trehalose in solubilisation of mutant huntingtin in heat shocked *Saccharomyces cerevisiae* cells. Biochim Biophys Acta - Mol Cell Res. 2014;1843:746–57.

48. Elliott B, Haltiwanger RS, Futcher B. Synergy between trehalose and Hsp104 for thermotolerance in *Saccharomyces cerevisiae*. Genetics. 1996;144:923–33.

49. van Leeuwe TM, Arentshorst M, Ernst T, Alazi E, Punt PJ, Ram AFJ. Efficient marker free CRISPR/Cas9 genome editing for functional analysis of gene families in filamentous fungi. Fungal Biol Biotechnol. 2019;6:1–13.

50. Labun K, Montague TG, Krause M, Torres Cleuren YN, Tjeldnes H, Valen E. CHOPCHOP v3: expanding the CRISPR web toolbox beyond genome editing. Nucleic Acids Res. 2019;47:171–4.

51. Arentshorst M, Ram AFJ, Meyer V. Using non-homologous end-joining-deficient strains for functional gene analyses in filamentous fungi. Methods Mol Biol. 2012;835:133–50.

52. Batth TS, Tollenaere MAX, Rüther P, Gonzalez-Franquesa A, Prabhakar BS, Bekker-Jensen S, et al. Protein aggregation capture on microparticles enables multipurpose proteomics sample preparation. Mol Cell Proteomics. 2019;18:1027–35.

53. Hughes CS, Foehr S, Garfield DA, Furlong EE, Steinmetz LM, Krijgsveld J. Ultrasensitive proteome analysis using paramagnetic bead technology. Mol Syst Biol. 2014;10:757.

54. Sielaff M, Kuharev J, Bohn T, Hahlbrock J, Bopp T, Tenzer S, et al. Evaluation of FASP, SP3, and iST protocols for proteomic sample preparation in the low microgram range. J Proteome Res. 2017;16:4060–72.

55. Zhang X, Smits AH, van Tilburg GB, Ovaa H, Huber W, Vermeulen M. Proteome-wide identification of ubiquitin interactions using UbIA-MS. Nat Protoc. 2018;13:530–50.

56. Aguilar-Pontes M V., Brandl J, McDonnell E, Strasser K, Nguyen TTM, Riley R, et al. The gold-standard genome of *Aspergillus niger* NRRL 3 enables a detailed view of the diversity of sugar catabolism in fungi. Stud Mycol. 2018;91:61–78.

57. Kim D, Paggi JM, Park C, Bennett C, Salzberg SL. Graph-based genome alignment and genotyping with HISAT2 and HISAT-genotype. Nat Biotechnol 2019 378. 2019;37:907–15.

58. Li H, Handsaker B, Wysoker A, Fennell T, Ruan J, Homer N, et al. The Sequence Alignment / Map (SAM) format and SAMtools 1000 genome project data processing subgroup. Bioinformatics. 2009;25:2078–9.

59. Anders S, Pyl PT, Huber W. HTSeq—a Python framework to work with high-throughput sequencing data. Bioinformatics. 2015;31:166–9.

60. Love MI, Huber W, Anders S. Moderated estimation of fold change and dispersion for RNA-seq data with DESeq2. Genome Biol 2014 1512. 2014;15:1–21.

61. Zhu A, Ibrahim JG, Love MI. Heavy-tailed prior distributions for sequence count data: removing the noise and preserving large differences. Bioinformatics. 2019;35:2084–92.

62. Hoi JWS, Lamarre C, Beau R, Meneau I, Berepiki A, Barre A, et al. A novel family of dehydrin-like proteins is involved in stress response in the human fungal pathogen *Aspergillus fumigatus*. Mol Biol Cell. 2011;22:1896.

63. Romsdahl J, Blachowicz A, Chiang AJ, Singh N, Stajich JE, Kalkum M, et al. Characterization of *Aspergillus niger* isolated from the international space station. mSystems. 2018;3:e00112-18.

64. Suzuki S, Sarikaya Bayram Ö, Bayram Ö, Braus GH. *conF* and *conJ* contribute to conidia germination and stress response in the filamentous fungus *Aspergillus nidulans*. Fungal Genet Biol. Academic Press; 2013;56:42–53.

65. Sales K, Brandt W, Rumbak E, Lindsey G. The LEA-like protein HSP12 in *Saccharomyces cerevisiae* has a plasma membrane location and protects membranes against desiccation and ethanol-induced stress. Biochim Biophys Acta - Biomembr. 2000;1463:267–78.

66. Sanchez Y, Taulien J, Borkovich KA, Lindquist S. Hsp104 is required for tolerance to many forms of stress. EMBO J. 1992;11:2357.

67. Grigoriev I V., Nikitin R, Haridas S, Kuo A, Ohm R, Otillar R, et al. MycoCosm portal: gearing up for 1000 fungal genomes. Nucleic Acids Res. 2014;42:D699–704.

68. Wong Sak Hoi J, Beau R, Latgé JP. A novel dehydrin-like protein from *Aspergillus fumigatus* regulates freezing tolerance. Fungal Genet Biol. Academic Press; 2012;49:210–6.

69. Park J, Hulsman M, Arentshorst M, Breeman M, Alazi E, Lagendijk EL, et al. Transcriptomic and molecular genetic analysis of the cell wall salvage response of *Aspergillus niger* to the absence of galactofuranose synthesis. Cell Microbiol. 2016;18:1268–84.

70. Nødvig CS, Nielsen JB, Kogle ME, Mortensen UH. A CRISPR-Cas9 system for genetic engineering of filamentous fungi. PLoS One. 2015;10:e0133085.

Additional Files

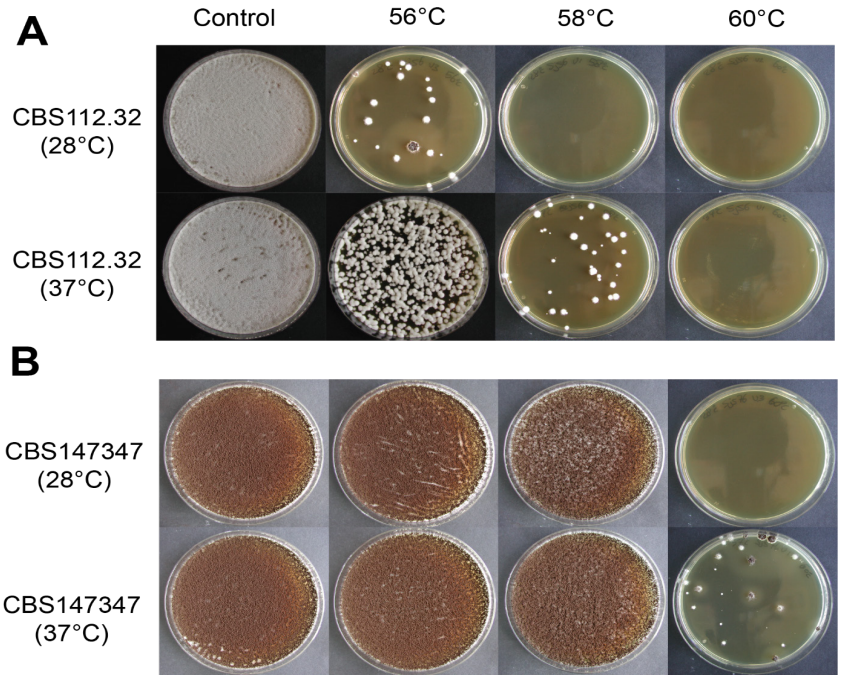

Figure 8.S1. Cultivation temperature impacts heat resistance of wild-type *A. niger* strains CBS112.32 and CBS147347. Heat resistance was investigated using the heat treatment assay, in which conidia are harvested, diluted and subsequently heat treated for 10 minutes in a thermocycler after which 10^6 conidia are plated. Pictures were taken after 5 days of incubation at 28°C. **A.** Heat resistance of wild-type strain *A. niger* CBS112.32. Conidial heat resistance increases when conidia were harvested from plates cultivated at 37°C versus 28°C as seen by the colony forming units obtained after a 10 minutes 58°C heat treatment. **B.** Heat resistance of wild-type strain *A. niger* CBS147347. Conidial heat resistance increases when conidia were harvested from plates cultivated at 37°C versus 28°C as seen by the colony forming units obtained after a 10 minutes 60°C heat treatment.

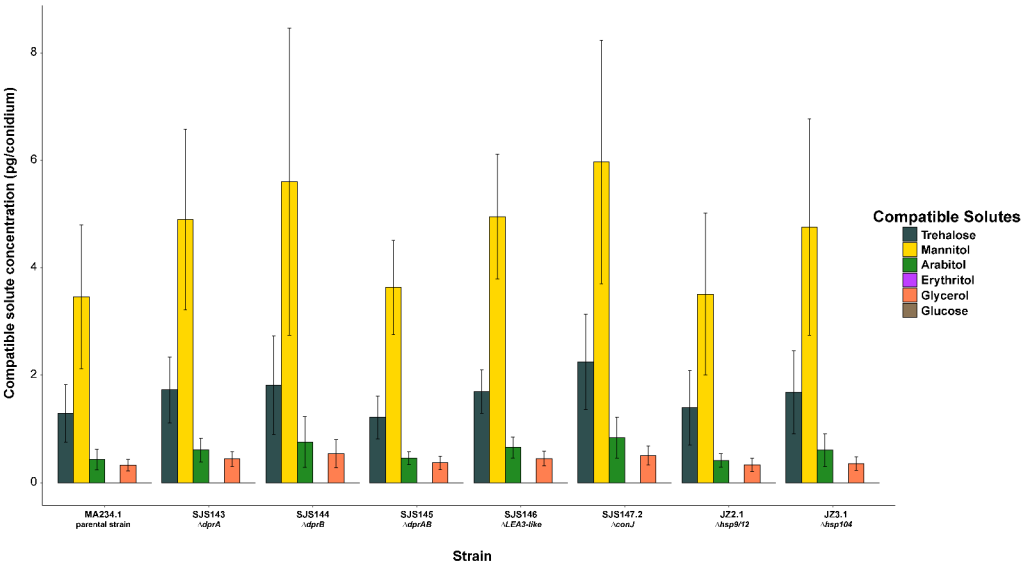

Figure 8.S2. HPLC analysis of knock-out mutants lacking protective proteins. No significant changes in compatible solute compositions were observed in any of the knock-out mutants when compared to the parental strain MA234.1 (*ΔkusA*).

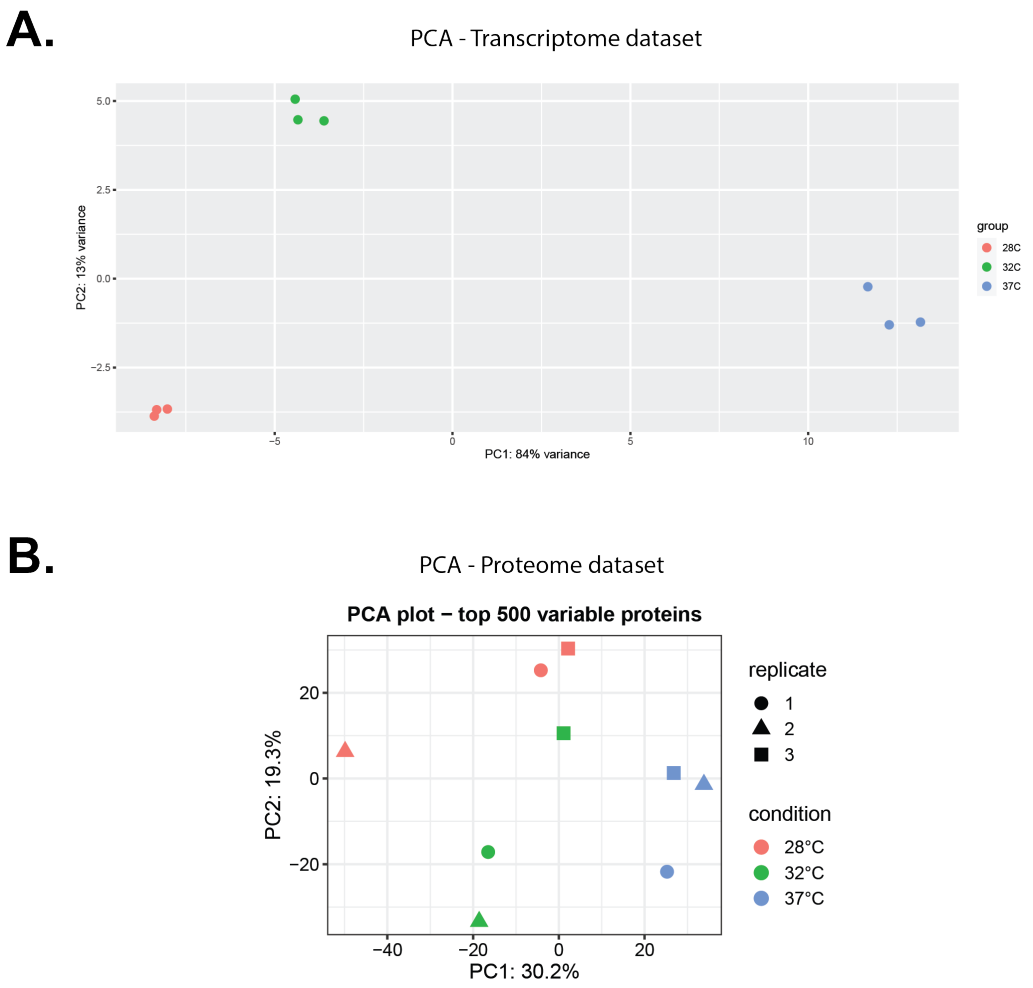

Figure 8.S3. Principle component analysis (PCA) on the transcriptome and proteome datasets. The three cultivation conditions; 28°C, 32°C and 37°C were compared. Most of the variance can be explained by the x-axis, of which the 37°C condition is the largest contributing factor in both cases. **A.** PCA of the transcriptome data, the PCA was made using the DESeq2 package in R [60]. 84% of the variance is found on the x-axis which is mostly due to the 37°C condition. **B.** PCA of the proteome data, the PCA was made using DEP package in R [55]. Variance is not as large as in the transcriptome dataset, but most of it is due to the x-axis difference which is due to the 37°C condition.

Table 8.S1. The 60 proteins significantly more or less present in conidia cultivated at 37°C. Positive values (green) in Log2 fold changes found significant ($p < 0.05$) show upregulation in conidia cultivated at 37°C, whereas negative values (red) show downregulation in conidia cultivated at 37°C. Descriptions are based on EuKaryotic Orthologous Groups (KOG) found as part of MycoCosm on the JGI website [67]. All descriptions are putative and solely based on homology. The baseMean DESeq2 values represent the average of normalized counts and the LFQ intensities represent quantified proteome data based on peptides found (higher values = more protein present). Normalization, Log2FC and their significance were calculated with the DESeq2 package in R for the transcriptome data and the DEP package in R for the proteome data.

			Transcriptome				Proteome		
NRRL3 number	An-number	Description	Base-Mean DESeq2	Log_2FC	p-value	Avg. LFQ intensity 28 °C	Avg. LFQ intensity 37°C	Log_2FC	p-value
NRRL3_10215	An18g00600	Molecular chaperone (small heat-shock protein Hsp26/Hsp42)	12309	2.43	2.44E-44	5900	1178113	7.5	2.6E-13
NRRL3_04002	An15g05410	Molecular chaperone (small heat-shock protein Hsp26/Hsp42)	1759	4.60	1.14E-65	0	130312	7.01	2.2E-08
NRRL3_09378	An11g09460	Sorting nexin SNX11	606	0.17	0.593362	0	97338	5.94	4.9E-04
NRRL3_10516	An18g04270	Parvulin-like peptidyl-prolyl cis-trans isomerase	237	-0.13	0.762198	0	46732	5.85	1.6E-03
NRRL3_11626	An06g01530	Glucan 1,3-beta-glucosidase	33	-0.04	0.940552	2858	196177	5.64	1.3E-06
NRRL3_05700	An02g07130	Mitochondrial large subunit ribosomal protein (Img2)	499	0.94	5.76E-07	0	149847	5.63	3.2E-04
NRRL3_11083	An08g04410	NADH-ubiquinone oxidoreductase subunit	568	-0.50	0.147736	0	125943	5.3	2.7E-03
NRRL3_03693	An15g01410	Possible oxidoreductase	460	0.17	0.626468	0	66393	5.28	1.4E-06
NRRL3_00318	An09g03890	Glyoxylate/ hydroxypyruvate reductase	361	-0.37	0.213897	0	99540	5.27	2.5E-07
NRRL3_11707	An06g00650 An06g00660	Oxoprolinase	1303	0.14	0.652759	218194	349483	5.16	2.0E-07
NRRL3_06627	An16g09040	N-acetyl-glucosamine-6-phosphate deacetylase	1674	-0.13	0.61331	4435	115895	5.05	1.1E-03

			Transcriptome				Proteome		
NRRL3 number	An-number	Description	Base-Mean DESeq2	Log_2FC	p-value	Avg. LFQ intensity 28 °C	Avg. LFQ intensity 37°C	Log_2FC	p-value
NRRL3_08471	An03g04500	Nucleoside diphosphate-sugar hydrolase of the MutT (NUDIX) family	286	-0.24	0.5011	2028	66817	4.85	3.7E-03
NRRL3_07783	An04g05750	hypothetical protein with signal peptide for secretion	460	-0.46	0.089005	0	55409	4.62	1.2E-02
NRRL3_09219	An11g11260	Protein-L-isoaspartate(D-aspartate) O-methyltransferase	3461	0.34	0.188724	11574	171360	4.57	3.6E-02
NRRL3_02034	An01g05040	dUTPase	85	-2.36	0.002346	0	30726	4.56	1.8E-02
NRRL3_07644	An04g07530	G protein-coupled receptor	1954	0.07	0.877749	58759	1304167	4.5	8.7E-03
NRRL3_05517	An02g09030	Nucleolar GTPase/ ATPase p130	27504	-0.22	0.05141	0	58260	4.44	2.1E-02
NRRL3_00602	An14g00300	1-Acyl dihydroxyacetone phosphate reductase and related dehydrogenases	115	-0.08	0.857974	0	40197	4.38	2.7E-02
NRRL3_06470	An17g00880	Damage-control phosphatase ARMT1-like domain	284	0.14	0.575414	0	83084	4.23	8.9E-05
NRRL3_02586	An01g11680	cis-muconate cyclase	170	0.03	0.940182	5144	99614	4.23	3.2E-03
NRRL3_00413	An09g05140	Saccharopine dehydrogenase NADP binding domain	83	-2.28	2.29E-12	0	26898	4.17	7.3E-06
NRRL3_11096	An08g04540	Putative cyclase	83	-0.26	0.561376	4433	80027	4.05	1.5E-02
NRRL3_05056	An02g14900 An02g14910	Ubiquitin activating E1 enzyme-like protein	1866	-0.14	0.415603	#N/A	#N/A	3.56	3.8E-02
NRRL3_04347	An07g01530	GatB domain	63	-0.19	0.666369	26075	258020	3.32	1.1E-02
NRRL3_04490	An07g03340	Fungal hydrophobin *hyp1*	293	0.00	0.995224	539587	5093167	3.26	2.3E-02
NRRL3_09330	An11g09920	Apoptosis-related protein/predicted DNA-binding protein	439	-0.21	0.521993	50923	374457	2.86	4.1E-02

			Transcriptome				Proteome		
NRRL3 number	An-number	Description	Base-Mean DESeq2	Log_2FC	p-value	Avg. LFQ intensity 28 °C	Avg. LFQ intensity 37°C	Log_2FC	p-value
NRRL3_03532	An05g00140	Signal recognition particle receptor, beta subunit (small G protein superfamily)	682	-0.28	0.114883	243067	67113	-2.08	4.2E-02
NRRL3_02666	An01g12550	Mannosyl-oligosaccharide alpha-1,2-mannosidase and related glycosyl hydrolases	3984	-0.66	0.149562	380070	69265	-2.53	5.9E-03
NRRL3_00410	An09g05110	Acyl-CoA synthetase	23559	-1.57	8.83E-05	256357	43786	-2.73	9.1E-03
NRRL3_02657	An01g12450	Chitinase	2316	-2.40	2.9E-05	1256357	176317	-2.83	9.6E-03
NRRL3_06237	An02g00210	Non-ribosomal peptide synthetase/ alpha-aminoadipate reductase and related enzymes	2397	-0.42	0.008291	101361	16332	-2.84	4.2E-02
NRRL3_03373	An12g04700	Dipeptidyl aminopeptidase	154	-0.79	0.069459	231517	34358	-3.04	5.2E-03
NRRL3_10599	An18g05500	Ceramidase	1652	-0.30	0.354418	166843	24713	-3.05	3.3E-02
NRRL3_04237	An07g00110	Beta-lactamase	406	-0.86	0.001611	905467	122393	-3.21	7.8E-03
NRRL3_00071	An09g00810	Zinc-binding oxidoreductase	303	-1.40	2.81E-08	176773	20027	-3.31	2.9E-03
NRRL3_00279	An09g03450	D-ribulose-5-phosphate 3-epimerase	922	-0.57	0.005181	16737	0	-3.49	9.2E-03
NRRL3_06024	An02g02930	ribose-5-phosphate isomerase	2280	-0.30	0.294115	701343	80009	-3.56	1.6E-02
NRRL3_10970	An08g03090	Calcium transporting ATPase	7420	0.15	0.457215	167843	19365	-3.67	4.6E-03
NRRL3_06352	An10g00800	Purine nucleoside permease (NUP)	32	-1.06	0.082256	325673	25999	-3.69	2.0E-04
NRRL3_02923	An12g10470	cyclin-dependent kinase	7273	-0.40	0.166186	1360567	119020	-3.84	3.4E-03
NRRL3_11047	An08g03960	Putative cargo transport protein ERV29	719	-0.39	0.142135	129678	7651	-4.15	2.1E-02
NRRL3_02139	An01g06310	hypothetical protein with DUF1793 domain	98	0.38	0.369748	52896	0	-4.36	3.7E-03
NRRL3_03251	An12g06060	hypothetical protein with YrdC-like domain	301	-1.87	6.26E-11	128167	6207	-4.41	2.2E-06

			Transcriptome				Proteome		
NRRL3 number	An-number	Description	Base-Mean DESeq2	Log_2FC	p-value	Avg. LFQ intensity 28 °C	Avg. LFQ intensity 37°C	Log_2FC	p-value
NRRL3_03449	An12g03850	ATP-dependent RNA helicase	1153	1.15	1.93E-12	42187	0	-4.42	9.7E-04
NRRL3_04236	An07g00100	Amidase	2983	-2.77	2.81E-50	50961	0	-4.5	4.8E-04
NRRL3_10468	An18g03780	Aminopeptidases of the M20 family	672	-0.13	0.662217	337473	14022	-4.58	8.0E-04
NRRL3_06750	An16g07450	Translation initiation factor 2C (eIF-2C) and related proteins	1599	-1.41	1.47E-10	239267	9344	-4.63	3.8E-08
NRRL3_03138	An12g07570	Synaptobrevin/VAMP-like protein	2175	0.97	1.39E-32	120507	2519	-4.73	1.7E-02
NRRL3_06942	An16g04640	Predicted membrane protein	318	0.00	0.998817	53285	0	-4.73	2.3E-02
NRRL3_02536	An01g11100	Predicted membrane protein	8115	0.33	0.011983	40871	0	-4.77	6.9E-03
NRRL3_03346	An12g04950	Mitochondrial F1F0-ATP synthase, subunit epsilon/ ATP15	937	-0.04	0.940168	54565	0	-4.84	2.2E-02
NRRL3_08244	An04g00150	Glutaredoxin-related protein	502	-0.06	0.8883	85849	6223	-4.85	2.4E-02
NRRL3_07734	An04g06310	hypothetical protein with signal peptide for secretion	1476	-0.45	0.000469	61747	0	-5.06	4.3E-02
NRRL3_09480	An11g08250	Glutamate decarboxylase and related proteins	185	-0.90	0.016693	290377	6787	-5.46	1.5E-05
NRRL3_11110	An08g04690	Dehydrogenases with different specificities (related to short-chain alcohol dehydrogenases)	141	-3.62	2.02E-09	192914	3916	-5.59	4.6E-04
NRRL3_04169	An15g07370	Chitinase	26	-0.35	0.414464	111428	0	-5.94	1.5E-06
NRRL3_03454	An12g03760	hypothetical protein	161	2.41	0.000117	1259540	21374	-6.04	2.3E-05
NRRL3_03951	An15g04790	Fungal specific transcription factor domain containing protein	372	0.35	0.135284	165789	0	-6.26	2.6E-03
NRRL3_10314	An18g01890	hypothetical protein	3670	-1.98	2.06E-12	1777000	23598	-6.44	2.6E-13
NRRL3_04228	An07g00020	alpha/beta hydrolase	206	0.35	0.394227	137507	0	-7.7	2.1E-02

Table 8.S2. Transcriptome and proteome changes of all chaperones and potentially protective proteins. Positive values (green) in Log2 fold changes found significant ($p < 0.05$) show upregulation in conidia cultivated at 37°C, whereas negative values (red) show downregulation in conidia cultivated at 37°C. Descriptions are based on EuKaryotic Orthologous Groups (KOG) found as part of MycoCosm on the JGI website [67]. All descriptions are putative and solely based on homology. The baseMean DESeq2 values represent the average of normalized counts and the LFQ intensities represent quantified proteome data based on peptides found (higher values = more protein present). Normalization, Log2FC and their significance were calculated with the DESeq2 package in R for the transcriptome data and the DEP package in R for the proteome data. The #N/A cells represent no proteome data for this gene present.

			Transcriptome				Proteome		
NRRL3 number	**An-number**	**Description**	**Base Mean DESeq2**	**log_2FC (37°C/28°C)**	**p-value**	**Avg.LFQ intensity 28°C**	**Avg. LFQ intensity 37°C**	**log_2FC (37°C/28°C)**	**p-value**
NRRL3_01017	An14g05070	*dprA*. Dehydrin-like protein. Homologue of DprA and DprB from *A. fumigatus*	9697	0.43	0.166	632040	495342	-1.30	0.92
NRRL3_01479	An13g01110	*dprB*. Dehydrin-like protein. Homologue of DprA and DprB from *A. fumigatus* [68]	7317	0.24	0.424	83526	191096	3.29	0.80
NRRL3_05684	An02g07350	LEA3-like protein	10188	0.33	0.2651	2480477	354129	-3.33	0.78
NRRL3_02511	An01g10790	*conJ*. Conidiation factor 10	10603	-2.27	2E-22	14067533	4508780	-2.15	0.859
NRRL3_11620	An06g01610	Heat shock protein 9/12	23695	0.55	0.006	706590	605488	-3.29	0.88
NRRL3_02725	An01g13350	Chaperone Hsp104	17811	-0.04	0.9218	7443467	7087667	-0.18	0.95
NRRL3_07278	An16g01760	Homologue of transcription factor HSF1 from *S. cerevisiae*	2312	0.29	0.0735	17626	26896	0.68	0.94
NRRL3_04002	An15g05410	Small heat-shock protein Hsp26/ Hsp42	1759	4.60	1E-65	0	130312	7.01	0.00
NRRL3_10215	An18g00600	Small heat-shock protein Hsp26/ Hsp42	12309	2.43	2E-44	5900	1178113	7.50	0.00
NRRL3_10695	An18g06650	Small heat-shock protein Hsp26/ Hsp42	374	-0.11	0.7312	#N/A	#N/A	#N/A	#N/A
NRRL3_08747	An03g00400	Small heat-shock protein Hsp26/ Hsp42	353	1.64	8E-10	#N/A	#N/A	#N/A	#N/A
NRRL3_09339	An11g09830	Small heat-shock protein Hsp26/ Hsp42	64	-0.41	0.3087	#N/A	#N/A	#N/A	#N/A
NRRL3_10998	An08g03480	Chaperone Hsp104 /Hsp98	675	-0.65	0.002	468723	441707	-0.19	0.96
NRRL3_10325	An18g02030	Heat shock factor binding protein 1	144	0.33	0.4264	#N/A	#N/A	#N/A	#N/A
NRRL3_00418	An09g05210 An09g05220	Molecular chaperone	1126	0.28	0.267	86884	19907	-2.51	0.27
NRRL3_00872	An14g03220	Molecular chaperone	780	0.41	0.0744	#N/A	#N/A	#N/A	#N/A

			Transcriptome				Proteome		
NRRL3 number	**An-number**	**Description**	**Base Mean DESeq2**	**log_2FC (37°C/28°C)**	**p-value**	**Avg.LFQ intensity 28°C**	**Avg. LFQ intensity 37°C**	**log_2FC (37°C/28°C)**	**p-value**
NRRL3_02772	An01g13900	Molecular chaperone	681	-0.60	0.0779	#N/A	#N/A	#N/A	#N/A
NRRL3_06094	An02g01990	Molecular chaperone	99	-1.19	0.0175	#N/A	#N/A	#N/A	#N/A
NRRL3_07907	An04g04050	Molecular chaperone	63	0.52	0.1181	#N/A	#N/A	#N/A	#N/A
NRRL3_10475	An18g03870	Molecular chaperone	440	-0.78	0.1306	#N/A	#N/A	#N/A	#N/A
NRRL3_10684	An18g06490	Molecular chaperone	648	-0.28	0.4742	11948	36447	0.53	0.96
NRRL3_11344	An08g07800	Molecular chaperone	88	-0.37	0.3794	#N/A	#N/A	#N/A	#N/A
NRRL3_01152	An14g06780	Molecular chaperone	194	0.75	0.0093	#N/A	#N/A	#N/A	#N/A
NRRL3_02701	An01g13070	Molecular chaperone	1111	-0.60	0.0236	145886	101211	-0.59	0.91
NRRL3_08150		Molecular chaperone	285	0.02	0.9815	#N/A	#N/A	#N/A	#N/A
NRRL3_09047	An12g01900	Molecular chaperone	1012	-0.53	0.0008	3182	34725	2.62	0.83
NRRL3_02005	An01g04620	DnaJ domain containing protein	41	-0.29	0.4593	#N/A	#N/A	#N/A	#N/A
NRRL3_00724	An14g01560	Zuotin and related molecular chaperones	730	0.27	0.3174	285847	142623	-0.98	0.82
NRRL3_10682	An18g06470	Zuotin and related molecular chaperones	490	-1.69	4E-13	0	0	#N/A	#N/A
NRRL3_09220	An11g11250	Contains TPR and DnaJ domains	1123	-0.66	9E-06	0	186719	#N/A	#N/A
NRRL3_05015	An07g09990	Molecular chaperones containing Hsp70 protein PFAM domain	53386	-0.12	0.4757	14114333	21501667	0.51	0.92
NRRL3_06609	An16g09260	SSB1 homologue. Molecular chaperones containing Hsp70 protein PFAM domain	10337	0.20	0.4875	15932667	15238667	-0.15	0.96
NRRL3_02714	An01g13220	Molecular chaperones containing Hsp70 protein PFAM domain (GRP170/ SIL1, HSP70 superfamily)	948	-0.49	0.0536	428753	358187	-0.33	0.95
NRRL3_06909	An16g05090	Molecular chaperones containing Hsp70 protein PFAM domain (mortalin/PBP74/ GRP75, HSP70 superfamily)	21561	0.56	1E-07	4467233	6191633	0.41	0.94
NRRL3_09797	An11g04180	Molecular chaperone *bipA*	10667	-1.70	6E-09	525263	1002440	1.06	0.86

			Transcriptome				Proteome		
NRRL3 number	**An-number**	**Description**	**Base Mean DESeq2**	**log_2FC (37°C/28°C)**	**p-value**	**Avg.LFQ intensity 28°C**	**Avg. LFQ intensity 37°C**	**log_2FC (37°C/28°C)**	**p-value**
NRRL3_11153	An08g05300	Molecular chaperones containing Hsp70 protein PFAM domain (HSP105/HSP110/ SSE1, HSP70 superfamily)	6370	-0.01	0.9894	3119067	3696733	0.14	0.96
NRRL3_03649	An15g00900	Metalloprotease with chaperone activity (RNAse H/ HSP70 fold)	223	-0.52	0.0946	#N/A	#N/A	#N/A	#N/A
NRRL3_04460	An07g03020	Metalloprotease with chaperone activity (RNAse H/ HSP70 fold)	285	0.39	0.1662	#N/A	#N/A	#N/A	#N/A
NRRL3_09481	An11g08220	Molecular chaperones containing Hsp70 protein PFAM domain	104	-4.57	5E-17	#N/A	#N/A	#N/A	#N/A
NRRL3_02989		Molecular chaperones containing Hsp70 protein PFAM domain	11	-0.01	0.9894	#N/A	#N/A	#N/A	#N/A
NRRL3_05751	An02g06500	Molecular chaperones containing Hsp70 protein PFAM domain	42	-5.35	0.0004	#N/A	#N/A	#N/A	#N/A
NRRL3_06901	An16g05270	Molecular chaperones containing Hsp70 protein PFAM domain	0	0.00	NA	#N/A	#N/A	#N/A	#N/A
NRRL3_08366	An03g05720	Molecular chaperones containing Hsp70 protein PFAM domain	9	0.48	0.2626	#N/A	#N/A	#N/A	#N/A
NRRL3_09070	An12g01630	Molecular chaperones containing Hsp70 protein PFAM domain	46	-0.01	0.9894	#N/A	#N/A	#N/A	#N/A
NRRL3_10894	An08g02030	Molecular chaperones containing Hsp70 protein PFAM domain	0	0.00	NA	#N/A	#N/A	#N/A	#N/A
NRRL3_10896	An08g02060	Molecular chaperones containing Hsp70 protein PFAM domain	0	0.00	NA	#N/A	#N/A	#N/A	#N/A
NRRL3_02732		Molecular chaperones containing Hsp70 protein PFAM domain	917	0.29	0.1689	#N/A	#N/A	#N/A	#N/A
NRRL3_06378		Molecular chaperones containing Hsp70 protein PFAM domain	9	-0.10	0.7838	#N/A	#N/A	#N/A	#N/A
NRRL3_00540	An09g06590	Molecular chaperone (HSP90 family)	29225	-0.36	0.0091	12163400	15786000	0.35	0.94

			Transcriptome				Proteome		
NRRL3 number	**An-number**	**Description**	**Base Mean DESeq2**	**log_2FC (37°C/28°C)**	**p-value**	**Avg.LFQ intensity 28°C**	**Avg. LFQ intensity 37°C**	**log_2FC (37°C/28°C)**	**p-value**
NRRL3_01036	An14g05320	HSP90 co-chaperone p23	1417	-0.33	0.0691	114657	603870	3.06	0.72
NRRL3_03609	An15g00480	Molecular chaperone (HSP90 family)	949	-0.15	0.6863	#N/A	#N/A	#N/A	#N/A
NRRL3_04680	An07g05920	HSP90 co-chaperone CPR7/ Cyclophilin	1023	0.09	0.7312	334040	554530	0.67	0.86
NRRL3_07788	An04g05700	HSP90 co-chaperone CPR7/ Cyclophilin	84	-0.31	0.3834	#N/A	#N/A	#N/A	#N/A
NRRL3_04490	An07g03340	Fungal hydrophobin *hyp1*/ *hfbC*	293	0.00	0.9952	539587	5093167	3.26	0.02
NRRL3_07571	An04g08500	Fungal hydrophobin *hfbC*-like	100	0.11	0.7865	#N/A	#N/A	#N/A	#N/A
NRRL3_08609	An03g02360	Fungal hydrophobin *hfbB*	1919	-1.25	0.0001	4848300	2510700	-1.10	0.81
NRRL3_08607	An03g02400	Fungal hydrophobin *hfbA*	2443	-1.78	4E-12	1245250	171940	-3.76	0.41
NRRL3_11516	An08g09880	Fungal hydrophobin *hfbD*	9284	-1.01	0.0005	#N/A	#N/A	#N/A	#N/A
NRRL3_03338	An12g05020	Fungal hydrophobin *hfbE*	109	-1.34	0.0179	#N/A	#N/A	#N/A	#N/A
NRRL3_01191	An14g07200	Catalase	11	-0.43	0.3174	#N/A	#N/A	#N/A	#N/A
NRRL3_02898	An12g10720	Catalase	14566	-0.62	7E-12	#N/A	#N/A	#N/A	#N/A
NRRL3_06040	An02g02750	Catalase *catC*	66	0.34	0.4285	0	676	#N/A	#N/A
NRRL3_08371	An03g05660	Catalase	10	-0.28	0.3861	#N/A	#N/A	#N/A	#N/A
NRRL3_11437	An08g08920	Catalase	1939	-1.35	7E-12	1368600	1184940	-0.35	0.94
NRRL3_00252	An09g03130	Catalase *catA*	30191	-0.29	0.0938	6520633	4676600	-0.45	0.94
NRRL3_00644	An14g00690	Catalase	190	-1.38	0.0002	1239393	469803	-1.48	0.51
NRRL3_01760	An01g01550	Catalase *catB*	57	-0.98	0.0775	2619867	2649100	0.04	0.96
NRRL3_01782	An01g01820	Catalase *catR*	37	-0.20	0.6581	6660	22055	0.56	0.95
NRRL3_04527	An07g03770	Super oxide dismutase *sodC*	8566	-0.78	0.0002	1284853	5670500	2.05	0.19
NRRL3_04944	An07g09250	Manganese superoxide dismutase	260	-0.41	0.199	0	9989	#N/A	#N/A
NRRL3_11040	An08g03890	Copper/zinc superoxide dismutase (SODC)	269	-1.23	7E-05	#N/A	#N/A	#N/A	#N/A
NRRL3_02664	An01g12530	Manganese superoxide dismutase	2551	0.25	0.4286	566903	717860	0.22	0.96
NRRL3_07844	An04g04870	Manganese superoxide dismutase	3297	-0.08	0.7549	325160	1082670	1.59	0.61
NRRL3_06880	An16g05520	Copper chaperone for superoxide dismutase	412	-0.88	0.0038	0	0	#N/A	#N/A

CHAPTER 9

Discussion

Discussion

The importance of transcription factors in the sorbic acid resistance of *A. niger*

In Chapter 2, the strain variability in sorbic acid resistance of 100 *A. niger* strains was investigated. We show that the minimal inhibitory concentration of undissociated sorbic acid towards *A. niger* can vary between 2 mM and 7 mM and depends on which strain was tested and which medium was used. A recent study conducted on three *A. niger* strains found MIC values between 2.88 mM – 4.80 mM undissociated sorbic acid [1]. These values are indeed consistent with our data, and fall nicely into the average MIC values found for 100 *A. niger* strains, where we show that the average *A. niger* strain has a MIC value between 2.9 ± 0.41 mM and 4.8 ± 0.83 mM depending on the medium. However, it is important to mention the outliers, such as CBS 113.50 that can even grow in the presence of 7 mM undissociated sorbic acid, as this strain might be the specific *A. niger* strain consistently found contaminating your food product. It is impossible to predict which *A. niger* strain will be encountered in which food production pipelines, and whether the average MIC among the 100 *A. niger* isolates presented here also represents the average *A. niger* conidium found in conidial populations within any given food production plant. In this thesis we show that strain diversity needs to be taken into account when designing effective preservation strategies, and in recent years other researchers have addressed this as well [2].

Transcription factors are important in the weak acid stress response of *A. niger*. The most sorbic acid sensitive wild-type strain CBS 147320 had a premature stop codon in the *sdrA* gene, and complementation of this strain with the *sdrA* gene from lab strain N402 increased the sorbic acid resistance. So, the natural strain variation found in *A. niger* isolates may in part be due to (point) mutations occurring in the transcription factors involved in the sorbic acid response. Additionally, in Chapter 2 we show that complementation of the *sdrA* gene in CBS 147320 leads to transformants with increased sorbic acid resistance, and that two transformants showed an even higher increase in sorbic acid resistance compared to the other transformants. This high sorbic acid resistance

could be due to the donor DNA, containing the complete *sdrA* gene, being inserted more than once into the genome of CBS 147320. Higher expression of *sdrA* may lead to higher sorbic acid resistance in those strains, which could also play a role in the high sorbic acid resistance observed in some *A. niger* isolates. Taken together, the results indicates that transcription factors play an important role in the sorbic acid stress response and contribute to the strain variability in sorbic acid stress resistance of *A. niger* isolates.

The screening of 240 transcription factor knock-out strains revealed the importance of multiple transcription factors, including WarB, in the weak acid stress response of *A. niger*. The *ΔwarB* strain was sensitive to sorbic, benzoic, cinnamic, propionic and acetic acid stress. Additionally, the triple knock-out strain lacking *sdrA, warA* and *warB* was more sorbic acid sensitive than any of the double knock-out strains, indicating that all three transcription factors contribute synergistically to the sorbic acid stress response.

Strain variability in heat resistance

Strain variability was also seen in heat resistance of conidia. In Chapter 3 we investigated the heat resistance of conidia isolated from *P. variotii*, *P. roqueforti* and *A. niger*. The conidia of *P. variotii* have the highest decimal reduction values, meaning that conidia from this species are generally the most heat resistant. When analysing heat resistance of three strains within *P. variotii* the D_{60}-values were 3.7 ± 0.08 minutes, 5.5 ± 0.35 minutes and 22.9 ± 2.00 minutes, which are the most heat resistant conidia known to date [3]. In order to ensure proper heat inactivation of conidia within a food production pipeline, the most heat resistant strain needs to be taken into account, since it is impossible to predict which specific strain will contaminate any given food product. The most heat resistant strain has a D-value that is roughly 6 times higher than the most heat sensitive strain in *P. variotii*. To put this heat resistance difference in perspective; after 23 minutes of 60°C heat stress 10% of the conidia from the heat resistant strain survive and only 0.0001% of the conidia of the heat sensitive strain survive. This difference in heat resistance between strains is also observed in *P. roqueforti* and *A. niger*. In fact, the impact of

strain on the variability of conidial heat resistance is consistent between the three fungi, suggesting that fluctuations in heat resistance due to strain is of a consistent factor, and therefore predictable, within filamentous fungi. Food industry can use these results to model and subsequently predict how the factor 'strain' could potentially impact heat stress resistance of conidia from any given filamentous fungus species.

The possibility of a sexual cycle in *Aspergillus niger*

Parasexual crossings between *A. niger sensu stricto* wild-type strains were attempted in order to use a bulk-segregant approach to pinpoint genes responsible for sorbic or heat resistant conidia. Unfortunately, parasexual crossings were often unsuccessful and heterokaryons could not be obtained, most likely due to heterokaryon incompatibility between most of the wild-type *A. niger sensu stricto* strains. Only 1 in 24 parasexual crossings attempted between wild-type strains were successful. This finding is in agreement with previous reports on the heterokaryon incompatibility between strains from *Aspergillus* section *Nigri* [4,5]. In our work, we limited the parasexual crossings between whole-genome sequenced *A. niger sensu stricto* strains that were genetically similar according to the phylogenetic tree (Chapter 5), but still encountered widespread heterokaryon incompatibility. Therefore, even between genetically similar *A. niger sensu stricto* strains, vegetative (heterokaryon) incompatibility is often observed.

However, vegetative incompatibility does not influence sexual compatibility in filamentous fungi. In fact, many heterothallic ascomycetes, especially heterothallic Aspergilli, show vegetative incompatibility between strains of different mating-type, such is the case for *Aspergillus flavus* and *Aspergillus heterothallicus* [6,7], which are still able to form sexual crosses. Therefore, vegetative incompatibility does not per definition affect the sexual reproduction, hence two heterokaryon incompatible strains could still potentially undergo sexual reproduction with each other (for more information, see Pál et al. [4]). Some of the molecular mechanisms behind this interplay between vegetative and sexual (in)compatibility between strains has been demonstrated in *Neuros-*

pora crassa, in which the *tol* gene mediates the mating-type associated heterokaryon incompatibility [8]. To conclude, even though a widespread vegetative incompatibility is observed between *A. niger sensu stricto* strains (Chapter 5), there is still a form of genetical exchange to be explored between *A. niger* strains; the sexual cycle. The discovery of a sexual state in *A. niger* would therefore open up the possibility to pinpoint genetic elements causing sorbic and heat resistance of conidia, by performing a bulk-segregant analysis using the sexual cycle.

No sexual state of *A. niger* has been observed to date. However, the equal distribution of mating types, and the equal distribution of these mating types throughout the phylogenetic tree (Chapter 4 and Chapter 5), indicate exchange of genetic material in nature. If *A. niger* would be a purely asexual fungus, and genetic exchange through the parasexual cycle is blocked, the presence of both MAT1-1 and MAT1-2 containing strains spread throughout the phylogenetic tree would be unexplainable. The genetical diversity observed between *A. niger sensu stricto* strains in SNPs is on average 6 ± 2 SNPs/kb (Chapter 5), which is not very different from ascomycetes with known sexual cycles. The diversity is higher than the average of 1.3 - 2.6 SNPs/kb found between 95 environmental and clinical strains from *Aspergillus fumigatus* [9]. This suggests ongoing genetical exchange between *A. niger* strains in nature, which due to heterokaryon incompatibility cannot be generated by chromosome shuffling through vegetative crossings. A closely related black Aspergillus species, *Aspergillus tubingensis*, has recently been described as having a sexual cycle [10,11]. Taken together, I hypothesize that a sexual cycle of *A. niger* is probably present and active in nature, however we currently do not know the right conditions to trigger it. By revealing the flipped orientation of the MAT1-1 locus in *A. niger* in Chapter 4, and creating a stable diploid strain between isolates of different mating types in Chapter 5, we gained more insight into the differences between *A. niger* and well-established sexual cycles of other closely related filamentous fungi such as *A. tubingensis*. Perhaps the unusual orientation of the MAT1-1 locus makes the fungus currently unable to perform a sexual cycle *in vitro*, and requires a unique activator or triggering molecule to start the sexual cycle. The ability to form a sta-

ble diploid containing two mating-types in the heterothallic species *A. niger* is, as far as I know, unique and suggests that this species, or at least the two parental strains, have no heterokaryon incompatibility mediated by the mating-type genes themselves, in contrast to this well-described phenomenon in *N. crassa* [12]. This finding indicates that genes involved in mating type gene heterokaryon incompatibility known from *N. crassa*, such as mediator *tol* [8,13], are probably not active in *A. niger*, although additional research is needed to confirm this. The unique diploid will enable to studies on environmental conditions and genetical modifications that could potentially trigger meiosis in *A. niger*.

Compatible solutes accumulate during conidial maturation on the spore chain and affect both stress resistance and germination

The conidium of *A. niger* is well-protected against heat stress, which is due to internal compatible solute composition (as shown in Chapter 7) and possible due to the presence of specific heat shock proteins (as shown in Chapter 8). The melanin present on the cell wall does not protect the cell against heat stress (as shown in Chapter 6), but it does protect the cell against UV-C radiation. All factors that contribute to a high heat stress resistance of the *A. niger* conidium, at least those studied in this thesis, are accumulating inside the cell, and are molecules or proteins that are suggested to stabilize macro-molecules [14–19]. Interestingly, in Chapter 7 we show that trehalose and polyols, the main compatible solutes found in *A. niger* conidia, are only present in small quantities in young conidia and increase in time with conidial age, thereby suggesting compatible solute accumulation is part of the conidial maturation. Taken together with the recent discovery that *A. nidulans* conidia are still transcriptionally active while attached to the spore chain [20], confirms the possibility that these compatible solutes are still actively accumulating inside the conidia after the conidia are formed, while being attached to the spore chain. Additionally, we show that germination kinetics are directly linked to internal compatible solute composition, where both a knock-out strain with conidia containing limited compatible solutes and young conidia with limited compatible solutes germinate better than

eight days old wild-type conidia in MM containing 10 mM arginine or 0.1 mM proline as the sole carbon and nitrogen source. We suggest in Chapter 7 that this could be a form of bet-hedging, where the conidia from a fungal colony are heterogenous in age and are therefore heterogenous in internal compatible solute composition. Some conidia are immature and contain limited internal compatible solutes, therefore these conidia are heat stress sensitive, but germinate better in low concentrations alanine, proline or arginine. Whereas some conidia are matured and contain high amounts of internal compatible solutes, therefore these conidia are heat resistant and germinate better in high concentrations of glucose. It suggests that a certain percentage of spores are primed for quick reproduction with minimal nutrient requirements, whereas other spores are primed for long term survival and stay dormant until ideal conditions are met.

The role of heat shock proteins in the heat resistance of *Aspergillus niger* conidia

In Chapter 8, we show that cultivation temperature increases conidial heat resistance and this correlates with both trehalose, Hsp20 and Hsp30 accumulation. The functionality of the Hsp20 and Hsp30 homologue proteins in *A. niger* still needs to be confirmed, however it is interesting to note that these two proteins are the best homologues of the two heat shock proteins found most upregulated in *A. nidulans* when conidia attached to the spore chain are heat treated. This suggests that the impact of cultivation temperature on conidial heat resistance might be established during this time-frame observed in *A. nidulans*, namely after the conidia are formed. Additionally, we show in Chapter 8 that a knock-out strain lacking the *hsp104* homologue produces heat sensitive conidia. It is interesting to note that small heat shock proteins of the *hsp26/42*-type (which the two upregulated proteins in Chapter 8 belong too) have a different mode of action than Hsp104 in *S. cerevisiae*, but both play a pivotal role in the heat stress response of yeast. In *S. cerevisiae*, Hsp26 and Hsp42 are referred to as “anti-aggregases” and bind proteins that were unfolded (due to heat shock or other stressors), thereby preventing aggregation of the unfolded proteins [21]. The yeast protein Hsp104 is unique and referred to as a dis-

aggregase or “unfoldase” and is the only yeast protein known to pull protein aggregates apart [22]. These three proteins are central in the main heat shock response of yeast, both Hsp26 and Hsp104 are regulated by Hsf1 and Msn2/4 [23], as reviewed in [24].

The effect of environmental factors during conidiation on spore heterogeneity

In Chapter 8, we describe accumulation of trehalose and heat shock proteins inside conidia upon cultivation at higher temperatures, which may seem solely beneficial for the cell. However, there might be trade-offs present; in *A. fumigatus* conidia cultivated at higher temperatures had significantly less DHN-melanin and were therefore more sensitive to UV-C resistance [25]. Reduced coloration was also observed in *A. niger* during growth at higher cultivation temperatures in our studies (data not shown). Perhaps these findings indicate that conidia are prepared for their current environment, during the maturation on the spore chain. This hypothesis is illustrated in Figure 9.1. Perhaps both compatible solute compositions and heat shock proteins concentrations are dependent on the environmental cues received, specifically during conidiation. Wang *et al.* have shown that conidia, while attached to the spore chain, are transcriptionally active in response to a heat shock. The study showed that conidia accumulate small heat shock proteins upon heat shock in *A. nidulans*, homologues of the Hsp20 and Hsp30 proteins found in Chapter 8 to accumulate inside conidia when the mycelium is cultivated at increased temperatures. Taken together, this could suggest that the cultivation temperature mainly impacts the heat resistance of conidia after their formation (by enhancing trehalose and heat shock protein accumulation), while on the spore chain, before they enter dormancy. However, more research is needed to confirm these hypotheses.

The impact of cultivation conditions during sporulation on the stress resistance has not been investigated in great detail, but could potentially be impactful and relevant for challenge tests undertaken in food industries. For example, conidia formed during a high cultivation temperature have increased heat resistance [25,26] (and Chapter 8), which means that food industries located in warmer climates face more food spoilage

due to heat resistant conidia than those located in colder climates, even when the conidia are from the same species or even strain. It would be interesting to know the other environmental cues that the conidia of the fungus can respond to during conidiation that would influence conidial resistance. A recent study shows that the nutrients the mycelium feeds on have an impact on the germination kinetics of the resulting conidia in *A. fumigatus* [27], similar results were obtained in Penicillium species [28]. Another recent study in *Penicillium rubens* showed that the water activity during conidiation affects the germination kinetics of the resulting conidia, when presented with conditions with low relative humidity [29].

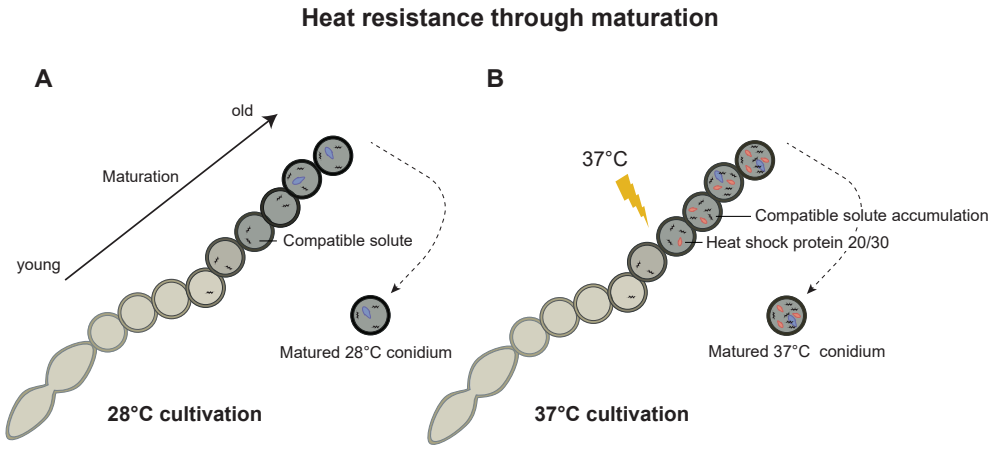

Figure 9.1. Heat resistance through maturation hypothesis. During maturation conidia are still transcriptionally active and respond to environmental cues as observed by Wang *et al.* [20] in *A. nidulans*. **A.** Conidia show maturation with age, compatible solutes start accumulating after conidia are formed (Chapter 7). **B.** At increased cultivation temperature (37°C), the conidia transcriptionally respond to the 'heat shock' environment, like described by Wang *et al.* [20], by accumulating extra trehalose and extra heat shock proteins (Hsp20 and Hsp30) in order to increase the heat resistance of the conidia (Chapter 8). As a result, a fungal colony from a single strain consists of conidia with varying heat resistance, dependent on both age and cultivation temperature experienced during conidiation.

Relevant to our study, also other research showed the impact of cultivation conditions on the stress resistance and germination of resulting conidia. The entomopathogenic filamentous fungus *Metarhizium robertsii* is used as a biocontrol agent in crop protection [30,31]. Conidia of this species are used as a product, sold to local farmers

to protect crops. Therefore, researchers and industries have been interested in generating preparations of long-lasting conidia from *Metarhizium* species, that are stress resistant in order to survive long-term storage conditions [32–34]. Previous research on *M. robertsii* has shown that growth conditions of the mycelium, i.e. the production process of these conidia (since they are a commercial product in this case), impact the stress resistance of resulting conidia [35,36]. The authors describe that the complexity of the medium, the water activity of the medium, osmotic stressors, illumination, hypoxic conditions and a heat shock during conidiation were all able to influence either the heat resistance or UV-B tolerance of the resulting conidia of *M. robertsii*. Additionally, the environmental conditions experienced during conidiation also impacted germination speeds and virulence of these conidia, which is understandably relevant for the use of *M. robertii* conidia as a natural biocontrol agent [37]. From this, we could conclude that the environmental conditions experienced during conidiation of consistently lead to changes in physical properties of conidia among filamentous fungi, including Aspergillus, Penicillium and Metharizium species.

Conclusion

Conidia are variable in their stress resistance and germination, either due to the species they belong to (Chapter 3 & 6), or the strain of a particular species they belong to (Chapter 2 & 3), or the age or environmental cues conidia of a particular strain received during conidiation (Chapter 7 and Chapter 8).

In this thesis, I show the effect of transcription factors on the natural variability in sorbic acid stress resistance of *A. niger* wild-type strains (Chapter 2), and identified novel weak acid response regulator WarB. Parasexual crosses were performed that revealed widespread heterokaryon incompatibility between *A. niger sensu stricto* strains and in the process, I created a unique diploid strain containing two mating types that can be used for future studies on sexual reproduction and/or heterokaryon incompatibility in *A. niger* (Chapter 5). The correlation between conidial age and internal compatible solute composition is shown (Chapter 7), and how compatible solutes are important for the wild-type heat stress resistance and germination kinetics. The relation between internal compatible solute composition and the germination kinetics of conidia should be further explored and could lead to new insights into molecular mechanisms behind spore germination and spore heterogeneity. Additionally, both transcriptomic and proteomic analysis on dormant conidia were performed, revealing the importance of heat shock proteins in the heat resistance of *A. niger* conidia.

The importance of transcription factors, compatible solutes and heat shock proteins described in this thesis provide new insight into molecular mechanisms behind food spoiling conidia, and could possibly be used as targets by food industry in future food preservation techniques.

References

1. Alcano M de J, Jahn RC, Scherer CD, Wigmann ÉF, Moraes VM, Garcia M V., et al. Susceptibility of Aspergillus spp. to acetic and sorbic acids based on pH and effect of sub-inhibitory doses of sorbic acid on ochratoxin A production. Food Res Int. 2016;81:25–30.

2. Rico-Munoz E, Samson RA, Houbraken J. Mould spoilage of foods and beverages: Using the right methodology. Food Microbiol. 2019;81:51–62.

3. van den Brule T, Punt M, Teertstra W, Houbraken J, Wösten H, Dijksterhuis J. The most heat-resistant conidia observed to date are formed by distinct strains of *Paecilomyces variotii*. Environ Microbiol. 2019;22:986–99.

4. Pál K, van Diepeningen AD, Varga J, Hoekstra RF, Dyer PS, Debets AJM. Sexual and vegetative compatibility genes in the Aspergilli. Stud Mycol. 2007;59:19–30.

5. van Diepeningen AD, Debets AJM, Hoekstra RF. Heterokaryon incompatibility blocks virus transfer among natural isolates of black Aspergilli. Curr Genet. 1997;32:209–17.

6. Kwon KJ, Raper KB. Heterokaryon formation and genetic analyses of color mutants in *Aspergillus heterothallicus*. Am J Bot. 1967;54:49–60.

7. Olarte RA, Horn BW, Dorner JW, Monacell JT, Singh R, Stone EA, et al. Effect of sexual recombination on population diversity in aflatoxin production by *Aspergillus flavus* and evidence for cryptic heterokaryosis. Mol Ecol. 2012;21:1453–76.

8. Shiu PKT, Glass NL. Molecular characterization of *tol*, a mediator of mating-type-associated vegetative incompatibility in *Neurospora crassa*. Genetics. 1999;15:545–55.

9. Knox BP, Blachowicz A, Palmer JM, Romsdahl J, Huttenlocher A, Wang CCC, et al. Characterization of *Aspergillus fumigatus* isolates from air and surfaces of the international space station. mSphere. 2016;1:5.

10. Horn BW, Olarte RA, Peterson SW, Carbone I. Sexual reproduction in *Aspergillus tubingensis* from section *Nigri*. Mycologia. 2013;105:1153–63.

11. Olarte RA, Horn BW, Singh R, Carbone I. Sexual recombination in *Aspergillus tubingensis*. Mycologia. 2015;107:307–12.

12. Staben C. The mating-type locus of *Neurospora crassa*. J Genet. 1996;75:341.

13. Jacobson DJ. Control of mating type heterokaryon incompatibility by the *tol* gene in *Neurospora crassa* and *N. tetrasperma*. Genome. 1992;35:347–53.

14. Mensink MA, Frijlink HW, van der Voort Maarschalk K, Hinrichs WLJ. How sugars protect proteins in the solid state and during drying (review): Mechanisms of stabilization in relation to stress conditions. Eur J Pharm Biopharm. 2017;114:288–95.

15. Allison SD, Chang B, Randolph TW, Carpenter JF. Hydrogen bonding between sugar and protein is responsible for inhibition of dehydration-induced protein unfolding. Arch Biochem Biophys. 1999;365:289–98.

16. Tapia H, Koshland DE. Trehalose is a versatile and long-lived chaperone for desiccation tolerance. Curr Biol. 2014;24:2758–66.

17. Glover J, Lindquist S. Hsp104, Hsp70, and Hsp40: a novel chaperone system that rescues previously aggregated proteins. Cell. 1998;94:73–82.

18. Sanchez Y, Taulien J, Borkovich KA, Lindquist S. Hsp104 is required for tolerance to many forms of stress. EMBO J. 1992;11:2357.

19. Pacheco A, Pereira C, Almeida M, Sousa M. Small heat-shock protein Hsp12 contributes to yeast tolerance to freezing stress. Microbiology. 2009;155:2021–8.

20. Wang F, Sethiya P, Hu X, Guo S, Chen Y, Li A, et al. Transcription in fungal conidia before dormancy produces phenotypically variable conidia that maximize survival in different environments. Nat Microbiol. 2021;6:1066–81.

21. Cashikar AG, Duennwald M, Lindquist SL. A chaperone pathway in protein disaggregation. Hsp26 alters the nature of protein aggregates to facilitate reactivation by Hsp104. J Biol Chem. 2005;280:23869–75.

22. Parsell DA, Kowal AS, Singer MA, Lindquist S. Protein disaggregation mediated by heat-shock protein Hsp104. Nature. 1994;372:475–8.

23. Amorós M, Estruch F. Hsf1p and Msn2/4p cooperate in the expression of *Saccharomyces cerevisiae* genes *HSP26* and *HSP104* in a gene- and stress type-dependent manner. Mol Microbiol. 2001;39:1523–32.

24. Verghese J, Abrams J, Wang Y, Morano KA. Biology of the heat shock response and protein chaperones: budding yeast (*Saccharomyces cerevisiae*) as a model system. Microbiol Mol Biol Rev. 2012;76:115–58.

25. Hagiwara D, Sakai K, Suzuki S, Umemura M, Nogawa T, Kato N, et al. Temperature during conidiation affects stress tolerance, pigmentation, and trypacidin accumulation in the conidia of the airborne pathogen *Aspergillus fumigatus*. PLoS One. 2017;12:e0177050.

26. Punt M, van den Brule T, Teertstra WR, Dijksterhuis J, den Besten HMW, Ohm RA, et al. Impact of maturation and growth temperature on cell-size distribution, heat-resistance, compatible solute composition and transcription profiles of *Penicillium roqueforti* conidia. Food Res Int. 2020;136:109287.

27. Earl Kang S, Celia BN, Bensasson D, Momany M. Sporulation environment drives phenotypic variation in the pathogen *Aspergillus fumigatus*. G3 Genes|Genomes|Genetics. 2021;11:jkab208.

28. Nguyen Van Long N, Vasseur V, Coroller L, Dantigny P, Le Panse S, Weill A, et al. Temperature, water activity and pH during conidia production affect the physiological state and germination time of Penicillium species. Int J Food Microbiol. 2017;241:151–60.

29. Ruijten P, Huinink HP, Adan OCG. *Penicillium rubens* germination on desiccated and nutrient-depleted conditions depends on the water activity during sporogenesis. Fungal Biol. 2020;124:1058–67.

30. Brunner-Mendoza C, Reyes-Montes M del R, Moonjely S, Bidochka MJ, Toriello C. A review on the genus *Metarhizium* as an entomopathogenic microbial biocontrol agent with emphasis on its use and utility in Mexico.

Biocontrol Sci Technol. 2018;29:83–102.

31. Shah PA, Pell JK. Entomopathogenic fungi as biological control agents. Appl Microbiol Biotechnol. 2003;61:413–23.

32. Moore D, Bateman RP, Carey M, Prior C. Long-term storage of *Metarhizium flavoviride* conidia in oil formulations for the control of locusts and grasshoppers. Biocontrol Sci Technol. 2010;5:193–200.

33. Moore D, Douro-Kpindou OK, Jenkins NE, Lomer CJ. Effects of moisture content and temperature on storage of *Metarhizium flavoviride* conidia. Biocontrol Sci Technol. Taylor & Francis; 1996;6:51–62.

34. Krell V, Jakobs-Schoenwandt D, Persicke M, Patel A V. Endogenous arabitol and mannitol improve shelf life of encapsulated *Metarhizium brunneum*. World J Microbiol Biotechnol. 2018;34:108.

35. Rangel DEN, Braga GUL, Fernandes ÉKK, Keyser CA, Hallsworth JE, Roberts DW. Stress tolerance and virulence of insect-pathogenic fungi are determined by environmental conditions during conidial formation. Curr Genet. 2015;61:383–404.

36. Rangel DEN, Fernandes ÉKK, Braga GUL, Roberts DW. Visible light during mycelial growth and conidiation of *Metarhizium robertsii* produces conidia with increased stress tolerance. FEMS Microbiol Lett. 2011;315:81–6.

37. Oliveira AS, Braga GUL, Rangel DEN. *Metarhizium robertsii* illuminated during mycelial growth produces conidia with increased germination speed and virulence. Fungal Biol. 2018;122:555–62.

Summary

In **Chapter 1** a general introduction to food preservation and challenges is given. Food and its preservation are crucial for human existence. However, efficient preservation of food has many challenges. Microbes, such as filamentous fungi, survive various preservation techniques and subsequently contaminate food products. The abundantly present asexual spores (conidia) of filamentous fungi survive stressors applied in preservation techniques, due to their relatively high stress resistance. Therefore, it is crucial for future improvements in preservation techniques to understand the molecular mechanisms behind the high stress resistance of fungal spores. Additionally, conidia are highly heterogeneous in their ability to survive preservation techniques and in their capacity to contaminate foods, which could be explained by genetic differences between strains or species. Next to the genetic factors influencing conidial stress resistance, reports suggest that conidia from the same strain, i.e. being genetically identical, can be heterogeneous in their ability to survive preservation treatments. Therefore, the work described in this thesis focused on the identification of genetic and environmental factors determining the heterogeneity in preservation stress resistance of *A. niger* conidia.

In **Chapter 2**, the impact of strain diversity on the sorbic acid resistance of 100 *A. niger* strains was investigated. The most sorbic acid sensitive wild-type strain, isolated from grape, was sorbic acid sensitive due to a disruption in the gene coding for transcription factor SdrA. Additionally, 240 *A. niger* strains deleted in a single putative transcription factor were screened on their weak acid stress resistance. Multiple single knock-out strains showed sensitivity to weak acid stress, and specifically a strain lacking the *warB* gene was sensitive to a large plethora of weak acids used as food preservatives. The *warB* gene has an additive effect on the weak acid stress resistance of *A. niger* when compared to previously reported transcription factors involved in weak acid stress resistance; *sdrA* and *warA*. This study revealed the importance of transcription factors as overall stress response regulators during weak acid stress in *A. niger*.

In **Chapter 3**, the impact of strain diversity on the heat resistance of *P. variotii*,

P. roqueforti and *A. niger* conidia was investigated. Heat resistance was quantified as D-values for each strain. The maximum difference in D-value between strains of a single species was a factor 5 to 8 and therefore considered consistent in the three fungal species investigated here. Statistically, the impact of strain difference is in the same order of magnitude when fungal spores are compared to bacterial spores. This indicates that the impact of strain difference on the heat resistance of spores is consistent between food spoiling species, and therefore predictable, which could help food industries model food spoilage risks.

In **Chapter 4**, the sequencing of the neotype *A. niger* strain CBS 554.65 is discussed. The *A. niger* neotype strain CBS 554.65 has a MAT1-2 locus, in contrast to most of the previously sequenced industrial strains that contain a MAT1-1 locus. The genetic architecture of the mating type loci MAT1-1 and MAT1-2 was compared. Many genes in the MAT1-1 mating type locus have a flipped orientation when compared to their homologues in the MAT1-2 locus. This altered orientation of the MAT1-1 locus is consistent when analysing 24 newly sequenced *A. niger sensu stricto* isolates, of which 12 were MAT1-1 and 12 were MAT1-2. The heterothallic fungus *A. niger* has so far been viewed as a purely asexual fungus, but the discovery of the flipped mating type locus might lead to new insights into the potential of *A. niger* to reproduce sexually. The CBS 554.65 strain is the first high-quality genome of a mating type MAT1-2 *A. niger* strain, making it a suitable reference strain to further investigate fungal development in *A. niger*.

In **Chapter 5**, the sequences of 24 *A. niger sensu stricto* strains were further analysed. A phylogenetic tree was made containing the 24 newly sequenced *A. niger sensu stricto* strains and eight previously sequenced *A. niger sensu stricto* strains obtained from literature. The *A. niger sensu stricto* strains could be divided into three clades, in which interestingly industrial enzyme producers clustered in clade A and organic acid producers clustered in clade B. The phylogenetic distances between strains was used to determine the likeliness of heterokaryon formation, and subsequent parasexual crossings were attempted (initially with the aim of performing bulk-segregant analysis to pinpoint genetic elements causing the heat or sorbic acid resistant phenotype of strains

analysed in Chapter 2 and Chapter 3). However, a wide-spread heterokaryon incompatibility was observed, even between closely related *A. niger sensu stricto* strains. Only a single parasexual crossing was successful, thereby creating a diploid strain containing both mating type loci. Unfortunately, no ascospores were found when sclerotium formation was induced in this strain. This diploid strain still provides us the unique opportunity to study the putative sexual cycle in *A. niger*.

In **Chapter 6**, the CRISPR/Cas9 genome editing techniques developed for *A. niger* were adopted to *P. variotii* and *P. roqueforti* in order to create DHN-melanin deficient mutant strains. Additionally, *kusA*$^{-}$ strains were developed in order to facilitate future gene replacement and gene knock-out studies in these two food spoilage fungi. The conidia of melanin mutant strains of the three food spoilers were tested for their heat and UV-C resistance. The melanin deficient strains were not altered in heat resistance compared to the wild-type strains in all three food spoilage fungi. However, the UV-C resistance was reduced in melanin mutant strains of the three food spoilage fungi, indicating that DHN-melanin protects conidia against UV-C but not heat stress in all three food spoilage fungi.

In **Chapter 7**, young conidia were investigated for their relative heat resistance compared to older conidia. Young conidia were significantly more heat sensitive than older conidia, and this sensitivity increased gradually with age. This gradual increase with age was also observed in the internal compatible solute levels, correlating with the observed gradual heat resistance increase. These results show that young conidia are still accumulating compatible solutes during the maturation process, and are therefore initially still relatively heat sensitive. Knock-out strains were created using CRISPR/Cas9 genome editing in order to further investigate the impact of compatible solutes on the heat resistance of conidia. Mature conidia of the *ΔmpdA ΔtpsACB* strain containing limited compatible solutes were more heat sensitive compared to the parental strain, comparable to the results obtained from young conidia from the parental strain. When investigating the germination of these conidia, the spores that contained limited compatible solutes germinated in higher percentages in 10 mM arginine and 0.1 mM

proline when compared to wild-type conidia. The conidia containing limited compatible solutes also showed consistently lower germination percentages in 10 mM glucose. Taken together, the germination kinetics and heat stress resistance of conidia depends on internal compatible solute concentrations, and these concentrations depend on the age of conidia. Therefore, in a population of conidia with different ages, some (young) conidia have significantly different germination kinetics and heat stress resistance when compared to other (old) conidia. This could potentially be an ecological advantage, a form of bet-hedging applied by the fungus, where the abundant population of airborne conidia consists of genetically identical cells that are heterogeneous in stress resistance and germination capacity dependent on internal compatible solute composition.

In **Chapter 8**, the impact of cultivation temperature on the heat resistance of the resulting conidia in *A. niger* is investigated. When mycelium is cultivated at higher temperatures, the resulting conidia contain more trehalose and are more heat resistant. However, the conidia of a trehalose null mutant still showed the increased heat resistance when the mycelium was cultivated at higher temperatures, without any correlating increase in the amount of internal trehalose. Therefore, a transcriptome and proteome study were conducted where conidia cultivated at 28°C, 32°C and 37°C were compared in order to find genetic elements that could explain the heat resistance increase when conidia are cultivated at higher temperatures. The comparison between conidia cultivated at 28C versus 37C was the most informative, and showed that only two genes were both significantly upregulated in transcripts and their translated proteins significantly more present. These two genes both encode predicted *hsp26/42*-type heat shock proteins. These two genes make promising candidates for the observed heat resistance increase in conidia when they were cultivated at higher temperatures.

Chapter 9 gives a detailed summary that places the work in broader context and gives hypotheses as well as potential future research topics to further our knowledge on the heterogeneity in preservation stress resistance of *A. niger* conidia.

The work described in this thesis enhanced our knowledge on preservation

stress resistance mechanisms in *A. niger*, and revealed environmental factors that influence this stress resistance. Conidia are diverse in preservation stress resistance, based on genetic differences (i.e. species or strain), but also age and cultivation temperature, which are in turn due to changes in internal compatible solute levels and heat shock proteins.

Samenvatting

In **Hoofdstuk 1** wordt een algemene introductie gegeven over voedsel conservering en de daarbij horende uitdagingen. Voedsel en voedsel conservering zijn cruciaal voor het menselijk bestaan. Echter, het efficiënt conserveren van voedsel brengt vele uitdagingen met zich mee. Microben, zoals filamenteuze schimmels, overleven sommige conserveringstechnieken en kunnen vervolgens leiden tot contaminatie van voedselproducten. De overvloedig aanwezige aseksuele sporen (conidia) van filamenteuze schimmels overleven de condities toegepast in conserveringstechnieken, door hun relatief hoge stress resistentie. Om conserveringstechnieken te kunnen verbeteren is het cruciaal om de moleculaire mechanismen achter de hoge stress resistentie beter te begrijpen. Bovendien zijn conidia ook zeer heterogeen in hun vermogen om conserveringstechnieken te overleven en voedsel te contamineren, wat deels verklaard kan worden door genetische verschillen tussen stammen en soorten. Daarnaast is er ook onderzoek dat suggereert dat conidia van dezelfde stam, die genetisch identiek zijn, ook heterogeen zijn in hun vermogen om conserveringstechnieken te overleven. Daarom concentreert het werk beschreven in dit proefschrift zich op de identificatie van genetische en omgevingsfactoren die de heterogeniteit in stress resistentie tegen conserveringstechnnieken van *Aspergillus niger* conidia bepaalt.

Hoofdstuk 2 beschrijft onderzoek over het effect stam variabiliteit op de sorbinezuur resistentie van 100 *A. niger* stammen. De stam met de hoogste sorbinezuur sensitiviteit, geïsoleerd van druiven, had een disruptie in het gen dat codeert voor transcriptie factor SdrA. Ook zijn 240 *A. niger* stammen, elk gedeleteerd in een enkele transcriptie factor, gescreend op hun resistentie tegen zwakke zuren. Een aantal mutanten lieten sensitiviteit zien tegen zwakke zuren, en specifiek een stam waar het gen *warB* was gedeleteerd was sensitief tegen een groot scala aan zwakke zuren die gebruikt worden als voedsel conserveringsmiddelen. Gen *warB* heeft een additief effect op de resistentie van *A. niger* tegen zwakke zuren vergeleken met stammen met mutaties in transcriptie factoren bekend uit de literatuur; *sdrA* en *warA*. Dit onderzoek toont het belang van tran-

scriptie factoren aan als regulators van de stressreactie van *A. niger* gedurende stress veroorzaakt door zwakke zuren.

In **Hoofdstuk 3** wordt het onderzoek naar het effect van stam diversiteit op de hitte resistentie van *P. variotii*, *P. roqueforti* en *A. niger* conidia beschreven. Hitte resistentie wordt daarbij voor elke stam gekwantificeerd in de vorm van zogenaamde D-waardes. Het maximale verschil in D-waarde tussen stammen binnen één soort was een factor 5 a 8, en daarom consistent tussen de drie schimmel soorten. Statistisch gezien is de impact van factor 'stam' in dezelfde orde grootte in schimmelsporen als in bacteriële sporen. Dit suggereert dat de impact van factor 'stam' op de hitte resistentie van sporen consistent is tussen voedsel bedervende soorten, en daardoor voorspelbaar, wat de voedsel industrie in staat stelt factor 'stam' te modeleren in voedselbederf risico's.

In **Hoofdstuk 4** wordt de sequentie van neotype *A. niger* stam CBS 554.65 gepresenteerd. De *A. niger* CBS 554.65 stam heeft een MAT1-2 locus, in contrast met de meeste bekende industriële stammen waarvan al een sequentie bekend is, deze industriële stammen hebben allemaal een MAT1-1 locus. De genetische compositie van de paringstype loci MAT1-1 en MAT1-2 zijn vergeleken. Veel van de genen in het MAT1-1 paringstype locus hebben een omgedraaide oriëntatie ten opzichte van hun homologen in het MAT1-2 locus. De omgedraaide oriëntatie van de genen in het MAT1-1 locus is consistent aanwezig, ook in de nieuwe sequenties van 12 MAT1-1 stammen. De filamenteuze schimmel *A. niger* wordt dusver gezien als een puur aseksuele schimmel, maar de ontdekking van het omgedraaide paringstype locus leidt tot nieuwe inzichten in de potentie van *A. niger* om zichzelf seksueel te reproduceren. De sequentie van stam CBS 554.65 is de eerste genetische sequentie van hoge kwaliteit van een stam met paringstype MAT1-2, waardoor dit een zeer geschikte stam is voor toekomstig onderzoek hieraan in *A. niger*.

In **Hoofdstuk 5** worden de genoomsequenties van 24 *A. niger sensu stricto* stammen verder geanalyseerd. Een fylogenetische boom met 24 nieuwe sequenties

en acht beschikbare sequenties van de literatuur liet zien dat *A. niger sensu stricto* stammen in drie groepen uiteenvallen. Interessant is dat de industriële stammen die enzymen produceren allemaal clusteren in groep A, terwijl de industriële stammen die organische zuren produceren clusteren in groep B. De verschillen tussen stammen in de fylogenetische boom zijn gebruikt om te bepalen hoe groot de kans is tot heterokaryon formatie, en vervolgens werden paraseksuele kruisingen ingezet met de doelstelling om paraseksuele kruisingen te gebruiken om genetische elementen te identificeren die hitte of sorbinezuur resistentie veroorzaken van de stammen besproken in Hoofdstuk 2 en Hoofdstuk 3. Echter, heterokaryon incompatibiliteit was wijd verspreid onder de stammen, zelfs tussen nauw verwante *A. niger sensu stricto* stammen, waardoor maar een enkele paraseksuele kruising succesvol was, en dus resulteerde in een diploïde stam die beide paringstypes bevat. De inductie van voor de seksuele ontwikkeling nodige sclerotia resulteerde helaas nog niet in ascosporen in deze diploïde stam. De diploïde stam biedt wel nieuwe kansen tot het bestuderen van de mogelijke seksuele cyclus in *A. niger*.

In **Hoofdstuk 6** wordt onderzoek beschreven waarin met CRISPR/Cas9 genoom modificatie technieken ontwikkeld voor *A. niger* in *P. variotii* en *P. roqueforti* DHN-melanine deficiënte stammen zijn gemaakt. Verder werden *kusA*$^{-}$ stammen gemaakt om zo toekomstige genetische modificatie in deze twee voedsel bedervende schimmels te vereenvoudigen. De conidia van melanine deficiënte stammen van de drie voedsel bedervende schimmels zijn getest op hun hitte en UV-C resistentie. De sporen van melanine deficiënte stammen zijn niet aangetast in hun hitte resistentie, maar wel gevoeliger voor UV-C straling in vergelijking met de ouderstammen. Concluderend is melanine van belang voor de UV-C resistentie, maar speelt geen rol in de hitte resistentie van schimmelsporen.

In **Hoodstuk 7** werden jonge conidia vergeleken met oudere conidia m.b.t. hun hitte resistentie. Jonge conidia zijn duidelijk meer gevoelig voor hitte dan oudere conidia, en deze hitte resistentie neemt gradueel toe met leeftijd. Deze graduele toename in hitte resistentie correleert met een toename in concentratie van de interne concen-

tratie osmolyten. Deze resultaten suggereren dat jonge sporen nog steeds osmolyten accumuleren tijdens de maturatie, waardoor jonge sporen hitte gevoeliger zijn dan oudere sporen. Mutanten gemaakt door CRISPR/Cas9 genoom modificatie zijn vervolgens gebruikt om zo de rol van interne osmolyten op de hitte resistentie van conidia verder te kunnen bestuderen. Conidia van de *ΔmpdA ΔtpsACB* stam hebben minimale hoeveelheden interne osmolyten en zijn hitte gevoeliger dan de sporen van de ouderstam. De hitte gevoeligheid voor hitte is vergelijkbaar met de hitte gevoeligheid van jonge sporen van de ouderstam. Tijdens het bestuderen van de ontkieming van deze conidia is verder gevonden dat sporen van mutanten met weinig interne osmolyten beter ontkiemde in medium met 10 mM arginine en 0.1 mM proline als koolstofbron in vergelijking met wild-type conidia. Deze conidia lieten ook consistent slechtere ontkieming zien in medium met 10 mM glucose als koolstofbron in vergelijking met wild-type conidia. Concluderend, de ontkieming en hitte resistentie van conidia hangen af van de concentraties interne osmolyten, en deze concentraties variëren met de leeftijd van de sporen. Dus in een sporenpopulatie waarbij verschillende leeftijden voorkomen hebben jonge schimmel sporen significant afwijkende ontkieming en lagere hitte resistentie in vergelijking met oudere schimmel sporen. Dit kan een ecologisch voordeel zijn, een vorm van een zogenaamde “bet-hedging” strategie van de schimmel, waarbij in een populatie genetisch identieke sporen heterogeniteit kan optreden in zowel stress resistentie als ontkieming efficiëntie afhankelijk van de interne compositie aan osmolyten.

In **Hoofdstuk 8** is de rol van de cultivatie temperatuur van het mycelium op de hitte resistentie van de resulterende conidia van *A. niger* onderzocht. Wanneer mycelium wordt gecultiveerd bij hogere temperaturen, neemt de interne concentratie trehalose en ook de hitte resistentie van de onder die omstandigheden gevormde sporen toe. Echter, de conidia van een trehalose deficiënte mutant laten nog steeds een toename in hitte resistentie zien wanneer ze gekweekt worden bij hogere temperaturen. Daarom is er aan het transcriptoom en proteoom van de verschillende sporen onderzoek gedaan waarbij de sporen bij 28°C, 32°C en 37°C zijn opgekweekt zijn om zo de genetische elementen te vinden die de toename in hitte resistentie kunnen verklaren. De sporen opgekweekt

bij 37°C leverden de meeste informatie op, en lieten zien dat voor twee genen zowel het transcript en als op basis daarvan gevormde eiwit meer aanwezig zijn in vergelijking met bij 28°C gevormde sporen. Deze twee genen coderen voor *hsp26/42*-achtige “heat shock” eiwitten. Deze twee genen hebben dus mogelijk een rol in de geobserveerde toename in hitte resistentie wanneer de sporen gevormd worden bij hogere temperaturen.

Hoofdstuk 9 geeft een gedetailleerde beschrijving van het totale onderzoek beschreven in dit proefschrift waarbij de resultaten in een bredere context worden geplaatst. Hypotheses en mogelijke toekomstige onderzoekslijnen worden besproken met als doel onze kennis over de heterogeniteit in stress resistentie van *A. niger* conidia te vergroten.

Het werk beschreven in dit proefschrift vergroot onze kennis over stress resistentie mechanismen in *A. niger*, en laat omgevingsfactoren zien die deze stress resistentie beïnvloeden. Conidia zijn divers in hun stress resistentie, door genetische verschillen (stammen of soorten), maar ook door hun leeftijd en de kweekomstandigheden waaronder ze worden gevormd. Een belangrijk aspect blijkt daarbij de verschillen in de concentraties van interne osmolyten en mogelijk heat shock eiwitten te zijn.

Curriculum vitae

Sjoerd Johan Seekles was born on Februari 20th, 1993 in Alkmaar, the Netherlands. He graduated from high school at the Petrus Canisius College (PCC), Alkmaar in 2011. Sjoerd followed chemistry courses for one year as part of a Bachelor Chemistry at the Universiteit van Amsterdam (UvA) in 2012. He transferred to a Bachelor Biology at the Vrije Universiteit (VU) which he obtained in 2015. During this time, he followed a minor Microbial Biotechnology & Health at the Leiden University. This sparked his interest in microbial biotechnology and he obtained his Master of Science with a specialization of Microbial Biotechnology and Health at the Leiden University in 2017. After obtaining his Master diploma, Sjoerd joined the group of dr. Arthur Ram to perform the work described in this thesis. Sjoerd is now a post-doctoral fellow in the lab of Prof. dr. Sophie G. Martin, University of Lausanne, Switzerland.

Publication list

Ellena V, **Seekles SJ**, Vignolle GA, Ram AFJ, Steiger MG. Genome sequencing of the neotype strain CBS 554.65 reveals the MAT1-2 locus of *Aspergillus niger*. BMC Genomics 22, 679 (2021). DOI: https://doi.org/10.1186/s12864-021-07990-8

Seekles SJ, Teunisse PPP, Punt M, van den Brule T, Dijksterhuis J, Houbraken J, Wösten HAB, Ram AFJ. Preservation stress resistance of melanin deficient conidia from *Paecilomyces variotii* and *Penicillium roqueforti* mutants generated via CRISPR/Cas9 genome editing. Fungal Biol Biotechnol 8, 4 (2021). DOI: https://doi.org/10.1186/s40694-021-00111-

